THE MECHANISMS OF LACTACYSTIN-INDUCED APOPTOSIS OF MOUSE PRIMARY CORTICAL NEURONS

CHOY MENG SHYAN

B.Sc (Hons), M.Sc, NUS

A THESIS SUBMITTED FOR THE DEGREE OF PHD IN THE FIELD OF

MEDICINE

DEPARTMENT OF BIOCHEMISTRY

NATIONAL UNIVERSITY OF SINGAPORE

2006

Acknowledgements

I thank my supervisors, Dr Steve Cheung Nam Sang and Dr Alan Lee Yiu Wah for their supervision and support in my study.

I am very grateful to my collaborator Heung-Chin Cheng from the Department of Biochemistry and Molecular Biology, Melbourne University for his help and guidance in the PTEN work. I also want to thank Dr Bay Boon Huat, Ms Chan Yee Gek and Ms Liu Ya Jun from the Department of Anatomy, National University of Singapore (NUS) for their assistance in the electron microscopy work. I also thank Jayapal Manikandan from the department of Physiology, NUS for his help in the Microarray data analysis using Genespring 7. I thank Dr Andrew M. Jenner for valuable advice on the measurement of neuronal cholesterol using gas chromatography mass spectrometry. Lastly, I want to thank Dr Markus Wenk and Guan Xue Li for their assistance in the lipidomic work of this project. I also wish to thank all the people in my laboratory, whom I have jointly published many papers.

I want to expression my sincere gratitude to my family and friends for their constant support. I am especially thankful to Joyce Koh for critical reading of this thesis.

Table of Contents

List of Figures

List of Tables

List of Publications

Papers

1. Cheung N.S., Choy M.S., Halliwell B., Teo T.S., Bay B.H., Lee A.Y.W., Qi R.Z., Koh C.H.V., Whiteman M., Koay E.S.C., Chiu L.L., Zhu H.J., Wong K.P., Beart P.M., and Cheng H.C. (2004) Lactacystin-induced apoptosis of cultured mouse cortical neurons is associated with accumulation of PTEN in the detergent-resistant membrane fraction. Cell Mol Life Sci. 61(15):1926-1934.

2. Choy MS, Halliwell B, Manikandan J, Jenner AM, Romero AJM and Cheung NS (2005). Proteasome inhibition by lactacystin induces the early up regulation of endoplasmic reticulum stress related genes in cultured cortical neurons. Submitted to Aging Cell.

3. Choy M.S., Bay B.H., Cheng H.C. and Cheung N.S. (2006). Recruitment of PTEN into the plasma membrane during lactacystin-induced neuronal apoptosis. Neuroscience Letters, in press.

4. Choy M.S. and Cheung N.S. (2006). Neuroprotective and pro-apoptotic responses of ubiquitin proteasome system. In: The ubiquitin Proteasome System in Central Nervous System: From Physiology to Pathology. Edited by Di Napoli M and Wojcik C, NovaScience Publisher, Inc. In press.

5. Choy M.S., Guan X.L., Wenk M.R. and Cheung N.S. (2006). Lipid profile of lactacystin-treated cortical neurons: the accumulation of ceramide and N-acyl phosphatidylethanolamine during neuronal apoptosis. In preparation.

Poster presentations:

1. M.S. Choy, H.C. Cheng, Q.T. Li, R.Z. Qi, A.Y.W. Lee, E.S.C. Koay, L. Chiu, D. Qi, H.J. Zhu P.M. Beart and N.S. Cheung (2003). PTEN expression in AMPA Receptor-mediated Apoptosis in Cultured Murine Cortical Neurons. Lorne Proteins 2003, Australia, P105

2. Lactacystin-induced apoptosis of cultured mouse cortical neurons is associated with accumulation of PTEN to specific detergent-resistant membrane micro-domains. Choy M.S., Cheng H.C., Halliwell B., Bay B.H., Lee A.Y.W., Qi R.Z., Koh C.H.V., and Cheung N.S. (2004) SfN Annual Meeting.

Other publications

1. Yew E.H.J., Cheung N.S., Choy M.S., Romero A.J.M., Manikandan J., Koay E.S. Chiu L.L., Ng W.L., Whiteman M., Kandiah J. and Halliwell B. (2005). Proteasome inhibition by lactacystin in primary neuronal cells induced both potentially neuroprotective and pro-apoptotic transcriptional responses: A microarray analysis. J Neurochem, 94: 943 – 956.

2. Cheung NS, Koh CHV, Bay BH, Qi RZ, Choy MS, Li QT, Wong KP, and Whiteman M (2004) Chronic exposure to U18666A induces apoptosis in cultured murine cortical neurons. Biochem Biophys Res Commun. 315(2):408-417.

3. Chen M.J., Yap Y.W., Choy M.S., Koh C.H.V., Seet S.J., Duan W., Whiteman M. and Cheung N.S. (2006). Early induction of calpains in rotenone-mediated neuronal apoptosis. Neurosci Lett, in press.

Abbreviations Used in the Text

ANOVA	Analysis of variance
ASK	Apoptosis-signal regulating kinase 1
ATF	Activating Transcription Factor
CHIP	Carboxyl terminus of Hsp70-interacting protein
CHOP	C/EBP-homologous protein
CNS	Central nervous system
COX-2	Cyclooxygenase 2
CREB	cAMP response element binding protein
DAB	3,4-diaminobenzidine
DUBs	Deubiquitinating enzymes
DMSO	Dimethyl sulfoxide
E1	Ubiquitin-activating enzyme
E2	Ubiquitin-conjugating enzyme
E3	Ubiquitin protein ligase
EGCG	(-)-Epigallocatechin-3-gallate
ER	Endoplasmic reticulum
ESI-MS	Electrospray-Ionisation Mass Spectrometry
ESTs	Expressed sequence tags
GC-MS	Gas Chromatography Mass Spectrometry
GSH	Glutathione
HSP	Heat shock protein
LDH	Lactate dehydrogenase
NAE	N-acylethanolamine

NAPE	N-acyl phosphatidylethanolamine
NB	Neurobasal™ medium
PI3-kinase	Phosphoinositide-3 kinase
PLD	Phospholipase D
PNS	Post nuclear supernatant
PtdIns(3,4,5)P_3	Phosphatidylinositol-(3,4,5)-triphosphate
PTEN	Phosphatase and tensin homolog deleted from chromosome 10
SMase	Sphingomyelinase
SREBP	Sterol regulatory element binding protein
TCA	Tricholroacetic acid
UPS	Ubiquitin-proteasome system

Summary

The Ubiquitin-proteasome system (UPS) is involved in the degradation of many proteins, including the short-lived regulatory proteins. Thus, UPS plays an important role in many biological processes, such as controlling the cell cycle, cell differentiation and cell death. UPS has another important role in the cell — it is able to degrade misfolded or unfolded proteins, thus protecting the cell against the accumulation of protein aggregates. Dysfunction of the proteasome is believed to be the main cause of neurodegenerative disease, since the presence of ubiquitinated protein aggregates is commonly found in diseased neurons. However, proteasome-inhibition-mediated apoptosis is still not well understood.

Exposure of the proteasome inhibitor lactacystin to mouse primary cortical neurons induced neuronal apoptosis. Upon the activation of cell death, the tumor suppressor PTEN (phosphatase tensin homolog deleted from chromosome 10) was cleaved and accumulated in the detergent-insoluble fraction of the plasma membrane, suggesting the translocation of PTEN to its membrane-bound substrate phosphatidylinositol-(3,4,5)-triphosphate during cell death. PTEN's tumor suppressor function is attributed to its phospholipid phosphatase activity, that specifically dephosphorylates the plasma membrane phospholipid secondary messenger phosphatidylinositol-(3,4,5)-triphosphate (PtdIns(3,4,5)P_3). The recruitment of PTEN, which is commonly localized in the cytosol, into the plasma membrane where PtdIns(3,4,5)P_3 accumulates is believed to be necessary during apoptosis. In this study, translocation of PTEN to the plasma membrane microdomain is demonstrated for the first time in primary cortical neurons treated with the proteasome inhibitor lactacystin. In addition,

proteolysis of PTEN to a shorter 50 kDa form that is preferentially targeted to the plasma membrane was observed. This truncated species of PTEN might play an important role in suppressing cell growth and promotes apoptosis by antagonizing the PI3-kinase/Akt signaling pathway.

Microarray analysis of neurons exposed to lactacystin reveals the early up-regulation of genes in response to unfolded proteins, such as those encoding proteasome subunits, heat shock proteins (HSPs), and endoplasmic reticulum (ER) stress. A mechanism of apoptotic cell death through the abnormal accumulation of protein and ER stress is suggested. ER stress can also cause the disruption of calcium homeostasis and oxidative stress in cells. The up-regulation of genes which encode calcium-binding proteins and enzymes involved in oxidative defense are likely to be regulated by the downstream effects of ER stress.

The lipid profile of the neural membrane reveals the accumulation of ceramides and N-acyl phosphatidylethanolamines (NAPEs) during lactacystin-induced apoptosis. Ceramide has been known to be involved in the apoptotic cell death pathway, but the role of NAPE is so far unclear. NAPE accumulation has been associated with excitotoxic or necrotic cell death, but the accumulation of NAPE in the apoptotic cell death pathway has not been reported.

(-)-Epigallocatechin-3-gallate (EGCG) from green tea extract is a naturally occurring proteasome inhibitor. Although high concentrations of EGCG were able to induce neuronal cell death through the activation of caspase-3, microarray analysis reveals that low concentrations of EGCG caused the up-regulation of genes encoding

proteasome subunits and ubiquitin, suggesting a potential neuroprotective effect against neurodegeneration.

CHAPTER 1

1 INTRODUCTION

1.1 The ubiquitin-proteasome system

The ubiquitin-proteasome system (UPS) and the lysosomal pathway constitute the major mechanisms of protein degradation in eukaryotic cells. Lysosomal degradation is responsible for the degradation of membrane-associated proteins and extracellular proteins taken up by endocytosis. On the other hand, UPS is an ATP-dependent protein degradation system which is responsible for the degradation of soluble proteins in the cytosol. UPS degrades proteins selectively — only proteins that have been tagged for degradation by a process called ubiquitination (or ubiquinylation) will be degraded. Many short-lived regulatory proteins are degraded by UPS; this selective degradation of regulatory proteins by UPS underlies the regulation of many cellular processes, including regulation of the cell cycle, modulation of cell surface receptors and ion channels, and antigen presentation (Ciechanover and Schowartz, 2002). In the central nervous system (CNS), UPS plays a role, among others, in neuronal signaling, synapse formation and function (review by Hegde, 2004), and in the prevention of abnormal protein accumulation. UPS is particularly important in the mechanism that controls the quality of newly synthesized proteins in the endoplasmic reticulum (ER), degrading any protein that fails to be folded properly in a process called ER-associated degradation (ERAD) (Travers et al, 2000; Hampton, 2002; Sitia and Braakman, 2003). It is becoming increasingly evident that the dysfunction or altered activity of UPS is involved in pathogenesis of neurodegenerative diseases such as Alzheimer's disease (Lam et al, 2000; Layfield, 2000; Lopez Salon et al, 2000; Hope et al, 2003; Song and Jung, 2004), Parkinson's disease (Shimura et al, 2000;

Snyder et al, 2003; Cookson, 2005; McNaugh and Olanow, 2005), Huntington's disease, Amyotrophic Lateral Sclerosis, prion diseases and spinocerebellar ataxia (Alves-Rodrigues et al, 1998; Sherman and Goldberg, 2001; Layfield et al, 2003). The molecular mechanisms that underlie these processes are presently being unraveled.

The UPS consists of different components: a multi-component protease, ubiquitin, ubiquitin-activating enzyme (E1), ubiquitin-conjugating enzyme (E2) and ubiquitin protein ligase (E3) (Fig. 1.1). The structures and functions of these components are described below.

1.1.1 Structure and function of proteasome

The proteasome is a multi-component protease (review by DeMartino and Slaughter, 1999). The fully assembled proteasome (26S) is a large 1500–2000 kDa protein complex. It is formed by the association of one core 20S proteasome (catalytic complex) with one or two 19S regulatory subunits (also known as PA700) at each end of the barrel-shaped 20S (Fig. 1.1). The eukaryotic 20S consists of two outer and two inner rings that are stacked to form a barrel structure. Each outer ring has seven α-subunits (α1 to α7) while each inner ring contains seven β-subunits (β1 to β7) (Groll and Clausen, 2003). The three main proteolytic activities of the 20S proteasome complex are: chymotrypsin-like (mediated by the β5-subunit), trypsin-like (mediated by the β2-subunit) and peptidyl-glutamyl peptide hydrolyzing or caspase-like (mediated by β1-subunit) (DeMartino and Slaughter, 1999). The chymotrypsin-like activity of the 20S proteasome is believed to be the rate-limiting step in the protein degradation pathway. Two additional

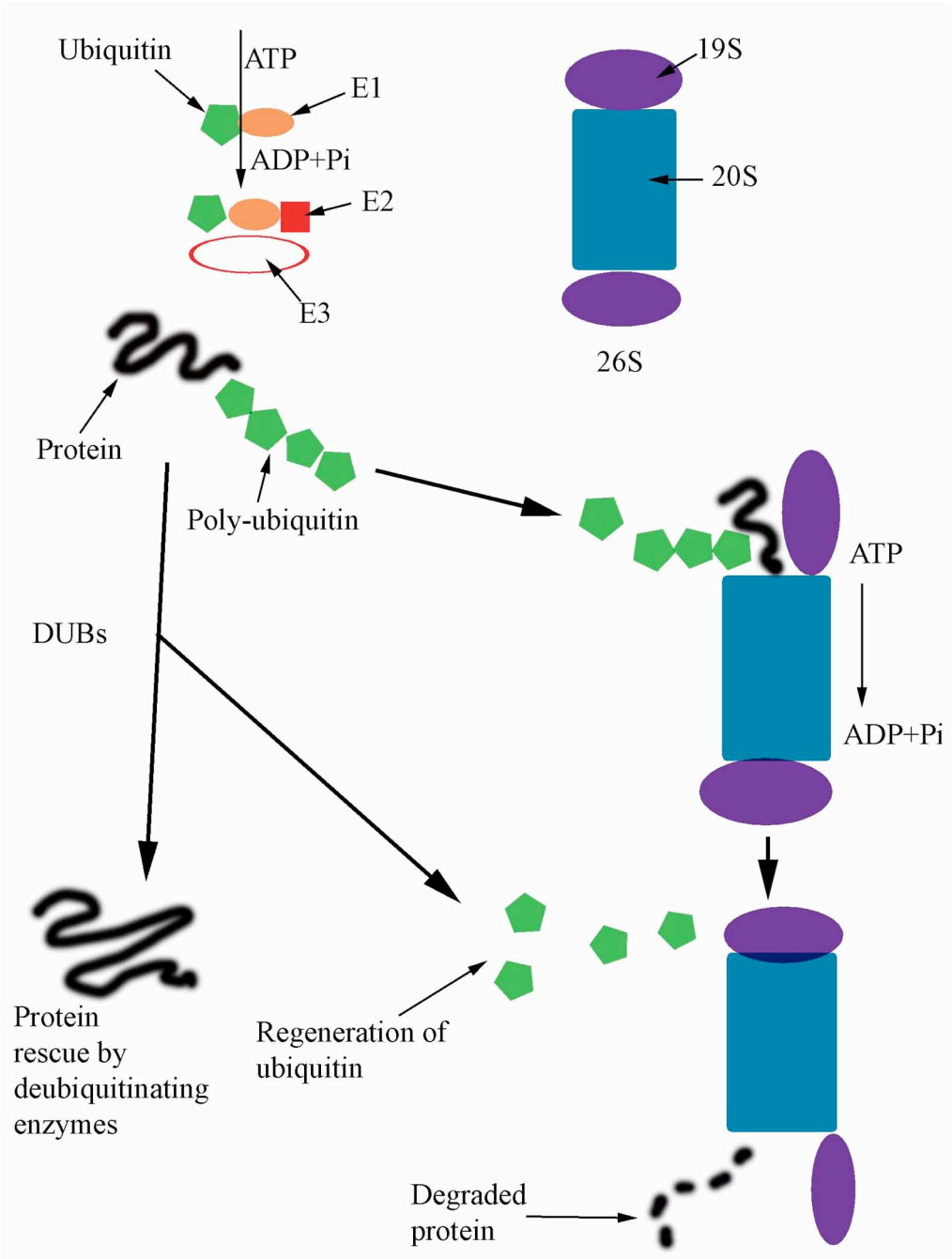

Figure 1.1. The ubiquitin-proteasome system. An E3 enzyme recognizes the substrate and mediates the transfer of ubiquitin from an E2. The latter receives its ubiquitin by transfer from an E1. Poly-ubiquitinated proteins are targeted for degradation by the 26S proteasome. The 26S proteasome is made up of the core 20S catalytic complex and the 19S regulator complexes. It releases free ubiquitin and degrades the substrate into short peptides. Poly-ubiquitinated proteins can be deubiquitinated by the action of numerous deubiquitinating enzymes (DUBs)

activities, called branched chain amino acid-preferring and small neutral amino acid-preferring activities have been recently described. Several evidences suggest that the peptidyl-glutamyl peptide hydrolyzing activity and the branched amino acid-preferring activity are expressed by the same active site, enabling the 20S proteasome alone to degrade a wide variety of protein substrates, such as poorly-folded or unfolded proteins, and oxidized proteins characterized by an increase of surface hydrophobicity (Amici et al, 2003).

Situated at both ends of the 20S catalytic complex, the 19S acts in an ATP-dependent fashion to unfold proteins for degradation and feed them into the catalytic barrel of the 20S proteasome for degradation (DeMartino and Slaughter, 1999). In addition to that, an ubiquitin recognition function is present in the 19S to selectively degrade proteins that are ubiquitinated. The functions of 19S are coupled to its ATPase activity, making it highly susceptible to ATP depletion, such as during ischemia.

1.1.2 Structure and function of ubiquitin

Ubiquitin is a small protein with 76 amino acids. It is present in all studied eukaryotic cells and tissues. Ubiquitin is encoded by the ubiquitin B (*Ubb*) gene and is one of the most conserved proteins known; the yeast's ubiquitin protein sequence differs from that of the human's in only 3 out of the 76 amino acids (Hershko and Ciechanover, 1998). Ubiquitin can be covalently attached to another protein, or to another ubiquitin, by a tightly controlled ATP-dependent process known as ubiquitination, involving an ubiquitin-activating enzyme (E1 or Uba), an ubiquitin-conjugating enzyme (E2, also known as Ubc) and an ubiquitin protein ligase (E3). The process of ubiquitination is as follows: first, an E1 activates the free ubiquitin in

an ATP-dependent manner. Next, the activated ubiquitin is transferred to an E2. Finally, an E3 brings together the target protein and the conjugating enzyme, facilitating the transfer of the activated ubiquitin to the targeted protein. The attachment of ubiquitin to the targeted protein is through the N-terminal of a lysine residue of the target. Subsequent rounds through the E1 ubiquitin-activating enzyme, E2 ubiquitin-conjugating enzyme and E3 ubiquitin ligase lead to the formation of a poly-ubiquitinated target protein, ready to be recognized and degraded by the 26S proteasome (DeMartino and Slaughter, 1999; Wójcik, 2002). The ubiquitination cascade leading to the degradation of the substrate by the 26S proteasome is depicted in Fig. 1.1. In some instances, the proteasome can degrade proteins through alternative regulatory mechanisms, which include the binding of adaptor proteins or covalent modification by ubiquitin-like proteins (eg. Nedd8). The UPS degradation pathway is further complicated by the existence of numerous deubiquitinating enzymes (DUBs). DUBs can cleave not only the free poly-ubiquitin chains released from tagged substrates which have already been degraded by the proteasome, but also the poly-ubiquitin chains bound to undegraded substrates. In the latter case, DUBs can perform a rescue function, releasing the tagged substrate from the fate of degradation (Wójcik, 2002).

1.2 Ubiquitin-proteasome system and neurodegeneration

The accumulation of unfolded proteins in the cell is a threat to its function and viability (Sherman and Goldberg, 2001; Schröder and Kaufman, 2005). Intra- or extra-cellular accumulation of often cross-linked and misfolded proteins is a characteristic feature of many neurodegenerative diseases, including Amyotrophic Lateral Sclerosis, Alzheimer's disease and Parkinson's disease (Sherman and

Goldberg, 2001; Shen et al, 2004; Grune et al, 2004). The protein aggregates found in diseased brains do not have a common terminology; the terms 'protein aggregates', 'plaques', 'inclusion bodies' or 'aggresomes' are commonly used (Wójcik and DeMartino, 2003). Johnston et al, defines an aggresome as a "peri-centriolar, membrane-free, cytoplasmic inclusion containing misfolded, ubiquitinated proteins ensheeted in a cage of intermediate filaments formed specifically at the microtubuli organization centre (MTOC)" (Johnston et al, 1998). On the other hand, the term 'protein aggregate' appears to have a rather wide specificity, requiring mainly the existence of aggregations of misfolded protein. For extracellular protein aggregates, the term 'plaque' is more common. The terms lipofuscin and ceroid are used in general to describe protein material that accumulates during the aging process (Grune et al, 2004).

Aggregation-prone proteins linked to neurodegenerative diseases have been shown to disrupt the function of the UPS (reviewed in Song and Jung, 2004). The majority of neurodegenerative disease cases are sporadic. However, the identification of a number of genes responsible for rare familial forms of neurodegenerative disease has provided insights into the underlying mechanisms of the disease's formation (Bossy-Wetzel et al, 2004; Moore et al, 2005). For example, loss-of-function mutation in the gene encoding the E3 ubiquitin ligase, Parkin, is linked to autosomal recessive juvenile parkinsonism (ARJP) (Shimura et al, 2000; Mizuno et al, 2001; Bossy-Wetzel et al, 2004). On the other hand, over-expression of Parkin could counter unfolded protein stress-induced cell death (Imai et al, 2000). Recent studies also found that a frame-shift mutation of the ubiquitin B gene produces a variant form of ubiquitin, UBB^{+1}, which is found in intracellular protein inclusions in Alzheimer's

diseases and progressive supranuclear palsy (de Vrij et al, 2001). This mutation abolishes the C-terminal G76 of ubiquitin, preventing the ligation of UBB^{+1} to target-protein substrates, or poly-ubiquitin chains. Instead, UBB^{+1} is readily poly-ubiquitinated and acts as a potent competitive inhibitor of the 26S proteasome (Lam et al, 2000; Hope et al, 2003; Song and Jung, 2004).

1.3 Ubiquitin-proteasome system in aging

Familial types of neurodegenerative diseases are linked to loss-of-function mutations of ubiquitin protein ligase, such as in the case of Parkinson's disease. However, sporadic forms of neurodegeneration are often associated with aging. Proteins, once synthesized, will be folded into their functioning conformation (Schröder and Kaufman, 2005). In the cell however, the properly folded proteins are subject to a highly reactive environment, and can undergo post-synthetic damage and modification through oxidation, isomerization or glycation (Goldberg, 2003). The rate of such damage inflicted will increase markedly upon the exposure of cells to stresses such as an increase of temperature, or reactive oxygen species (Sherman and Goldberg, 2001). Eukaryotic cells have two main strategies to counteract these stresses and avoid the accumulation of protein aggregates. These include the (i) induction of heat shock proteins (HSPs) and molecular chaperones that are involved in the protein refolding systems and (ii) targeted degradation of damaged and unfolded proteins by the UPS (Taylor et al, 2005). In an aging cell, the capacity to handle the building up of unfolded or damaged proteins becomes insufficient to prevent their accumulation and toxic consequences (Keller et al, 2002). Recent studies report that the expression of neuroprotective antioxidants and molecular chaperones decrease in aging cells (Keller et al, 2004). The decrease in

neuroprotective antioxidants exposes proteins to oxidative stress and enhances the building up of protein aggregates. This building up of protein aggregates contributes to the overloading and inhibition of the UPS, causing it to be less effective (Keller et al, 2004). Much remains to be discovered about the inducibility and functioning of heat shock proteins, molecular chaperones and the UPS in mammalian cells. Such studies appear very important to undertake, since genetic polymorphism in these protective systems, and in their expression with aging may play critical roles in the accumulation of abnormal proteins and pathogenesis of neurodegenerative diseases. Moreover, pharmacological induction or activation of these protein repair-and-degradative systems could present an attractive new approach to treatment or delaying the neurodegenerative process (Sherman and Goldberg, 2001).

1.4 Proteasome-inhibition-induced neuronal cell death

The use of proteasome inhibitors to inhibit proteasome activities in cells is sufficient to induce both the formation of protein aggregates and neuronal apoptosis (Sawada et al, 2004). Therefore, research on the prevention of neurodegenerative diseases has to be focused on the mechanisms of protein aggregation and the resultant neuronal cell death that is caused by the inhibition of proteasome activities. The mechanism of cell death through the inhibition of the proteasome is, however, unclear. Proteasome inhibition has been found to mediate several cell death signaling pathways, including the activation of the cysteine-dependent aspartate-directed (caspase) protease family, the c-jun N-terminal kinase (JNK) pathway, and its upstream kinase and apoptosis-signal regulating kinase 1 (ASK) pathway. Recently, studies have also proposed the ER stress-mediated cell death pathway to be involved in the toxicity of proteasome inhibition (Nakagawa et al, 2000; Rao et al, 2005). Caspase-12 is an ER-localized

caspase, which is activated by ER stress and can possibly lead to the cleavage of caspase-3 (Rutkowski and Kaufman, 2004). It is worth noting that caspase-12 was identified in the mouse, but its presence in human tissues is controversial (Rao et al, 2005). Nevertheless, pro-apoptotic signals resulting from ER stress can also be sent through the induction of the pro-apoptotic transcription factor C/EBP-homologous protein (CHOP). CHOP is normally undetectable, but is expressed at high levels in cells exposed to conditions that perturb protein folding in the ER, and induces ER stress-mediated apoptosis (Wang et al, 1996). The increase in CHOP protein expression is believed to suppress the anti-apoptotic Bcl-2 expression in cells, which makes them more susceptible to apoptosis induction (McCullough et al, 2001; Rao et al, 2004). Furthermore, ER stress can also cause the disruption of calcium homeostasis in cells, which in turn activates the calcium-regulated protease calpain and subsequently induces cell death (Rutkowski and Kaufman, 2004).

1.5 Proteasome inhibitors

Proteasome inhibitors can be divided into 5 classes: (1) peptide aldehydes, (2) peptide vinyl sulfones, (3) peptide boronates, (4) peptide epoxyketones (epoxomycine and eponomycin), and (5) β-lactones (lactacystin and its derivatives), based on the pharmacophore that reacts with the threonine residue in the active site of the proteasome (reviewed by Adam, 2003). In addition to being useful research tools for dissecting the roles of the proteasome, these inhibitors elicit appreciable interest because of their potential applications in biotechnology and medicine. For example, through their ability to block the activation of NFκB, proteasome inhibitors can dramatically reduce in vitro and in vivo production of inflammatory mediators, as well as that of various leukocyte adhesion molecules, which play crucial roles in

many diseases (Lee and Goldberg, 1998; Di Napoli and Papa, 2003; Wójcik and Di Napoli, 2004). Also of appreciable promise is the potential use of these proteasome inhibitors in cancer therapy (Rajkumar et al, 2005). The proteasome inhibitor PS-341 (generic name bortezomib) has become the first proteasome inhibitor to be used in clinical practice to treat relapse cases of multiple myeloma (Adams, 2003; Rajkumar et al, 2005; Elliott and Ross, 2001). The other potential proteasome inhibitor is MLN-519, a small-molecular-weight lactacystin analog developed by Millennium (Leukosite) for the potential treatment of inflammatory disease and stroke (Wojcik and De Napoli, 2004). However, of all the inhibitors mentioned above, only two currently exhibit properties that are suitable for clinical development. Reasons to reject a proteasome inhibitor for future clinical development include metabolic instability (Adams et al, 2003), lack of enzyme specificity, and irreversible binding to the proteasome, such as in the case of β-lactone. Nonetheless, proteasome inhibitors such as peptide aldehydes and lactacystin have been useful in the study of UPS in cancer cell lines or in neurons (Adam, 2003).

1.5.1 Many effects of proteasome inhibitors

Although the inhibition of proteasomes by proteasome inhibitors leads to cell death and is related to neurodegenerative disease, other studies have also shown that proteasome inhibition can cause the induction of various HSPs, which increase cell tolerance to stressful conditions (Bush et al, 1997). For example, Meriin et al reported that proteasome inhibition using peptidyl aldehyde MG-132 was able to trigger both pro-apoptotic and anti-apoptotic responses in U937 lymphoid and 293 kidney human tumor cells (Meriin et al, 1998). In their study, the prolonged incubation of cells with MG132 activates the apoptotic program through the c-Jun N-

terminal kinase (JNK) pathway. However, a short incubation of cells with MG-132, followed by its withdrawal caused the accumulation of the heat shock protein 72 (Hsp72) and thus suppressed the JNK-dependent apoptosis caused by heat-shock or ethanol treatment (Meriin et al, 1998). In another study using cultured rat cerebellar granule neurons, prolonged incubation with MG132 increased the expression and phosphorylation of c-Jun and the pro-apoptotic protein Bim, and triggered neuronal apoptosis. Short-term incubation, on the other hand, exerted a neuroprotective effect by stabilizing the MEF2 transcription factor (Butts et al, 2005). Drug exposure time is not the only factor that determines the fate of cells. In a separate report, Suh et al observed that a lower concentration of MG-132 (0.1 μM) induced neuronal apoptosis in mouse cortical neuronal cultures, while a higher concentration (10 μM) attenuated apoptosis (Suh et al, 2005). The authors concluded that the complete inhibition of proteasome activity might have prevented neuronal cell death through the regulation of mitochondrial-mediated apoptotic pathways. Therefore, both the concentrations and the times of exposure to the proteasome inhibitor might define the fate of cells.

1.5.2 Lactacystin

Lactacystin, a proteasome inhibitor, was first isolated from the soil bacteria *Streptomyces sp.* OM-6519 because of its ability to promote differentiation in mouse neuroblastoma cell line (Neuro 2a) and rat Oligodendroglial cells (Nakagawa, 1994; Pasquini et al, 2003). Lactacystin was found to induce apoptosis in actively dividing cancerous cell lines (Imajoh-Ohmi et al, 1995), and more recently, in cultured cortical neurons (Qiu et al, 2000). Lactacystin is specific, non-reversible and potent as a proteasome inhibitor. It can inhibit the chymotrypsin-like and trypsin-like activities of 20S proteasome; many studies suggest that chymotrypsin-like activity is the rate-

limiting step in protein degradation (Lee and Goldberg, 1998). Lactacystin does not react with the proteasome; rather, it undergoes a spontaneous conversion (lactanization) to the active proteasome inhibitor, clasto-lactacystin β-lactone (or β-lactone in short). When β-lactone is added to mammalian cells in culture, it rapidly enters the cells, where it can react with the sulfhydryl of glutathione (GSH) to form a thioester adduct that is both structurally and functionally analogous to lactacystin (called lactathione). Like lactacystin, lactathione does not react with the proteasome, but can undergo lactanization to yield back the active β-lactone (Dick et al, 1996). In cells, β-lactone binds specifically to the β5 subunit of 20S and inhibits its chymotrypsin-like activities (Dick et al, 1996). Fig. 1.2 illustrates the mechanism of proteasome inhibition by lactacystin in cells.

1.6 The aims of this study

Aberration of the UPS has been implicated in the pathogenesis of many neurodegenerative disorders. The mechanism of proteasome inhibition-induced neuronal apoptosis is still not well understood. Therefore, the aim of this study is to address the mechanism of proteasome dysfunction-mediated neuronal apoptosis, using the proteasome inhibitor lactacystin. Understanding the underlying mechanism involved in this cell death system is important for the development of novel, mechanism-based drugs for the treatment of neurodegeneration.

I started out my research by studying the role of the tumor suppressor PTEN (phosphatase and tensin homolog deleted from chromosome 10) in lactacystin-induced neuronal apoptosis. PTEN is a novel phospholipid and protein phosphatase.

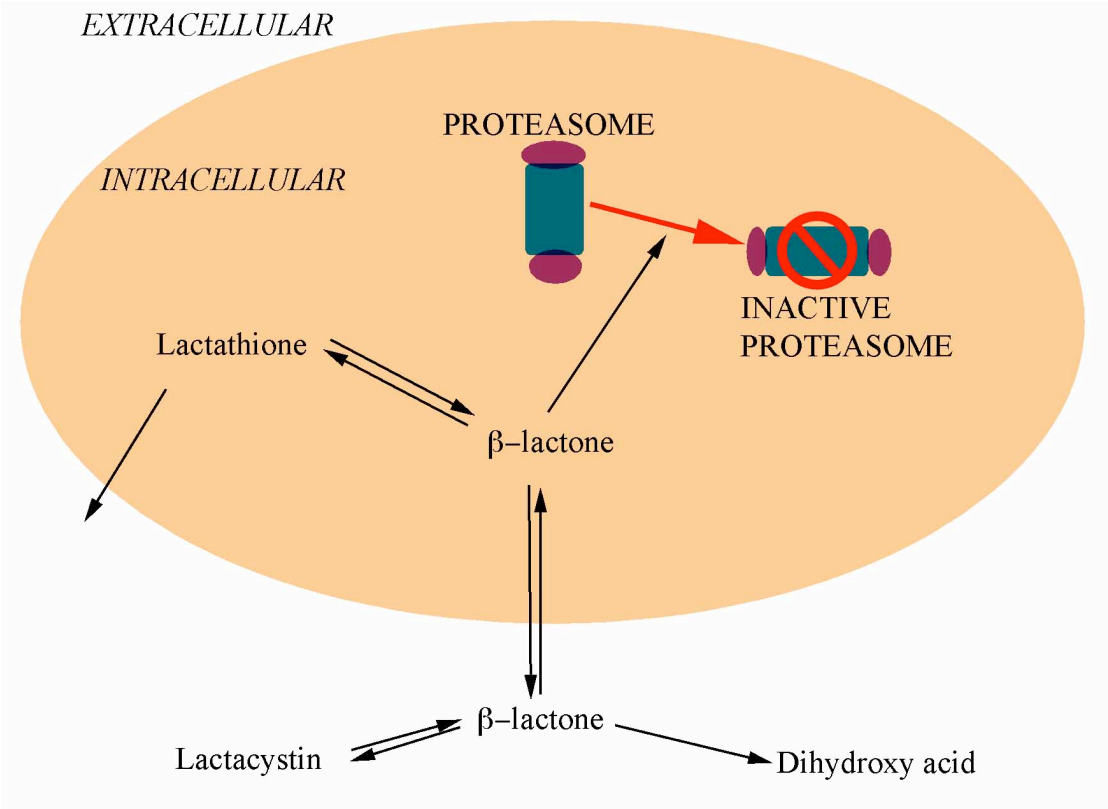

Figure 1.2. Mechanism of proteasome inhibition by lactacystin in cells. The detailed information of proteasome inhibition by lactacystin is described in the text. This diagram is according to the report of Dick et al, 1997.

Mutation of the *PTEN* gene is associated with many cancer types such as gliomas and endometrial cancers (Leslie and Downes, 2002; Waite and Eng, 2002), mammalian cells transfected with the *PTEN* gene are more sensitive to the induction of apoptosis (Wang et al, 1999; Gary and Mattson, 2002), suggesting that its interplay with PI3-kinase is an important regulatory step in the cellular cascades related to apoptosis. It has been suggested that PTEN needs to be translocated to the plasma membrane during apoptosis to dephosphorylate the phospholipid secondary messenger phosphatidylinositol-(3,4,5)-triphosphate (PtdIns(3,4,5)P_3), a product of PI3-kinase. It is tempting to speculate that PTEN regulates neuronal cell death and is involved in the pathogenesis of neurodegeneration. The initial aim of this study was therefore to demonstrate that translocation of PTEN occurred during proteasome inhibition-induced neuronal cell death. Using mouse primary cortical neurons as a cell death model, it was tedious but not difficult to prove that PTEN was recruited into the detergent-insoluble fraction or lipid raft of the plasma membrane during neuronal cell death. The tough part however, would have been to demonstrate that this translocation could actually result in the dephosphorylation of the PtdIns(3,4,5)P_3 on the neural membrane. Furthermore, recent studies have shown that PTEN has a complex role in the central nervous system, and is involved in the differentiation and maturation of neurons. This led to a decision to switch the research interest to focus on the study of the mechanisms of proteasome inhibition-induced neuronal apoptosis using microarray GeneChip® technology.

Gene expression studies lie at the heart of a wide variety of medical and biological research projects, including classifying diseases, understanding basic biological processes, and identifying new drug targets. Until recently, comparing expression

levels across different tissues or cells was limited to tracking one or a few genes at a time. Using GeneChip® arrays, it is possible to simultaneously monitor the activities of thousands of genes. Global views of gene expression are often essential for obtaining comprehensive pictures of complex biological processes. For example, microarray technology has been applied to study neuroprotective gene expression in ischemic preconditioned in vitro and in vivo models (Stenzel-Poore et al, 2003). In this study, Affymetrix GeneChip® was used to study the global gene expression of cultured cortical neurons exposed to lactacystin.

The breakdown of the neuronal membrane is a characteristic feature of neuronal degeneration (Klein, 2000). Changes in plasma membrane phospholipid compositions might increase the susceptibility of neurons to pro-apoptotic signals (Farooqui et al, 2004). Furthermore, neural plasma membrane is also a rich source of lipid messengers, which are known to regulate cell death and survival. Differential lipid profiling (analogous to differential protein expression profiling) between healthy and dying cells will provide insight into the changes of lipid compositions in apoptotic cells. Information on alterations in lipid metabolites in dying cells may facilitate subsequent studies to examine the kinetics of lipid metabolism and the interactions of lipids with cellular proteins, and provide new insight into the function of cellular networks. Lipid profiling can thus be integrated with genomics and proteomics to provide a multidimensional perspective of the biological system. In this study, lipid profiling was carried out to complement the results obtained from the microarray analysis.

(-)-Epigallocatechin-3-gallate (EGCG) is the major flavonoid (or polyphenol) in green tea (*Camelliea sinensis*) leaf extract. Most of the experimental and epidemiological studies with green tea extract have been targeted at its possible cardiovascular, anticarcinogenic and anti-inflammatory activities, which are thought to rely on the antioxidant and iron-chelating actions of its polyphenol constituents, and on modulation of endogenous metabolizing and antioxidant enzymes (Mandel and Youdim, 2004). However, it has been found that EGCG can selectively inhibit the chymotrypsin-like activity of proteasomes by binding to the active site of the β5-subunit of 20S proteasome (Wan et al, 2004). Furthermore, Nam et al shows that EGCG can potently inhibit proteasome activity in vitro and in vivo (Nam et al, 2001). Recent studies suggest that the neuroprotective effect of EGCG is due to its ability to inhibit proteasomes (Mandel and Youdim, 2004; Shay and Banz, 2005). EGCG was therefore chosen as a comparative proteasome inhibitor to lactacystin in the microarray study.

This thesis therefore contains the following topics of interest:

1) PTEN accumulation in the detergent-insoluble fraction during lactacystin-induced neuronal apoptosis

2) Microarray GeneChip® study of gene expression during lactacystin-induced neuronal apoptosis

3) Lipid profile of neural membrane during lactacystin-induced neuronal apoptosis

4) Microarray GeneChip® study of gene expression of cultured cortical neurons during exposure to (-)-epigallocatechin-3-gallate

CHAPTER 2

2 MATERIALS AND METHODS

2.1 Primary cortical neurons

Cultures of mouse neocortical neurons (gestational days 15–16) were prepared from cortices microdissected from the brains of fetuses and subjected to trypsin digestion and mechanical trituration (Cheung et al, 1998). The dissociated cells were harvested by centrifugation and resuspended in Neurobasal™ (NB) medium with 2.5% B-27 supplement, 0.25% GlutaMAX™-I supplement (all of the above are from GIBCO™), 10% fetal calf serum and 1% penicillin and streptomycin. Cells were seeded to a density of 2×10^5 cells per cm^2 culture area previously coated with 100 μg/ml poly-D-lysine. The cultures were maintained in a humidified 5% CO_2 incubator at 37°C. After 24 h in vitro, the culture medium was replaced with serum-free NB medium with 2.5% B-27 supplement, 0.25% GlutaMAX™-I supplement and 1% penicillin and streptomycin and cultured for 5 days in vitro before treatment. Immunocytochemical staining of the cultures for microtubule-associated protein 2 (MAP-2) and glia fibrillary acidic protein (GFAP) indicated >95% of the cells were neurons with minimal contamination by glia (Fig. 2.1).

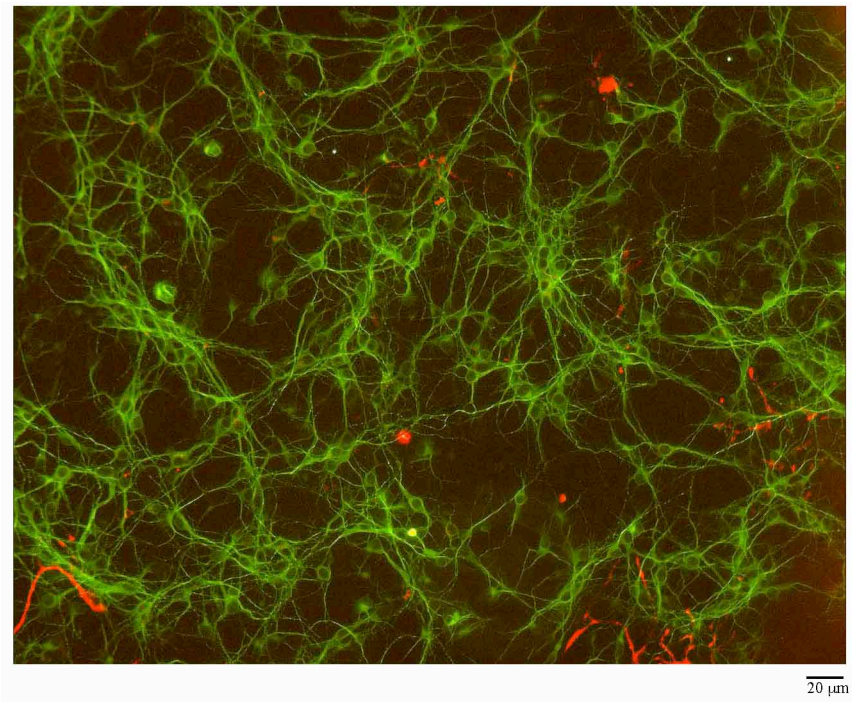

Figure 2.1. Immunocytochemical staining of the mouse cortical neurons for microtubule-associated protein-2 (Map-2) and glia fibrillary acidic protein (GFAP). Green color (Map-2) indicates cortical neurons while red color (GFAP) indicates glial cells

2.2 Drug treatment

2.2.1 Lactacystin stock solution preparation

The synthetic lactacystin (cat# 426100, CALBIOCHEM®, Lajolla, CA, USA) was dissolved and maintained as a 10 mM stock solution [200 μg in 53 μl Dimethyl sulfoxide (DMSO)]. The 10 mM stock solution was stored at -20° for not more than 6 months. The stock solution was further diluted to 2 mM in DMSO and added into NB medium to obtain the final concentrations of drug in the range of 0.1 to 5 μM for cell culture treatment. The same volume of DMSO was used in the control treatment as the drug vehicle.

2.2.2 (-)-Epigallocatechin-3-gallate from green tea

EGCG from green tea (≥95%, cat# E-4143, Sigma-Aldrich, USA) was dissolved in water to make a 10 mM stock solution. The stock solution was further diluted to concentrations (0.1–10 μM) in NB before treatment. Fresh stock solution was prepared from the powder for each set of experiments.

2.2.3 Caspase and calpain inhibitors

The irreversible, cell-permeable, broad-spectrum caspase inhibitor z-VAD-FMK (cat# P-416, BIOMOL®, PA, USA), caspase-3 inhibitor IV (cat# 235421, CALBIOCHEM®, Lajolla, CA, USA) and calpain inhibitor calpeptin (cat#03-34-0051, CALBIOCHEM®, Lajolla, CA, USA) were prepared as 50 mM stock solutions in DMSO. All stock solutions were kept at -20°C for not more than two months. For

treatment with cultured neurons, the stock solutions were diluted to 50–100 μM concentrations using NB medium before treatment.

2.3 Immunocytochemistry

Fixed cells were quenched in 1% H_2O_2 and non-specific binding was subsequently blocked with 10% normal goat serum and 0.1% Triton X-100 in Tris buffered saline (TBS) for 1 h at 4°C. Cells were incubated with polyclonal antibody to PTEN (1:2000) overnight at 4°C and then secondary antibody for 3 h in solution with 2% normal goat serum and 0.1% Triton X-100 in TBS. Detection of immunoreactive cells was carried out using 3,4-diaminobenzidine (DAB) substrate solution (0.5 mg/ml DAB and 0.01% H_2O_2 in TBS). Immunoreactive cells were visualized under bright-field microscopy.

2.4 Immunofluorescence and confocal microscopy

Cells were fixed with 4% paraformaldehyde in phosphate-buffered saline (PBS). Fixed cells were treated with 100 mM NH_4Cl and with 0.2% Triton X-100 and then blocked with 10% goat serum in PBS, immuno-labeled with primary antibodies and with Alexa Fluor® 488 goat anti-rabbit IgG or Alexa Fluor® 594 goat anti-mouse IgG (Molecular Probes). Images were obtained using laser scanning confocal microscope (Carl Zeiss LSM510).

2.5 Transmission electron microscopy

Cells were fixed in 3% glutaraldehyde and 2% paraformaldehyde. After osmication in 2% osmium tetroxide, samples were dehydrated in an ascending series of ethanol

and embedded in araldite. Ultra-thin sections (70 nm) were cut and mounted on formvar-coated copper grids. Grids were stained with uranyl acetate and lead citrate before viewing in a Philips BioTwin CM 120 transmission electron microscope.

2.6 Preparation of plasma membrane sheet and gold labeling for transmission electron microscopy

Plasma membrane rip-off and gold labeling was done according to Wilson et al (Wilson et al, 2004). In brief, coverslips with cultured cortical neurons on it were rapidly chilled by immersion in ice-cold HEPES buffer (25 mM HEPES, pH 7, 25 mM KCl, 2.5 mM Mg acetate) and inverted onto nickel electron microscopy grids that had been coated with Formvar and carbon and, on the day of the experiment, glow discharged and floated on poly-L-lysine (0.8 mg/ml for 30 min, followed by 10 s distilled water rinse and air drying. Pressure was applied to the coverslip for 20 s by bearing down with a cork. The coverslips were lifted, leaving sections of the upper cell surface adherent to the poly-L-lysine-coated grid. Membranes were then fixed in 2% paraformaldehyde for 10 min at 4°C immediately after cell membrane sheet preparation. PTEN were labeled from the inside by incubating sequentially with primary antibodies and gold-conjugated secondary reagents, by inverting the grids onto the droplets. Samples were then post-fixed in 2% glutaraldehyde in phosphate-buffered saline. The samples were then incubated with antibodies specific for PTEN (10 nm gold) and Flottilin-1 (15 nm gold) at the dilution of (1:100). Next, samples were stained for 10 min with 1% OsO_4 prepared in 0.1 M cacodylate buffer, then washed for 5 min with cacodylate buffer and then twice for 5 min in H_2O. Samples were then processed for 10 min in 1% aqueous tannic acid, followed by two 5-min

rinses with H_2O, 10 min with 1% aqueous uranyl acetate, and two 1-min rinses with H_2O. Grids were air-dried and examined using a TEM.

2.7 MTT cell viability assay

3-(4,5-dimethylthiazole-2-yl)-2,5-diphenyltetrazolium bromide (MTT) was dissolved in RPMI medium 1640 (GIBCO™) at a stock concentration of 5 mg/ml. MTT solution (30 μl) was added to each well of the 24-well plate containing cells in 300 μl culture medium and the plate was incubated at 37°C for 30 min. The culture medium was then removed by aspiration. An aliquot of 200 μl DMSO was added to dissolve the formazan formed in each well and the absorbance of the solution at the wavelength of 570 nm was read using a TECAN plate reader. MTT assay measures the loss of mitochondrial Krebs cycle activity.

2.8 Western blotting

For whole cell lysate preparation, neurons were lysed in 5× sample buffer (0.5 M Tris (pH 6.8), 10% SDS, 20% glycerol, 0.05% bromophenol blue, 20% β-mercaptoethanol). When RIPA buffer (10 mM Tris HCl (pH 7.4), 1 mM EDTA, 150 mM NaCl, 1% Nonidet P-40, 0.5% Deoxycholate, 0.1% SDS) was used for extraction, cells were lysed in RIPA buffer and the insoluble materials were pelleted by centrifugation at 14,000 rpm for 10 min. Pellets were re-dissolved in 5× sample buffer. Equal volumes of the whole cell lysate and the pellet obtained from extraction using RIPA buffer were loaded onto SDS-PAGE gels. An aliquot of the supernatant containing an equal amount of proteins was used for Western blot analysis. After

SDS-PAGE, proteins were electro-transferred to PVDF membranes and probed with antibodies.

2.9 Antibodies

A PTEN polyclonal antibody was raised by immunizing rabbits with 5 synthetic peptides from different regions of PTEN. The peptides were K^{352}ANRYFSDNFKVKLYF^{367}, T^{2}AIIKEIVSRNKRRYQED^{19}, T^{232}RREDKFMYFEF^{243}, E^{388}NEPFDEDQHTQITKV^{403} and K^{260}QNKMLKKDKMF^{271}. Two other PTEN antibodies, one of which recognizes the N-terminal of PTEN [anti-PTEN (N-19), sc-6818] from Santa Cruz Inc. (CA, USA) and the other of which recognizes the C-terminal of PTEN [anti-PTEN (26H9), cat#9556] from Cell Signaling Technology (Beverly, MA, USA) were obtained commercially. Anti-β-tubulin (ATN01) was purchased from Cytoskeleton Inc. (Denver, CO, USA). Anti-β-actin (clone AC-74, cat#A-5316) and anti-MAP-2 (clone AP-20, cat# M 1406) were obtained from Sigma, USA. Anti-active caspase-3 (cat# 557035) was obtained from BD Biosciences PharMingen (San Diego, CA, USA). Anti-PARP (AB-2) (Clone C-2-10, cat# AM30) was obtained from Oncogene Research Products (San Diego, CA, USA). Anti-p35 (cat# sc-820) was obtained from Santa Cruz Inc. CA, USA.

2.10 Caspase activities measurement

Caspase activities were measured using 9 types of fluorogenic substrates from BioVision, California, USA according to the manufacturer protocol. The substrates used were Ac-YVAD-AFC (caspase-1), Ac-VDVAD-AFC (caspase-2), Ac-DEVD-

AFC (caspase-3), Ac-LEVD-AFC (caspase-4), Ac-WEHD-AFC (caspase-5), Ac-VEID-AFC (caspase-6), Ac-IETD-AFC (caspase-8), Ac-LEHD-AFC (caspase-9) and Ac-AEVD-AFC (caspase-10). In brief, 2.25×10^6 cells were lysed in 150 µl chilled cell lysis buffer (Cat# 1201-1). The protein concentrations were determined using BCA protein assay kit (Pierce, USA). In a black 96-well plate, 10 µg of total proteins were added into each well, containing 50 µl of 2× reaction buffer (Cat# 1068-20) with 10 mM DTT (freshly added). 25 µM of AFC conjugated substrates were added into each well last, and incubated at 37ºC for one hour. The samples were read in the TECAN ULTRA 384 plate reader (Tecan, Austria) using 400 nm excitation filter and 505 nm emission filters. The fold-increase in caspase activity was determined by comparing the fluorescence of the treated sample with that of the non-induced control.

2.11 Proteasome activity measurement using fluorogenic substrates

The fluorogenic peptide substrates: substrate II (Z-Leu-Leu-Glu-AMC), substrate III (Suc-Leu-Leu-Val-Tyr-AMC) and substrate VI (Z-Ala-Arg-Arg-AMC) were used respectively to assay for the postglutamate, chymotrypsin-like and trypsin-like peptidase activities of the neuronal cell proteasomes. Cells were lysed in ice-cold homogenization buffer (10 mM Tris, pH 7.5, 5 mM EDTA, 1 mM DTT, 5 mM ATP, 20% glycerol, 0.04% Nonidet P-40). The protein concentration was determined, and an equal amount of protein (5 µg) was incubated with 50 µM of substrate II, substrate III, or substrate VI in assay buffer (50 mM Tris and 0.5 mM DTT) prior to protease activity measurement using a TECAN plate reader with excitation wavelength of 360 nm and emission wavelength of 465 nm. All fluorogenic substrates were purchased from Calbiochem®, San Diego, CA, USA.

2.12 Plasma membrane isolation using Percoll gradient

All steps were carried out at 4°C. Each well was washed once with 3 ml of buffer A (0.32 M sucrose, 1 mM EDTA, 20 mM Tris, pH 7.8) containing a protease inhibitor cocktail (Complete mini™, Roche, Switzerland) and phosphatase inhibitors (25 mM sodium fluoride, 2 mM sodium orthovanadate and 10 mM sodium pyrophosphate), and the cells were scraped off and collected in 3 ml of buffer A. The cells were pelleted by centrifugation for 5 min at 1,000 g. Cells were resuspended in 0.5 ml buffer A, placed in a Dounce homogenizer and homogenized using a tight-fitted plunger for 20 strokes. The suspension was transferred to a 1.5-ml Eppendorf tube and centrifuged at 1,000 g for 10 min. The post nuclear supernatant (PNS) were stored on ice and the pellet from each tube was resuspended in 0.5 ml buffer A, homogenized and centrifuged again. The PNS were combined and layered on top of 30% Percoll in buffer A and centrifuged at 84,000 g for 30 min in a Beckman SW 41 Ti rotor. This method was modified from Smart et al, 1995. Plasma membrane fractions were determined using anti-flotillin-1 (BD Transduction Laboratories, 610820) and anti-caveolin-1 (Santa Cruz, sc-894). Cytosolic fractions were determined by measuring lactate dehydrogenase (LDH) using the CytoTox 96®Non-Radioactive Cytotoxicity Assay (Promega). Protein concentrations of fractions were determined using BCA protein assay kit (Pierce, USA).

2.13 Microarray GeneChip®

2.13.1 Experimental design for lactacystin treatment

A total of 15 murine genome U74Av2 GeneChips® (Affymetrix, Santa Clara, CA, USA) were used in this experiment. U74Av2 was selected for the experiment

because it contains all the known genes of mouse and some ESTs. The following treatments were used: 24 h control (n=4), 4.5 h 1 μM lactacystin treatment (n=2), 7.5 h 1 μM lactacystin treatment (n=3), 24 h 1 μM lactacystin treatment (n=3) and 48 h 1 μM lactacystin treatment (n=3).

2.13.2 Experimental design for (-)-epigallocatechin-3-gallate treatment

A total of 7 murine genome U74Av4 GeneChips® were used in this experiment. The following treatments were used: control 24 h (n=2), 1 μM 24 h EGCG treatment (n=2), 25 μM 24 h EGCG treatment (n=3).

2.13.3 Total RNA isolation

Total RNA was extracted from cultured cortical neurons using RNeasy mini Kit (Qiagen, Valencia, CA) according to manufacturer protocol. Total RNA from a 6-well plate was pooled by adding 350 μl of RLT buffer into each well and scrapping with a cell scraper. The cell lysate collected was passed through a 20-gauge needle 10 times, after which 350 μl of 70% ethanol was added to the homogenized lysate. The mixture was then applied into an RNeasy mini column and subjected to centrifugation. The flow-through was discarded. The column was washed with 700 μl RW1 and after that twice with 500 μl RPE buffer. The column was spun dry and the total RNA eluted using 30 μl RNase-free water. The quality and the yield of the total RNA extracted were determined by spectrophotometer (A260 and A280) and by running a 1% agarose formaldehyde denaturing gel to check the integrity of the 28S and 18S ribosomal RNA bands.

2.13.4 One-cycle cDNA synthesis

One Cycle Kit (Affymetrix, Santa Clara, CA, USA) was used to synthesize biotinylated cRNA according to manufacturer protocol. 10 μg of total RNA was used for the cDNA synthesis. For details of microarray GeneChip® protocol, reagents and suppliers, please refer to the technical manual (expression_print_manual.pdf) which can be obtained from the Affymetrix website (www.affymetrix.com). This section of the thesis documents the conditions under which the microarray experiments were conducted.

2.13.4.1 First-strand cDNA synthesis

The RNA sample, diluted poly-A RNA controls and T7-Oligo(dT) primer were mixed as in Table 2.1.

Table 2.1. Preparation of RNA/T7-Oligo(dT) Primer Mix

Component	Volume/μl
Sample RNA	10 μg (variable volume)
Diluted poly-A RNA controls	2
T7-Oligo(dT) primer, 50 μM	2
RNAse-free water	Variable
Total volume	11

The above mixture was subjected to incubations in a thermal cycler with the following program:

70°C	10 min
4°C	Hold for the addition of First-Strand Master Mix
42°C	2 min, then SuperScript II was added
42°C	1 h
4°C	Hold

The First-strand Master Mix is assembled as in Table 2.2:

Table 2.2. Preparation of First-Strand Master Mix

Component	Volume/μl
5× 1st Strand Reaction Mix	4
DTT, 0.1 M	2
DNTP, 10 mM	1
Total volume	7

SuperScript II (2 μl) was added after 2 min of incubation at 42°C. After incubation for 1 h at 42°C, the sample was cooled for at least 2 min at 4°C before the second-strand cDNA synthesis.

The following program was used to perform the second-strand cDNA synthesis in a thermal cycler:

16°C	2 h
4°C	Hold for the addition of T4 DNA Polymerase
16°C	5 min
4°C	Hold

A Second-Strand Master Mix was prepared according to Table 2.3.

Table 2.3. Preparation of Second-Strand Master Mix

Component	Volume/μl
RNase-free water	91
5×2nd Strand Reaction Mix	30
dNTP, 10 mM	3
E. coli DNA ligase	1
E. coli DNA polymerase I	4
RNase H	1
Total volume	130

The Second-Strand Master Mix (130 μl) was added to each first-strand synthesis sample for a total volume of 150 μl. The mixtures were incubated for 2 h at 16°C. T4 DNA polymerase (2 μl) was added to each sample and incubated for another 5

min at 16°C. After that, 10 μl of 0.5 M EDTA was added into each sample before the cleanup of double-strand cDNA.

2.13.4.2 Cleanup of double-stranded cDNA for one-cycle target labeling assay

cDNA Bidding Buffer (600 μl) was added to the double-stranded cDNA synthesis preparation. This mixture was applied into the cDNA Cleanup Spin Column, centrifuged and the flow-through was discarded. The spin column was then washed with 750 μl cDNA Wash Buffer, dried and the cDNA was eluted from the column with 14 μl cDNA Elution Buffer. The average volume of eluate was 12 μl from 14 μl Elution Buffer.

2.13.4.3 Synthesis of biotin-labeled cRNA for one-cycle target labeling assay

The template cDNA (6 μl) was transferred to RNAse-free microfuge tubes and the following reaction components were added in the order indicated in Table 2.4.

Table 2.4. In vitro transcription (IVT) reaction

Reagent	Volume/μl
Template cDNA	6
RNase-free water	14
10× IVT Labeling NTP Mix	4
IVT Labeling NTP Mix	12
IVT Labeling enzyme Mix	4
Total volume	40

The mixtures were incubated at 37°C for 16 h. To prevent condensation, incubation was carried out in a thermal cycler with a heated lid.

2.13.4.4 Cleanup and quantification of biotin-labeled cRNA

RNase-free H_2O (60 μl) was added into the IVT reaction and mixed for 3 s. After that 350 μl of IVT cRNA Binding Buffer was added, followed by 750 μl 96–100% ethanol. The samples were applied to the IVT Cleanup Spin Column sitting on a 2 ml collection tube. The column was centrifuged and the flow-through was discarded. The column was then washed with 500 μl IVT cRNA Wash Buffer, followed by 500 μl 80% (v/v) ethanol. The column was spun dry and the cRNA was eluted by 11 μl RNase-free water. A second elution using 10 μl was performed to maximize the yield. The cRNA was diluted 1:100 fold for quantification.

The yield of cRNA was determined by: 1 absorbance unit at 260 nm equals 40 μg/ml RNA. The purity of the cRNA was checked by calculating the A260/A280 ratio. Ratios between 1.9 and 2.0 were considered acceptable.

For quantification of cRNA using total RNA as starting material, an adjusted cRNA yield must be calculated to reflect carryover of unlabeled total RNA. The following formula was used to determine adjusted cRNA yield:

Adjusted cRNA yield = RNA_m-(total RNA_i) (y)

Where,

RNA_m = amount of cRNA measured after IVT (μg)

Total RNA_i = starting amount of total RNA (μg)

y = fraction of cDNA reaction used in IVT

2.13.4.5 Fragmenting the cRNA for target preparation

Fragmentation of cRNA target before hybridization onto GeneChip probe arrays has been shown to be critical in obtaining optimal assay sensitivity. The reaction mix was set up as in Table 2.5.

Table 2.5. Sample fragmentation reaction

Component	For 49 (standard)/64 array format
cRNA	20 μg
5× Fragmentation Buffer	8 μg
RNase-free water	Top up to 40 μl final volume

The reaction was incubated at 94°C for 35 min and cooled down on ice following incubation. The fragmented sample cRNA can be stored at -20°C (or -70°C for longer-term storage) until ready to perform the hybridization. An aliquot of the fragmented cRNA was run on 1% agarose gel to check the quality of the fragmentation. The standard fragmentation procedure should produce a distribution of RNA fragment sizes from approximately 35 to 200 bases.

2.13.4.6 Eukaryotic target hybridization

Table 2.6 shows the components in the hybridization cocktail for a single probe array.

Table 2.6. Hybridization cocktail for a single 49 format (standard)/64 format array

Component	Volume/μl
Fragmented cRNA	15 μg (variable volume)
Control oligonucleotide B2 (3 nM)	5
20X Eukaryotic Hybridization Control	15
Herring Sperm DNA (10 mg/ml)	3
Acetylated BSA (50 mg/ml)	3
2× hybridization buffer	150
DMSO	30
Water	Top up to final volume of 300 μl

The frozen stock of 20× GeneChip® Eukaryotic Hybridization Control cocktail was heated to 65°C for 5 min to completely resuspend the cRNA before aliquoting. It contains bioB, bioC, bioD and cre prokaryotic enzymes. *bioB, bioC* and *bioD* are

genes of the biotin synthesis pathway from the bacteria *E. coli*. *cre* is the recombinase gene from P1 bacteriophage. These genes can be labeled and serve as hybridization controls when mixed with labeled eukaryotic cRNA samples. The probe array was equilibrated to room temperature immediately before use. The array was wetted by filling it through the lower septa with 100 µl of 1×hybridization buffer while the array was held in a vertical position. The probe array was incubated at 45°C for 10 min in an incubator with rotation. The hybridization cocktail was heated to 99°C for 5 min in a heat block, cooled down to 45°C for 5 min and centrifuged for 5 min at maximum speed to spin down any insoluble material from the hybridization mixture. After incubation, the 1× hybridization buffer was aspirated out and the hybridization cocktail was added into the probe array. Test chips were used before the actually probe arrays (U74Av2) to ensure the quality of the targets and reagents. Tapes were stuck over the septa to prevent leakage. The probe array was placed into the hybridization oven at 45°C, rotated at 60 rpm and hybridized for 16 h.

2.13.4.7 Washing, staining and scanning of the probe array

After 16 h of hybridization, the hybridization cocktail was removed from the probe array and kept in a centrifuge tube. The probe array was filled with 200 µl of non-stringent wash buffer. For staining, Streptavidin phycoerythrin (SAPE) staining reagent was prepared before use as in Table 2.7. For each probe array to be stained, the following components were combined in a microfuge tube:

Table 2.7. SAPE solution mix

Component	Volume/µl
2× MES stain buffer	600
50 mg/ml acetylated BSA	48
1 mg/ml SAPE	12
Milli-Q water	540
Total volume	1,200

The SAPE solution was mixed well and divided into 2 aliquots of 600 µl each to be used for the first and third staining respectively. An antibody mixture was prepared with the following reagents as in Table 2.8.

Table 2.8. Antibody solution mix

Component	Volume/µl
2×MES stain buffer	300.0
50 mg/ml acetylated BSA	24.0
10 mg/ml normal goat IgG	6.0
0.5 mg/ml biotinylated antibody	3.6
Milli-Q water	266.4
Total volume	600.0

The staining and washing of probe arrays were performed in GeneChip® Fluidics Station 450. The fluidic protocol (Micro_1v1, Appendix B) was used for the test chip. For the U74Av2 probe array, the EukGE-WS2v5 Fluidics Scripts (Appendix B) were used. At the end of the wash protocol, the probe array was scanned using Affymetrix® GeneChip® Scanner 3000. The data obtained was saved. The probe id, signal, detection and detection p value from the absolute analysis results file were extracted and saved as .txt file for analysis using GeneSpring® (Silicon Genetics, Redwood City, CA, USA; www.silicongenetics.com).

2.13.5 Microarray data analysis

The microarray analysis was conducted with GeneSpring 7 Software (Silicon Genetics, Redwood City, CA). The raw data from the treatments were normalized to the median of the control values. GeneSpring 7 calculates the median expression for each gene in the control samples, then uses that value to normalize all the samples. The data is represented as fold change, relative to the median of all four control samples. All genes demonstrating smaller than 2-fold change were eliminated from further consideration. Furthermore, the genes that showed absence in all the treatments were removed from the differentially expressed gene list. To determine whether the difference in gene expression in response to the treatments was significant, a one-way ANOVA test was performed and genes with values of $p<0.05$ were considered to be significant. To further test the integrity of the gene list, Bonferroni Correction, a very stringent statistical analysis (Jung et al, 2005) was performed. The gene list with comprehensive functional annotations (molecular and/or biological) was exported to Microsoft Excel for further analysis. Genes were then clustered according to their biological function in Excel spreadsheet with reference to Gene Ontology Mining Tool from Affymetrix® NetAffx™ Analysis Center (www.affymetrix.com/analysis/). Follow-up experiments were done to address the biological relevance of the findings.

2.14 RNA gel electrophoresis

Denaturing agarose-formaldehyde gel electrophoresis was used for the size fractionation of RNA. A 1% (w/v) agarose-formaldehyde was prepared by melting 0.5 g of agarose in 43.5 ml of milli-Q water and cooled to 60%. 5 ml of 10× MOPS

and 1 ml of 37% formaldehyde were added and casting of the gel was carried out in the fume hood. The RNA samples were prepared as follows:

RNA (1 μg)	4.5 μl
10× MOPS buffer	2.0 μl
Formaldehyde (pH>4, 37%)	3.5 μl
Deionized formamide	10 μl
RNA loading buffer	3.5 μl

The sample was mixed and heated to 60°C for 10 min prior to loading and electrophoresis was carried out in 1× MOPS buffer. RNA bands were visualized under UV-light after electrophoresis. The image was recorded using Chemi Genius gel documentation system (Syngene, Cambridge, UK).

2.15 Quantitative real-time PCR

Total RNA was extracted using the High Pure RNA Isolation Kit (Roche Applied Science, Indianapolis, IN, USA) with on-column DNase treatment according to manufacturer's specifications. The RNA was then reverse transcribed using TaqMan® Reverse Transcription Reagents (Applied Biosystems, Foster City, CA). The final reverse transcription reaction includes 200 ng of RNA, 1×RT Buffer, 5.5 mM $MgCl_2$, 0.5 μM per dNTP mixture, 2.5 μM Random Hexamers, 4 U RNase Inhibitor and 12.5 U MultiScribe™ Reverse Transcriptase. Reaction conditions were 25°C for 10 min, 37°C for 60 min and 95°C for 5 min. The reaction was carried out using a thermocycler (PTC-100™ Peltier Thermal Cycler, MJ Research). A Multiplex real-time PCR amplification was then carried out in the TagMan® 7000 Sequence Detection System (Applied Biosystems) using TagMan® Universal PCR Master Mix (Applied Biosystems) and the specific primers and probes according to

the manufacturer's protocol. The probes were labeled with 6-carboxyfluorescein as the reported fluorescent dye at their 5' ends while the 3' ends were labeled with 6-carboxy-tetramethyl-rhodamine as the quencher. 18S ribosomal RNA was used as the internal control and its probe was labeled with reporter dye VIC at the 5' end instead. All primers and probes were synthesized by Applied Biosystems and details of sequences are available upon request.

The PCR conditions were: an initial incubation of 50°C for 2 min and 95°C for 10 min followed by 40 cycles of 94°C for 15 s and 60°C for 1 min. All reactions were carried out in triplicates. The threshold cycle, CT, which correlates inversely with the levels of target mRNA, was measured as the cycle number at which the reporter fluorescence emission exceeded a preset threshold level. The amplified transcripts were quantified using the comparative CT methods as described previously (Livak and Schmittgen, 2001), with the formula for relative fold change = $2^{-\Delta\Delta CT}$, where ΔΔCT = [ΔCT gene of interest (treated sample)-ΔCT 18S rRNA (treated sample)]-[ΔCT gene of interest (control sample)-ΔCT 18 rRNA (control sample)]. ΔCT represents the mean CT value of each sample. Data were obtained by carrying out at least three independent experiments.

2.16 Cellular ATP and GSH measurement

Cells were washed twice in ice-cold PBS. A volume of 250 µl of ice-cold tricholroacetic acid (TCA) 6.5% (w/v) was added and the plate was left on ice for 10 min. The TCA extract was removed and either stored at -80ºC or used immediately for analysis. NaOH (200 µl of 1 M solution) was then added to solubilize cellular protein. Protein concentration then was measured using BioRad protein assay.

Cellular ATP concentration was assessed by using firefly lantern extract (Sigma, FLE-50). Each sample (3 µl) was incubated with 200 µL of sodium arsenite buffer (comprising 26.67 mM $MsSO_4.7H_2O$/3.33 mM KH_2PO_4/33.33 mM $Na_2HASO_4.7H_2O$, pH 7.4). After the addition of 25 µL of firefly lantern extract per sample, light emission was measured for 3 s per sample by using TECAN ULTRA 384. The concentrations of ATP were determined by comparing the values obtained with a freshly prepared standard curve of ATP.

For cellular GSH measurement, 7.5 µl of TCA extract was added to a 96-well black plate followed by the addition of 227.5 µl of 100 mM KH_2PO_4-KOH buffer, pH 10 and 15 µl of o-phthaldialdehyde (10 mg/ml freshly prepared in methanol). Samples were stored in the dark at room temperature for 25 min and measured by fluorescence (excitation=350 nm; emission=420 nm) using TECAN ULTRA 384. Concentrations of GSH were then determined by comparing the values obtained with a freshly prepared standard curve of GSH. The GSH concentrations were normalized with the protein concentrations to get the final value.

2.17 Cholesterol measurement using gas chromatography mass spectrometry

Cells were washed twice with PBS. The internal standard, consisting of a cholesterol control containing heavy isotopes was added into each well before the extraction. Cholesterol was extracted by adding 200 µl methanol, followed by 200 µl of KOH (1 M). Cells from each well were scraped, collected into glass vials and hydrolyzed at RT for 2 h in the dark. Twenty-five µl of HCl (5 M) were added into each glass vial to neutralize the KOH. The samples were dried under a stream of N_2 for 15 min in a fume hood. One hundred microliters of 200 mM formic acid (pH 4.5) were added

into each vial followed by 1 ml of ethyl ether / Hexane (30:70) and mixed by vortexing. The aqueous phase was removed from the bottom of the glass vial and the solvent was dried under a stream of N_2. The samples were then subjected to derivatisation with acetonitrile (20ul) and BSTFA + 1% TMCS (20ul, Pierce, USA) for 1 h in the dark, and then injected into gas chromatography mass spectrometer (GC-MS).

Derivatised samples were analyzed by a Hewlett-Packard 5973 mass selective detector interfaced with a Hewlett- Packard 6890 gas chromatograph and equipped with an automatic sampler and a computer workstation. The injection port, MS source and GC-MS interface were kept at 280°C, 180°C and 290°C, respectively. Separations were carried out on a fused silica capillary column (12m x 0.2mm i.d.) coated with cross-linked 5% phenylmethylsiloxane (film thickness 0.33µm), (Agilent, J and W). Helium was the carrier gas with a flow rate of 0.8 ml/min (average velocity = 55cm/sec). Derivatised samples (1 µl) were injected with a 10:1 split into the GC injection port (280°C). Column temperature was increased from 240°C to 300°C at 25°C/min after 1 min at 240°C, then held at 300°C for 4 min. Selected-ion monitoring was performed using the EI mode at 70eV with the ion source maintained at 230°C and the quadrapole at 150°C. Selected-ion monitoring was performed to monitor one target ion and two qualifier ions selected from each compound mass spectrum to optimize sensitivity and specificity. Quantitation of cholesterol was achieved by relating the peak area of the cholesterol with its corresponding internal standard 5a-cholestane peak and comparison with a standard calibration curve.

2.18 Lipid profiling using Electro-Ionization Mass Spectrometry

2.18.1 Lipid extraction from cultured neurons

All buffers and reagents were kept chilled in an icebox. Control and treated cells were washed with 3 ml of PBS twice. Once all trace amounts of PBS was removed, 0.3 ml of 50% Methanol/HCl was added into each well of a 6-well culture plate. Cells were scraped immediately and transferred to a microfuge tube (cells from two wells were combined into one tube). Internal standards were spiked into the sample prior to lipid extraction. Tubes were vortexed and stored on ice until all the cells had been collected. Prechilled chloroform (0.6 ml) was added into each tube and the mixtures were subjected to vigorous vortexing for 30 s. This was repeated twice. Tubes were then centrifuged for 2 min at 9,000 rpm in a microcentrifuge. The organic layer (bottom layer) was transferred to clean microfuge tubes, pooling organic layers from two tubes into one. The organic layers were dried in a speed vac. The lipid film was later resuspended in 0.5 ml choloroform:methanol (1:1).

2.18.2 Electrospray-Ionization mass spectrometry

Electrospray-Ionisation Mass Spectrometry (ESI-MS) was performed using a Waters Micromass Q-Tof micro (Waters Corp., Milford, MA) mass spectrometer. Typically, 2 µl of sample were injected for mass spectrometry analysis. The capillary voltage and sample cone voltage were maintained at 3.0 kV and 50 V respectively. The source temperature was 80°C and the nano-flow gas pressure was 0.7 bar. The mass spectrum was acquired from m/z 400–1200 in the negative ion mode with an acquisition time of ten minutes [mrw], and the scan duration was 1 sec. The HPLC system, consisting of a Waters CapLC Autosampler and a Waters CapLC Pump, was

used to provide the mobile phase and to inject samples. Chloroform-methanol 1:1 (v/v) at a flow rate of 3 µl/min was used as the mobile phase. Individual molecular species were identified using tandem mass spectrometry and in general, the collision energy used ranged from 25–80 eV.

CHAPTER 3

3 PTEN accumulation in detergent-insoluble fraction during lactacystin-induced neuronal apoptosis

3.1 Introduction

3.1.1 PTEN and cell death

PTEN (phosphatase and tensin homolog deleted from chromosome 10) is a novel phospholipid and protein phosphatase. Its tumor suppressor function is attributed to its phospholipid phosphatase activity that specifically dephosphorylates the plasma membrane phospholipid secondary messenger phosphatidylinositol-(3,4,5)-triphosphate (PtdIns(3,4,5)P_3), a product of phosphoinositide-3 kinase (PI3-kinase) (Fig. 3.1). Mutation of the *PTEN* gene is associated with many cancer types such as gliomas and endometrial cancer (Leslie and Downes, 2002; Waite and Eng, 2002). Furthermore, mammalian cells transfected with the *PTEN* gene are more sensitive to the induction of apoptosis (Wang et al, 1999; Gary and Mattson, 2002), suggesting that its interplay with PI3-kinase is an important regulatory step in the cellular cascades related to apoptosis.

3.1.2 The role of PTEN in central nervous system

In the central nervous system (CNS), PTEN is a regulatory molecule with multiple functions at multiple subcellular sites (Review by Ross et al, 2001). PTEN plays a very important role in brain development. Recent in vivo studies have revealed a novel role for PTEN in the size control of neurons; dysregulation of cell growth

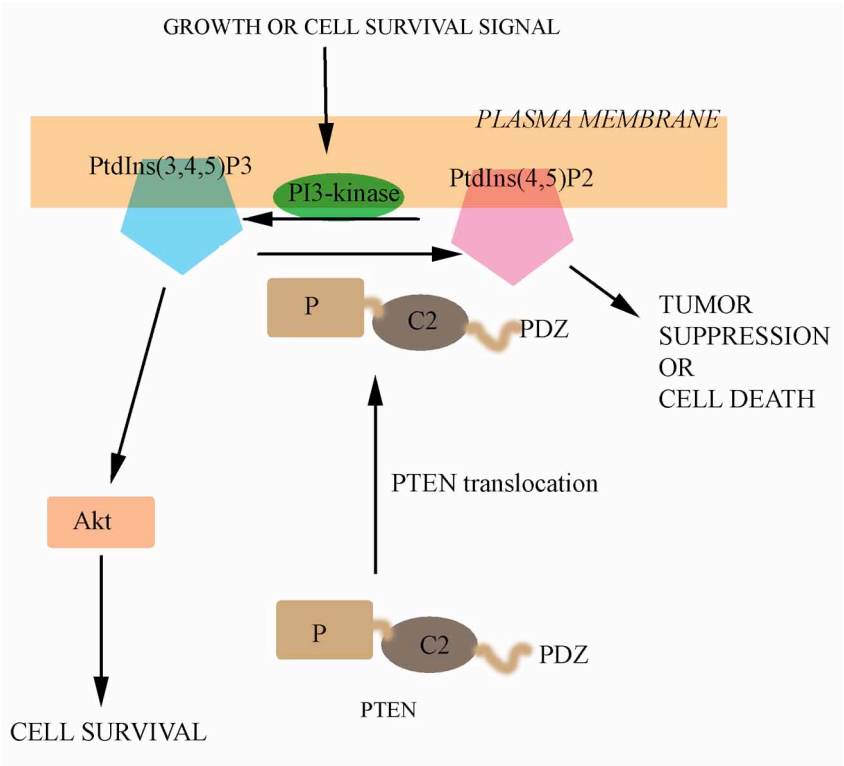

Figure 3.1. PTEN translocation and the PI3-kinase/Akt cell survival pathway. Figure shows the hypothetical model for pro-apoptotic PTEN translocation during neuronal cell death.

control by PTEN is associated with the neurological disorder Lhermitte-Duclos disease, a rare CNS manifestation of Cowden's disease caused by a hamartomatous overgrowth of the cerebellum (Backman et al, 2002). In addition, PTEN also regulates migration of precursor cells in the subventricular zone to the olfactory bulb (Li et al, 2003). Recently, Perandones et al reported an observation that PTEN might be involved in synaptogenesis during brain development (Perandones et al, 2004). Furthermore, the lost and altered distribution of PTEN in Alzheimer's diseased neurons suggests the important role of PTEN in the pathogenesis of neurodegenerative diseases (Griffin et al, 2005).

3.1.3 The structure of PTEN

The PTEN structure can be divided into a phosphatase domain in the N-terminal portion, a C2 domain and a C-terminal tail (Fig. 3.2). The phosphatase domain contains the active site responsible for catalyzing the dephosphorylation reaction. Mutations abolishing PTEN phosphatase activity are frequently found in cancer. Both phosphatase- and C2- domains contain phospholipid-binding motifs that are essential for targeting PTEN to the plasma membrane and activation of PTEN (Waite and Eng, 2002; Das et al, 2003). The 50-residue C-terminal tail contains the physiological phosphorylation sites Ser-380, Thr-382 and Thr-383 and the ITKV-motif at the C-terminus that mediates binding of PTEN to PDZ domain-containing cellular proteins (Georgescu et al, 1999; Leslie and Downes, 2002). In most mammalian cells, PTEN is mainly localized in the cytosol, with little or no association with the plasma membrane (Leslie et al, 2001). In the PC12 cell line, a significant portion of PTEN is also localized in the nucleus (Lachyanker et al, 2000; Ross et al, 2001; Lian and Di Cristofano, 2005). Since PtdIns(3,4,5)P_3 is located on

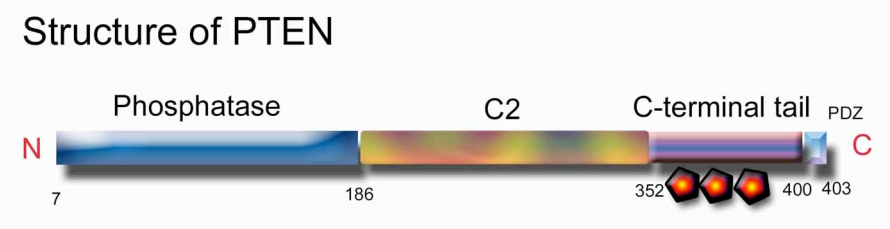

Figure 3.2. A cartoon drawing of the structure of PTEN. PTEN protein contains 3 main parts, the phosphatase at the N-terminal, the C2 domain and the C-terminal tail with the PDZ sequence. The C-terminal tail contains 3 main phosphorylation sites at Ser-380, Thr-382 and Thr-383.

the plasma membrane, PTEN needs to translocate from the cytosol and/or the nucleus to the plasma membrane before it can dephosphorylate the phospholipid substrate. However, the mechanism of recruitment of PTEN to the plasma membrane is still poorly understood. Data presented in a recent report by Das et al. suggests dephosphorylation of Ser-380, Thr-382 and Thr-383 in the C-terminal tail enhances PTEN targeting to the plasma membrane and nucleus (Das et al, 2003). In spite of this, physiological and pathological conditions that induce PTEN targeting to the plasma membrane have not been identified.

3.1.4 The possible role of PTEN in proteasome inhibition-induced neuronal apoptosis

Inhibition of the proteasome has been postulated to be responsible for the pathogenesis of neurodegenerative diseases such as Alzheimer's and Parkinson's diseases (Keller et al, 2000; Naujokat and Hoffmann, 2002; Halliwell, 2002; Song and Jung, 2004; Bossy-Wetzel et al, 2004). Inhibition of proteasome function by lactacystin treatment induces apoptosis of cultured cortical neurons and cerebellar granule cells via stimulation of mitochondrial cytochrome c release and activation of a caspase-3-like protease activity (Qiu et al, 2000; Pasquini et al, 2000). Herein, this study reports that neuronal apoptosis and activation of caspase-3 induced by lactacystin treatment is associated with conversion of PTEN to a truncated form that lacks parts of the C-terminal tail, and accumulation of both PTEN and its truncated fragment to the detergent-insoluble membrane fraction. This data suggests the association of PTEN with the plasma membrane in a pathological condition.

3.2 Results and discussions

3.2.1 Lactacystin-induced neuronal apoptosis

Lactacystin treatment suppresses proteasome activity and induces apoptosis of cultured cortical neurons. The morphological and biochemical changes of cultured cortical neurons induced by treatment with the proteasome inhibitor lactacystin were examined. As shown in Fig. 3.3, treatment of cultured neuronal cells with 1 μM lactacystin for 48 h induced apoptosis-associated phenotypic changes such as cell shrinkage, DNA condensation and chromatin fragmentation. The MTT assay confirmed that the viability of the treated cells decreased in a dose- and time-dependent manner (Fig. 3.4A). Decrease in cell viability was concomitant with the dose-dependent decrease in proteasome activities — the postglutamyl peptidase (caspase-like) activity, chymotrypsin-like peptidase activity and the trypsin-like peptidase activity of the proteasome in the treated cells (1 μM for 48 h) were decreased to 54.3 ± 1.2 %, 40.6 ± 2.4 % and 42.8 ± 2.7 %, respectively, of the level in untreated cells (Fig. 3.4B). To ascertain if the caspase-3 signaling pathway is involved in lactacystin-induced neuronal cell death, the level of the active caspase-3 generated from proteolysis of procaspase-3, and the caspase-3 activity level in cultured neurons treated with different doses of lactacystin were measured. As shown in Fig. 3.5, Western blotting of the whole cell lysate extracted from lactacystin-treated neurons reveals the presence of a cleaved form of caspase-3. The appearance of the cleaved form of caspase-3 is accompanied with a dose-dependent activation of caspase-3 activity in the lactacystin-treated neurons. Taken together, the results demonstrate that treatment with lactacystin at 1 μM for 48 h could efficiently inhibit proteasome activity, activate caspase-3 activity and induce apoptosis of cultured neuronal cells.

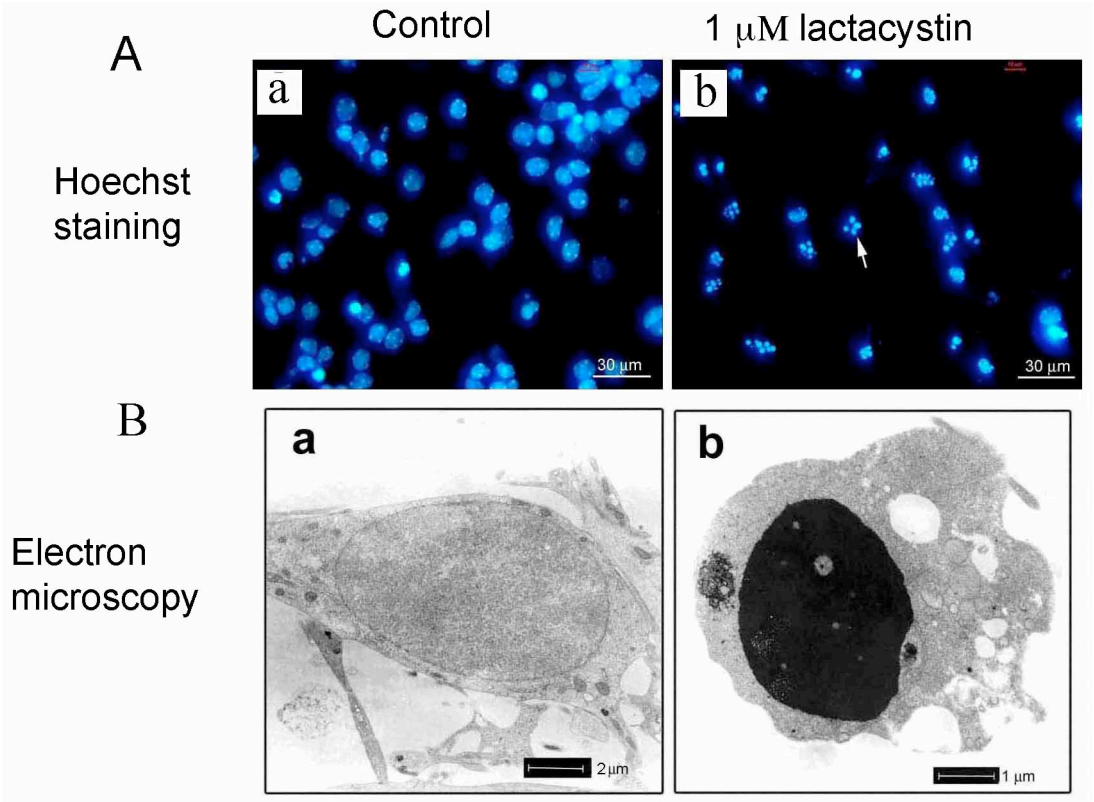

Figure 3.3. Morphological changes of cultured cortical neuronal cells induced by lactacystin treatment. (A) Staining of apoptotic nuclei using Hoechst 33258. Control and treated (1 μM lactacystin for 48 h) cells were stained and viewed under the fluorescence microscope (Carl Zeiss LSM510). White arrow indicates the apoptotic nuclei in treated cells. (B) Transmission electron micrographs of cultured cortical neurons. Control and lactacystin-treated (1 μM lactacystin for 48 h) cells showing the normal (a) and condensed nuclei (b).

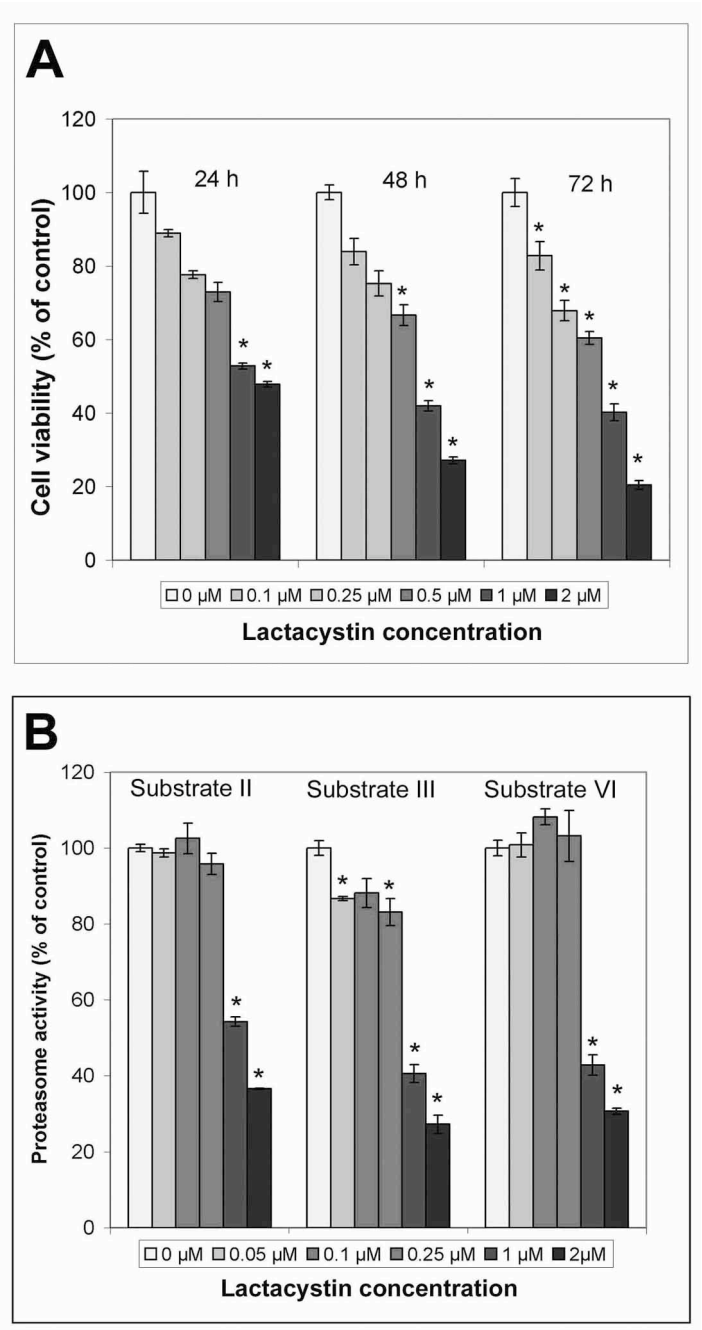

Figure 3.4. The effects of lactacystin treatment on viability and proteasome activity of cultured cortical neurons. (A) Cell viability of lactacystin-treated (1 µM lactacystin for 48 h) cultured cortical neurons was determined using the MTT assay (as described in materials and methods). Cell injury was found to be concentration- and time-dependent. Values are mean ± standard error of at least 3 independent samples and *$p<0.05$ (ANOVA with Tukey's test) compared with the corresponding control. (B) Proteasome activity measurement of cultured cortical neurons treated with lactacystin (0, 0.05, 0.1, 0.25, 1 and 2 µM for 48 h) using fluorogenic peptide substrate. Five micrograms of total protein were incubated with substrate II, substrate III or substrate VI for the measurements of postglutamyl, chymotrypsin-like or the trypsin-like peptidase activities respectively and the fluorescent products were detected using a TECAN plate reader. Values are mean ± standard error of at least 3 independent samples and *$p<0.05$ (ANOVA with Tukey's test) compared with the corresponding control.

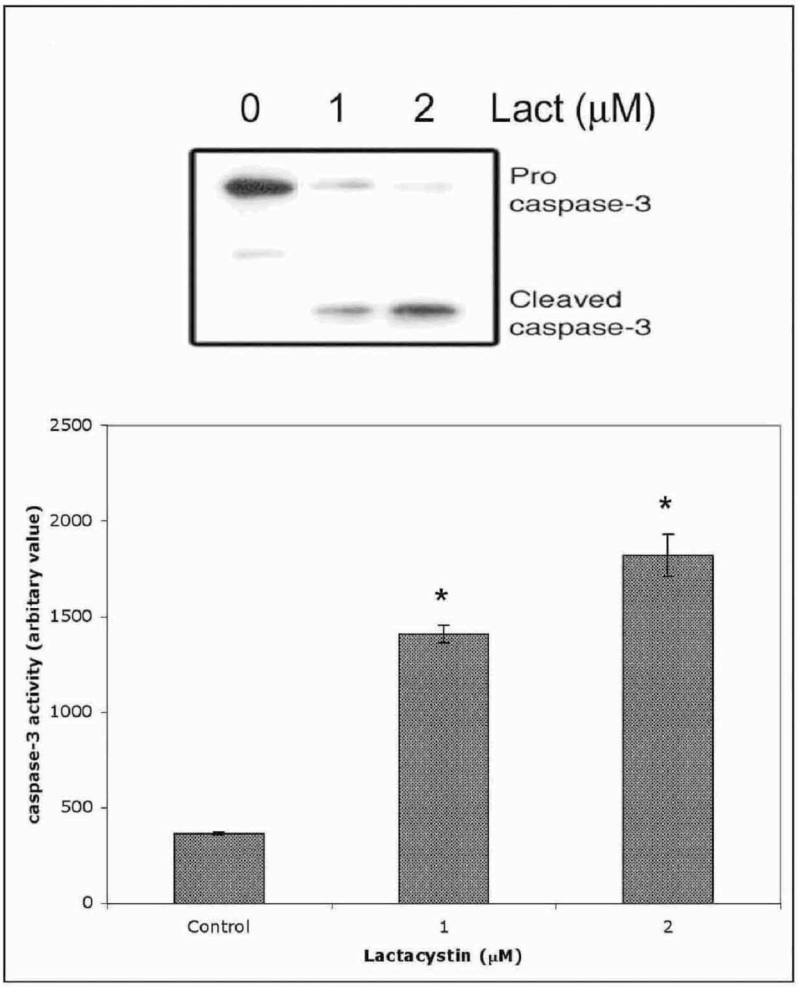

Figure 3.5. Detection of active caspase-3 in cultured cortical neurons treated with lactacystin. Western blot showing the presence of a cleaved form of caspase-3 and the increase in caspase-3 activity in lactacystin-treated (0, 1 and 2 μM for 48 h) cells. Statistically significant (*$p < 0.01$) over control cells determined by one-way ANOVA with Tukey's test.

3.2.2 Changes of PTEN level in cultured neuronal cells during development

PTEN has been implicated in enhancing the apoptosis of neurons induced by several pathological conditions (Gary and Mattson, 2002). Since the regulatory properties of PTEN are not fully understood, the exact role played by PTEN in enhancing neuronal apoptosis is not known. As a part of the ongoing study of the molecular mechanism of lactacystin-induced neuronal cell death, this study examined if lactacystin treatment induced biochemical changes of PTEN. As a background study, the time-dependent changes in PTEN expression levels in cultured primary cortical neurons were examined. Fig. 3.6 shows that PTEN expression could be detected from as early as day 2 in the in vitro culture, and the expression level increased in a time-dependent fashion until it reached the maximum level on day 6–9 in culture. This observation is reminiscent of the report by Luukko et al. of the high level of PTEN expression in embryonic mouse brain (Luukko et al, 1999). Since the PTEN expression level of cultured neurons was relatively high at day 5, reaching a maximum level at day 7 in culture, and neuronal cells required treatment with lactacystin for 48 h before they exhibited prominent apoptotic phenotypes (Fig. 3.3), neurons at day 5 to day 7 in culture were used for this investigation into the effect of lactacystin on PTEN expression level and subcellular localization.

3.2.3 Lactacystin treatment enhances the conversion of PTEN to a 50kDa truncated fragment and accumulation of both forms of PTEN in the detergent-insoluble membrane fraction

Western blot analysis of the whole cell lysate of neurons in treated and untreated cells revealed two forms of PTEN — a 55 kDa form

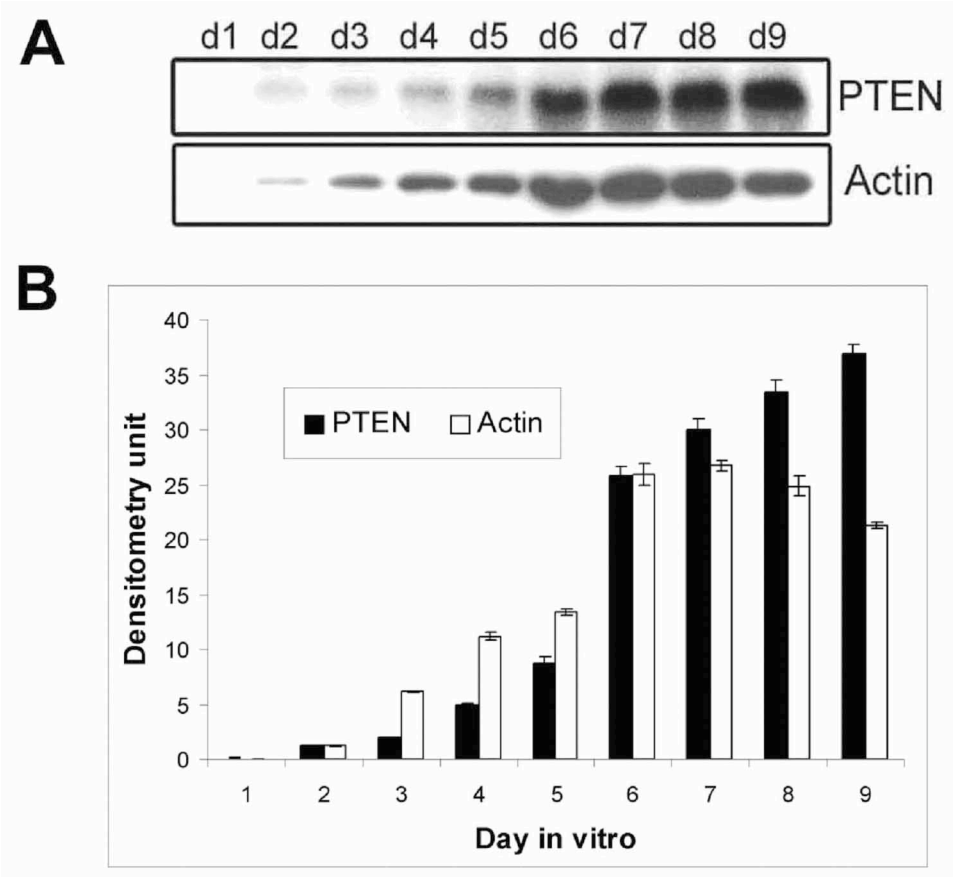

Figure 3.6. Western blot analysis of PTEN expression in cultured mouse primary cortical neurons. (A) PTEN expression in cultured mouse cortical neurons from day 1 to day 9 in vitro. Equal amount of proteins (5 μg) were loaded and run on a SDS-PAGE, transferred to PVDF membrane and immuno-labeled with anti-PTEN and anti-actin. Since the expression of actin increased from day 1 to 6 before reaching a plateau, it was used as an internal control for cultures from day 6 onwards only. (B) Graph represents the densitometric intensities of the bands in (A).

and a 50 kDa truncated form (Fig. 3.7). PTEN in untreated cells exists predominantly as the 55 kDa form. Treatment with increasing concentrations of lactacystin decreased the total expression level of PTEN (Fig. 3.7). Intriguingly, the treatment also caused the conversion of a significant amount of the 55 kDa species to the truncated 50 kDa species. After lysis of the neuronal cells with RIPA buffer, PTEN levels in the soluble and the insoluble fractions were determined by Western blotting. As shown in Fig. 3.8A, only the 55 kDa species appeared in the soluble fraction while both the 55 kDa and the 50 kDa species were present in the insoluble fraction (Fig. 3.8B). Since RIPA buffer contains detergents (NP40, deoxycholate and SDS), the soluble portion represents the cytosolic fraction and the detergent-soluble membrane fraction of the neuronal cells, while the insoluble portion represents the detergent-resistant plasma membrane. To establish the identity of the 50 kDa species, the blots were re-probed with two other PTEN antibodies, the PTEN-N-19 and PTEN 26H9, that target the N-terminal segment and the C-terminal segment, respectively. The PTEN 26H9 antibody failed to recognize the 50 kDa truncated PTEN (Fig. 3.8B), indicating that the latter lacks part of the C-terminal tail. Taken together, the data in Fig. 3.8 demonstrate that lactacystin treatment of neuronal cells induced proteolysis of PTEN to the truncated 50 kDa form of PTEN, which is preferentially targeted to the detergent-resistant fraction.

Recently, Torres et al. reported that PTEN is cleaved by caspase-3 at several target sites located in unstructured regions within the C-terminus of the molecule (Torres et al, 2003) (Fig. 3.9). In this study, caspase-3 was activated upon treatment with lactacystin (Fig. 3.5). This makes caspase-3 the most likely candidate that cleaved PTEN to its 50 kDa truncated form during lactacystin-induced apoptosis.

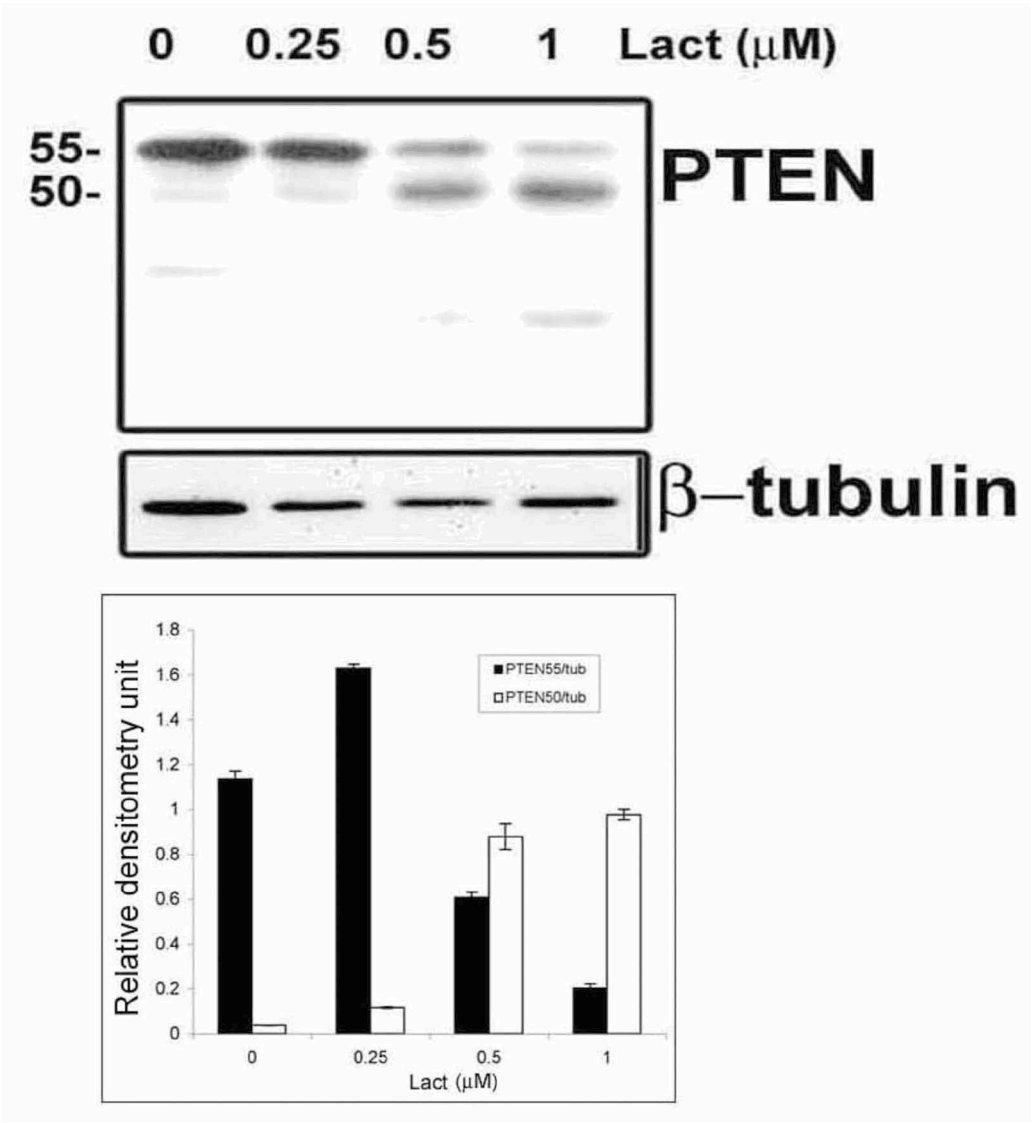

Figure 3.7. Western blots and graphic representation of the relative amounts of 55 kDa and 50 kDa PTEN species found in the whole cell lysate of cortical neurons treated with increasing concentrations of lactacystin. Mouse cortical neurons were treated with increasing concentrations of lactacystin (0, 0.25, 0.5 and 1 μM) for 48 h and proteins were harvested using 5× sample loading buffer. Proteins were resolved in a 10% gel SDS-PAGE and electro-transferred to PVDF membrane. The blot was later immuno-labeled with PTEN polyclonal antibody raised from 5 peptides chemically synthesized according to 5 regions of the PTEN protein. β-tubulin is the internal control for equal loading of protein. The graph represents the densitometric intensities of the 50 and 55 kDa PTEN species found in different concentrations of lactacystin treatments.

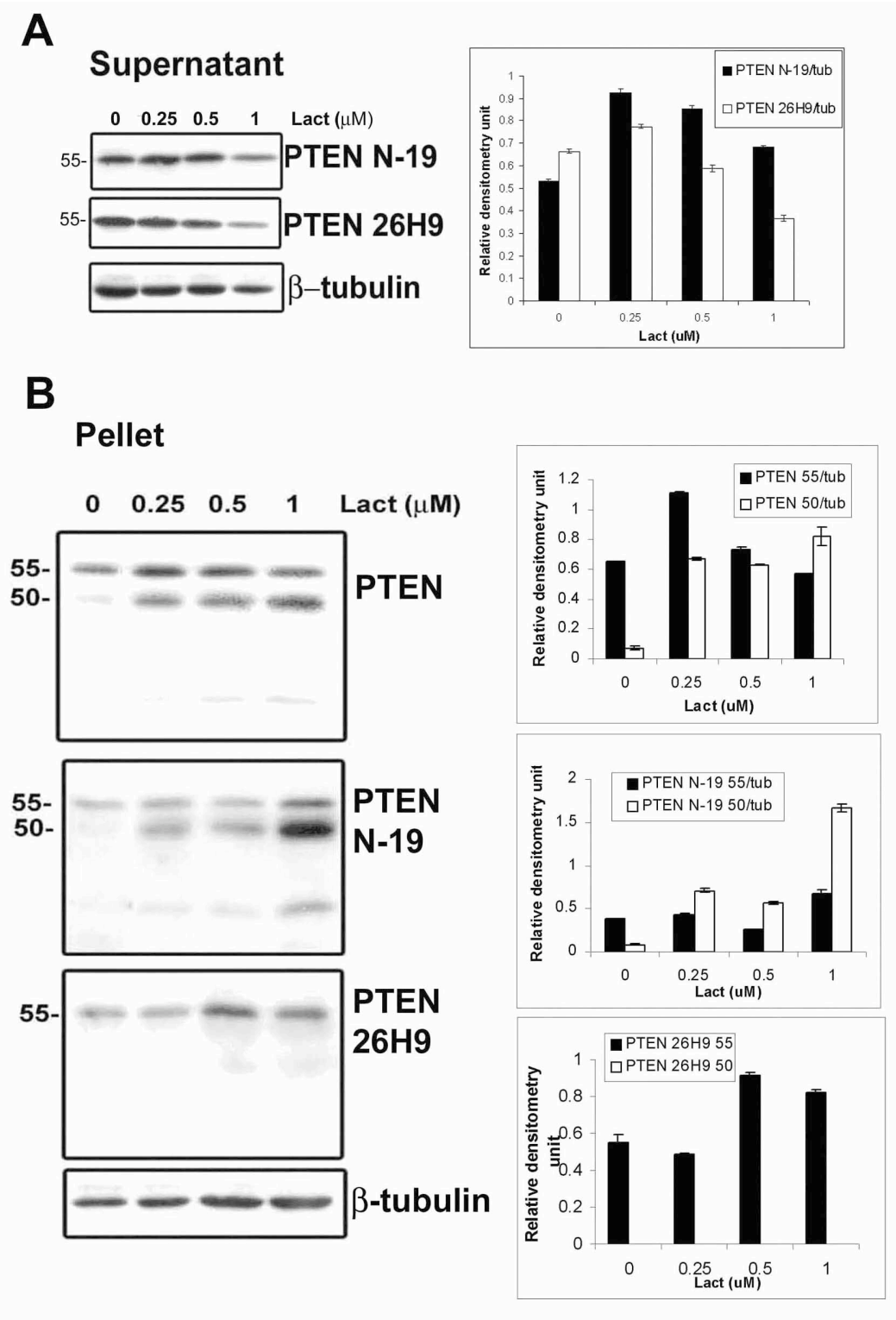

Figure 3.8. Distribution of the 55 kDa PTEN and the 50 kDa PTEN species in the soluble and insoluble fractions of cortical neurons treated with lactacystin. (A) The 55 kDa PTEN species in the detergent-soluble fraction of the lactacystin-treated cells. (B) The 55 kDa and 50 kDa species of PTEN in the detergent-insoluble fraction of the lactacystin-treated (1 μM for 48 h) cells. Relative amounts of the 55 kDa and 50 kDa species of PTEN were quantitated by densitometric scan of the immunoreactive bands in the Western blots and were expressed in densitometry units.

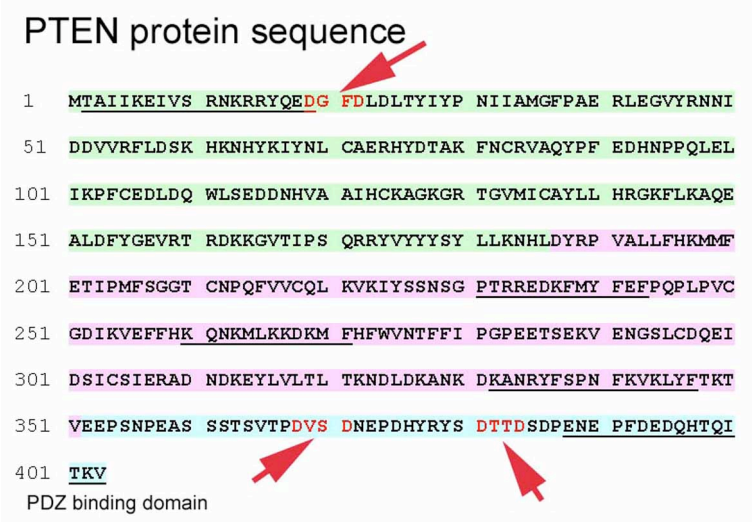

Figure 3.9. PTEN protein sequence and potential caspase-3 cut sites. Arrows indicates potential caspase-3 cleavage sites. The underlined protein sequences are the sequences of peptides generated for poly-clonal anti-PTEN antibody, as described in Materials and Methods sections.

3.2.4 Lactacystin treatment enhances accumulation of PTEN in the detergent-insoluble fraction that has been co-purified with plasma membrane protein markers

As PtdIns(3,4,5)P_3 is localized on the plasma membrane, it is likely that the detergent-insoluble fraction in which PTEN and its truncated form accumulate upon lactacystin treatment are part of the plasma membrane. To examine this notion, immunocytochemistry was performed to investigate how lactacystin treatment affected localization of PTEN in cultured cortical neurons. Fig. 3.10A shows that PTEN in the untreated neurons was localized predominantly in the cytosol and nucleus. The image, however, could not reveal if PTEN was associated with the plasma membrane. Since flotillin-1 is expressed exclusively in specific micro-domains of the plasma membrane such as the lipid-raft, its localization was therefore compared with that of PTEN. As shown in Fig. 3.10B, the localization of flotillin-1 had little, if any, overlap with that of PTEN in the untreated cells. In contrast, the significant overlap of the confocal images of PTEN and flotillin-1 in the lactacystin-treated neurons suggests that PTEN was co-localized with flotillin-1 in the lactacystin-treated cells.

To further investigate the subcellular distribution of PTEN in lactacystin-treated and untreated neuronal cells, the post-nuclear supernatants of cell lysates from both the treated and untreated cells were subjected to Percoll gradient centrifugation. Analysis of the centrifugation fractions with various protein markers revealed: (i) the plasma membrane lipid-raft markers caveolin-1 and flotillin-1 resided predominantly in fractions 4-6 (Fig. 3.11A), corresponding to the low-density membrane fraction; (ii)

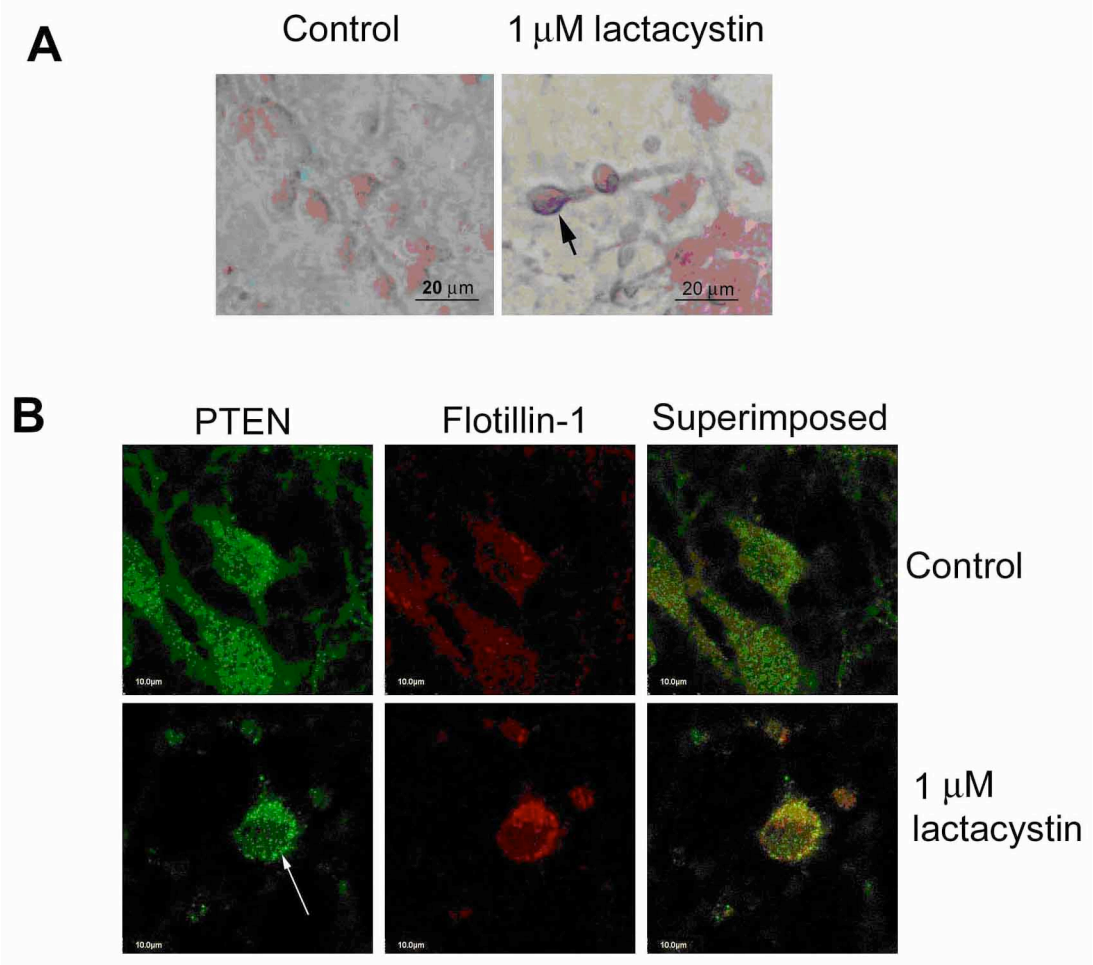

Figure 3.10. Effects of lactacystin treatment on PTEN subcellular localization in cultured neuronal cells. (A) Immunocytochemistry showing PTEN localized at the plasma membrane during neuronal apoptosis (arrow). (B) Immunofluorescence showing PTEN co-localized with flotillin-1 during neuronal apoptosis. Cortical neurons were treated with 1 μM lactacystin for 48 h for the induction of neuronal apoptosis.

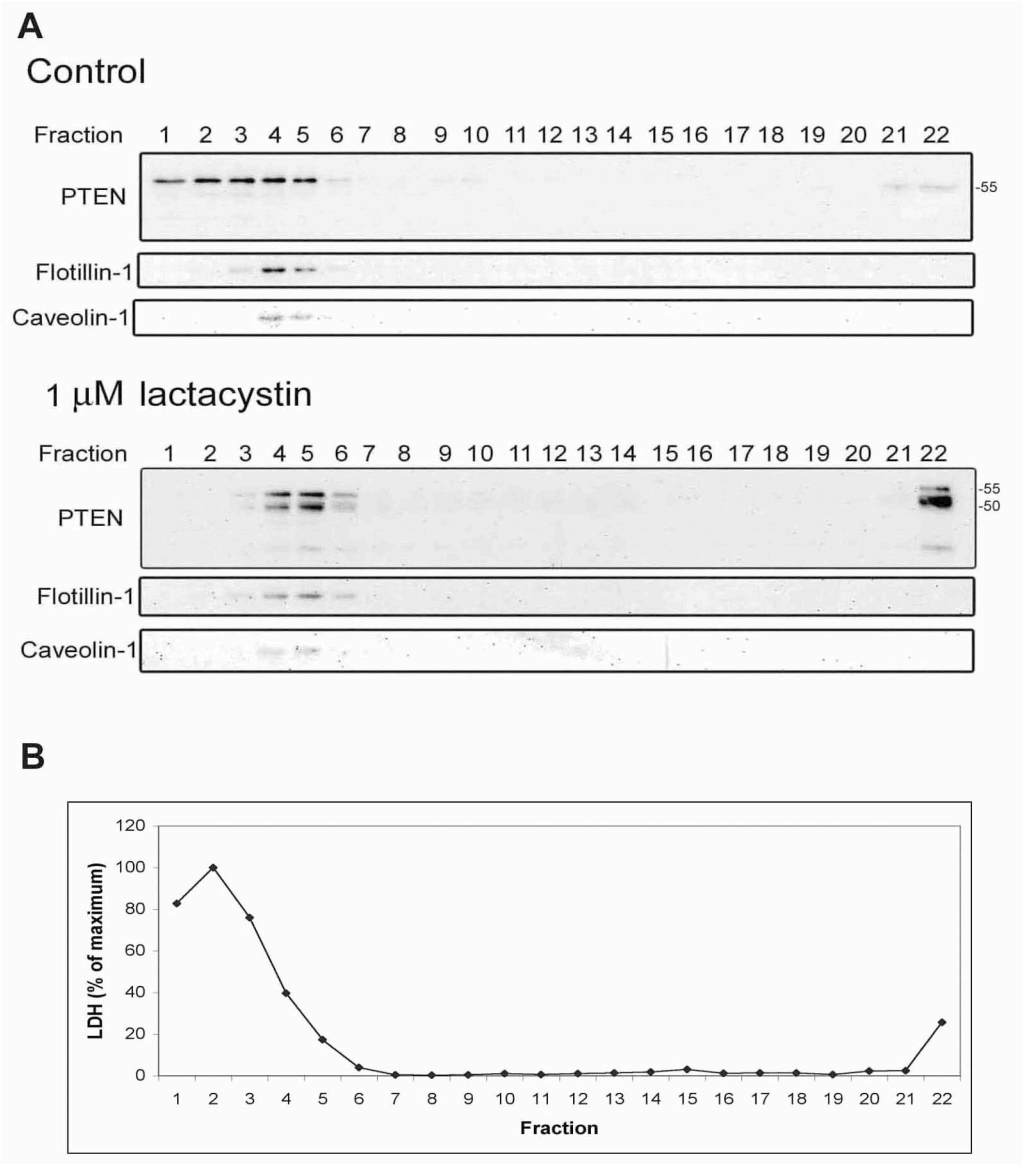

Figure 3.11. Lactacystin-induced changes in PTEN distribution in the various subcellular compartments of neuronal cells separated by Percoll gradient centrifugation. (A) The plasma membranes of cortical neurons treated and untreated with 1 μM lactacystin for 48 h were isolated with Percoll gradient centrifugation. Fractions (from top to bottom of the gradient) were collected and immunoblotted for PTEN, flotillin-1 and caveolin-1 (plasma membrane lipid-raft markers). (B) LDH enzyme activity measurement of fractions from cells treated with 1 μM lactacystin for 48 h. Graph shows the majority of LDH was in fraction 2, which corresponds to the cytosolic fraction.

besides residing in fractions 4-6, the plasma membrane-bound protein tyrosine kinase c-Src was also present in fractions 21-22, which correspond to the high-density membrane fraction; and (iii) the catalytic activity of the cytosolic protein marker lactate dehydrogenase (LDH) peaked at fraction 2 (Fig. 3.11B), suggesting that fractions 1-3 were derived from the cytosolic compartment of the neuronal cells. In the untreated cells, PTEN was present in the cytosol (fractions 1-3), the low-density membrane fraction (fractions 4-6) and the high-density membrane fraction (fractions 21-22). However, in the lactacystin-treated cells, PTEN and its truncated fragment were almost absent in the cytosol and accumulated in both the low-density and high-density membrane fractions. In summary, the data shown in Fig. 3.10 and 3.11 lend further support to the conclusion drawn from the biochemical data (Fig. 3.8) that lactacystin treatment induced accumulation of PTEN and its truncated fragment to the membrane fraction.

Co-localization of anti-PTEN and anti-flotillin-1 immunoreactivities in the lactacystin-treated cells (Fig. 3.10) and co-migration of PTEN and its truncated fragment with the plasma membrane markers in Percoll density gradient centrifugation (Fig. 3.11), suggest that the detergent-insoluble fraction at which both forms of PTEN accumulate (Fig. 3.8) are parts of the plasma membrane. However, unequivocal proof that both forms of PTEN are targeted to the plasma membrane such as the lipid-raft upon lactacystin treatment entails demonstration of a correlative decrease in plasma membrane PtdIns(3,4,5)P_3 level and/or binding of PTEN and its fragments to protein complexes that are found exclusively in the plasma membrane.

3.2.5 Implications of the appearance of the 50kDa truncated PTEN in neuronal cells induced by lactacystin treatment

Previously, Das et al. 2003 demonstrated that deletion of the segment corresponding to residues 354 to 403, or prevention of PTEN C-terminal tail phosphorylation by replacing Ser-380, Thr-382 and Thr-383 with alanine, targets the "phosphatase-dead" [C124A] PTEN mutant to the plasma membrane. Their results suggest that the C-terminal tail, upon phosphorylation, prevents PTEN from targeting to the plasma membrane. This notion is reminiscent of this study's finding that the C-terminally truncated 50 kDa PTEN species preferentially accumulated to the detergent-insoluble membrane fraction in the lactacystin-treated neuronal cells. It is possible that the truncated PTEN species is an activated form of PTEN, which upon dephosphorylation of PtdIns(3,4,5)P_3 in the plasma membrane, suppresses cell growth and promotes apoptosis by antagonizing the PI-3 kinase/PKB signaling pathway. A model of PTEN phosphorylation or truncation corresponding to its tumor suppressor activity or pro-apoptotic role is therefore proposed (Fig. 3.12). Since PTEN phosphorylation and dephosphorylation are reversible processes, the regulation of PTEN through phosphorylation might play a role in PTEN tumor suppressor activity. On the other hand, the deletion of the C-terminal tail during apoptosis is most likely to be associated with cell death since this process is not reversible. Cells undergoing apoptosis probably activate proteases such as caspase-3 to cleave PTEN, causing the latter to translocate to the plasma membrane to suppress the PI3-kinase/Akt survival pathway.

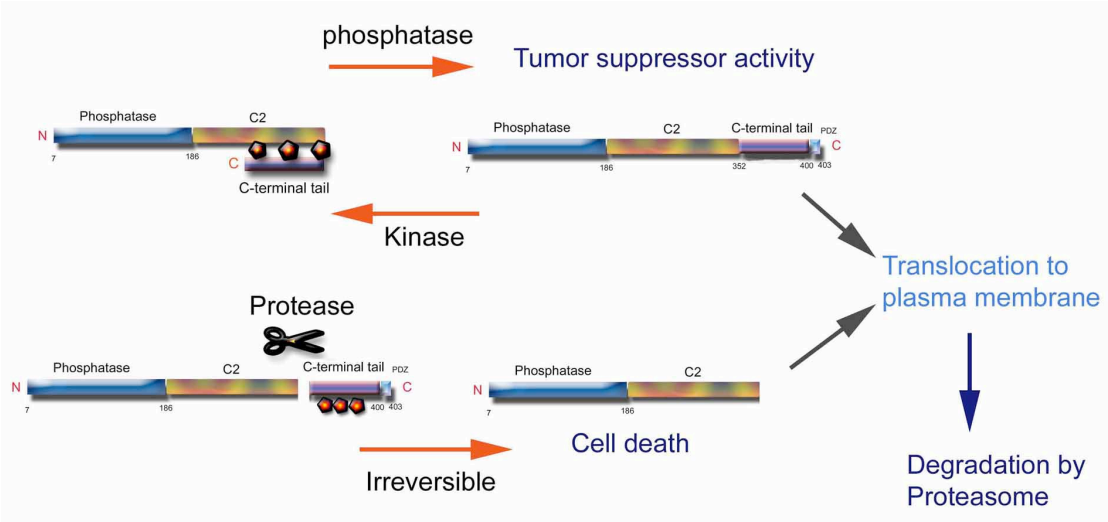

Figure 3.12. Hypothetical model of PTEN regulation associated with its tumor suppressor activity and cell death.

In spite of these findings, the exact mechanism of PTEN in mediating apoptotic effects during lactacystin treatment is still not known. Future investigation should focus on (i) identifying the proteases responsible for converting the full length PTEN to the truncated PTEN, (ii) defining the segments deleted from PTEN to generate the 50 kDa truncated form in neurons, (iii) ascertaining how the deletion facilitates targeting of PTEN to the plasma membrane and (iv) ascertaining if the truncated PTEN is enzymatically active.

3.3 Follow-up work

3.3.1 Identification of the protease responsible for converting the full length PTEN to the truncated PTEN

Western blot analysis of α-fodrin, a caspase-3 substrate, showed a clear 120 kDa band associated with caspase-3 cleavage 24 h after lactacystin treatment. Interestingly, a very faint doublet (145 and 150 kDa), which is associated with calpain cleavage, was observed too (Fig. 3.13A). Calpain is known to cleave p35, the neuronal-specific activator of cyclin-dependent kinase 5 (Cdk5) to produce the truncated form called p25. p25 has been reported to accumulate in the brains of patients with Alzheimer's disease (Patrick et al, 1999; Lee et al, 2000). Unlike p35, p25 is not readily degraded, and the binding of p25 to cdk5 constitutively activates cdk5 and hyper-phosphorylates tau to disrupt the cytoskeleton and promote neuronal death (Patrick et al, 1999; Lee et al, 2000). Incidentally, p35 was found to have been cleaved into its truncated form of p25 24 h after lactacystin treatment (Fig. 3.13A). The cleavage of p35 into p25 in lactacystin-treated neurons strongly supports the involvement of calpain in lactacystin-induced neuronal cell death. To further confirm this observation, caspase

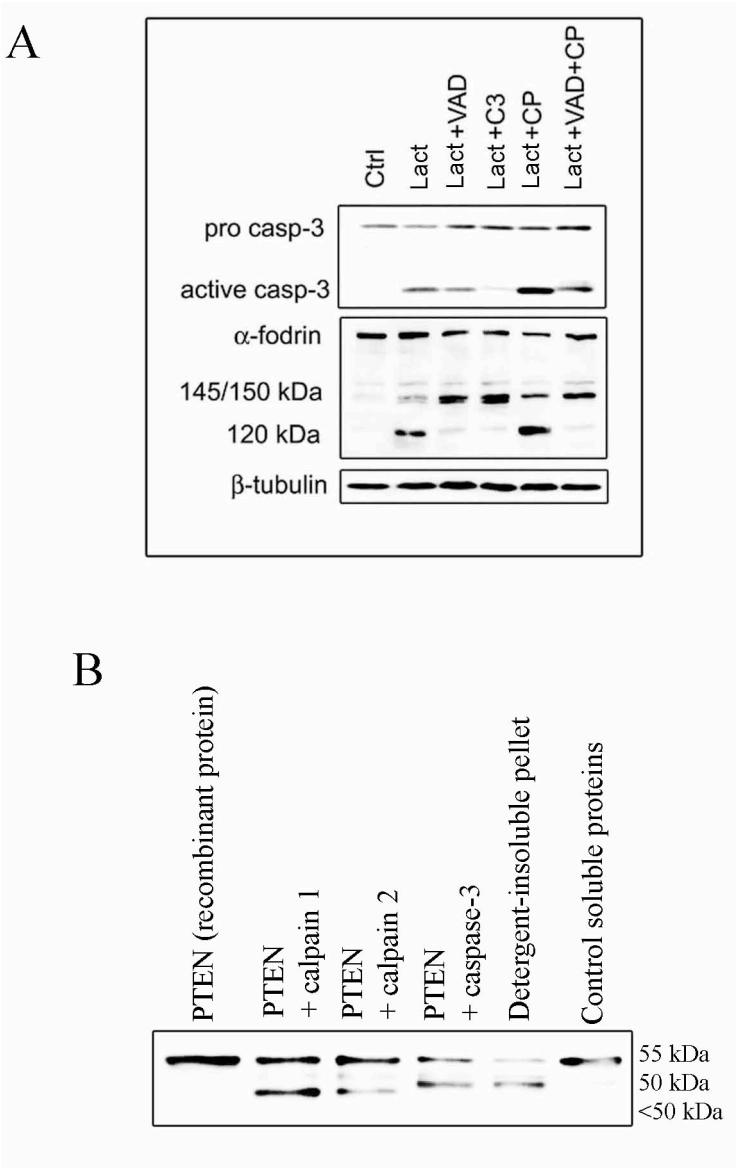

Figure 3.13. PTEN is cleaved by caspase-3 during lactacystin-induced neuronal apoptosis. (A) Western blot analysis of the cleavage of caspase-3 and α-fodrin in protein samples obtained from cultured cortical neurons treated with 1 μM lactacystin alone (Lact), or with 100 μM z-VAD-FMK caspase inhibitor (Lact+VAD), or with 100 μM caspase-3 inhibitor IV (Lact+C3), or with 10 μM calpeptin (Lact+CP), or with both 100 μM z-VAD-FMK and 10 μM calpeptin (Lact+VAD+CP) for 24 h. The 120 kDa α-fodrin fragment corresponds to caspase-3 cleavage and the 145/150 doublet corresponds to calpain cleavage. (B) In vitro digestion of recombinant PTEN by calpains and caspase-3. Recombinant PTEN (1 μg) was incubated with calpain 1, calpain 2 and caspase-3 for 3 h and the products were analyzed using Western blot. Both calpain 1 and calpain 2 produced truncated TPEN with molecular size <50 kDa. Caspase-3-digested recombinant PTEN produced 50 kDa truncated PTEN, similar to those observed in the detergent-insoluble pellets of lactacystin-treated cultured cortical neurons. The control soluble proteins were extracted from untreated cultured cortical neurons using RIPA buffer.

and calpain inhibitors were used in the following experiments. As expected, Western blot showed a more intense caspase-3-cleavage-associated 120 kDa α-fodrin fragment compared to the 145/150 kDa calpain-cleavage-associated doublet (Fig. 3.13A) in protein samples extracted from cultured neurons exposed to lactacystin (1 μM) alone. When caspase pan-specific inhibitor z-VAD-FMK (100 μM) or caspase-3 inhibitor IV (100 μM) were used together with lactacystin (1 μM), Western blot analysis of α-fodrin cleavage showed a more intense calpain-cleavage-associated 145/150 kDa doublet but a faint 120 kDa caspase-3-cleavage-associated band, indicating that calpain activity was dominant when caspase-3 activity was blocked (Fig. 3.13A). On the other hand, when the calpain inhibitor calpeptin (10 μM) was used together with lactacystin (1 μM), the absence of the 145 kDa calpain-cleavage-associated band and the presence of a more prominent caspase-3-cleavage associated 120 kDa band in the western blot of α-fodrin suggest an increase in caspase-3 activity (Fig. 3.13A). This western blot result indicates that the inhibition of caspase-3 activity using inhibitors could affect the activity of calpain or vice versa. This observation suggests that a cross-talk between caspase-3 and calpain exists in lactacystin-induced neuronal apoptosis.

To confirm if caspase-3 was the protease that cleaved PTEN to generate the truncated form of 50 kDa during lactacystin-induced neuronal apoptosis, in vitro enzymatic digestion was performed on recombinant PTEN obtained from an insect cell line (a gift from Heung-Chin Cheng, Department of Biochemistry and Molecular Biology, Melbourne University) using recombinant caspase-3 enzyme (recombinant protein expressed in *E. coli*, cat#14-264, Upstate Biotechnology, Lake Placid, NY, USA).

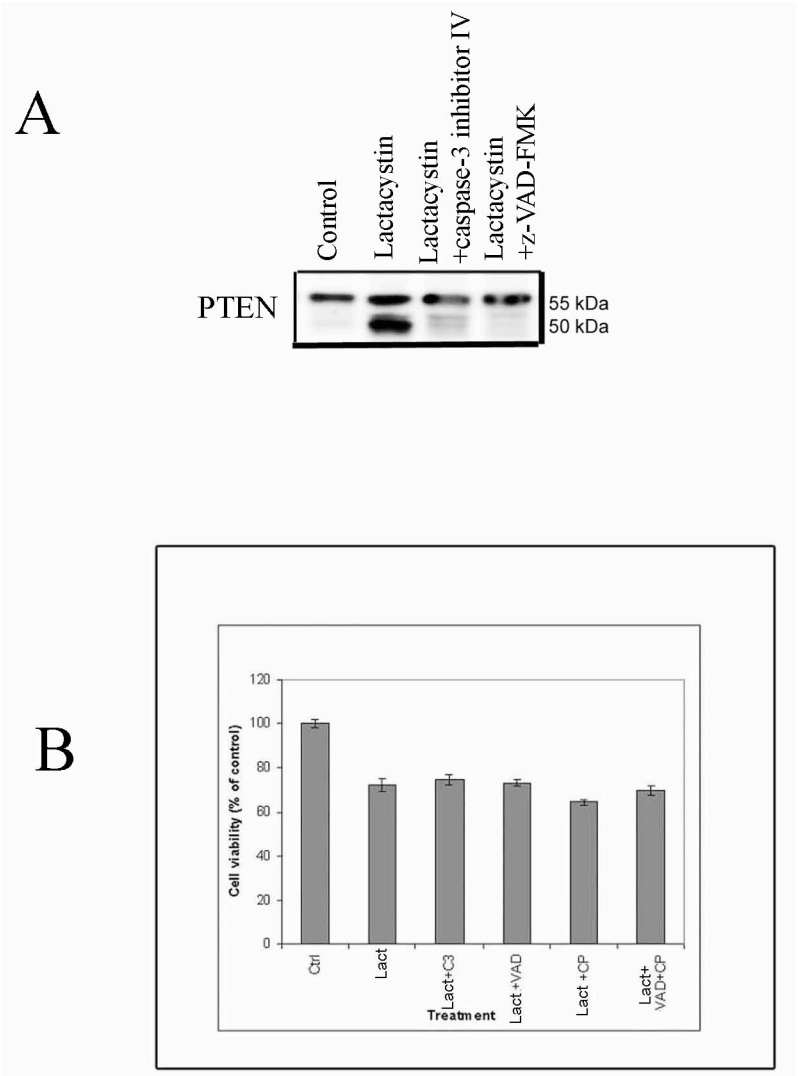

Figure 3.14. The effects of caspase and calpain inhibitors on the cleavage of PTEN and cell viability. (A) Both caspase-3 inhibitor IV and z-VAD-FMK can effectively inhibit the cleavage of PTEN. (B) Caspase-3 inhibitor IV, z-VAD-FMK and calpeptin when co-treated with lactacystin cannot protect the cultured neuron against cell death.

The Western blotting result shows that the recombinant PTEN was cleaved to exactly the same truncated form as the lactacystin-treated control (Fig. 3.13B). This observation supports the hypothesis that caspase-3 was the protease responsible for the cleavage of PTEN to the 50 kDa-truncated form. Both calpain-1 and -2 generated a smaller (<50 kDa) truncated PTEN fragment (Fig. 3.13B), indicating a different cut site. Furthermore, both z-VAD-FMK and caspase-3 inhibitor IV could effectively inhibit the cleavage of PTEN during lactacystin-induced neuronal apoptosis (Fig. 3.14A).

Cell viability assay was performed on cultured cortical neurons treated with lactacystin (1 μM), caspase-3 and calpain inhibitors to investigate whether these inhibitors could effective attenuate cell death. MTT assay shows that they were ineffective in protecting neurons from lactacystin-induced apoptosis (Fig. 3.14B). The result shows that inhibition of caspase-3 and calpain activity could not block lactacystin-induced neuronal apoptosis in cultured cortical neurons.

Caspase-3 was identified as the protease responsible for the cleavage of PTEN to the truncated 50 kDa form during lactacystin-induced neuronal apoptosis. Calpain was found to be activated, although not as much as caspase-3, and was found to cleave p35 into p25. In vitro digestion study using recombinant PTEN showed that PTEN could be cleaved by calpain, but the cleavage generates a smaller PTEN fragment compared to those generated by caspase-3. In lactacystin-treated cultured cortical neurons, this <50 kDa PTEN fragment was not observed and probably served no physiological role in the cell death.

3.3.2 Recruitment of PTEN onto the plasma membrane during lactacystin-induced neuronal apoptosis

In this study, an attempt was made to demonstrate the recruitment of PTEN onto the plasma membrane of cultured cortical neurons treated with lactacystin using immunogold TEM. Under the TEM, the plasma membrane sheets contained dark (electron-dense) patches (Fig. 3.15). These patches were caused by the accumulation of Osmium, which is a stain for lipids with double bonds; therefore the dark patches indicated areas rich in lipids or cholesterol, such as the lipid raft or the detergent-insoluble plasma membrane microdomain (Wilson et al, 2004). In this experiment, the immuno-reactivity of anti-flotillin-1 against the antigens on the membrane sheets was not as good as that of anti-PTEN antibody. Nevertheless, both treated and untreated neurons showed small clusters of flotillin-1 (2–5 size 15-nm gold particles) on the inner surface of the membrane sheets (Fig. 3.15A). In contrast, lactacystin-treated neurons showed a marked increased of the 10-nm gold particles corresponding to PTEN on the inner membrane sheets, compared to the untreated neurons (Fig. 3.15B). A closer examination revealed the localization of gold particles in the electron-dense patches (Fig 3.15B, inset), confirming that PTEN accumulated in the lipid-rich membrane microdomain or lipid-raft.

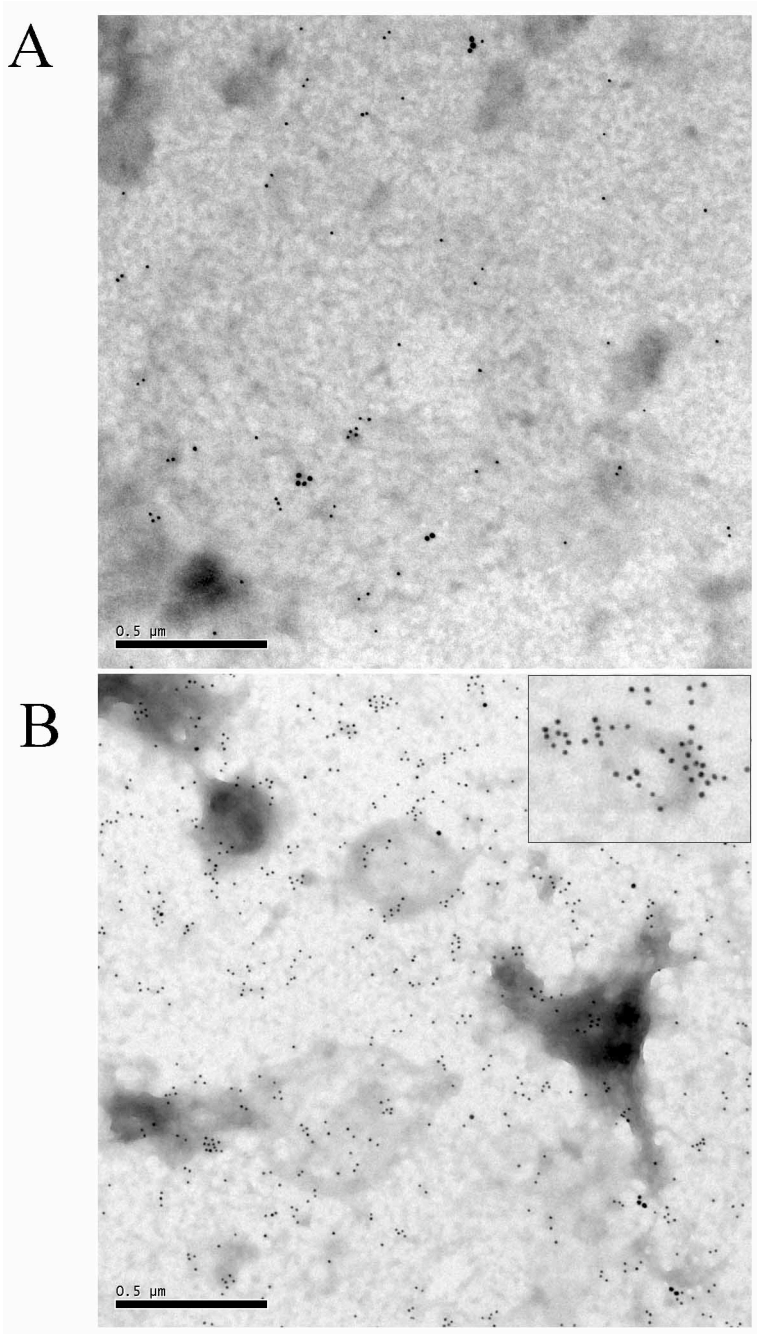

Figure 3.15. Accumulation of PTEN at the plasma membrane of mouse cortical neurons treated with lactacystin. (A) Control membrane sheet showing some immunogold labeling of PTEN (10 nm) and flotillin-1 (15 nm). (B) Membrane sheet from lactacystin-treated neurons showing marked increased in PTEN immunogold labeling.

Lipid rafts are plasma membrane microdomains that contain high concentrations of cholesterol and glycosphingolipids (Pike, 2003). Lipid rafts exist as liquid-ordered regions of membrane that are resistant to extraction with nonionic detergents such as Triton X-100 (Schroeder et al, 1998). A variety of proteins, especially those involved in cell signaling have been shown to partition into lipid rafts (Pike, 2003). PTEN accumulation into the detergent-insoluble fraction during lactacystin-induced neuronal apoptosis was previously reported. In this study, the localization of PTEN in the electron-dense and lipid-rich microdomains was shown using immuno-gold TEM on the plasma membrane sheets.

CHAPTER 4

4 Microarray GeneChip® analysis of gene expression during lactacystin-induced neuronal apoptosis

4.1 Introduction

Global views of gene expression are often essential for obtaining comprehensive pictures of cell function. Understanding the critical relative changes among all the genes would be impossible without the use of whole-genome analysis. Whole-genome analyses also provide an efficient tool to sort through the activities of thousands of genes, and to recognize the key players. Global analyses frequently provide insights into multiple facets of a biological process and may also reveal clues about the basic biology of disorders, and suggest novel drug targets.

The GeneChip® probe array, with its sensitivity, specificity, and reproducibility, is an excellent tool for the study of global gene expression. Taking advantage of these capabilities, many researchers have used GeneChip® probe arrays to study the regulation of gene expression associated with a wide variety of basic biological functions and disease conditions (Stenzel-Poore et al, 2003; Fribley et al, 2004).

Microarray GeneChip® technology has also been used to study the global response of proteasome inhibition in *Saccharomyces cerevisiae* (Flemming et al, 2002) and in human breast carcinoma cells, demonstrating the up-regulation of members of various transcription factor families (Zimmermann et al, 2000). Recently, the chronic effect of proteasome inhibitors was tested on SH-5Y5Y neural cell lines (Ding et al, 2004). However, a similar analysis of the effects of proteasome inhibition upon primary

neurons has not been reported. Because proteasome inhibition is likely to contribute to neurodegeneration and is also able to generate initial neuroprotective proteins, the identification of genes that are differentially expressed upon proteasome inhibition in a primary neuronal culture model might enable us to have a clearer idea of the possible pro-apoptotic and neuroprotective pathways activated in this process. The fundamental objective in any neurodegeneration and neuroprotection research is to determine which of these factors constitutes the primary event, the sequence in which these events occur, and whether they act in concurrence in the pathogenic process (Mandel and Youdim, 2004). In this study, Affymetrix U74Av2 microarray was used to analyze the changes in gene expression upon lactacystin treatment of mouse primary cortical neurons at different time points. The microarray result showed that lactacystin-induced proteasome inhibition caused differential expression of genes involved in the UPS, heat shock protein (HSP), ER stress, oxidative stress and cholesterol biosynthesis among others.

4.2 Results

4.2.1 Time course of lactacystin-induced proteasome inhibition and neuronal apoptosis

Proteasomal chymotrypsin-like activity was assayed using flurogenic substrate on the cell lysate extracted from cultured cortical neurons treated with 1 μM lactacystin. The chymotrypsin-like activity was inhibited considerably (94% decrease in activity compared to the control) at the earliest time point (4.5 h) measured (Fig. 4.1A). The slight recovery of chymotrypsin-like activity was observed at 24 h after lactacystin

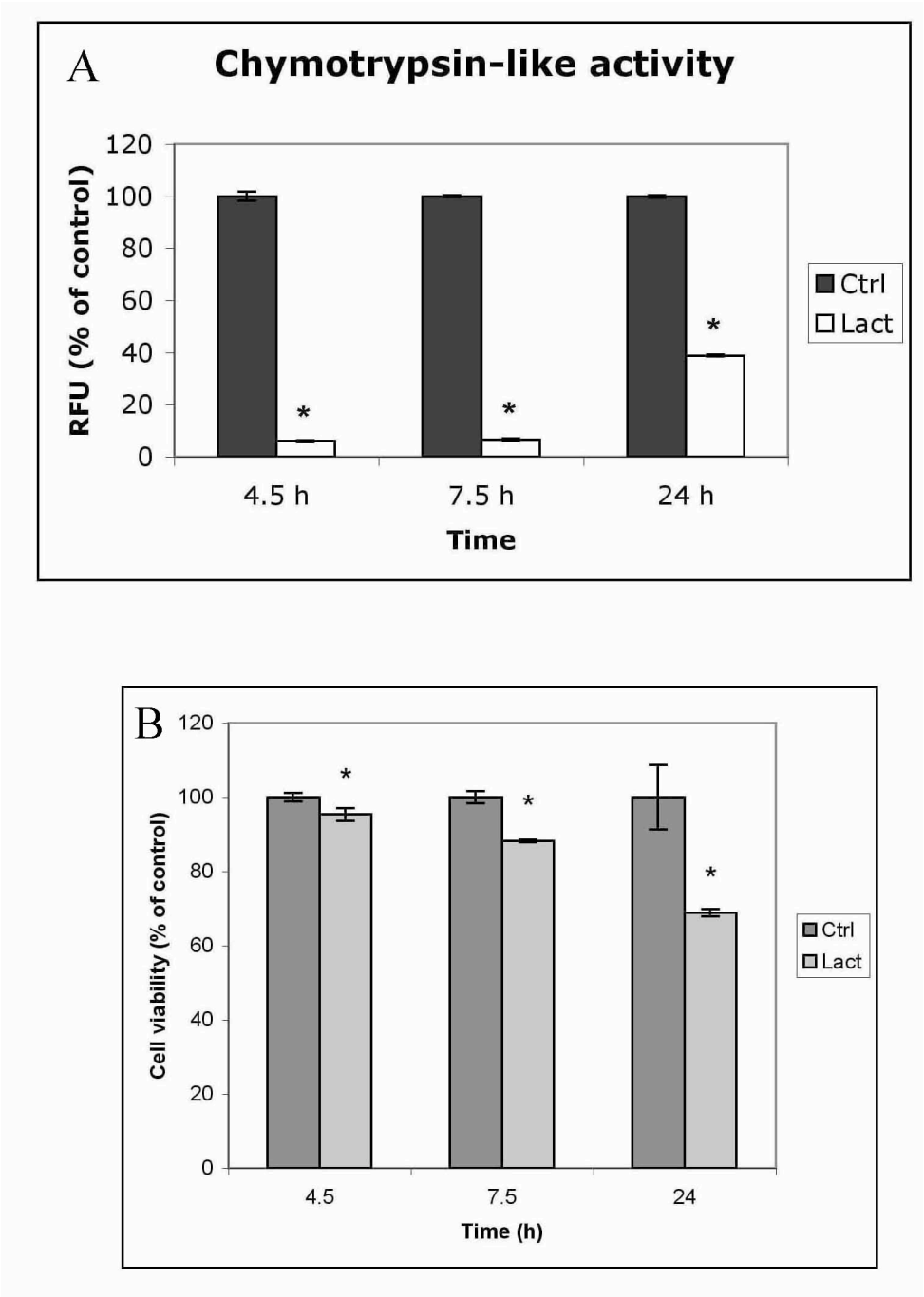

Figure 4.1. Effects of lactacystin (Lact) on proteasome activities and cell viability of mouse cultured cortical neurons. (A) Proteasomal chymotrypsin-like activity was measured using fluorogenic substrate III. Activity was presented as percent relative fluorescence unit (RFU) compared to the control. * denotes significant difference compared to the control according to the one-sample t test, $p<0.05$. (B) MTT cell viability assay showing cell viability of cultured cortical neurons treated with 1 μM lactacystin at 4.5 h, 7.5 h and 24 h time points. * indicates significant difference according to ANOVA with post hoc Tukey's test, $p<0.05$.

treatment; this was probably due to the degradation of fluorogenic substrates by other proteases during apoptosis. The calpain inhibitor calpeptin (10 μM) effectively suppressed the increase of chymotrypsin-like activity at 24 h, suggesting that calpain could be involved in the interference of chymotrypsin-like activity measurement. MTT cell viability assay showed a time-dependent decrease of neuronal cell viability after treatment by 1 μM of lactacystin; a more significant decrease was observed at the 24 h time point (Fig. 4.1B).

Western blot analyses were performed to investigate when caspase-3 was activated during lactacystin-induced neuronal apoptosis. Pro-caspase-3 (32 kDa) was cleaved to its active form (17 kDa) at 15 h after lactacystin treatment (Fig. 4.2A). Similarly, the caspase-3 substrates (α-fodrin and poly (ADP-ribose) polymerase or PARP) were cleaved at the same time point as when caspase-3 was activated (Fig. 4.2A). Likewise, measurement of caspase activity in the cell lysate of cultured cortical neurons treated with 1 μM lactacystin showed a maximum increase (1,200% caspase-3 activity compared to the untreated control) at the 15 h time point (Fig. 4.2B). Other caspases activated during lactacystin-induced neuronal apoptosis include: caspase-2 (700% at 15 h), caspase-10 (600% at 15 h), caspase-4 (400% at 15 h), caspase-6 (250% at 15 h), caspase-8 (160% at 15 h) and caspase-9 (200% at 15 h). Caspase-1, caspase-4 and caspase-5 are caspases involved in inflammation (Salvesen and Dixit, 1997; Nicholson, 1999) but among them, only caspase-4 was activated (400% increase) at the 15 h time point. Taken together, the data above suggest that apoptosis, as determined by the activation of caspase-3, was initiated at 15 h after lactacystin treatment.

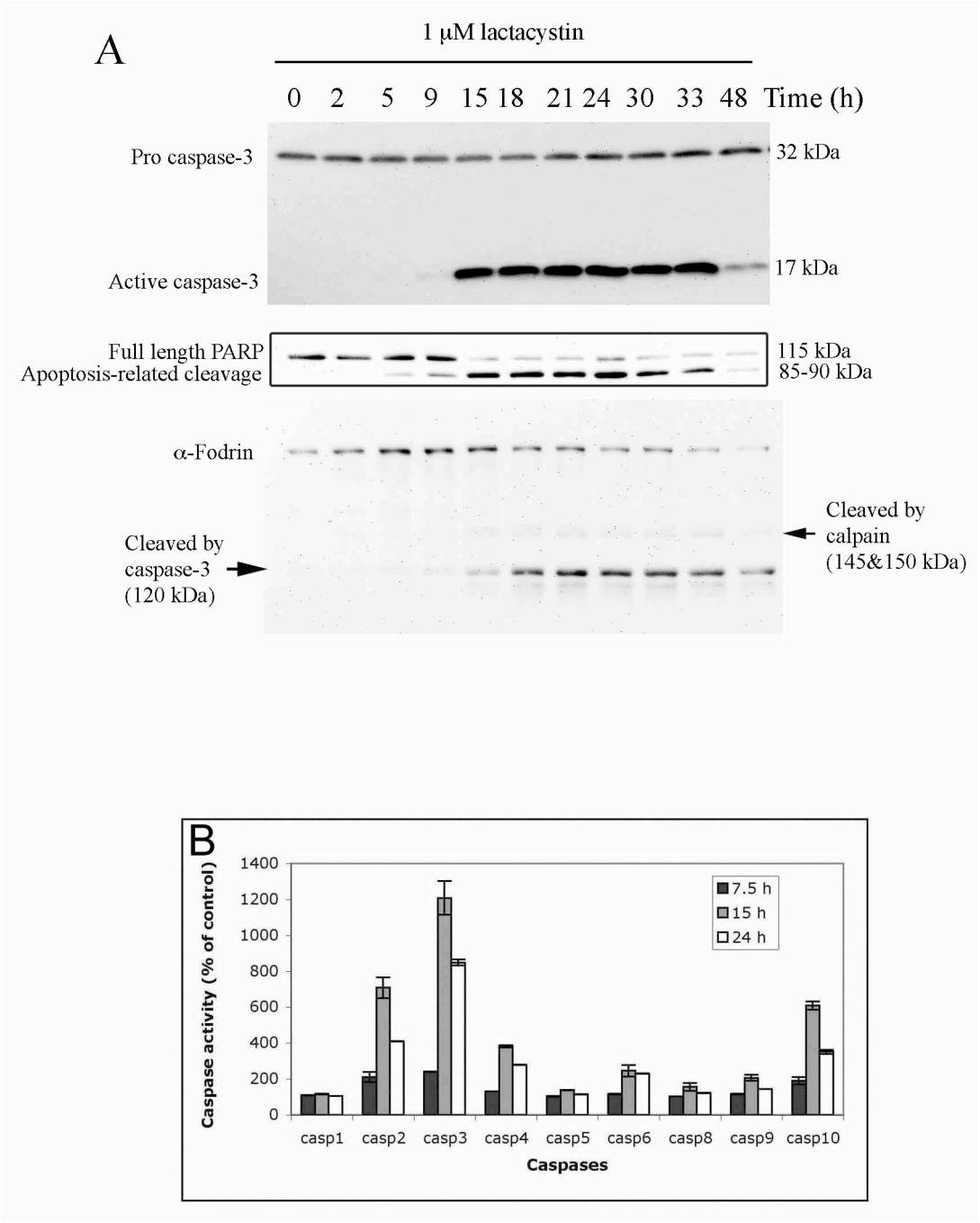

Figure 4.2. Time-course study of caspase-3 activation and substrate cleavage during lactacystin-induced neuronal apoptosis. (A) Western blots show the cleavage of pro-caspase-3 to active caspase-3, and the cleavage of caspase-3 substrates PARP and α-fodrin. (B) The measurement of caspase activities using caspase-family fluorogenic substrates detected a maximum increase (12-fold) of caspase-3 activities 15 h after 1 μM lactacystin treatment.

To investigate whether there were any apoptotic cells in the neuronal cultures 7.5 h after exposure to 1 μM lactacystin, the fixed cells were stained with DNA-staining dye (Hoechst 33258) at 7.5 h and 24 h after lactacystin exposure and observed under the microscope. As expected, no chromatin fragmentation was observed at the 7.5 h time point, confirming the absence of apoptotic cells at this time point (Fig. 4.3A). On the other hand, nuclear condensation and chromatin fragmentation were observed in the neuronal cultures 24 h after treatment with lactacystin (Fig. 4.3). Apoptotic cells can also be detected using annexin V-FITC dye. The change in the apoptotic cell plasma membrane exposes phosphatidylserine to the outer cell surface without compromising membrane integrity; annexin V-FITC binds to the exposed phosphatidylserine on the surface of the apoptotic cell, giving out green fluorescence under FITC excitation/emission wavelengths (485/530 nm). According to the annexin V-FITC staining assay, only neuronal cultures subjected to 24 h lactacystin treatment contained apoptotic cells (Fig. 4.3B).

4.2.2 RNA isolation from lactacystin-treated cultured cortical neurons

The quality of RNA extracted from cells needs to be evaluated before microarray analysis. Fig. 4.4 shows gel photos of total RNA extracted from cultured cortical neurons, taken from RNA samples used in both microarray analysis and verification real-time PCR analysis. Using the Qiagen RNeasy Mini Kit for RNA extraction, the yield of total RNA obtained was in the range of 40–80 μg with a purity of 1.4–1.8 (A260/A280 ratio) from each 6-well culture plate. A yield of 2.1–5.9 μg of total RNA with a purity of 1.3–1.6 (A260/A280 ratio) could be obtained from a single well of cultured neurons in a 6-well plate using High Pure Isolation Kit (Roche, Penzberg, Germany).

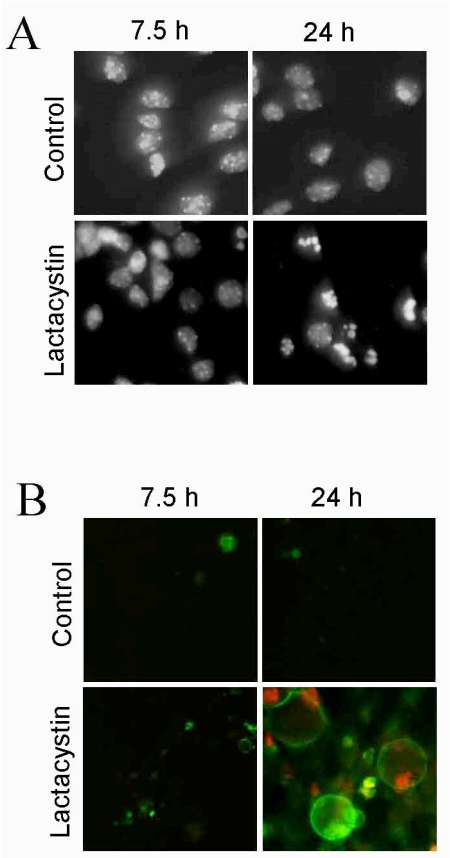

Figure 4.3. Apoptotic cell death of cultured cortical neurons exposed to lactacystin. (A) Hoechst staining showing the presence of chromatin fragmentation in cultures treated with lactacystin (1 μM) for 24 h. (B) Annexin V-FITC staining showing apoptotic cells (round and green) in cultures treated with lactacystin (1 μM) for 24 h. During the late stage of apoptosis, the nuclei of dead cells are stained red with propedium iodide, indicating that the plasma membranes have been disrupted.

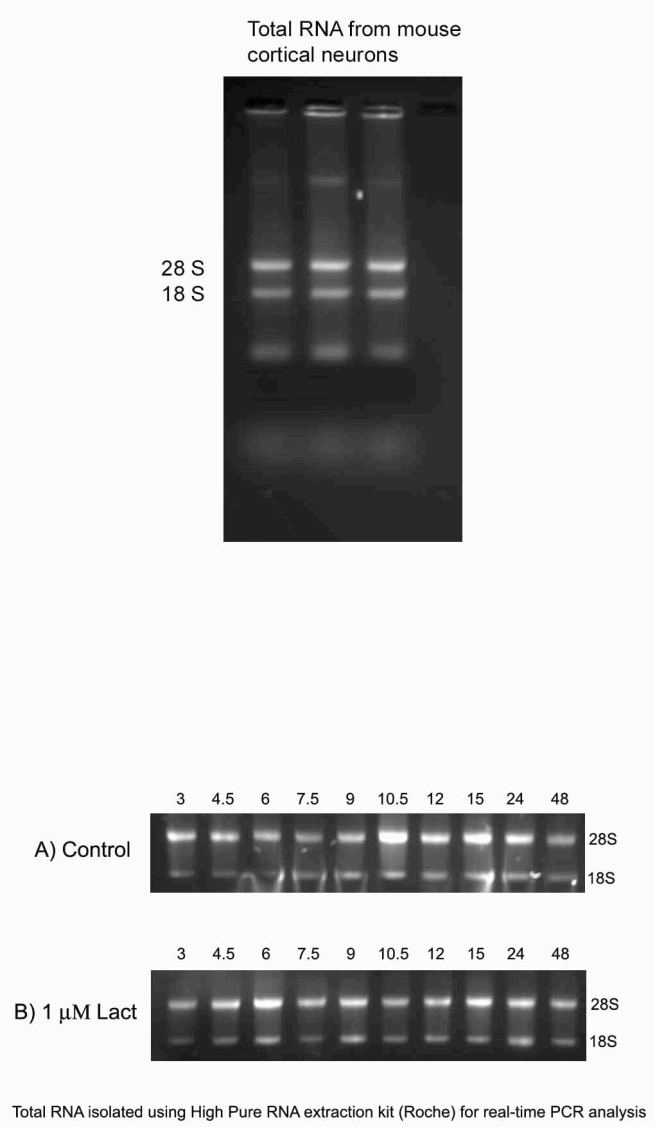

Figure 4.4. Total RNA extracted from cultured cortical neurons. (A) Total RNA extracted from cultured cortical neurons treated with 1 μM lactacystin for 7.5 h using RNeasy Mini Kit (Qiagen) for microarray analysis and (B) total RNA extracted from untreated and treated (1 μM lactacystin) cultured cortical neurons in time-course real-time PCR study.

4.2.3 Microarray analysis

Microarray analyses revealed that a large number of genes were differentially expressed in cultured cortical neurons which underwent neuronal apoptosis after treatment with 1 μM lactacystin; out of a total of 12,488 genes and Expressed Sequence Tags (ESTs) in the murine genome GeneChip® U74Av2, 1,168 genes were differentially expressed by more than two-fold according to the one-way ANOVA, $p<0.01$. To reduce the number of genes to a manageable size, a more stringent condition was applied; genes that were differentially expressed by more than three-fold at least once in any of the time points (4.5 h, 7.5 h, 24 h and 48 h) tested were selected for analysis. Under this condition, the number of genes was reduced to 342. These genes were then arranged according to their biological functions and listed in Tables 4.1–4.13. Bonferroni correction, a very stringent statistical analysis was performed to check the integrity of the gene list. Genes that passed the Bonferroni correction were indicated by an asterisk (*). More than one-third of genes (123 genes) passed the Bonferroni test, indicating a highly significant set of data.

For an overview of the changes in global gene expression across the time points, selected genes from Tables 4.1–4.13 are shown in Fig. 4.5 as gene clusters with their expression profile indicated by colors: red for up-regulation and blue for down-regulation (Fig 4.5). Most genes were up-regulated during earlier time points compared to later time points, as shown in Figure 4.5.

Table 4.1. Differentially expressed genes after lactacystin treatment: Ubiquitin-proteasome system. Gene expression is indicated as fold change±Standard Error. Only genes differentially expressed >3-fold and significantly expressed according to one-way ANOVA, $p<0.05$ are included in this list. * indicates genes that passed the Bonferroni Correction.

Probe id	Symbol	Gene Title	Time points (h)				Genbank
			4.5	7.5	24	48	
Ubiquitin-proteasome system							
95600_at	Arih2*	ariadne homolog 2 (Drosophila)	2.61±0.14	4.11±0.14	1.24±0.15	-1.05±0.19	AJ130975
96892_at	Psma1*	proteasome subunit, alpha type 1	2.79±0.09	3.37±0.10	2.49±0.20	-1.06±0.14	AI836804
93988_at	Psma7*	proteasome subunit, alpha type 7	2.60±0.08	3.53±0.07	2.35±0.13	-1.09±0.19	AI836676
94025_at	Psmb3	proteasome subunit, beta type 3	2.78±0.06	4.50±0.20	3.22±0.21	1.10±0.24	AW045339
160152_at	Psmc1*	proteasome 26S subunit, ATPase 1	2.28±0.12	3.79±0.09	2.29±0.16	-1.06±0.13	U39302
93734_i_at	Psmc3*	proteasome 26S subunit, ATPase 3	2.71±0.07	3.13±0.11	2.27±0.12	-1.05±0.13	D49686
160305_at	Psmd11	proteasome 26S subunit, non-ATPase, 11	5.34±0.07	5.03±0.27	2.75±0.17	1.02±0.12	AW121693
93971_f_at	Psmd12	proteasome 26S subunit, non-ATPase, 12	3.34±0.06	3.62±0.20	2.56±0.31	-1.09±0.17	AI838669
94302_at	Psmd4	proteasome 26S subunit, non-ATPase, 4	2.85±0.07	5.29±0.12	3.07±0.35	-1.05±0.21	AF013099
103350_at	Psmd7	proteasome 26S subunit, non-ATPase, 7	2.38±0.08	3.03±0.08	1.88±0.30	-1.31±0.15	M64641
95124_i_at	Rbx1	ring-box 1	3.18±0.11	2.00±0.19	1.13±0.15	-1.21±0.17	AW122337
97906_at	Siah2	seven in absentia 2	1.54±0.12	2.90±0.08	-1.06±0.26	-1.51±0.19	Z19581
101255_at	Ubb*	ubiquitin B	3.10±0.07	3.62±0.06	1.08±0.15	-1.19±0.14	X51703
95215_f_at	Ubc*	ubiquitin C	4.04±0.09	4.79±0.07	1.39±0.16	-1.25±0.12	D50527
101581_at	Ube3a*	ubiquitin protein ligase E3A	3.65±0.08	1.93±0.09	1.24±0.11	-1.20±0.10	U82122
93303_at	Ufd1l*	ubiquitin fusion degradation 1 like	2.49±0.07	4.45±0.07	2.05±0.34	-1.43±0.16	U64445
161870_at	Usp15	ubiquitin specific protease 15	-3.77±0.09	-3.28±0.12	-1.57±0.12	1.50±0.24	AV359471
101069_g_at	Mkrn1*	makorin, ring finger protein, 1	1.96±0.09	3.10±0.08	-1.25±0.12	-1.32±0.12	AA656621
161814_f_at	Rnf19*	ring finger protein (C3HC4 type) 19	4.51±0.12	2.67±0.18	-1.03±0.10	-1.48±0.10	AV355427
102131_f_at	Rnf20*	ring finger protein 20	-3.05±0.08	-2.93±0.06	1.01±0.13	1.08±0.13	AU014874
101966_s_at	Rnf13*	ring finger protein 13	2.09±0.09	3.13±0.12	1.00±0.10	1.13±0.12	AF037206
93164_at	Rnf2*	ring finger protein 2	1.79±0.10	3.25±0.17	-1.57±0.10	-1.12±0.14	Y12783

Table 4.2. Differentially expressed genes after lactacystin treatment (continued): ER stress; heat shock proteins and molecular chaperones; apoptosis. Gene expression is indicated as fold change±Standard Error. Only genes differentially expressed >3-fold and significantly expressed according to one-way ANOVA, $p<0.05$ are included in this list. * indicates genes that passed the Bonferroni Correction.

Probe id	Symbol	Gene Title	Time points (h)				Genbank
			4.5	7.5	24	48	
ER stress							
104155_f_at	Atf3*	activating transcription factor 3	3.77 ± 0.13	11.13 ± 0.38	6.68 ± 1.76	2.06 ± 0.27	U19118
100599_at	Atf4	activating transcription factor 4	3.52 ± 0.06	3.73 ± 0.09	-1.03 ± 0.25	-2.13 ± 0.12	M94087
92925_at	Cebpb	CCAAT/enhancer binding protein (C/EBP), beta	-1.13 ± 0.18	4.26 ± 0.14	3.44 ± 0.34	1.32 ± 0.13	M61007
101429_at	Ddit3	DNA-damage inducible transcript 3	2.90 ± 0.10	5.01 ± 0.12	2.65 ± 0.42	1.02 ± 0.15	X67083
95057_at	Herpud1	homocysteine-inducible, endoplasmic reticulum stress-inducible, ubiquitin-like domain member 1	1.93 ± 0.08	3.18 ± 0.16	1.17 ± 0.22	-1.32 ± 0.11	AI846938
96773_at	Txndc4*	thioredoxin domain containing 4 (endoplasmic reticulum)	2.45 ± 0.11	3.46 ± 0.11	1.38 ± 0.11	1.28 ± 0.18	AW125408
Heat shock proteins and molecular chaperones							
96254_at	Dnajb1	DnaJ (Hsp40) homolog, subfamily B, member 1	2.11 ± 0.20	3.52 ± 0.15	1.42 ± 0.26	-1.12 ± 0.12	AB028272
93875_at	Hspa1a	heat shock protein 1A (HSP70)	-1.27 ± 0.13	4.70 ± 0.53	13.82 ± 6.14	1.78 ± 0.53	M12571
97914_at	Hspa9a	heat shock protein, A	1.68 ± 0.07	3.68 ± 0.07	2.18 ± 0.27	1.07 ± 0.16	D17666
160139_at	Hspb8*	heat shock 27kDa protein 8	-1.37 ± 0.12	1.67 ± 0.16	8.08 ± 0.47	2.22 ± 0.48	AI848798
94817_at	Serpinh1*	serine (or cysteine) proteinase inhibitor, clade H, member 1 (HSP47)	1.14 ± 0.08	3.10 ± 0.06	6.16 ± 0.15	3.30 ± 0.43	X60676
Apoptosis							
161980_f_at	Bag3	Bcl2-associated athanogene 3	1.37 ± 0.29	1.97 ± 0.24	6.36 ± 1.02	3.41 ± 0.70	AV373612
97724_at	Cry2	cryptochrome 2 (photolyase-like)	1.85 ± 0.26	3.47 ± 0.09	-1.75 ± 0.17	-1.29 ± 0.22	AB003433
95545_at	Igf1	insulin-like growth factor 1	-4.23 ± 0.08	-2.11 ± 0.07	-1.49 ± 0.11	-1.45 ± 0.14	X04480
95750_at	Nipa	nuclear interacting partner of anaplastic lymphoma kinase (Alk)	2.07 ± 0.08	3.06 ± 0.07	1.55 ± 0.37	-1.25 ± 0.17	AI848853

Table 4.3. Differentially expressed genes after lactacystin treatment (continued): proteolysis; inflammatory response; glutathione synthesis; metal ion homeostasis. Gene expression is indicated as fold change±Standard Error. Only genes differentially expressed >3-fold and significantly expressed according to one-way ANOVA, $p<0.05$ are included in this list. * indicates genes that passed the Bonferroni Correction.

Probe id	Symbol	Gene Title	Time points (h)				Genbank
			4.5	7.5	24	48	
Proteolysis							
93048_at	Clpp	caseinolytic protease, ATP-dependent, proteolytic subunit homolog (E. coli)	2.43 ± 0.10	3.38 ± 0.10	1.75 ± 0.18	-1.15 ± 0.19	AJ005253
92256_at	Ctsb*	cathepsin B	2.85 ± 0.27	3.18 ± 0.16	2.20 ± 0.12	1.82 ± 0.20	AI853714
101019_at	Ctsc	cathepsin C	1.79 ± 0.45	3.27 ± 0.26	6.64 ± 1.10	3.65 ± 0.87	U74683
161358_r_at	Dpep3	dipeptidase 3	-1.64 ± 0.13	-3.89 ± 0.09	-1.48 ± 0.11	-1.13 ± 0.11	AV209030
98287_at	Dpp6	dipeptidylpeptidase 6	-3.44 ± 0.07	-2.61 ± 0.06	-1.41 ± 0.11	-1.26 ± 0.14	AF092507
160290_at	Ide*	insulin degrading enzyme	3.17 ± 0.07	3.03 ± 0.08	2.78 ± 0.43	-1.04 ± 0.10	AI574278
94238_at	2310046G 15Rik*	RIKEN cDNA 2310046G15 gene	-1.24 ± 0.11	-2.06 ± 0.09	1.65 ± 0.23	3.29 ± 0.21	AW228316
Inflammatory response							
98088_at	Cd14*	CD14 antigen	-2.35 ± 0.13	-3.62 ± 0.07	-1.13 ± 0.11	1.33 ± 0.13	X13333
101341_at	H2-M9	histocompatibility 2, M region locus 9	-5.34 ± 0.14	-5.30 ± 0.06	-1.52 ± 0.10	-1.01 ± 0.13	AF016308
102029_at	Il16	interleukin 16	-5.36 ± 0.17	-1.82 ± 0.18	-1.12 ± 0.16	-1.14 ± 0.13	AF017111
Glutathione biosynthesis							
160335_at	Gclm	glutamate-cysteine ligase , modifier subunit	2.97 ± 0.10	2.63 ± 0.14	3.25 ± 0.48	1.51 ± 0.25	U95053
96085_at	Gsta4*	glutathione S-transferase, alpha 4	1.17 ± 0.10	1.03 ± 0.08	5.07 ± 0.12	4.56 ± 1.18	L06047
97681_f_at	Gstm3	glutathione S-transferase, mu 3	-5.19 ± 0.15	-3.77 ± 0.07	-1.11 ± 0.11	1.06 ± 0.11	J03953
93026_at	Mgst1*	microsomal glutathione S-transferase 1	1.63 ± 0.14	1.07 ± 0.12	4.13 ± 0.61	2.97 ± 0.36	AW124337
Metal ion homeostasis							
93573_at	Mt1	metallothionein 1	-1.24 ± 0.07	-2.35 ± 0.06	2.98 ± 0.10	4.14 ± 1.04	V00835
95340_at	Mt3	metallothionein 3	-4.44 ± 0.06	-3.65 ± 0.06	1.15 ± 0.11	1.85 ± 0.27	M93310

Table 4.4. Differentially expressed genes after lactacystin treatment (continued): calcium homeostasis and calcium binding; cell adhesion. Gene expression is indicated as fold change±Standard Error. Only genes differentially expressed >3-fold and significantly expressed according to one-way ANOVA, $p<0.05$ are included in this list. * indicates genes that passed the Bonferroni Correction.

Probe id	Symbol	Gene Title	Time points (h)				Genbank
			4.5	7.5	24	48	
Calcium homeostasis and calcium binding							
102815_at	Anxa11	annexin A11	-6.37 ± 0.18	-6.68 ± 0.13	1.41 ± 0.16	1.85 ± 0.11	U65986
100569_at	Anxa2*	annexin A2	1.45 ± 0.09	1.80 ± 0.08	4.56 ± 0.25	2.84 ± 0.43	M14044
101393_at	Anxa3*	annexin A3	-1.81 ± 0.18	-2.57 ± 0.24	12.33 ± 3.14	9.26 ± 0.80	AJ001633
104006_at	Eps15	epidermal growth factor receptor pathway substrate 15	1.78 ± 0.09	3.26 ± 0.38	1.02 ± 0.10	1.16 ± 0.11	L21768
98475_at	Matn2	matrilin 2	-5.18 ± 0.36	-1.81 ± 0.11	-1.06 ± 0.15	1.34 ± 0.13	U69262
92539_at	S100a10*	S100 calcium binding protein A10 (calpactin)	-1.80 ± 0.10	-1.23 ± 0.06	4.77 ± 0.55	2.54 ± 0.22	M16465
98600_at	S100a11*	S100 calcium binding protein A11 (calizzarin)	-3.12 ± 0.08	-3.10 ± 0.06	5.31 ± 0.85	8.03 ± 0.50	U41341
100959_at	S100a13	S100 calcium binding protein A13	-3.02 ± 0.08	-3.37 ± 0.13	-1.23 ± 0.12	1.52 ± 0.11	X99921
162428_I_at	S100a14*	S100 calcium binding protein A14	-3.78 ± 0.06	-3.92 ± 0.06	-1.46 ± 0.10	-1.28 ± 0.12	AV293396
101051_at	S100a3	S100 calcium binding protein A3	-5.37 ± 0.13	-2.44 ± 0.16	-1.20 ± 0.10	1.00 ± 0.10	AF004941
Cell adhesion							
94886_at	Canx*	calnexin	-3.08 ± 0.08	-3.06 ± 0.06	-1.14 ± 0.15	-1.16 ± 0.11	L18888
94305_at	Col1a1	procollagen, type I, alpha 1	-1.71 ± 0.38	-8.55 ± 0.07	-1.14 ± 0.22	1.38 ± 0.22	U03419
99800_at	L1cam	L1 cell adhesion molecule	1.39 ± 0.11	2.49 ± 0.10	-3.41 ± 0.13	-3.06 ± 0.27	X12875
99669_at	Lgals1*	lectin, galactose binding, soluble 1	-1.06 ± 0.07	-1.03 ± 0.06	4.01 ± 0.36	5.89 ± 0.72	X15986
95706_at	Lgals3	lectin, galactose binding, soluble 3	2.70 ± 0.29	1.91 ± 0.24	8.66 ± 2.94	7.08 ± 1.46	X16834
161708_f_at	Mpdz	multiple PDZ domain protein	-1.01 ± 0.39	-3.97 ± 0.16	1.48 ± 0.14	1.29 ± 0.17	AV244715
160469_at	Thbs1*	thrombospondin 1	-2.17 ± 0.07	-3.20 ± 0.06	2.16 ± 0.39	2.91 ± 0.31	M62470
103088_at	Chl1*	cell adhesion molecule with homology to L1CAM	3.83 ± 0.08	1.93 ± 0.11	-1.83 ± 0.11	-1.79 ± 0.12	X94310
103492_at	Cpxm1*	carboxypeptidase X 1 (M14 family)	1.16 ± 0.35	3.05 ± 0.22	3.44 ± 0.21	1.38 ± 0.18	AF077738

Table 4.5. Differentially expressed genes after lactacystin treatment (continued): lipid and cholesterol. Gene expression is indicated as fold change±Standard Error. Only genes differentially expressed >3-fold and significantly expressed according to one-way ANOVA, $p<0.05$ are included in this list. * indicates genes that passed the Bonferroni Correction.

Probe id	Symbol	Gene Title	Time points (h)				Genbank
			4.5	7.5	24	48	
Lipid and Cholesterol							
95425_at	Acadl	acetyl-Coenzyme A dehydrogenase, long-chain	1.99±0.39	1.35±0.28	3.85±0.22	4.33±0.70	U21489
101006_at	Acat2*	acetyl-Coenzyme A acetyltransferase 2	1.10±0.07	-2.20±0.06	-3.50±0.09	-2.90±0.10	M35797
93320_at	Cpt1a*	carnitine palmitoyltransferase 1a, liver	1.03±0.08	1.05±0.06	2.79±0.13	3.23±0.49	AF017175
94916_at	Cyp51	cytochrome P450, 51	-1.41±0.06	-1.47±0.10	-3.21±0.10	-3.12±0.10	AW122260
98989_at	Dhcr7	7-dehydrocholesterol reductase	-1.64±0.07	-2.25±0.06	-3.65±0.11	-3.52±0.10	AF057368
97518_at	Fdft1	farnesyl diphosphate farnesyl transferase 1	1.25±0.08	1.71±0.10	-3.17±0.10	-3.22±0.10	D29016
99098_at	Fdps	farnesyl diphosphate synthetase	1.22±0.06	1.21±0.06	-4.21±0.10	-4.63±0.09	AW045533
161682_f_at	Gpaa1	GPI anchor attachment protein 1	-3.57±0.07	-2.88±0.07	-1.90±0.13	-1.08±0.15	AV161234
104285_at	Hmgcr*	3-hydroxy-3-methylglutaryl-Coenzyme A reductase	-1.77±0.06	-1.53±0.06	-2.43±0.10	-3.38±0.09	M62766
96269_at	Idi1*	isopentenyl-diphosphate delta isomerase	-1.53±0.06	-2.39±0.06	-5.82±0.09	-4.78±0.09	AA716963
160737_at	Lss	lanosterol synthase	-1.23±0.12	-1.11±0.13	-2.65±0.11	-3.17±0.11	AW060927
160770_at	Mvd	mevalonate (diphospho) decarboxylase	-3.06±0.07	-2.61±0.06	-6.96±0.08	-4.98±0.09	AW049778
95632_f_at	Mvk*	mevalonate kinase	1.51±0.15	1.17±0.09	-8.26±0.09	-7.52±0.09	AW122653
98631_g_at	Nsdhl*	NAD(P) dependent steroid dehydrogenase-like	1.51±0.06	-1.28±0.06	-4.73±0.09	-3.41±0.11	AW106745
100927_at	Pltp*	phospholipid transfer protein	-3.48±0.09	-3.43±0.09	1.45±0.27	3.04±0.12	U28960
160388_at	Sc4mol*	sterol-C4-methyl oxidase-like	-1.12±0.07	-1.59±0.06	-2.95±0.10	-3.66±0.09	AI848668
94056_at	Scd1*	stearoyl-Coenzyme A desaturase 1	-2.08±0.06	-2.02±0.07	-5.64±0.09	-7.42±0.09	M21285
160865_at	Vldlr*	very low density lipoprotein receptor	3.68±0.16	1.83±0.15	-1.68±0.12	-1.46±0.16	L33417

Table 4.6. Differentially expressed genes after lactacystin treatment (continued): protein biosynthesis; protein modification. Gene expression is indicated as fold change±Standard Error. Only genes differentially expressed >3-fold and significantly expressed according to one-way ANOVA, $p<0.05$ are included in this list. * indicates genes that passed the Bonferroni Correction.

Probe id	Symbol	Gene Title	Time points (h)				Genbank
			4.5	7.5	24	48	
Protein biosynthesis							
104048_at	Cars	cysteinyl-tRNA synthetase	2.11±0.07	3.77±0.11	1.23±0.34	-1.32±0.13	AI848732
100636_at	Eif4ebp1	eukaryotic translation initiation factor 4E binding protein 1	3.25±0.25	3.89±0.31	3.17±0.33	1.55±0.21	U28656
98141_at	Eif5b*	eukaryotic translation initiation factor 5B	3.76±0.11	1.78±0.13	1.52±0.14	-1.30±0.11	AA647048
103891_i_at	Ell2	elongation factor RNA polymerase II 2	1.69±0.14	1.72±0.16	3.50±0.41	1.49±0.15	AI197161
161683_r_at	Gtpbp1*	GTP binding protein 1	-2.94±0.07	-3.60±0.06	-1.31±0.09	-1.16±0.10	AV239949
93752_at	Iars	isoleucine-tRNA synthetase	2.12±0.07	3.22±0.07	1.17±0.26	-1.32±0.14	AI848393
103630_at	Lars	leucyl-tRNA synthetase	1.85±0.06	2.97±0.08	1.42±0.29	-1.30±0.14	AI844089
96693_at	Rars	arginyl-tRNA synthetase	2.10±0.10	3.57±0.26	2.54±0.37	-1.16±0.16	AI849453
Protein modification							
93219_at	Acp1	acid phosphatase 1, soluble	1.94±0.12	3.74±0.13	1.13±0.19	-1.10±0.12	Y17343
92383_at	Dyrk1a	dual-specificity tyrosine-(Y)-phosphorylation regulated kinase 1a	1.01±0.17	2.91±0.24	-1.03±0.10	-1.23±0.12	U58497
98771_at	Ephb2	Eph receptor B2	2.86±0.08	2.67±0.13	-2.00±0.17	-1.42±0.17	L25890
161492_i_at	Mgat1*	mannoside acetylglucosaminyltransferase 1	-2.72±0.07	-3.21±0.06	-1.02±0.13	-1.03±0.11	AV089873
102047_at	Nmt1*	N-myristoyltransferase 1	2.84±0.12	3.45±0.11	2.46±0.20	1.23±0.15	AF043326
95079_at	Pdgfra	platelet derived growth factor receptor, alpha polypeptide	-3.86±0.08	-3.31±0.07	-1.75±0.19	-1.10±0.15	M57683
97096_at	Prkar2a	protein kinase, cAMP dependent regulatory, type II alpha	3.58±0.17	3.63±0.09	-2.13±0.23	-1.76±0.23	J02935
161964_r_at	Prkcz	protein kinase C, zeta	-2.07±0.12	-3.14±0.08	-1.38±0.12	-1.10±0.12	AV367375
161270_i_at	Prkwnk1	protein kinase, lysine deficient 1	1.22±0.13	-5.24±0.07	1.55±0.14	-1.07±0.25	AV319920
92380_r_at	Ptprz1	protein tyrosine phosphatase, receptor type Z, polypeptide 1	1.45±0.17	-3.42±0.07	-1.81±0.12	1.26±0.12	AJ133130

Table 4.7. Differentially expressed genes after lactacystin treatment (continued): transport. Gene expression is indicated as fold change±Standard Error. Only genes differentially expressed >3-fold and significantly expressed according to one-way ANOVA, $p<0.05$ are included in this list. * indicates genes that passed the Bonferroni Correction.

Probe id	Symbol	Gene Title	Time points (h)				Genbank
			4.5	7.5	24	48	
Transport							
100074_at	2400003B06Rik*	RIKEN cDNA 2400003B06 gene	-6.99±0.06	1.31±0.20	1.59±0.14	-1.34±0.13	AW046723
104453_at	2310079P12Rik	RIKEN cDNA 2310079P12 gene	2.78±0.12	3.44±0.06	1.89±0.34	-1.02±0.21	AW046336
92288_at	Ap1g1	adaptor protein complex AP-1, gamma 1 subunit	2.53±0.10	3.99±0.22	-1.48±0.16	-1.50±0.30	X54424
100492_at	Ap2a2*	adaptor protein complex AP-2, alpha 2 subunit	-3.73±0.07	1.17±0.08	-1.18±0.11	-1.29±0.11	AW122807
102704_at	Aqp4	aquaporin 4	-1.59±0.08	-6.24±0.09	-6.17±0.10	1.22±0.16	U88623
96032_at	Atp5g1*	ATP synthase, H+ transporting, mitochondrial F0 complex, subunit c (subunit 9), isoform 1	-3.88±0.08	-2.23±0.07	-1.69±0.10	-1.34±0.11	L19737
102854_s_at	Atp7a*	ATPase, Cu++ transporting, alpha polypeptide	3.21±0.13	2.24±0.16	1.23±0.13	1.04±0.12	U03434
95654_at	Clic1*	chloride intracellular channel 1	1.45±0.11	1.76±0.09	3.64±0.18	3.20±0.45	AF109905
97248_at	Dbi*	diazepam binding inhibitor	-1.52±0.06	-3.44±0.06	-1.91±0.09	1.19±0.14	X61431
94376_s_at	Mre11a*	meiotic recombination 11 homolog A (S. cerevisiae)	3.09±0.21	3.00±0.23	1.52±0.13	-1.18±0.11	U60318
92952_f_at	Napb*	N-ethylmaleimide sensitive fusion protein attachment protein beta	3.63±0.15	2.19±0.09	-1.18±0.13	-1.91±0.14	X61455
93466_at	Sec8l1	SEC8-like 1 (S. cerevisiae)	3.02±0.08	2.60±0.09	-1.16±0.21	-1.10±0.34	AF022962
98457_at	Slc4a4	solute carrier family 4 (anion exchanger), member 4	-1.30±0.13	-3.96±0.11	-1.48±0.13	1.46±0.15	AF020195
161573_at	Slc4a7*	solute carrier family 4, sodium bicarbonate cotransporter, member 7	-3.75±0.07	-2.01±0.07	-1.12±0.10	1.02±0.16	AV278013
102319_at	Snx12	sorting nexin 12	1.55±0.08	3.10±0.13	1.31±0.12	-1.22±0.13	AF062484
96019_at	Sypl	synaptophysin-like protein	2.22±0.18	3.17±0.22	1.51±0.11	-1.01±0.18	AI843476
98339_at	Syt11	synaptotagmin 11	2.85±0.07	3.38±0.11	-1.59±0.17	-1.61±0.19	AB026808
160190_at	Syt4*	synaptotagmin 4	3.50±0.20	1.10±0.06	-1.45±0.10	-1.40±0.10	U10355
101420_at	Viaat	vesicular inhibitory amino acid transporter	-2.76±0.07	-3.23±0.06	-1.45±0.12	-2.57±0.14	AJ001598

Table 4.8. Differentially expressed genes after lactacystin treatment (continued): electron transport; cytoskeleton. Gene expression is indicated as fold change±Standard Error. Only genes differentially expressed >3-fold and significantly expressed according to one-way ANOVA, p<0.05 are included in this list. * indicates genes that passed the Bonferroni Correction.

Probe id	Symbol	Gene Title	Time points (h)				Genbank
			4.5	7.5	24	48	
Electron transport							
101991_at	Fmo1*	flavin containing monooxygenase 1	-2.32 ± 0.08	-4.02 ± 0.07	-2.35 ± 0.12	-1.45 ± 0.11	D16215
98984_f_at	Gpd2*	glycerol phosphate dehydrogenase 2, mitochondrial	3.92 ± 0.22	2.12 ± 0.14	1.19 ± 0.12	-1.54 ± 0.10	D50430
98918_at	Txndc5	thioredoxin domain containing 5	-3.23 ± 0.12	-1.25 ± 0.06	1.18 ± 0.15	1.10 ± 0.17	AI841920
94209_g_at	Txndc7*	thioredoxin domain containing 7	2.11 ± 0.14	3.17 ± 0.17	1.04 ± 0.10	-1.26 ± 0.10	AW045202
102000_f_at	Uqcrc2*	ubiquinol cytochrome c reductase core protein 2	3.40 ± 0.10	2.28 ± 0.11	1.19 ± 0.10	-1.03 ± 0.12	AI842835
103922_f_at	1500005G05Rik	RIKEN cDNA 1500005G05 gene	-1.38 ± 0.08	1.73 ± 0.10	4.87 ± 0.97	1.32 ± 0.34	AI839690
Cytoskeleton							
93100_at	Acta2*	actin, alpha 2, smooth muscle, aorta	-2.11 ± 0.07	-4.06 ± 0.08	1.68 ± 0.37	3.89 ± 0.49	X13297
95705_s_at	Actb	actin, beta, cytoplasmic	-10.94 ± 0.06	-6.82 ± 0.05	1.45 ± 0.22	-1.67 ± 0.26	J04181
94863_r_at	Dncl2a	dynein, cytoplasmic, light chain 2A	3.05 ± 0.16	1.88 ± 0.17	1.27 ± 0.17	-1.16 ± 0.19	AI850000
101698_f_at	Krt2-17	keratin complex 2, basic, gene 17	-3.27 ± 0.15	-1.89 ± 0.07	-1.17 ± 0.13	1.07 ± 0.13	AI852429
98059_s_at	Lmna*	lamin A	1.26 ± 0.07	2.82 ± 0.19	3.54 ± 0.18	1.34 ± 0.18	D49733
102742_g_at	Mapt*	microtubule-associated protein tau	3.07 ± 0.07	2.10 ± 0.06	-1.16 ± 0.12	-1.51 ± 0.11	M18775
160308_at	Msn*	moesin	-2.05 ± 0.07	-1.19 ± 0.08	5.12 ± 0.35	2.80 ± 0.61	AI839417
102108_f_at	Myh9	myosin heavy chain IX	1.69 ± 0.31	1.30 ± 0.07	3.20 ± 0.24	1.82 ± 0.16	AI505453
93541_at	Tagln	transgelin	-1.63 ± 0.09	-2.06 ± 0.07	2.53 ± 0.49	4.16 ± 0.53	Z68618
93413_at	Terf2	telomeric repeat binding factor 2	2.95 ± 0.17	1.97 ± 0.10	1.05 ± 0.16	-1.09 ± 0.18	AF003000
101543_f_at	Tuba6*	tubulin, alpha 6	2.41 ± 0.06	3.07 ± 0.06	1.06 ± 0.12	-1.19 ± 0.14	M13441
162379_r_at	Vim*	vimentin	-8.34 ± 0.07	-7.48 ± 0.08	-1.49 ± 0.10	-1.01 ± 0.12	AV245272

Table 4.9. Differentially expressed genes after lactacystin treatment (continued): cell cycle; signalosome complex; carbohydrate metabolism. Gene expression is indicated as fold change±Standard Error. Only genes differentially expressed > 3-fold change and significantly expressed according to one-way ANOVA, $p<0.05$ are included in this list. * indicates genes that passed the Bonferroni Correction.

Probe id	Symbol	Gene Title	Time points (h)				Genbank
			4.5	7.5	24	48	
Cell cycle							
96146_at	Btg3	B-cell translocation gene 3	1.65±0.08	2.12±0.14	4.15±0.43	1.62±0.35	D83745
96236_at	Cdc16	CDC16 cell division cycle 16 homolog (S. cerevisiae)	3.04±0.23	2.92±0.11	1.81±0.21	-1.34±0.18	AW122965
98067_at	Cdkn1a	cyclin-dependent kinase inhibitor 1A (P21)	1.27±0.09	1.25±0.08	3.14±0.33	1.19±0.17	U09507
97411_at	Ect2	ect2 oncogene	2.94±0.09	2.13±0.16	1.10±0.19	2.20±0.23	L11316
160901_at	Fos*	FBJ osteosarcoma oncogene	1.84±0.20	2.05±0.13	3.11±0.30	2.66±0.21	V00727
100130_at	Jun	Jun oncogene	4.76±0.45	8.30±0.13	1.91±0.42	-1.45±0.14	X12761
161931_r_at	Mki67	antigen identified by monoclonal antibody Ki 67	-4.08±0.18	-1.83±0.13	-1.29±0.10	1.22±0.13	AV309347
103418_at	Rfc4	replication factor C (activator 1) 4	3.54±0.17	2.36±0.10	1.34±0.11	1.21±0.26	AW122092
103520_at	Vegfa	vascular endothelial growth factor A	2.88±0.43	4.89±0.21	-1.07±0.22	-1.38±0.14	M95200
102292_at	Gadd45a*	growth arrest and DNA-damage-inducible 45 alpha	2.49±0.12	4.20±0.16	4.73±0.62	1.98±0.26	U00937
101979_at	Gadd45g*	growth arrest and DNA-damage-inducible 45 gamma	2.45±0.12	3.10±0.07	1.78±0.20	2.57±0.18	AF055638
Signalosome complex							
99113_at	Cops3	COP9 (constitutive photomorphogenic) homolog, subunit 3 (Arabidopsis thaliana)	3.73±0.20	3.08±0.09	1.37±0.17	-1.12±0.18	AF071313
95460_at	Cops5*	COP9 (constitutive photomorphogenic) homolog, subunit 5 (Arabidopsis thaliana)	2.90±0.07	3.30±0.08	1.55±0.18	-1.07±0.12	U70736
Carbohydrate metabolism							
96803_at	Gbe1	glucan (1,4-alpha-), branching enzyme 1	2.78±0.32	1.57±0.42	2.95±0.22	2.33±0.49	AW210370
103637_at	Naga	N-acetyl galactosaminidase, alpha	-3.61±0.27	1.23±0.07	-1.17±0.14	1.52±0.11	AJ223966
100573_f_at	Gpi1	glucose phosphate isomerase 1	1.93±0.07	2.49±0.13	3.13±0.16	1.28±0.21	M14220

Table 4.10. Differentially expressed genes after lactacystin treatment (continued): cell signaling. Gene expression is indicated as fold change±Standard Error. Only genes differentially expressed >3-fold and significantly expressed according to one-way ANOVA, $p<0.05$ are included in this list. * indicates genes that passed the Bonferroni Correction.

Probe id	Symbol	Gene Title	Time points (h)				Genbank
			4.5	7.5	24	48	
Cell signaling							
95022_at	Akap12*	A kinase (PRKA) anchor protein (gravin) 12	1.19 ± 0.09	-1.03 ± 0.08	3.13 ± 0.30	1.02 ± 0.10	AB020886
99481_at	Atp1a2	ATPase, Na+/K+ transporting, alpha 2 polypeptide	1.02 ± 0.08	-1.64 ± 0.07	-3.57 ± 0.09	-1.03 ± 0.26	AI839697
94006_at	Azi2*	5-azacytidine induced gene 2	3.29 ± 0.28	2.49 ± 0.15	-1.19 ± 0.13	-1.21 ± 0.11	AB007141
102773_at	Car8	carbonic anhydrase 8	-1.54 ± 0.37	-3.26 ± 0.14	-1.69 ± 0.13	-1.63 ± 0.11	X61397
102896_at	Dok1*	downstream of tyrosine kinase 1	3.28 ± 1.07	6.24 ± 0.31	3.79 ± 0.14	1.17 ± 0.17	U78818
97740_at	Dusp16	dual specificity phosphatase 16	2.35 ± 0.26	3.35 ± 0.11	2.67 ± 0.51	1.02 ± 0.20	AI642662
103550_at	Ednrb	endothelin receptor type B	1.63 ± 0.09	-3.50 ± 0.07	-1.62 ± 0.10	1.98 ± 0.17	U32329
98446_s_at	Ephb4*	Eph receptor B4	2.48 ± 0.09	3.16 ± 0.09	1.53 ± 0.11	-1.11 ± 0.12	U06834
101096_s_at	Hs1bp1	HS1 binding protein	2.20 ± 0.09	2.88 ± 0.06	1.42 ± 0.14	-1.07 ± 0.13	AF023482
99491_at	Il10rb*	interleukin 10 receptor, beta	-2.07 ± 0.16	-3.73 ± 0.07	-1.01 ± 0.11	1.25 ± 0.13	U53696
161796_r_at	Kcnq1*	potassium voltage-gated channel, subfamily Q, member 1	-2.37 ± 0.07	-4.41 ± 0.07	-1.56 ± 0.10	-1.19 ± 0.12	AV367240
103235_at	Npy*	neuropeptide Y	1.09 ± 0.08	-1.19 ± 0.06	-3.07 ± 0.09	-3.12 ± 0.10	AI848386
93007_at	Npy1r	neuropeptide Y receptor Y1	1.92 ± 0.10	1.15 ± 0.15	-4.01 ± 0.15	-2.59 ± 0.14	Z18280
102255_at	Osmr	oncostatin M receptor	-1.83 ± 0.41	-1.59 ± 0.25	3.84 ± 0.17	2.70 ± 0.21	AB015978
102049_at	Pdk4	pyruvate dehydrogenase kinase, isoenzyme 4	-1.74 ± 0.18	-4.52 ± 0.19	1.25 ± 0.16	1.81 ± 0.16	AJ001418

Table 4.11. Differentially expressed genes after lactacystin treatment (continued): growth and development. Gene expression is indicated as fold change±Standard Error. Only genes differentially expressed >3-fold and significantly expressed according to one-way ANOVA, $p<0.05$ are included in this list. * indicates genes that passed the Bonferroni Correction.

Probe id	Symbol	Gene Title	Time points (h)				Genbank
			4.5	7.5	24	48	
Growth and development							
101475_at	Bmi1	B lymphoma Mo-MLV insertion region 1	3.02 ± 0.14	2.88 ± 0.07	1.13 ± 0.12	-1.14 ± 0.16	M64068
100022_at	Cish*	cytokine inducible SH2-containing protein	2.16 ± 0.40	3.02 ± 0.14	-1.34 ± 0.10	-1.12 ± 0.10	D89613
93294_at	Ctgf	connective tissue growth factor	2.94 ± 0.70	2.11 ± 0.28	14.63 ± 0.63	7.93 ± 1.62	M70642
97426_at	Emp1*	epithelial membrane protein 1	1.18 ± 0.15	1.04 ± 0.08	4.98 ± 0.45	4.06 ± 0.14	X98471
100277_at	Inhba	inhibin beta-A	-2.15 ± 0.09	-3.25 ± 0.06	-1.77 ± 0.12	-1.59 ± 0.10	X69619
160463_at	Myd116	myeloid differentiation primary response gene 116	1.93 ± 0.09	4.30 ± 0.09	2.71 ± 0.47	1.12 ± 0.15	X51829
97474_r_at	Ptn*	pleiotrophin	-1.04 ± 0.08	-3.79 ± 0.07	1.04 ± 0.10	1.46 ± 0.13	D90225
95387_f_at	Sema4b	sema domain, immunoglobulin domain (Ig), transmembrane domain (TM) and short cytoplasmic domain, (semaphorin) 4B	8.87 ± 0.47	3.89 ± 0.12	1.07 ± 0.20	-1.36 ± 0.17	AA266467
99911_at	Sema6b	sema domain, transmembrane domain (TM), and cytoplasmic domain, (semaphorin) 6B	-4.00 ± 0.07	-2.12 ± 0.06	-1.66 ± 0.10	-1.82 ± 0.12	AF036585
103302_r_at	Sox3*	SRY-box containing gene 3	-3.45 ± 0.07	-2.25 ± 0.06	-1.12 ± 0.11	1.29 ± 0.11	AA866668
95436_at	Sst	somatostatin	1.35 ± 0.11	1.64 ± 0.08	-1.19 ± 0.19	-4.06 ± 0.10	X51468
161258_at	Wt1*	Wilms tumor homolog	-3.34 ± 0.10	-3.99 ± 0.07	-1.23 ± 0.10	-1.20 ± 0.10	AV322247
99549_at	Ogn	osteoglycin	1.03 ± 0.31	-6.87 ± 0.19	1.62 ± 0.49	4.77 ± 0.64	D31951

Table 4.12. Differentially expressed genes after lactacystin treatment (continued): other processes. Gene expression is indicated as fold change±Standard Error. Only genes differentially expressed >3-fold and significantly expressed according to one-way ANOVA, $p<0.05$ are included in this list. * indicates genes that passed the Bonferroni Correction.

Probe id	Symbol	Gene Title	Time points (h)				Genbank
			4.5	7.5	24	48	
Other processes							
97689_at	F3*	coagulation factor III	-1.16 ± 0.11	1.42 ± 0.14	3.29 ± 0.17	2.14 ± 0.17	M26071
98372_at	Aldh1a3	aldehyde dehydrogenase family 1, subfamily A3	1.43 ± 0.29	-1.94 ± 0.29	3.25 ± 0.21	-1.31 ± 0.13	AW050387
95133_at	Asns	asparagine synthetase	1.74 ± 0.07	3.13 ± 0.13	1.11 ± 0.24	-1.50 ± 0.17	U38940
96775_at	Cbx1	chromobox homolog 1 (Drosophila HP1 beta)	4.97 ± 0.10	1.47 ± 0.13	-1.36 ± 0.14	1.16 ± 0.12	X56690
160711_at	Decr1	2,4-dienoyl CoA reductase 1, mitochondrial	-1.97 ± 0.17	-4.46 ± 0.21	1.31 ± 0.37	2.94 ± 0.34	AI844846
160101_at	Hmox1	heme oxygenase (decycling) 1	1.11 ± 0.14	2.34 ± 0.11	5.39 ± 0.82	2.23 ± 0.49	X56824
162387_f_at	Mfn1	mitofusin 1	-4.95 ± 0.09	-2.55 ± 0.21	-1.31 ± 0.10	1.20 ± 0.11	AV255723
94485_at	Peci*	peroxisomal delta3, delta2-enoyl-Coenzyme A isomerase	2.00 ± 0.10	2.23 ± 0.09	3.11 ± 0.12	2.42 ± 0.38	AI840013
93542_at	Pter	phosphotriesterase related	1.33 ± 0.15	1.02 ± 0.12	1.56 ± 0.11	3.54 ± 0.51	U28016
162317_r_at	Rps12	ribosomal protein S12	-5.09 ± 0.18	1.30 ± 0.19	1.13 ± 0.22	-1.23 ± 0.16	AV064697
95049_at	Snrpd2	small nuclear ribonucleoprotein D2	3.17 ± 0.12	2.52 ± 0.18	1.21 ± 0.12	-1.10 ± 0.19	AI837853
94564_at	Sult4a1	sulfotransferase family 4A, member 1	1.40 ± 0.13	3.05 ± 0.07	-2.26 ± 0.16	-2.37 ± 0.19	AF059257
93794_at	Appbp1	amyloid beta precursor protein binding protein 1	3.45 ± 0.16	1.85 ± 0.13	1.13 ± 0.13	-1.21 ± 0.14	AI846393
102780_at	Npn3	neoplastic progression 3	4.13 ± 0.19	8.60 ± 0.52	18.46 ± 0.98	2.64 ± 1.18	Z31362

Table 4.13. Differentially expressed genes after lactacystin treatment (continued): unknown biological functions. Gene expression is indicated as fold change±Standard Error. Only genes differentially expressed >3-fold and significantly expressed according to one-way ANOVA, $p<0.05$ are included in this list. * indicates genes that passed the Bonferroni Correction.

Probe id	Symbol	Gene Title	Time points (h)				Genbank
			4.5	7.5	24	48	
Unknown biological processes							
97012_f_at	0610033H09Rik	RIKEN cDNA 0610033H09 gene	3.00 ± 0.23	2.44 ± 0.27	1.73 ± 0.14	1.08 ± 0.18	AI838702
104400_at	0610042I15Rik	RIKEN cDNA 0610042I15 gene	2.11 ± 0.10	2.97 ± 0.10	-1.80 ± 0.21	-1.98 ± 0.17	AF076956
95732_at	1110005L13Rik	RIKEN cDNA 1110005L13 gene	3.23 ± 0.12	2.17 ± 0.09	1.20 ± 0.10	-1.11 ± 0.16	AW047746
103773_at	1110020K19Rik	RIKEN cDNA 1110020K19 gene	1.66 ± 0.09	3.01 ± 0.46	1.06 ± 0.15	-1.30 ± 0.13	AW047874
104314_r_at	1110032A03Rik	RIKEN cDNA 1110032A03 gene	3.12 ± 0.95	4.51 ± 0.25	-1.08 ± 0.16	-1.03 ± 0.19	AI851206
96068_at	1500034J20Rik	RIKEN cDNA 1500034J20 gene	3.48 ± 0.19	1.97 ± 0.12	1.31 ± 0.16	1.10 ± 0.26	AI848821
95561_at	1700013H19Rik	RIKEN cDNA 1700013H19 gene	3.10 ± 0.27	1.53 ± 0.17	-1.05 ± 0.25	1.27 ± 0.12	AW120867
161004_at	1700097N02Rik*	RIKEN cDNA 1700097N02 gene	-2.14 ± 0.12	-3.37 ± 0.06	-1.03 ± 0.11	-1.01 ± 0.10	AA250414
98942_r_at	2310032D16Rik	RIKEN cDNA 2310032D16 gene	-2.99 ± 0.10	-4.97 ± 0.06	1.03 ± 0.19	1.14 ± 0.30	AW125284
92703_at	2310032M22Rik	RIKEN cDNA 2310032M22 gene	3.33 ± 0.15	1.95 ± 0.08	-1.05 ± 0.14	-1.37 ± 0.13	AI325791
104100_at	2310075E07Rik*	RIKEN cDNA 2310075E07 gene	-3.46 ± 0.10	-2.52 ± 0.07	1.31 ± 0.14	1.65 ± 0.11	AI845915
95449_at	2310075G12Rik	RIKEN cDNA 2310075G12 gene	-3.12 ± 0.11	-1.83 ± 0.06	-1.10 ± 0.11	1.16 ± 0.12	AW049793
161906_f_at	2410022L05Rik*	RIKEN cDNA 2410022L05 gene	-3.11 ± 0.09	-3.26 ± 0.06	-1.28 ± 0.10	-1.61 ± 0.12	AV113045
97864_at	2510049I19Rik	RIKEN cDNA 2510049I19 gene	3.66 ± 0.36	2.42 ± 0.13	1.15 ± 0.17	1.26 ± 0.17	AW258842
93802_at	2610103J23Rik	RIKEN cDNA 2610103J23 gene	5.92 ± 0.55	3.46 ± 0.62	1.56 ± 0.19	1.12 ± 0.21	AA815890
98973_at	2610318G08Rik*	RIKEN cDNA 2610318G08 gene	3.15 ± 0.22	4.09 ± 0.35	1.39 ± 0.18	1.10 ± 0.11	AA982595
100306_at	2700007P21Rik	RIKEN cDNA 2700007P21 gene	2.70 ± 0.22	6.66 ± 0.34	1.29 ± 0.18	-1.13 ± 0.15	AI510297
92268_at	2700007P21Rik	RIKEN cDNA 2700007P21 gene	2.60 ± 0.10	4.08 ± 0.22	1.49 ± 0.21	1.06 ± 0.14	AI854851
104470_at	2700066J21Rik	RIKEN cDNA 2700066J21 gene	2.61 ± 0.67	4.61 ± 0.13	1.77 ± 0.22	1.20 ± 0.18	AI957346
160752_at	2810002D13Rik	RIKEN cDNA 2810002D13 gene	-4.05 ± 0.17	-1.20 ± 0.14	-1.13 ± 0.10	1.00 ± 0.13	AA667021
104089_at	2810026P18Rik*	RIKEN cDNA 2810026P18 gene	3.53 ± 0.23	5.50 ± 0.23	1.35 ± 0.11	1.05 ± 0.10	AW045664
103071_at	2810429C13Rik*	RIKEN cDNA 2810429C13 gene	3.33 ± 0.10	2.52 ± 0.09	1.22 ± 0.11	1.35 ± 0.13	AI843655
92840_at	3110079L04Rik*	RIKEN cDNA 3110079L04 gene	4.91 ± 0.58	6.87 ± 0.17	1.54 ± 0.32	1.04 ± 0.12	AA683712
104356_at	4921516M08Rik	RIKEN cDNA 4921516M08 gene	3.39 ± 0.22	1.75 ± 0.25	1.10 ± 0.13	1.13 ± 0.11	AI465543
104639_i_at	4930553M18Rik	RIKEN cDNA 4930553M18 gene	3.05 ± 0.35	5.24 ± 0.18	1.13 ± 0.24	1.12 ± 0.28	AI464596
92992_i_at	5730497N03Rik*	RIKEN cDNA 5730497N03 gene	4.26 ± 0.39	3.11 ± 0.32	-1.20 ± 0.12	1.12 ± 0.15	AI324972
94426_at	6330575P11Rik	RIKEN cDNA 6330575P11 gene	2.72 ± 0.11	2.86 ± 0.08	-1.04 ± 0.26	-2.08 ± 0.18	AI851052
161104_at	9430099J10Rik	RIKEN cDNA 9430099J10 gene	3.82 ± 0.25	1.91 ± 0.22	1.10 ± 0.17	1.79 ± 0.13	AI846811

160713_at	AA407930	expressed sequence AA407930	2.08 ± 0.07	3.61 ± 0.21	2.74 ± 0.52	1.01 ± 0.15	AI841579
93464_at	Akap9	A kinase (PRKA) anchor protein (yotiao) 9	1.54 ± 0.08	-3.17 ± 0.07	-1.27 ± 0.10	-1.35 ± 0.14	AI561567
93900_at	Bat2	HLA-B associated transcript 2	1.42 ± 0.21	3.01 ± 0.12	-1.67 ± 0.13	-1.69 ± 0.18	AW050268
100946_at	Bat9	HLA-B-associated transcript 9	-1.21 ± 0.07	1.92 ± 0.07	5.47 ± 2.18	-1.07 ± 0.20	AF109906
103485_at	BC030046	cDNA sequence BC030046	-2.20 ± 0.07	-4.47 ± 0.07	-1.32 ± 0.26	1.07 ± 0.16	AA795415
100410_at	C330027G06Rik	RIKEN cDNA C330027G06 gene	3.24 ± 0.31	1.82 ± 0.15	1.14 ± 0.15	-1.04 ± 0.16	AW122781
103016_s_at	Cd68*	CD68 antigen	-1.39 ± 0.11	1.01 ± 0.09	3.10 ± 0.23	2.79 ± 0.51	X68273
162251_f_at	Centg2	centaurin, gamma 2	-1.51 ± 0.08	-3.15 ± 0.09	-1.38 ± 0.10	-1.22 ± 0.12	AV335015
160330_at	Chordc1*	cysteine and histidine-rich domain (CHORD)-containing, zinc-binding protein 1	1.66 ± 0.07	3.00 ± 0.07	1.56 ± 0.20	-1.24 ± 0.10	AW122453
97352_f_at	Coxvib2	cytochrome c oxidase subunit VIb, testes-specific	-1.93 ± 0.08	-3.61 ± 0.08	1.00 ± 0.27	2.66 ± 0.11	AW123567
95432_f_at	D16Wsu109e*	DNA segment, Chr 16, Wayne State University 109, expressed	3.00 ± 0.07	2.78 ± 0.10	-1.04 ± 0.11	-1.57 ± 0.10	AI844034
103861_s_at	D7Wsu128e*	DNA segment, Chr 7, Wayne State University 128, expressed	1.62 ± 0.07	3.86 ± 0.10	1.88 ± 0.13	-1.14 ± 0.11	AA388099
103862_r_at	D7Wsu128e*	DNA segment, Chr 7, Wayne State University 128, expressed	1.96 ± 0.08	3.01 ± 0.11	1.51 ± 0.11	-1.05 ± 0.10	AA388099
103460_at	Ddit4	DNA-damage-inducible transcript 4	2.36 ± 0.11	3.79 ± 0.19	1.11 ± 0.17	-1.03 ± 0.19	AI849939
100037_at	Ddx18	DEAD (Asp-Glu-Ala-Asp) box polypeptide 18	1.82 ± 0.23	2.98 ± 0.16	1.01 ± 0.12	-1.12 ± 0.21	AW213225
99096_at	Ddx24	DEAD (Asp-Glu-Ala-Asp) box polypeptide 24	1.82 ± 0.10	3.05 ± 0.07	1.35 ± 0.16	-1.30 ± 0.13	U46690
99366_at	E030024M05Rik*	RIKEN cDNA E030024M05 gene	-1.32 ± 0.13	1.01 ± 0.10	3.48 ± 0.21	3.24 ± 0.34	AI553536
98525_f_at	Erdr1	erythroid differentiation regulator 1	1.64 ± 0.12	3.02 ± 0.07	1.51 ± 0.24	-1.12 ± 0.18	AJ007909
92553_at	Es10	esterase 10	1.78 ± 0.09	1.67 ± 0.08	4.08 ± 0.11	2.21 ± 0.50	AB025408
96569_at	Fignl1*	fidgetin-like 1	-2.61 ± 0.07	-3.11 ± 0.06	-1.17 ± 0.10	1.13 ± 0.11	AA266298
93443_at	Fndc1	fibronectin type III domain containing 1	-3.37 ± 0.11	-1.90 ± 0.09	-1.38 ± 0.10	1.08 ± 0.16	AW212271
98531_g_at	Gas5*	growth arrest specific 5	2.25 ± 0.07	3.20 ± 0.08	2.08 ± 0.20	1.30 ± 0.14	AI849615
94805_f_at	Hist1h2ac	histone 1, H2ac	4.05 ± 0.10	3.04 ± 0.10	1.03 ± 0.14	1.03 ± 0.21	M33988
98090_at	Hrb2*	HIV-1 Rev binding protein 2	4.04 ± 0.21	3.24 ± 0.24	1.75 ± 0.11	-1.10 ± 0.13	AW210014
99109_at	Ier2	immediate early response 2	1.77 ± 0.08	3.53 ± 0.07	1.72 ± 0.14	1.24 ± 0.18	M59821
94384_at	Ier3*	immediate early response 3	4.75 ± 0.30	7.40 ± 0.48	7.33 ± 0.22	1.29 ± 0.28	X67644
102152_f_at	Igh-VS107*	immunoglobulin heavy chain (S107 family)	-3.88 ± 0.07	-3.28 ± 0.08	-1.36 ± 0.10	-1.12 ± 0.10	M16724
162006_r_at	Immt*	inner membrane protein, mitochondrial	-1.34 ± 0.07	-3.01 ± 0.07	-1.32 ± 0.10	-1.07 ± 0.10	AV334115
101501_r_at	Impact	imprinted and ancient	1.86 ± 0.26	1.29 ± 0.11	3.21 ± 0.56	1.19 ± 0.14	D87973
103523_at	Leng8	leukocyte receptor cluster (LRC) member 8	-5.32 ± 0.11	-1.12 ± 0.13	1.43 ± 0.24	1.10 ± 0.10	AI851703

101214_f_at	LOC14433	similar to glyceraldehyde-3-phosphate dehydrogenase	2.78 ± 0.07	3.07 ± 0.11	1.51 ± 0.17	-1.07 ± 0.16	M32599
92564_at	Lrrfip1	leucine rich repeat (in FLII) interacting protein 1	2.84 ± 0.35	1.22 ± 0.26	3.92 ± 0.30	2.37 ± 0.22	AI891475
98440_at	Ltb4dh*	leukotriene B4 12-hydroxydehydrogenase	1.13 ± 0.22	1.33 ± 0.16	10.74 ± 1.04	6.95 ± 1.90	AA596710
96151_at	Mocos*	molybdenum cofactor sulfurase	2.25 ± 0.28	2.16 ± 0.29	3.26 ± 0.13	1.08 ± 0.13	AA839813
96285_at	Myadm	myeloid-associated differentiation marker	-2.24 ± 0.10	-3.54 ± 0.07	-1.10 ± 0.12	1.03 ± 0.10	AJ001616
101366_f_at	Nvl*	nuclear VCP-like	3.47 ± 0.26	2.60 ± 0.20	1.26 ± 0.11	-1.26 ± 0.11	AA250299
100626_at	Odf2	outer dense fiber of sperm tails 2	1.64 ± 0.19	3.04 ± 0.31	1.08 ± 0.10	-1.16 ± 0.16	AF034105
103388_at	P42pop	Myb protein P42POP	-3.59 ± 0.06	-3.12 ± 0.07	-1.25 ± 0.13	-1.10 ± 0.12	AW047050
99926_at	Pigr*	polymeric immunoglobulin receptor	-4.91 ± 0.11	-3.78 ± 0.06	-1.42 ± 0.09	-1.11 ± 0.10	AB001489
96145_at	Pigt	phosphatidylinositol glycan, class T	-3.12 ± 0.08	-1.78 ± 0.07	-1.28 ± 0.16	1.03 ± 0.16	AW211407
95631_at	Ppp4c*	protein phosphatase 4, catalytic subunit	1.52 ± 0.10	3.06 ± 0.09	1.11 ± 0.11	1.02 ± 0.11	AF088911
97496_f_at	Prkcdbp*	protein kinase C, delta binding protein	1.17 ± 0.23	1.23 ± 0.18	5.96 ± 0.65	3.36 ± 0.17	AW048944
161006_at	R75096	expressed sequence R75096	-2.93 ± 0.10	-3.07 ± 0.07	-1.36 ± 0.10	-1.38 ± 0.11	AI853978
102724_at	Rabep1*	rabaptin, RAB GTPase binding effector protein 1	5.36 ± 0.50	3.28 ± 0.26	-1.14 ± 0.10	-1.43 ± 0.10	AI608324
95077_at	Rabggtb*	RAB geranylgeranyl transferase, b subunit	2.60 ± 0.09	3.77 ± 0.07	1.51 ± 0.26	-1.04 ± 0.10	U12922
97838_at	Rnu22*	RNA, U22 small nucleolar	3.38 ± 0.13	4.31 ± 0.22	2.16 ± 0.19	1.14 ± 0.12	AA684508
95664_at	Sec14l1*	SEC14-like 1 (S. cerevisiae)	2.21 ± 0.08	3.43 ± 0.09	-1.43 ± 0.11	-1.44 ± 0.13	AW048159
97160_at	Sparc	secreted acidic cysteine rich glycoprotein	1.28 ± 0.07	-1.84 ± 0.10	3.00 ± 0.17	3.64 ± 0.59	X04017
94387_at	Spata5	spermatogenesis associated 5	1.94 ± 0.11	2.87 ± 0.19	1.36 ± 0.26	-1.47 ± 0.19	AF016544
101995_at	Sqstm1*	sequestosome 1	3.11 ± 0.06	5.59 ± 0.09	3.58 ± 0.34	1.17 ± 0.27	U40930
104283_at	Tbc1d15*	TBC1 domain family, member 15	3.18 ± 0.11	3.82 ± 0.22	1.98 ± 0.14	1.39 ± 0.12	AI037493
99144_s_at	Tgoln1	trans-golgi network protein	1.74 ± 0.18	3.11 ± 0.10	1.25 ± 0.16	1.14 ± 0.20	D50031
92437_at	Tm7sf2	transmembrane 7 superfamily member 2	-1.29 ± 0.11	-1.09 ± 0.07	-4.50 ± 0.10	-2.69 ± 0.10	AW047445
100039_at	Tmem4	transmembrane protein 4	2.86 ± 0.24	2.93 ± 0.13	1.34 ± 0.10	1.25 ± 0.17	AW125880
162362_f_at	Tnc	tenascin C	3.27 ± 0.24	2.00 ± 0.16	2.46 ± 0.39	1.03 ± 0.33	AV230686
162463_at	Tpd52	tumor protein D52	-3.26 ± 0.25	-2.46 ± 0.09	-1.07 ± 0.10	-1.07 ± 0.15	AV059497
100717_at	U90926*	cDNA sequence U90926	-2.99 ± 0.07	-3.01 ± 0.06	-1.38 ± 0.10	1.02 ± 0.10	U90926
103753_at	Zzz3*	zinc finger, ZZ domain containing 3	3.06 ± 0.10	2.43 ± 0.18	1.29 ± 0.15	1.05 ± 0.11	AI159572

95685_at	Adult male testis cDNA, RIKEN full-length enriched library, clone:1700092M07 product:unknown EST, full insert sequence	2.55 ± 0.08	3.74 ± 0.11	1.22 ± 0.18	-1.30 ± 0.13	AI849678
161535_at	---	-2.76 ± 0.07	-3.37 ± 0.06	-1.31 ± 0.11	-1.23 ± 0.11	AV234882
162311_f_at	---	-2.22 ± 0.07	-3.54 ± 0.08	-1.11 ± 0.10	-1.20 ± 0.10	AV050648
161528_r_at	---	-1.14 ± 0.11	-3.51 ± 0.11	-1.99 ± 0.10	-1.06 ± 0.14	AV227261
161737_at	---	-5.94 ± 0.08	-2.93 ± 0.17	1.13 ± 0.12	-1.05 ± 0.13	AV312560
96963_s_at	Anti-PC rearranged Ig kappa chain V-J region mRNA, hybridoma 31-23-1, partial cds.	-5.41 ± 0.19	-3.10 ± 0.19	-1.41 ± 0.11	1.00 ± 0.11	L14553
101863_at	---	-5.45 ± 0.18	-1.42 ± 0.22	-1.18 ± 0.13	1.00 ± 0.16	C78246
161655_at	---	-1.78 ± 0.18	-8.10 ± 0.20	-1.02 ± 0.11	1.02 ± 0.13	AV099898
101217_at	---	-11.95 ± 0.15	-3.15 ± 0.11	-1.30 ± 0.10	1.06 ± 0.12	D18865
95891_at	Hypothetical LOC328660 (LOC328660), mRNA	-3.83 ± 0.10	-2.60 ± 0.09	-1.48 ± 0.10	1.10 ± 0.13	AI591977
102348_at	---	-2.41 ± 0.07	-4.37 ± 0.06	1.66 ± 0.25	1.17 ± 0.19	AI551087
96316_at	Transcribed sequences	3.01 ± 0.23	1.82 ± 0.15	-1.08 ± 0.12	1.21 ± 0.15	AI839289
103709_at	---	-5.41 ± 0.12	-3.78 ± 0.07	-1.27 ± 0.10	1.24 ± 0.18	AA763466

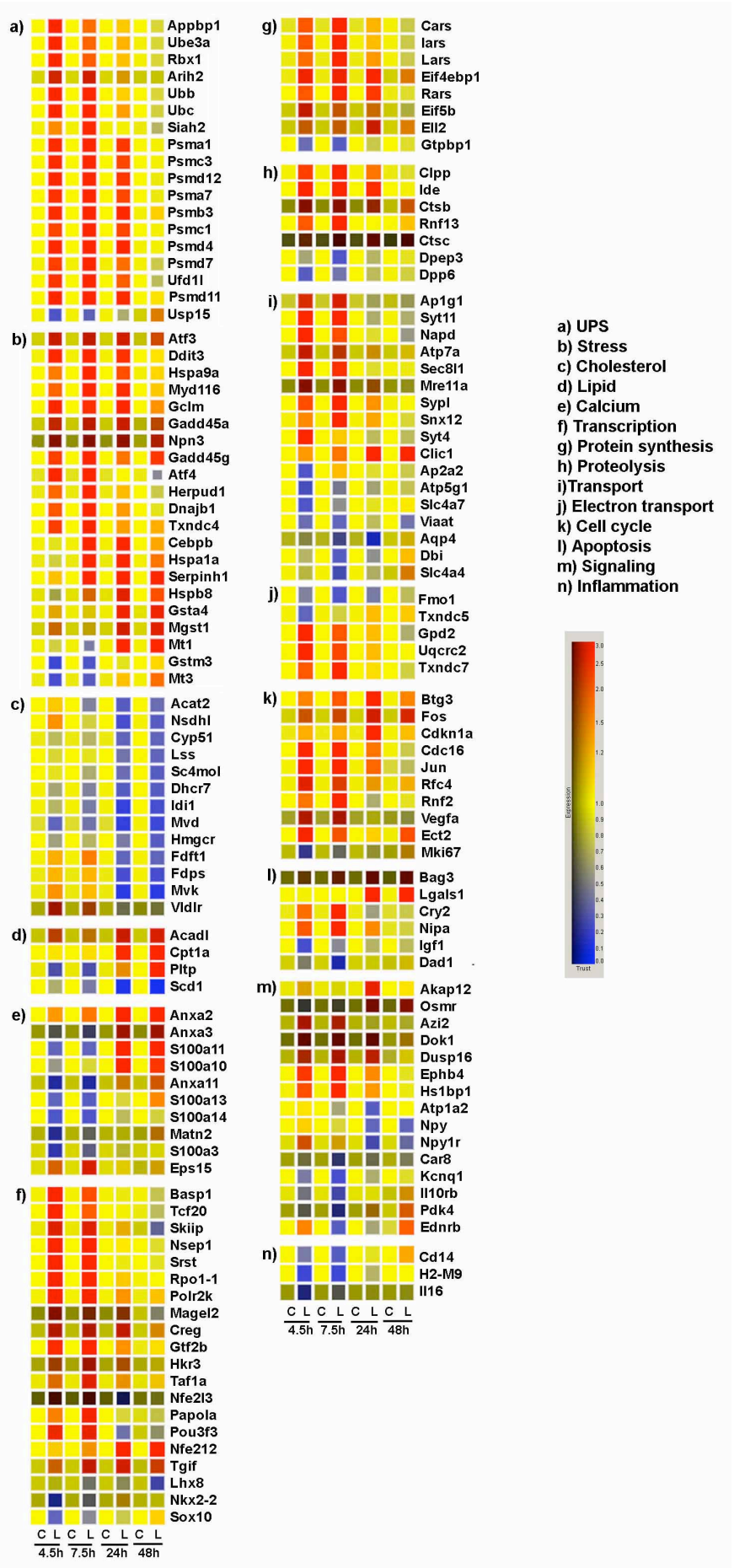
a)
Appbp1
Ube3a
Rbx1
Arih2
Ubb
Ubc
Siah2
Psma1
Psmc3
Psmd12
Psma7
Psmb3
Psmc1
Psmd4
Psmd7
Ufd1l
Psmd11
Usp15
b)
Atf3
Ddit3
Hspa9a
Myd116
Gclm
Gadd45a
Npn3
Gadd45g
Atf4
Herpud1
Dnajb1
Txndc4
Cebpb
Hspa1a
Serpinh1
Hspb8
Gsta4
Mgst1
Mt1
Gstm3
Mt3
c)
Acat2
Nsdhl
Cyp51
Lss
Sc4mol
Dhcr7
Idi1
Mvd
Hmgcr
Fdft1
Fdps
Mvk
Vldlr
d)
Acadl
Cpt1a
Pltp
Scd1
e)
Anxa2
Anxa3
S100a11
S100a10
Anxa11
S100a13
S100a14
Matn2
S100a3
Eps15
f)
Basp1
Tcf20
Skiip
Nsep1
Srst
Rpo1-1
Polr2k
Magel2
Creg
Gtf2b
Hkr3
Taf1a
Nfe2l3
Papola
Pou3f3
Nfe212
Tgif
Lhx8
Nkx2-2
Sox10
C L C L C L C L
4.5h 7.5h 24h 48h
g)
Cars
Iars
Lars
Eif4ebp1
Rars
Eif5b
Ell2
Gtpbp1
h)
Clpp
Ide
Ctsb
Rnf13
Ctsc
Dpep3
Dpp6
i)
Ap1g1
Syt11
Napd
Atp7a
Sec8l1
Mre11a
Sypl
Snx12
Syt4
Clic1
Ap2a2
Atp5g1
Slc4a7
Viaat
Aqp4
Dbi
Slc4a4
j)
Fmo1
Txndc5
Gpd2
Uqcrc2
Txndc7
k)
Btg3
Fos
Cdkn1a
Cdc16
Jun
Rfc4
Rnf2
Vegfa
Ect2
Mki67
l)
Bag3
Lgals1
Cry2
Nipa
Igf1
Dad1
m)
Akap12
Osmr
Azi2
Dok1
Dusp16
Ephb4
Hs1bp1
Atp1a2
Npy
Npy1r
Car8
Kcnq1
Il10rb
Pdk4
Ednrb
n)
Cd14
H2-M9
Il16
C L C L C L C L
4.5h 7.5h 24h 48h
a) UPS
b) Stress
c) Cholesterol
d) Lipid
e) Calcium
f) Transcription
g) Protein synthesis
h) Proteolysis
i)Transport
j) Electron transport
k) Cell cycle
l) Apoptosis
m) Signaling
n) Inflammation
Expression
Trust

Figure 4.5. The gene expression profile of lactacystin-treated cultured cortical neurons. Total RNAs were isolated from lactacystin-treated cultured cortical neurons at different time points: Control (n=4), 4.5 h (n=2), 7.5 h (n=3), 24 h (n=3) and 48 h (n=3). Expression of each gene was determined using Affymetrix GeneChip U74Av2. The data analysis was carried out using GeneSpring 7. The differentially expressed genes were grouped according to their biological processes: a) UPS, b) stress, c) cholesterol, d) lipid, e) calcium, f) transcription, g) protein synthesis, h) proteolysis, I) transport, j) electron transport, k) cell cycle, l) apoptosis, m) signaling and n) inflammation. The color bar=scale bar denotes changes in expression in fold-change, red indicates up-regulation and blue indicates down-regulation of genes.

4.2.3.1 Genes differentially expressed during the early phase of lactacystin-induced neuronal apoptosis

Ubiquitin-proteasome system

Almost all genes in cluster a) UPS were up-regulated in the early time points, as shown in red (Fig. 4.5). Genes that encode the proteasome subunits (*Psma1*, *Psmd12* and *Psmd7*), ubiquitins (*Ubb*), E2 ubiquitin conjugating enzyme (*Ubc*), ubiquitin protein ligase E3A (*Ube3a*) and ubiquitin fusion degradation 1-like (*Ufd1l*) were up-regulated as early as 4.5 h after lactacystin treatment. Most of the genes encoding the proteasome subunits were up-regulated persistently (until 24 h after lactacystin treatment), while others like *Ubb* and *Ubc* lasted only until 7.5 h after treatment (Table 4.1).

Heat shock proteins and molecular chaperones

The genes encoding heat shock proteins (HSPs) such as DnaJ (Hsp40) homolog subfamily B (*Dnajb1*), HSP A (*Hspa9a*), HSP70 (*Hspala*), HSP27 (*Hspb8*) and HSP47 (*Serpinh1*) were up-regulated later (at 7.5 h) compared with genes that encode proteasome subunits and ubiquitin. There was hardly any HSP gene expression detected at the 4.5 h time point (Table 4.2).

Endoplasmic reticulum stress

The group of genes that encodes protein response to ER stress consisted of the earliest pro-apoptotic genes to be up-regulated at early time points (Table 4.2). Genes encoding the transcription factor DNA-damage inducible transcript 3 (*Ddit3*), also known as C/EBP-homologous protein (*CHOP*), as well as its interaction partner

CCAAT/enhancer binding protein (C/EBP) beta (*Cebpb*), are involved in the induction of apoptosis mediated by ER stress (Rutkowski and Kaufman, 2004).

Inflammation

Genes associated with in inflammatory response, such as CD14 antigen (*Cd14*), histo-compatibility 2, M region locus 9 (*H2-M9*) and interleukin 16 (*Il16*), were down-regulated at early time points (Table 4.3).

4.2.3.2 Genes differentially expressed during the late phase of lactacystin-induced neuronal apoptosis

Antioxidant

Microarray data shows late up-regulation of genes involved in glutathione (GSH) biosynthesis, such as the glutamate-cysteine ligase, modifier subunit (*Gclm*), glutathione S-transferase, alpha 4 (*Gsta4*) and microsomal glutathione S-transferase 1 (*Mgst1*). Similarly, the gene encoding metallothionein 1 (*Mt1*) was also up-regulated at a later time point (Table 4.3).

Calcium homeostasis and binding

Genes encoding calcium-binding proteins such as Annexin A2 (*Anxa2*), Annexin A11 (*Anxa11*), S100 calcium-binding protein A10 (*S100a10*) and S100 calcium-binding protein A11 (*S100a11*) were also up-regulated at a later time point (24 h) (Table 4.4).

Cholesterol biosynthesis

Interestingly, most of the genes involved in the biosynthetic pathway of cholesterol were down-regulated after lactacystin treatment (Table 4.5). Genes encoding

enzymes involved in determining the rate of cholesterol biosynthesis, such as 3-hydroxy-3-methylglutaryl-Coenzyme A reductase (*Hmgcr*), as well as others such as cytochrome P450, 51 (*Cyp51*) 7-dehydrocholesterol reductase (*Dhcr7*), lanosterol synthase (*Lss*), mevalonate kinase (*Mvk*) and NAD(P)-dependent steroid dehydrogenase-like (*Nsdhl*) were all down-regulated during lactacystin-induced neuronal apoptosis.

4.2.4 Validation of differentially expressed genes identified by microarray analysis

4.2.4.1 Endoplasmic reticulum stress

Western blot analysis of proteins extracted from cultured cortical neurons treated with lactacystin (1 μM) for 7.5 h and 24 h detected CHOP protein expression (Fig. 4.6A). Similarly, the stress-associated activating transcription factor 3 (Atf3) protein was detected in protein samples from these two time points (Fig. 4.6A). Since ER stress-mediated cell death is associated with the disruption of calcium homeostasis and the activation of calpain, a calcium-regulated protease (Rutkowski and Kaufman, 2004), Western blot analysis was performed on the cell lysate of cultured cortical neurons treated with lactacystin, to check whether the calpain substrate p35 was cleaved into its truncated form of p25. Fig. 4.6A shows the presence of p25, the product of calpain cleavage, in the cell lysate 24 h after lactacystin treatment. Fig. 4.6B shows that the intracellular calcium chelator BAPTA-AM (2.5 μM), when co-applied with lactacystin (1 μM), could mildly improve the cell viability of cultured cortical neurons. This observation suggests that calcium homeostasis disruption might be involved in lactacystin-induced neuronal apoptosis (Fig. 4.6B).

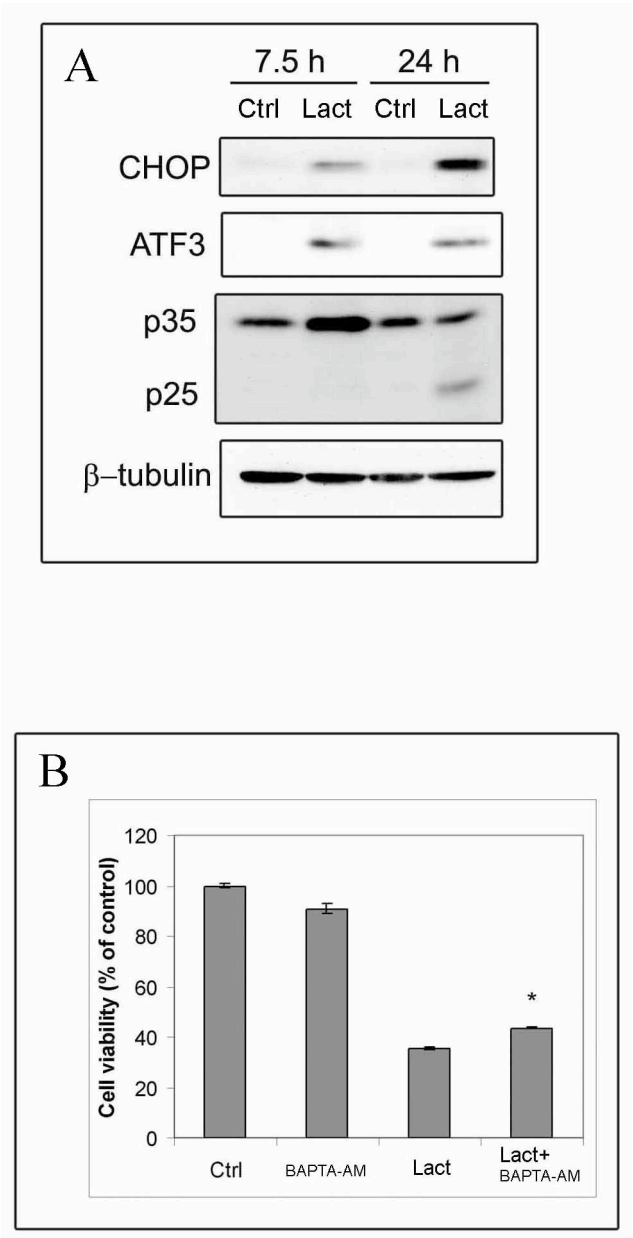

Figure 4.6. Lactacystin-induced ER stress-associated cell death events. (A) Western blotting showing the induction of Atf3 and Ddit3/CHOP proteins at 7.5 h and 24 h after lactacystin treatment. p35 was cleaved to p25 24 h after the cultured cortical neurons were exposed to 1 μM lactacystin. Since p35 is degraded by the UPS (Patrick et al, 1999), the increased p35 expression at the 7.5 h time point could have been due to the inhibition of proteasome degradation by 1 μM lactacystin. (B) MTT cell viability assay demonstrates a mild neuroprotective effect of 2.5 μM BAPTA-AM on lactacystin-induced neuronal apoptosis. * denotes significant difference compared to the treatment with 1 μM lactacystin (Lact), according to ANOVA with post hoc Tukey's test, $p<0.05$.

ER stress can also lead to the production of reactive oxygen species (ROS) (Pahl, 1999). ROS production can lead to the reduction of cellular GSH and ATP. The level of cellular GSH in lactacystin-treated cortical neurons decreased to 60% at 7.5 h, but rebounded to 80% at 24 h after lactacystin treatment (Fig 4.7). This could be due to the up-regulation of the GSH biosynthesis genes (Table 4.3).

4.2.4.2 The down-regulation of cholesterol biosynthesis

Real-time quantitative PCR reveals the down-regulation of mRNA expression of both acetyl-Coenzyme A acetyltransferase 2 (*Acat2*) and mevalonate (diphospho) decarboxylase (*Mvd*), confirming the microarray data (Fig 4.8A, Table 4.5). Corresponding to that, the total cholesterol levels in the lactacystin treated neurons were found to be significantly decreased compared to the untreated control (Fig 4.8B).

4.3 Discussion

Most microarray analyses are done at a single time point. This approach provides only a snapshot of molecular events. However, by performing a time course microarray study, we can determine the sequence in which these events occur, and whether they act in concurrence in a process like apoptosis. The time course microarray analysis revealed that a large number of genes were differentially expressed during lactacystin-induced neuronal apoptosis. Some of these genes were potentially neuroprotective while others were potentially pro-apoptotic. When these differentially expressed genes were grouped according to their biological functions, it

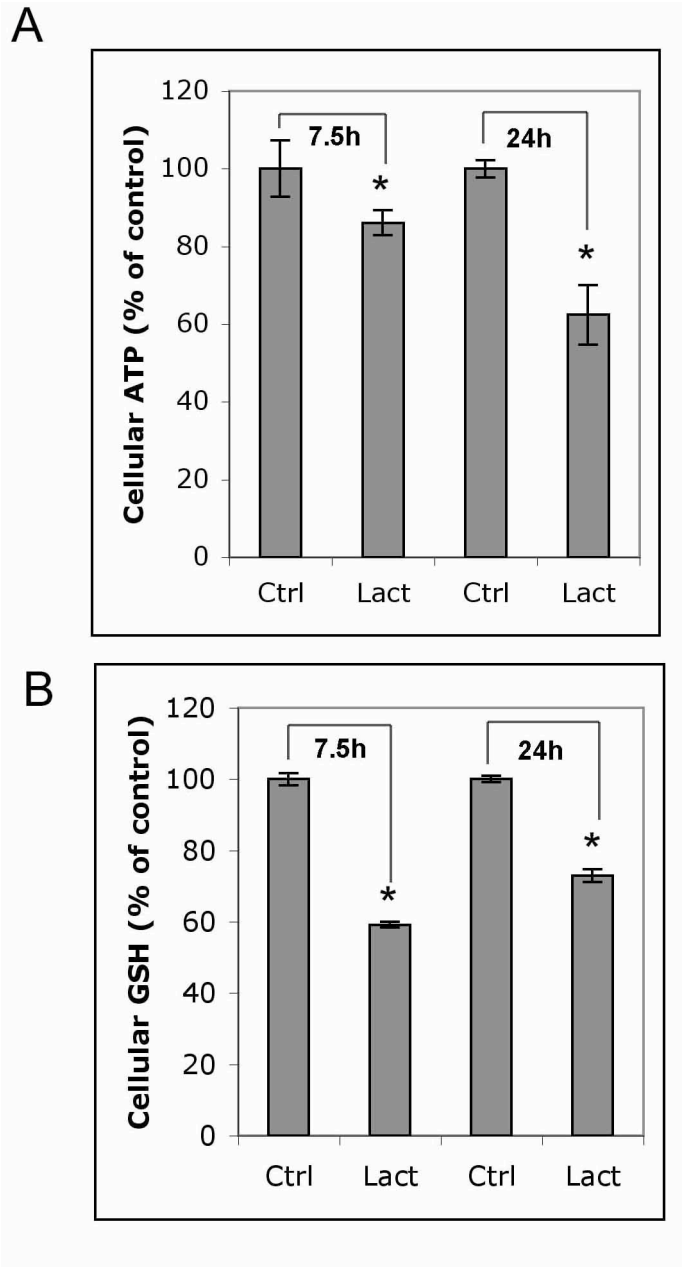

Figure 4.7. GSH and ATP levels in lactacystin-treated cultured cortical neurons. (A) Cellular ATP of cultured cortical neurons treated with 1 μM lactacystin decreased significantly 24 h after treatment. (B) Cellular GSH of cultured cortical neurons treated with 1 μM lactacystin decreased 7.5 h and 24 h after treatment. * denotes significant difference compared to the control according to ANOVA with post hoc Tukey's test, $p<0.05$.

became obvious that some groups of genes were differentially expressed at early time points while others were expressed at later time points. The following section discusses, in detail, the different groups of genes that might play important roles during lactacystin-induced neuronal apoptosis.

4.3.1 Ubiquitin-proteasome system

It is now evident that UPS plays an important role in the degradation of misfolded and unfolded proteins in neurons (Sherman and Goldberg, 2001; Schroder and Kaufman, 2005). The abnormal accumulation of proteins in neurons might be the main cause of neurodegeneration (Halliwell, 2002). Consistent with this hypothesis, alterations in proteasome function have been found in many biological processes, including aging (review in Gaczynska et al, 2001) and neurodegenerative diseases (Mandel et al, 2005). A recent study showed that genes encoding proteasome subunits were down-regulated in the Parkinson's diseased substantia nigra pars compacta, suggesting that a robust transcription of proteasome subunits might play an important role in the survival of cells under stress conditions (Mandel et al, 2005). In another study, pretreatment of cultured neocortical neurons with sub-lethal concentrations of proteasome inhibitors (for example with 10–100 nM MG-132, 0.1–3 nM epoxomicin or 10–30 nM clasto-lactacystin β-lactone) could increase proteasomal activity and promote resistance to oxidative injury (Lee et al, 2004). Recently, Chondrogianni et al demonstrated that stable over-expression of the proteasome β5 subunit alone was able to increase the amount of assembled proteasomes and confer protection against oxidative stress in primary IMR90 human fibroblasts (Chondrogianni et al, 2005). All these observations imply that enhancement of proteasomal activity is neuroprotective.

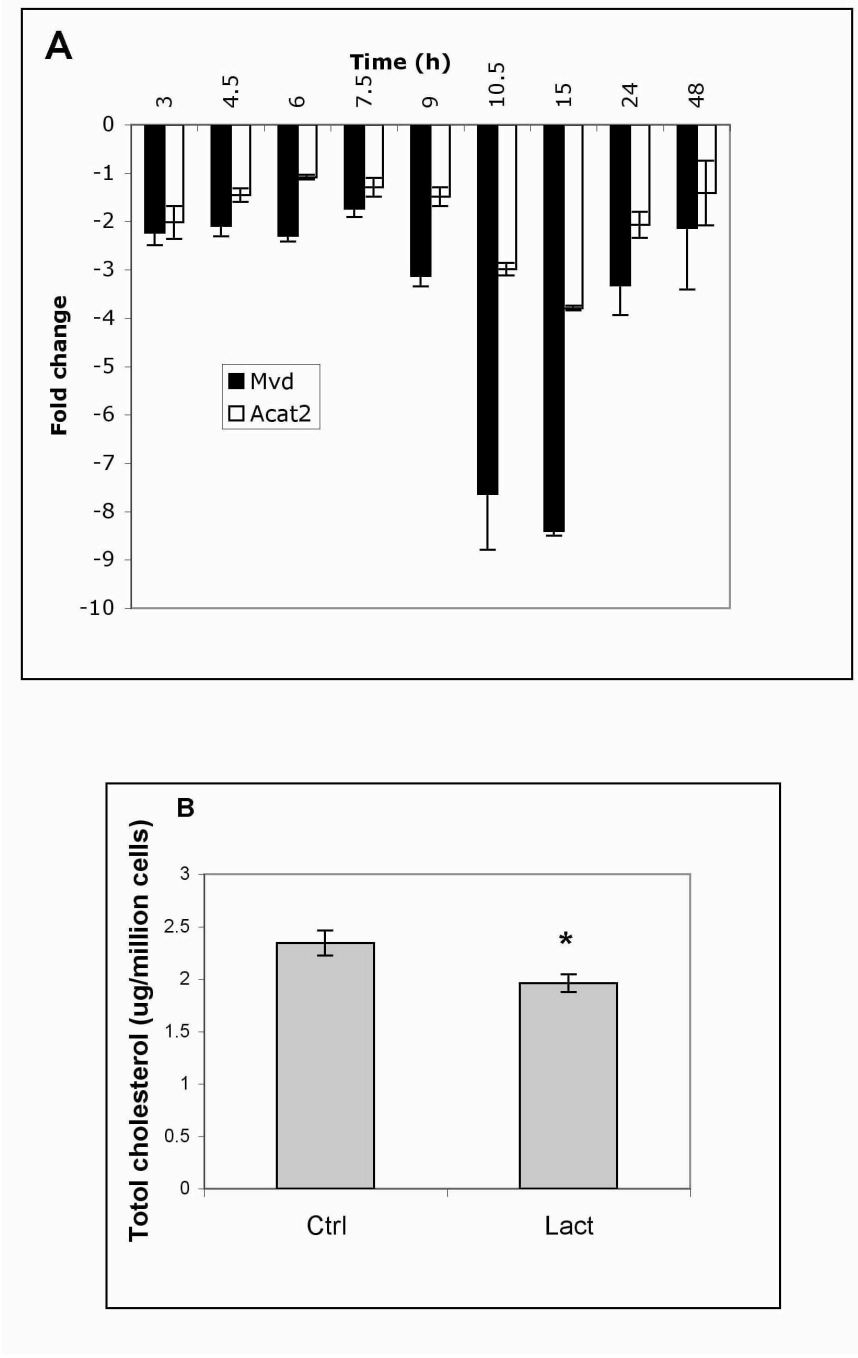

Figure 4.8. Exposure to lactacystin caused the down-regulation of genes associated with cholesterol biosynthesis. (A) Real-time quantitative PCR performed on total RNA extracted from cultured cortical neurons treated with 1 μM lactacystin at different time points show the down-regulation of *Mvd* and *Acat2* gene expression after treatment. (B) Total cholesterol of cells treated with 1 μM lactacystin was significantly lower compared to the control according to one sample t test ($p<0.05$), 24 h after treatment. * denotes significant difference compared to the control according to ANOVA with post hoc Tukey's test, $p<0.05$.

In this study, the microarray results revealed that genes encoding various proteasome subunits were up-regulated after lactacystin treatment (Table 4.1). This result is consistent with a similar study using primary cultures of rat vascular smooth muscle cells (Meiners et al, 2003). In the yeast *Saccharomyces cerevisiae*, genes encoding proteasomal subunits are preceded by a common upstream activating cis-element called the proteasome-associated control element. This proteasome-associated control element serves as a target sequence for the transcription factor Rpn4 that activates proteasomal gene expression in a concerted manner (Mannhaupt et al, 1999). Interestingly, Rpn4 is also a substrate of the 26S proteasome: the same protein that controls the induction of proteasome formation is also destroyed by the proteasome; such a combination, or regulatory mechanism, yields a negative feedback circuit in yeast. More recently, Rnp4 was found to be responsible for the elevation of proteasome subunit mRNA levels in response to various stress conditions such as the abnormal accumulation of proteins, suggesting that Rpn4 is indeed a master regulator responsible for the ability of the cell to compensate for proteasome inhibition (London et al, 2004; Glickman and Raveh, 2005).

Knowledge of the mechanisms by which mammalian proteasome formation is regulated is still very limited. Meiners et al showed that not only was there a transient and concerted up-regulation of the genes encoding the 26S proteasome subunit mRNA during proteasome inhibition, the inhibitor-induced proteasome gene activation resulted in enhanced de novo protein synthesis of all subunits, increasing the de novo formation of proteasomes. Their experiments present the first evidence that the amount of proteasomes in mammalian cells is regulated at the transcriptional level, and that there exists an autoregulatory feedback mechanism that compensates

for reduced proteasomal activity (Meiners et al, 2003; Goldbaum and Richter-Landsberg, 2004).

Besides that of proteasome subunits, the genes encoding ubiquitin (*Ubb*), ubiquitin-conjugating enzyme E2 (*Ubc*) and ubiquitin protein ligase E3A (*Ube3a*) were also significantly up-regulated, according to the microarray data (Table 4.1). The up-regulation of these genes might be neuroprotective, since they encode proteins that are essential for the UPS. Both *Ubb* and *Ubc* genes were reported to be up-regulated following ischemic injury in animal models, and therefore might play a role in the degradation of the denatured proteins resulting from oxidative stress during the injury (Noga and Hayashi, 1996). A recent report revealed that the presence of wild type or mutant ubiquitin transgenes resulted in a small but significant delay in the onset of clinical symptoms, and mild acceleration, respectively, of familial amyotrophic lateral sclerosis in animal models, although the neuroprotective mechanism at present is still not clear (Gilchrist et al, 2005).

The other group of genes that shows an early up-regulation during proteasomal inhibition is that of the ring finger protein. The ring finger proteins are proteins with the consensus sequence CX2CX(9-39)CX(1-3)HX(2-3_C/HX2CX(4-48)CX2C, with the Cys and His representing zinc-binding residues (Joazeiro and Weissman, 2000). Recent studies demonstrated that many ring finger-containing proteins are E3s that catalyze autoubiquitination and/or ubiquitination of their substrates (Joazeiro and Weissman, 2000; Yang and Yu, 2003). Ring finger-containing E3s play pivotal roles in diverse cellular processes and have been implicated in contributing to disease, such as in the case of the *Parkin* gene mutation and juvenile parkinsonism (Joazeiro and

Weissman, 2000). Ring finger E3 also plays key roles in the quality control of protein synthesis. For example, Hrd1p is a yeast ER membrane ring finger protein that regulates the degradation of abnormal ER protein via the UPS (Shen et al, 2004). Therefore, the up-regulation of these ring finger proteins might have a neuroprotective role against the accumulation of abnormal unfolded protein in neurons.

4.3.2 Heat shock proteins and molecular chaperones

Heat shock proteins (HSPs) with chaperoning function work together with the UPS to prevent the accumulation of misfolded, potentially toxic proteins, as well as to control catabolism of the bulk of cytoplasmic, cellular protein. The levels of these proteins are often increased in response to stress and they have been shown to enhance cell resistance to various insults (Bush et al, 1997; Ding and Keller, 2001). HSPs and molecular chaperones facilitate the refolding of misfolded proteins to prevent them from aggregating in the cell (Meriin and Sherman, 2005). Mammalian cells possess a number of HSPs, which are induced in response to stresses and display protective chaperone activity (Ohtsuka and Suzuki, 2000).

HSPs can act via two mechanisms to confer cellular protection. First, as molecular chaperones, where HSPs are active in the formation and maintenance of the native conformation of cytosolic proteins and the stabilization of actin filaments which make up the cytoskeleton of the cell. Second, both Hsp70 and Hsp27 can inhibit the release of cytochrome c by suppressing Bid, a pro-apoptotic member of the Bcl-2 family (review by Franklin et al, 2005).

Hsp70 proteins and their associated co-chaperones CHIP (carboxyl terminus of Hsp70-interacting protein)and Hsp40 are the best characterized among these proteins. Functionally, Hsp70 are ATPases that can bind newly exposed hydrophobic sequences on denatured proteins. The co-chaperones from the Hsp40 (Dnaj) family play essential roles in this process by stimulating the ATPase activity of Hsp70. When correct refolding is not possible, Hsp70/Hsp40 target bound substrates to proteasomal degradation in collaboration with other Hsp70-interacting proteins such as CHIP, and ubiquitin E3 ligase (McDonough and Patterson, 2003). Hsp70 can suppress both necrosis and apoptosis induced by various injuries in vivo and in vitro (Mosser et al, 2000; Sun et al, 2005; Lai et al, 2005). Although the majority of studies on the protective effect of individual HSPs have concentrated on the major inducible Hsp70, a variety of evidence suggests that the small Hsp27 may have a more potent protective effect in the nervous system (Latchman, 2005).

Another group of HSPs, called the small HSPs (sHSPs), consists of 10 members in humans and mice (Hspb1–10), of which Hsp27 (Hspb1) and Hsp22 (Hspb8) are the best-known representatives (Carra et al, 2005). Unlike Hsp70, sHSPs have no ATPase activity and binding to substrates appears to be modulated by the de-oligomerization of the sHSPs, a process itself modulated by mechanisms such as phosphorylation or temperature change (Giese and Vierling, 2002).

According to the microarray analysis, genes encoding both HSPs and sHSPs were up-regulated (Table 4.2). Recent findings have demonstrated that mutation of either Hsp27 or the related protein Hsp22 can be observed in specific families with hereditary motor neuropathy caused by premature axonal loss, possibly due to

neuronal death and subsequent degeneration. Therefore, Hsp27 appears to be a potent protective factor for neuronal cells whose mutation results in neuronal cell death and disease, whilst enhanced expression of the wild type protein may be a therapeutic option for human diseases involving excessive neuronal cell death (Latchman, 2005). A recent report demonstrated that Hsp27 expression is regulated by members of the cAMP response element binding protein (CREB)/ATF families, such as Atf3 and c-Jun. Atf3 is considered to be a nerve injury marker because it is not normally found in neuronal cells but is highly expressed in response to nerve injury (Takeda et al, 2000; Tsujino et al, 2000). Atf3 is also known as a stress-inducible gene (Liang et al, 1996; Hai et al, 1999). Recently, the expression of Atf3 is linked to proteasome inhibition (Zimmermann et al, 2000) and ER stress (Jiang et al, 2004). The Atf3 homodimer is known to function as a repressor, whereas the heterodimer, for instance in combination with c-Jun, functions as an activator for Hsp27, conferring neuroprotection against nerve injury (Nakagomi et al, 2003). Consistent with this observation, the microarray results (Table 4.2) show that up-regulation of the genes encoding both Atf3 and c-Jun preceded the up-regulation of the *Hsp27* gene.

Much of the research to date has focused on the actions of Hsp27 and Hsp70 individually, whereas the full therapeutic benefit of these molecules may be dependent on a better understanding of their combined neuroprotective action.

4.3.3 Endoplasmic reticulum stress

The ER is the site of protein synthesis in eukaryotic cells. The UPS regulates the removal of misfolded proteins in cells. Proteasome inhibitors can, however, disrupt this process and cause ER stress. Genes encoding these ER stress-associated

transcription factors, such as DNA-damaged inducible transcript 3 (Ddit3), also known as C/EBP-homologous protein (CHOP), CCAAT/enhancer binding protein (C/EBP) beta (Cebpb), and activating transcription factor 4 (Atf4), have been reported to be up-regulated during proteasomal inhibition and ER stress (Reimertz et al, 2003; Yew et al, 2005).

Ddit3/CHOP is a small nuclear protein transcription factor of the C/EBP family that is normally undetectable, but expressed at high levels in cells exposed to conditions that perturb protein folding in the ER and induce the ER stress response (Wang et al, 1996). The expression of Ddit3/CHOP in stressed cells is linked to the development of programmed cell death (Wang et al, 1998; Zimmermann et al, 2000, Fribley et al, 2004, Rao et al, 2004). The increase in Ddit3/CHOP protein expression is believed to lead to the suppression of Bcl-2 expression in cells, making them more susceptible to apoptosis (McCullough et al, 2001; Rao et al, 2004).

Besides being a principal site for protein synthesis and folding, the ER also acts as a site for calcium storage and calcium signaling (Rao et al, 2004). The pro-apoptotic response of ER stress can also be due to the disruption of calcium homeostasis in the cells. Thus, ER stress may result in the activation of calpain and subsequently trigger apoptosis through the activation of caspase-3 (Rutkowski and Kaufman, 2004). The calcium-regulated calpain is known to cleave p35, the neuronal-specific activator of cyclin-dependent kinase 5 (Cdk5), to produce p25, which is known to accumulate in the brains of patients with Alzheimer's disease (Lee et al, 2000). p25 could hyper-phosphorylate tau to disrupt the cytoskeleton and promote neuronal death (Lee et al, 2000; Kusakawa et al, 2000).

4.3.4 Inflammation

Neuroinflammation plays a key role in the pathophysiology of cerebral ischemia. Proteasomal inhibition is able to attenuate the inflammatory cascade in cerebral ischemia and reduce ischemic damage (Wojcik and Di Napoli, 2004). The mechanism of this neuroprotection involves the deactivation of NF-κB by stabilizing the inhibitor IκB, and preventing the translocation of NF-κB to the nucleus where it can bind to the promoter regions of pro-inflammatory genes. The effect of proteasome inhibitors on animal models has been recently evaluated. Intravenous infusion of PS-519 (analog of clasto-lactacystin β-lactone) effectively attenuated the expression of cell adhesion proteins, reducing the invasion of leukocytes and hence limiting brain tissue damage (Phillips et al, 2000). The microarray analysis shows that proteasomal inhibition by lactacystin caused an early down-regulation of genes associated with the inflammatory response (Table 4.3). This is so far consistent with the anti-inflammatory effect of proteasome inhibitors.

Other studies, however, reported that proteasome inhibition induced cyclooxygenase-2 (COX-2) activation in neuronal culture (Rockwell et al, 2000; Yew et al, 2005). Inflammatory pathways involving COX-2 enzymes and the subsequent generation of prostaglandins are potential causes of neurodegeneration such as amyotrophic lateral sclerosis (Consilvio et al, 2004) and Alzheimer's disease. Several regulatory elements on the murine COX-2 promoter, including a cyclic AMP response element, two C/EBP sites and a single NFκB site, have been shown to be involved in COX-2 promoter activation (Cieslik et al, 2002). The regulation of COX-2 expression during proteasome inhibition is unlikely to be mediated by NF-κB (Rockwell et al, 2000).

Instead, COX-2 may be activated by CCAAT/enhancer-binding protein-β (C/EBP-β) binding to the promoter region of COX-2 (Cieslik et al, 2002). Since C/EBP-β expression is mediated by ER stress, ER stress may be the trigger for the activation of COX-2 in neurons during proteasome inhibition.

Furthermore, the caspase activity assay reveals that both caspase-1 and caspase-5 were not activated in the course of lactacystin treatment; only caspase-4 activity was detected (Fig. 4.2B). Caspase-1, -4 and -5 are primarily involved in inflammatory response (Salvesen and Dixit, 1997). These caspases are needed in the maturation of cytokines. ER stress triggers apoptosis via an alternative intrinsic pathway that might involve the activation of caspase-12 (Rao et al, 2004). The involvement of caspase-12 during ER stress-mediated apoptosis in humans is still unclear since human counterparts of murine caspase-12 have not yet been identified. Recently, caspase-4 has been suggested to be involved in ER stress-mediated cell death (reviewed in Katayama et al, 2004). This report is consistent with the results of the current study.

4.3.5 Antioxidants

Oxidative stress has been linked to ER stress. The release of calcium into the cytosol could lead to the production of reactive oxygen species (ROS) (Pahl, 1999; McCullough et al, 2001). In our study, the groups of genes which are associated with antioxidant response, such as glutathione S-transferase, alpha 4 (*Gsta4*), microsomal glutathione S-transferase 1 (*Mgst1*) and metallothionein 1 (*Mt1*), were up-regulated at the later time points (Table 4.3). Besides their role in sequestration and distribution of metal ions such as copper and zinc, metallothioneins are known to provide cryoprotection from ROS. The down-regulation of metallothioneins is implicated in

redox status and increased susceptibility to oxidative stress and metal-induced neurotoxicity (Aschner et al, 1997). Cells also respond to oxidative stress by increasing the expression of genes associated with the antioxidant GSH, such as *Gsta4*, *Mgst1* and *Gclm* (Coppedè et al, 2005; Maeda et al, 2005; Chen et al, 2005). The *Gsta4* gene was previously reported to be up-regulated at a later time point after lactacystin treatment (Yew et al, 2005). Gsta4 is known for its high catalytic efficiency in the conjugation of 4-hydroxinonenal and other genotoxic products of lipid peroxidation during oxidative stress (Hubatsch et al, 1998). Mgst1, an ER-bound enzyme known for its oxidative stress protection, was also up-regulated. Cellular GSH is an important antioxidant in the cell. A decrease in its level was reported to be an early event in the pathogenesis of Parkinson's disease (Owen et al, 1996). In our study, the depletion of cellular ATP and GSH indicated that the neurons were under oxidative stress after lactacystin treatment (Fig. 4.7A and 4.7B). Since Gclm is the rate-limiting enzyme in GSH biosynthesis, an increased *Gclm* expression might have accounted for the 'rebound synthesis' of cellular GSH in the cultured neurons treated with lactacystin at the 24 h time point (Fig. 4.7B).

4.3.6 Cholesterol biosynthesis

Cholesterol, an essential component of cellular membranes, is synthesized on the ER surface (Chapman et al, 1998; Pahl, 1999). The disruption of cholesterol homeostasis in neurons has been associated with Alzheimer's disease. Furthermore, the down-regulation of the rate-limiting enzyme 3-hydroxy-3-methylglutaryl-Coenzyme A reductase (Hmgcr), encoded by the *Hmgcr* gene, causes cell death. The microarray data reveals that all genes involved in cholesterol biosynthesis were down-regulated 24 h after lactacystin treatment (Table 4.5). This data is supported by the decrease of

total cholesterol in neurons treated with lactacystin (Fig. 4.8B). In cultured neurons, the inhibition of Hmgcr using inhibitors such as pravastatin is sufficient to cause the reduction of neurite growth and ultimately cell death (Schulz et al, 2004; Tanaka et al, 2000). Not much is understood about the regulation of fatty acid and cholesterol synthesis in neurons (Koudinova et al, 2003; Pfrieger 2003). Cholesterol is a multifaceted molecule that serves as an essential membrane component (lipid raft) as well as a precursor for steroid hormone synthesis. In neurons, cholesterol is important for the stability of the synapse, in addition to maintaining synaptic plasticity (Pfrieger 2003).

How lactacystin treatment induces the down-regulation of lipid and cholesterol biosynthesis genes is not clear, but it is not unexpected that the synthesis of lipid and cholesterol will be affected during ER stress, since cholesterol is synthesized in the ER. A recent report suggests that cholesterol and fatty acid biosynthesis are controlled by a common family of transcription factors, known as the sterol regulatory element binding proteins (SREBPs) (Eberlé et al, 2004). Upon activation (eg. when the ER is deficient in lipid and sterol), the ER-anchored SREBP precursor transits to the Golgi, where it undergoes a sequential two-step cleavage process to release the NH2-terminal active domain, the designated nuclear form of SREBP, SREBP(N), which is transported to the nucleus and promotes the expression of many genes involved in cholesterol and fatty acid synthesis. Similarly, activating transcription factor 6 (ATF6), an ER membrane-bound transcription factor, can also undergo a similar two-step cleavage process to form ATF6(N) during ER stress. This proteolytic cleavage can cause the nuclear translocation of ATF6(N) to direct the transcriptional activation of chaperone molecules and enzymes essential for protein

folding. Zeng et al showed that over-expression of ATF6(N) in HepG2 (liver cell line) could suppress the SREBP(N)-mediated transcription of *HMGCR* and 3-hydroxy-3-methylglytaryl-Coenzyme A synthase (*HMGCS*) (Zeng et al, 2004). This report suggests a direct link between ER stress and the down-regulation of lipid and cholesterol biosynthesis.

Cholesterol biosynthesis is a complex synthetic pathway that requires dozens of enzymes and large amounts of energy (Pfrieger 2003). The down-regulation of cholesterol synthesis genes might be a step taken by cells to conserve energy, especially when cells are under stress.

4.3.7 Apoptosis

The microarray analysis picks up other genes that might be involved in the survival and cell death action of lactacystin. The gene encoding Bcl-2-associated athanogene 3 (*Bag3*) was found to be up-regulated strongly 24 h after lactacystin treatment (Table 4.2). Bag3 can form a complex with more than one apoptosis-modulating factor such as Hsp70 and Bcl-2 proteins, and thus can participate in apoptosis regulation (Antoku et al, 2001). An earlier study showed that the down-regulation of Bag3 enhanced the apoptotic response to chemotherapy in human primary B chronic lymphocytic leukemia cells (Romano et al, 2003). The role of Bag3 in neurons is, however, less clear, but based on the microarray results, it might have an important role in neuroprotection.

Insulin-like growth factor 1 (Igf1) is a 70-amino acid protein that is structurally similar to insulin. It acts as a major neurotrophic factor, promoting neuronal

proliferation and differentiation during normal brain development. Igf1 also acts as a neuroprotective survival factor under pathological conditions such as stroke, brain trauma, multiple sclerosis and Alzheimer's disease (Trejo et al, 2003; Carro and Torres-Aleman, 2004). The biological functions of Igf1 are mediated by the Igf1 receptor. Binding of Igf1 to the extracellular domain of the Igf1 receptor leads to the phosphorylation of the insulin receptor substrates IRS-1 and IRS-2, which results in the activation of two downstream signaling cascades for cell survival, namely the mitogen-activated protein kinase (ERK) and PI3-kinase/Akt pathways (Mendez et al, 2005). A recent study showed that direct administration of Igf1 into the intrathecal space may have a therapeutic benefit for amyotrophic lateral sclerosis (Nagano et al, 2005). In this microarray study, *Igf1* gene expression was down-regulated as early as 4.5 h after lactacystin treatment. This down-regulation of *Igf1* might contribute to the apoptosis of the neurons treated with lactacystin.

4.4 Conclusion

The UPS is involved in the regulation of many important biological processes in neurons. The study using microarray GeneChip® revealed that many potentially neuroprotective and pro-apoptotic genes were differentially expressed during proteasome inhibition by lactacystin. The early up-regulation of some genes is important in determining the fate of cells; genes encoding the proteasome subunits and HSPs were up-regulated early, before the onset of apoptosis in the lactacystin-treated cells. These genes seemed to have responded to the abnormal build-up of unfolded proteins in the cells caused by the inhibition of proteasome activity. Since lactacystin is an irreversible proteasome inhibitor, cells exposed to lactacystin can undergo apoptosis. The microarray data shows an early ER stress response after

lactacystin treatment, in spite of the up-regulation of neuroprotective genes such as those encoding proteasome subunits and HSPs.

The microarray data also reveals that some genes encoding neuroprotective antioxidants were up-regulated later, after the onset of apoptosis. This suggests the neurons were under oxidative stress at the later stages of proteasome inhibition. ER stress has been reported to cause oxidative stress in many cell death models (McCullough et al, 2001). The fact that ER stress-associated genes were up-regulated before the genes encoding antioxidants might suggest that ER stress is the main cause of cell death in lactacystin-induced cultured cortical neurons.

CHAPTER 5

5 Lipid profile of the neural membrane during lactacystin-induced neuronal apoptosis

5.1 Introduction

The microarray analysis of cultured cortical neurons subjected to proteasome inhibition using lactacystin reveals a significant down-regulation of genes associated with cholesterol and lipid biosynthesis, metabolism and homeostasis (Chapter 4, Table 4.5). The collective evidence from many studies suggests that neural membrane phospholipid metabolism is disrupted in neural trauma neurodegenerative diseases (review by Farooqui et al, 2004). The neural membrane is very complicated and diverse. It contains three major categories of lipids, phospholipids, cholesterol and sphingolipids, that form the membrane lipid bilayer. The cytoplasmic leaflets of membranes are enriched in the negatively-charged phospholipids that interact with positively-charged protein surfaces. Phosphoinositides play a particularly important role in the regulation of protein binding, because the number and location of negative charges on the inositol ring are controlled by a variety of kinases and phosphatases. The non-cytoplasmic leaflet of the membrane contains a variety of glycolipids, that, together with their interacting proteins, may contribute to the generation of lipid microdomains (Wenk and De Camilli, 2004). Phospholipids and sphingolipids not only form the lipid bilayer of membranes, but also act as reservoirs for the precursors of lipid signaling molecules or messengers such as acetylcholine, eicosanoids, diacylglycerol and ceramides (Review by Araki and Wurtman, 1998; Ariga et al, 1998; Buccoliero and Futerman 2003; Colombaioni and Garcia-Gil, 2004; Bazan et

al, 2005). Specific lipid messengers can be released from this reservoir of lipids by a class of proteins known as the phospholipases (Farooqui et al, 2004). This can happen in response to signals such as hormones, growth factors, cytokines, membrane depolarization, ion channel activation and neurotransmitters such as glutamate (Bazan et al, 2005). These lipid messengers are known to play important roles in the regulation of cell proliferation, differentiation and death.

The electrospray ionization mass spectrometry (ESI-MS) has been used successfully to study the lipid profile in complex lipid mixtures from human fibroblasts and cultured cortical neurons (Wenk et al, 2003). ESI-MS was used in this study to investigate the lipid profile of cultured cortical neurons during lactacystin-induced neuronal apoptosis. By comparing the lipid profile of apoptotic neurons with the control cells, it was observed that two groups of lipids were prominently accumulated in lactacystin-treated cultured neurons undergoing apoptosis. Ceramide, a second messenger, can be generated in cells undergoing cell death (review by Goswami and Dawson, 2000). Ceramide accumulation in neurons has been reported in various disorders associated with acute or chronic neurodegeneration. For example, recent studies have shown that ceramides accumulate in the normal aging brain and in the diseased brains of Alzheimer's disease patients (Goswami and Dawson, 2000). More interestingly, the lipid profile analysis also shows the accumulation of N-acyl phosphatidylethanolamine (NAPE) during lactacystin-induced neuronal apoptosis. NAPE is the precursor of anandamide (N-arachidonoylethanolamine) and other N-acylethanolamines (NAEs). Anandamide is an endogenous cannabinoid receptor ligand and has been reported to have neuroprotective property in vivo (Veldhuis et al, 2003). Therefore the accumulation of NAPE during lactacystin-induced neuronal

apoptosis might be a neuroprotective response. The significance of these results will be discussed subsequently.

5.2 Results

5.2.1 Lipid profile of lactacystin-treated cultured neurons

Lipids were extracted from mouse cultured cortical neurons and analyzed using negative-ion ESI-MS. The differences in the lipid profiles between control and lactacystin-treated cells (1 μM for 24 h) were computed using a chemometric method in a semi-quantitative fashion (Fig. 5.1). Among the most pronounced differences are (i) an increase in levels of ions with m/z 536, 564 and 600, (ii) a drop in levels of ions with m/z of 597, 714, 732, 760, 786, 965, and 967 and (iii) increased signals in m/z 980, 1004, and 1030. Some of these m/z correspond to small yet readily visible peaks in the single mass spectrum (e.g. 564, 760), while others, such as 965, 980, 1004, and 1030, are minor ions (Fig 5.1). Based on tandem mass spectrometry, the following trends were observed: (i) an increase in m/z which corresponds to ceramides; (ii) a drop in lysophosphatidylinositol, phosphatidylinositol phosphate (PIP), phosphatidylethanolamine (PE) and phosphatidylserine (PS) and (iii) up-regulation of levels of N-acyl phosphatidylethanolamines (NAPEs) (Fig. 5.2). In order to better characterize some of the ions which showed differential response, we used tandem mass spectrometry to show the MSMS of ions at m/z (A) 744, (B) 812 and (C) 976, which correspond to 34:1 PC or 36:1 PE, 38:3 PS and 54:2 NAPE (Fig. 5.3). The up-regulation of ceramide was confirmed by employing the precursor ion scan with the use of an internal standard (C-19-ceramide).

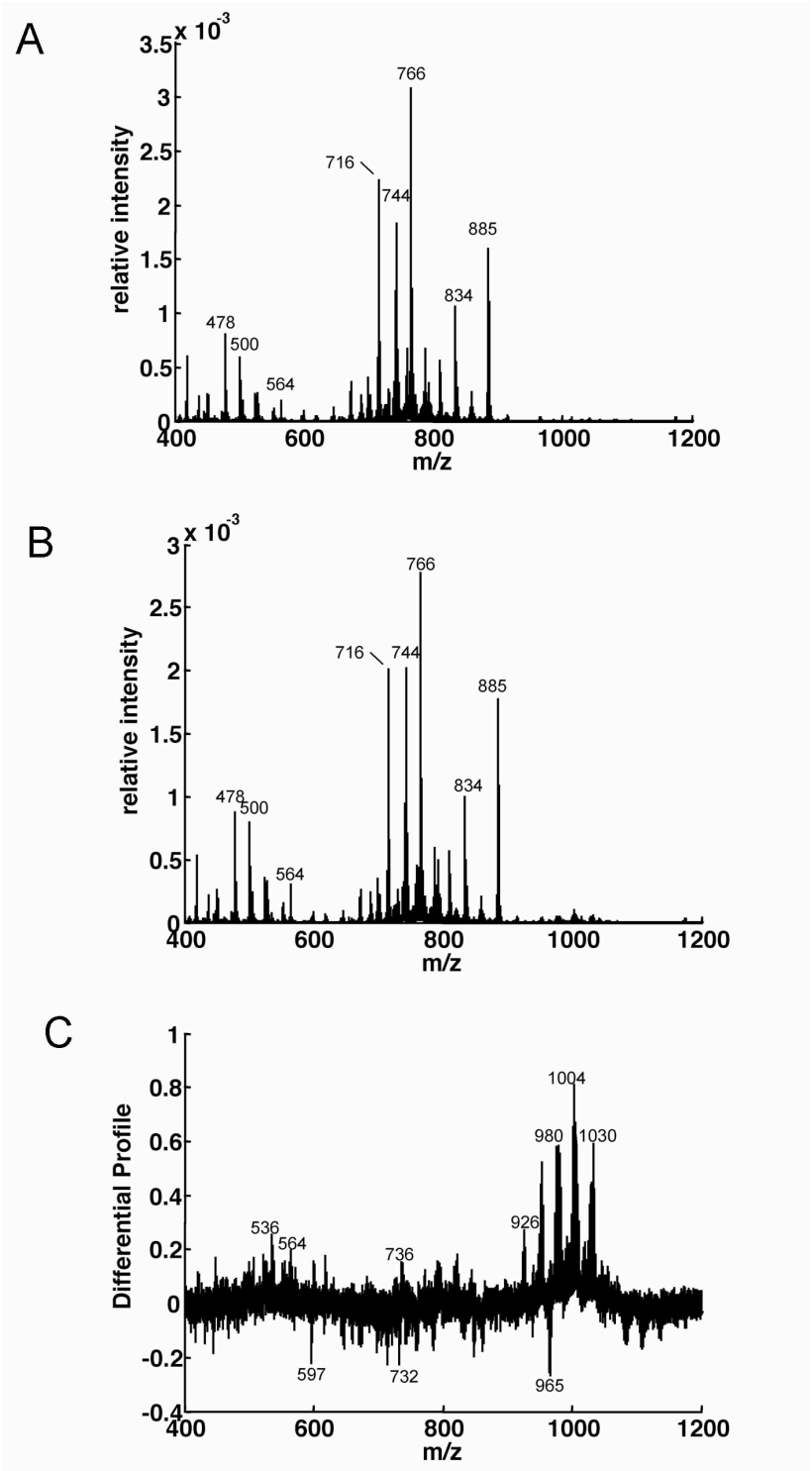

Figure 5.1. Differential analysis of lipid profile. Negative ion mode ESI-MS of control (A) and lactacystin-treated (B) cultured mouse cortical neuron lipids 24 h after treatment. Average spectra of independent experiments (n=4) for each condition was aligned and the relative difference (Lactacystin/Control) in peak intensity of negative molecular ions within the scan range of 400–1200 was computed (C).

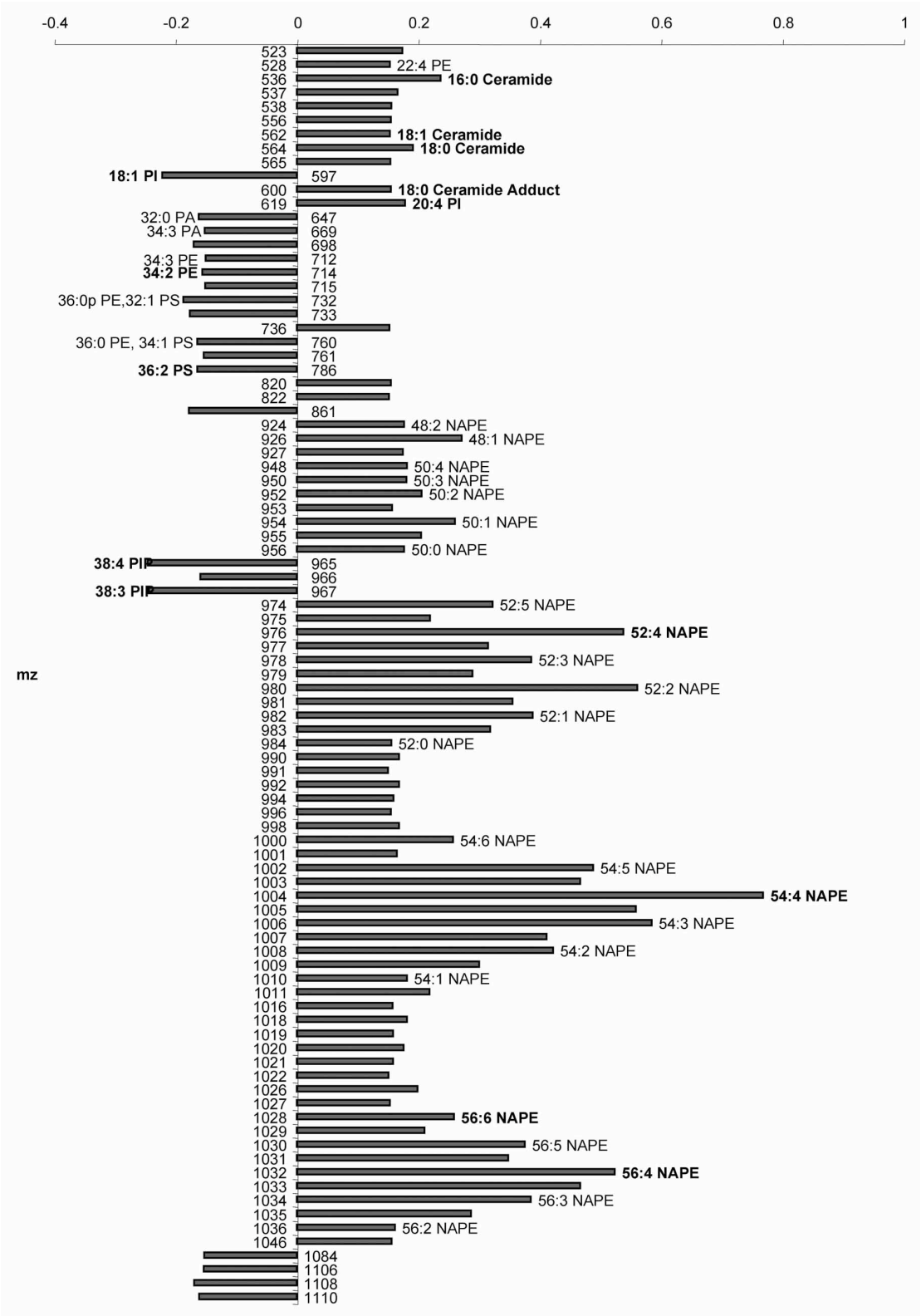

Figure 5.2. Lactacystin-induced changes in lipid profile of neurons and identification of lipid molecular species as revealed by ESI-MS and ESI-MSMS. Relative changes in lipid compositions 24 h after lactacystin exposure.

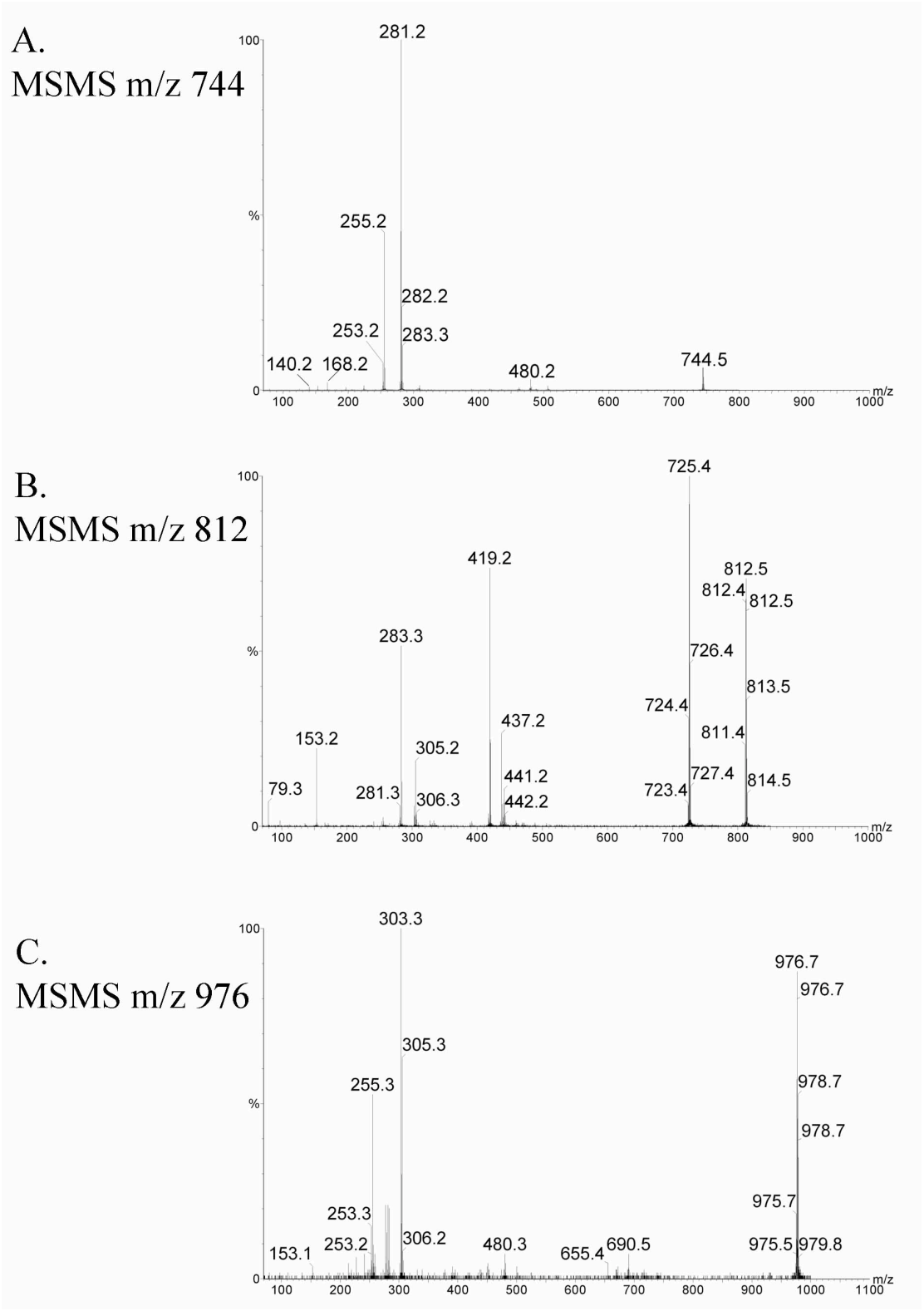

Figure 5.3. MSMS of ions at m/z (A) 744, (B) 812 and (C) 976, corresponding to 34:1 PC or 36:1 PE, 38:3 PS and 54:2 NAPE.

To check whether the changes of lipid profile changes in response to neuronal apoptosis, ESI-MS was used to analyze lipids extracted from cultured cortical neurons treated with 1 μM lactacystin for 7.5 h. Under this condition, neurons have yet to undergo apoptosis (Fig. 4.3B). The lipid profile obtained at this time point (Fig. 5.4) is different from that of cultures 24 h after lactacystin treatment. The changes in lipids from the early time point (7.5 h) are primarily of the ethanolamine/choline-containing lipids (note: ethanolamine and choline lipids can share the same mass and a single stage scan MS cannot differentiate the two). Other phospholipids (eg. Phosphatidyl-inositol-serine) did not show an observable change (Fig. 5.4). In contrast to the lipid profile obtained from apoptotic neurons (24 h time point), there were no elevations of NAPEs or ceramides at this time point.

5.3 Discussion

5.3.1 Lactacystin induces the accumulation of ceramide during neuronal apoptosis

The role of ceramide in neuronal cell death is well documented (Ariga et al, 1998; Goswami and Dawson, 2000; Buccoliero and Futerman, 2002). Ceramides can be generated in the cell either from de novo synthesis, by the action of sphingomyelinases (SMase) or from breakdown of complex glycolipids (Goswami and Dawson, 2000; Buccoliero and Futerman, 2003). Experimental manipulations that increase intracellular ceramide levels, for example, by treatment with bacterial sphingomyelinase or exposure to synthetic preparations of ceramide, potently induce apoptosis in mammalian cells (Ariga et al, 1998). Numerous signaling systems are associated with ceramide action, including activation of the mitogen-activated protein

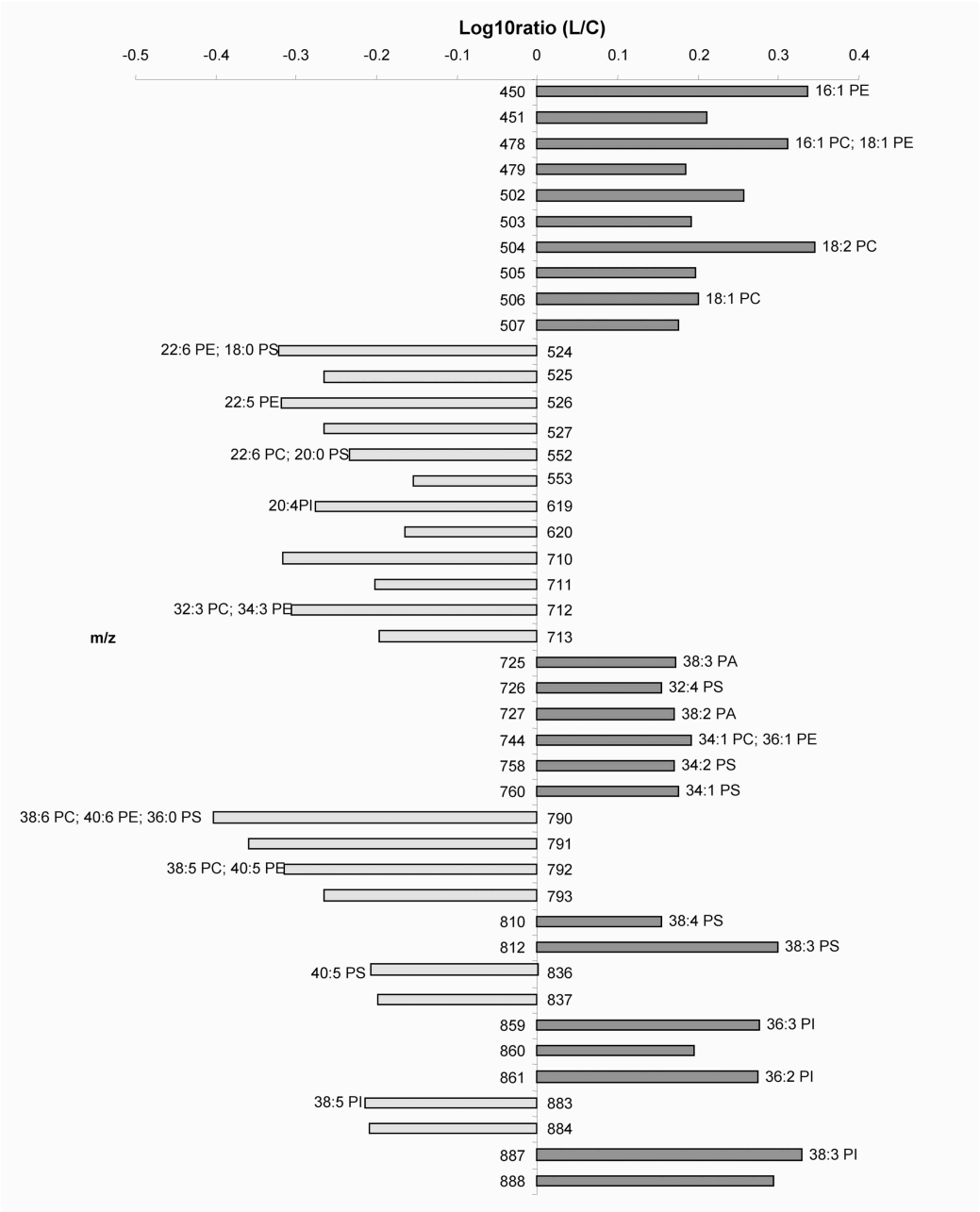

Figure 5.4. Lactacystin-induced changes in the lipid profile of neurons and identification of lipid molecular species as revealed by ESI-MS and ESI-MSMS. Relative changes in lipid compositions of mouse cultured cortical neurons 7.5 h after lactacystin exposure.

kinase (MAPK) cascade (Sotica et al, 2005) and death-associated protein kinase (DAPK) cascade (Pelled et al, 2002). Cutler et al recently reported that the accumulation of long-chain ceramides and cholesterol in the brain of Alzheimer's disease patients suggests the involvement of ceramides in the pathogenesis of Alzheimer's disease (Cutler et al, 2004). In spite of these, the role of ceramides in neuronal apoptosis induction is still debatable, since some data suggests that the formation of ceramides might be a post-apoptotic event (Sillence and Allan, 1998)

5.3.2 Lactacystin induces accumulation of NAPE during neuronal apoptosis

NAPE in which the free amino group of phosphatidylethanolamine is acylated by a further fatty acid is a common constituent of cereal grains (eg. wheat, barley and oats), and of some other seeds, but it may occur in other plant tissues too, especially under conditions of physiological stress (Chapman, 2000; Holmback et al, 2001). NAPE can be found in very small amounts in brain tissue. NAPE is the precursor of N-arachidonoylehtanolamine (anandamide) and N-acylethanolamines (NAEs). In animal tissues, anandamide and NAEs are principally biosynthesized through the transacylation-phosphodiesterase pathway, which consists of two enzyme reactions. The first reaction is the transfer of an acyl group from sn-1 position of glycerophospholipid to the amino group of phophatidylethanolamine (PE) and this is catalyzed by calcium-dependent N-acyltransferase. The resultant NAPE is then hydrolyzed to become NAE and phosphatidic acid by a phosphodiesterase of the phospholipase D (PLD)-type, generally abbreviated to NAPE-PLD (Ueda et al, 2005). The gene of NAPE-PLD has recently been cloned, and over-expression of NAPE-PLD was able to cause significant decreases in the NAPE level in transfected cells (Okamoto et al, 2005).

Anandamide is an endocannabinoid (or endogenous ligand) of the brain cannabinoid receptor (Maccarrone and Ainazzi-Agró, 2003). Anandamide is involved in many biological processes such as pain relief, regulation of cell growth, differentiation and even apoptosis (Calignano et al, 1998; Maccarrone and Ainazzi-Agró, 2003). The levels of anandamide and its precursor NAPE were markedly increased upon post-decapitative brain ischemia, experimental stroke and traumatic brain injury (Hansen et al, 2001; Ueda et al, 2005). The role of NAPE accumulation in cultured cortical neurons undergoing neuronal apoptosis is not clear, but recent studies have shown that anandamide was able to protect neurons against excitotoxicity and ischemic injury (Shen and Thayer, 1998; Sinor et al, 2000). Therefore, NAPE accumulation might indirectly confer neuroprotective effect on cells under cellular insults (Hansen et al, 2001).

So far, the accumulation of NAPE has been reported only in necrotic cell death models such as decapitative brain ischemia, experimental stroke and traumatic brain injury models (Hansen et al, 2001). In this study, however, the accumulation of NAPE was observed in an apoptotic cell death model. The apoptotic nature of the lactacystin-induced cell death model has been demonstrated in Chapter 3 of this thesis. One possible explanation for the accumulation of NAPE species during lactacystin-induced neuronal apoptosis is the involvement of ER stress in this cell death pathway. In the previous chapter, the microarray and Western blot data show that exposure of lactacystin (1 μM) to cultured cortical neurons can induce the up-regulation of ER stress-associated genes and proteins. Since ER is the main calcium store in cells, ER stress can cause the elevation of cellular calcium levels in affected

cells (Verkhratsky and Toescu, 2003). The elevation of cellular calcium could cause the activation of N-acyltransferase, and this would lead to the accumulation of NAPE species in neural membranes undergoing apoptosis.

The role of NAPE in neurons during neuronal apoptosis remains to be explored. Currently, there are only a handful of laboratories working on NAPE-related projects. With the recent successful cloning of the NAPE-PDL gene from mouse (Okamoto et al, 2005), a step closer to understanding the role of NAPE in neurons has been taken.

CHAPTER 6

6 Microarray analysis of gene expression during exposure to (-)-epigallocatechin-3-gallate on cultured cortical neurons

6.1 Introduction

The leaves of green tea (*Camellia sinensis*) contain many constituents; among these are the polyphenolic catechins, which are thought to confer beneficial biological effects such as neuroprotective, anti-carcinogenic and anti-inflammatory activities. Fresh tea leaves contain high amounts of polyphenolic catechins, which constitute 30–40% of the solid green tea extract (Wang et al, 1994). Among the tea catechins, (-)-epigallocatechin-3-gallate (EGCG) is the major constituent, accounting for more than 10% of the extract dry weight (Mandel and Youdim, 2004).

Initially, the beneficial biological effects of these polyphenolic catechins were thought to rely on the antioxidant and/or iron-chelating actions of its polyphenol constituents, and on modulation of endogenous metabolizing and antioxidant enzymes (reviewed in Mandel and Youdim, 2004). However, several recent studies have begun to associate the biological activity of the polyphenols present in green tea, especially EGCG, with the inhibition of proteasome activity (Wan et al, 2004; Shay and Banz, 2005). Like lactacystin, EGCG is found to specifically inhibit the chymotrypsin-like activity of the proteasome (Nam et al, 2001; Wan et al, 2004). The experiments carried out by Nam et al demonstrated that EGCG, at concentrations typically observed in the serum of green tea drinkers (1–10 μM), can inhibit proteasome activity and cause growth

arrest in the G1 phase of the cell cycle in several tumor and transformed cell lines (Nam et al, 2001).

In addition to its role in reducing the risk of cancers, consumption of EGCG-containing tea has also been shown to lessen the risk of atherosclerosis and to improve blood lipid levels (Shay and Banz, 2005). These clinically observed improvements were probably due to the inhibitory effect of EGCG on proteasomes. In this case, the target of proteasomal regulation may be the sterol regulatory element-binding proteins (SREBPs). SREBPs are a family of transcription factors that regulate lipid homeostasis in cells. Three isoforms of SREBPs have been known to control the expression of more than 30 genes required for the biosynthesis of cholesterol, fatty acids, triacylglycerols and phospholipids (Horton, 2002). Two SREBP genes encode three different isoforms; the isoform most directly related to cholesterol regulation is SREBP-2. Genes regulated by SREBP-2 include that of the low-density lipoprotein (LDL) receptor, and genes encoding enzymes of the cholesterol biosynthetic pathway, such as *Hmgcr*. Thus, the activation of SREBP-2 can lead to an increase in the transcription and synthesis of receptors that promote the uptake of cholesterol-containing lipoprotein from the serum into cells. Concurrently, intracellular cholesterol synthesis will also be promoted by the up-regulation of genes encoding the cholesterol biosynthetic enzymes. Since proteasome inhibition can stabilize the active SREBP-2 and induce the expression of LDL receptors (Hirano et al, 2001), the proteasomal inhibitory effect of EGCG might contribute to the cholesterol lowering (in serum) and heart disease-preventive effects of green tea (Kuhn et al, 2003).

In Chapter 4, the differentially expressed genes during lactacystin-induced neuronal apoptosis were analyzed using microarray GeneChip. In this chapter, microarray analysis was carried out once again to study the genes that were differentially expressed after the cultured cortical neurons were exposed to EGCG. The special focus for this study was to investigate whether EGCG could induce a gene expression profile similar to that observed for cultured cortical neurons treated with lactacystin (1 μM).

6.2 Results

6.2.1 EGCG induced apoptosis in primary cortical neurons with caspase-3 activation and proteasome inhibition

The MTT assay results showed decreasing cell viability with increasing EGCG concentrations, with about 67.46±2.08% and 31.64±1.61% residual cell viability with treatment with 20 μM and 50 μM EGCG for 24 h respectively; treatment with 1 μM EGCG for 24 h had little effect on cell viability (Fig. 6.1A). The caspase activity measurement using fluorogenic substrates indicated a 491% increase in caspase-3 activity (compared with the control) with treatment with 25 μM EGCG for 24 h. Treatment with 1 μM EGCG for 24 h, however, did not activate the caspase-3 activity (Fig. 6.1B). Other caspases that were found to be activated 24 h after treatment with 25 μM EGCG were caspase-2 (238%), caspase-4 (207%), caspase-6 (184%) and caspase-10 (248%) (Fig. 6.1B). The proteasomal activity (chymotrypsin-like) assay reveals that chymotrypsin-like activity in the cell lysate decreased to 60±0.3% after the cells were exposed to 25 μM EGCG for 24 h. The decrease of chymotrypsin-like activity was not detected in cells exposed to 25 μM EGCG for 7.5 h. Cells exposed to

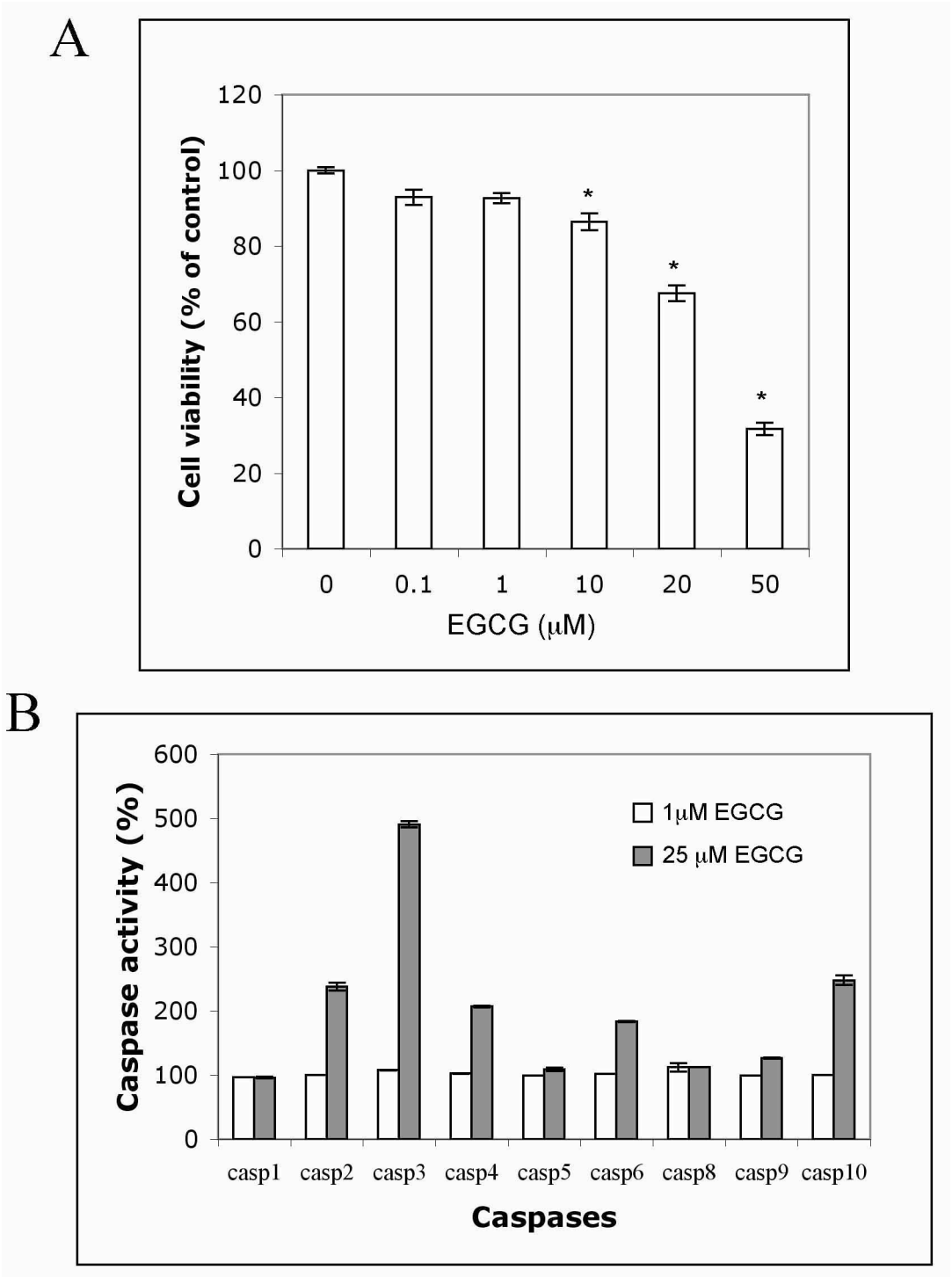

Figure 6.1. The effects of EGCG treatment on cell viability and caspase-3 activity activation of cultured cortical neurons. (A) The viability of EGCG-treated primary cortical neurons was quantified using the MTT assay. Cell injury was found to be concentration-dependent. * indicates significant difference according to ANOVA with post hoc Tukey's test, $p<0.05$. (B) Caspase activity measurement reveals the activation of caspase-3, as well as other caspases (caspase-2, caspase-4, caspase-6 and caspase-10) after treatment with 25 μM EGCG for 24 h.

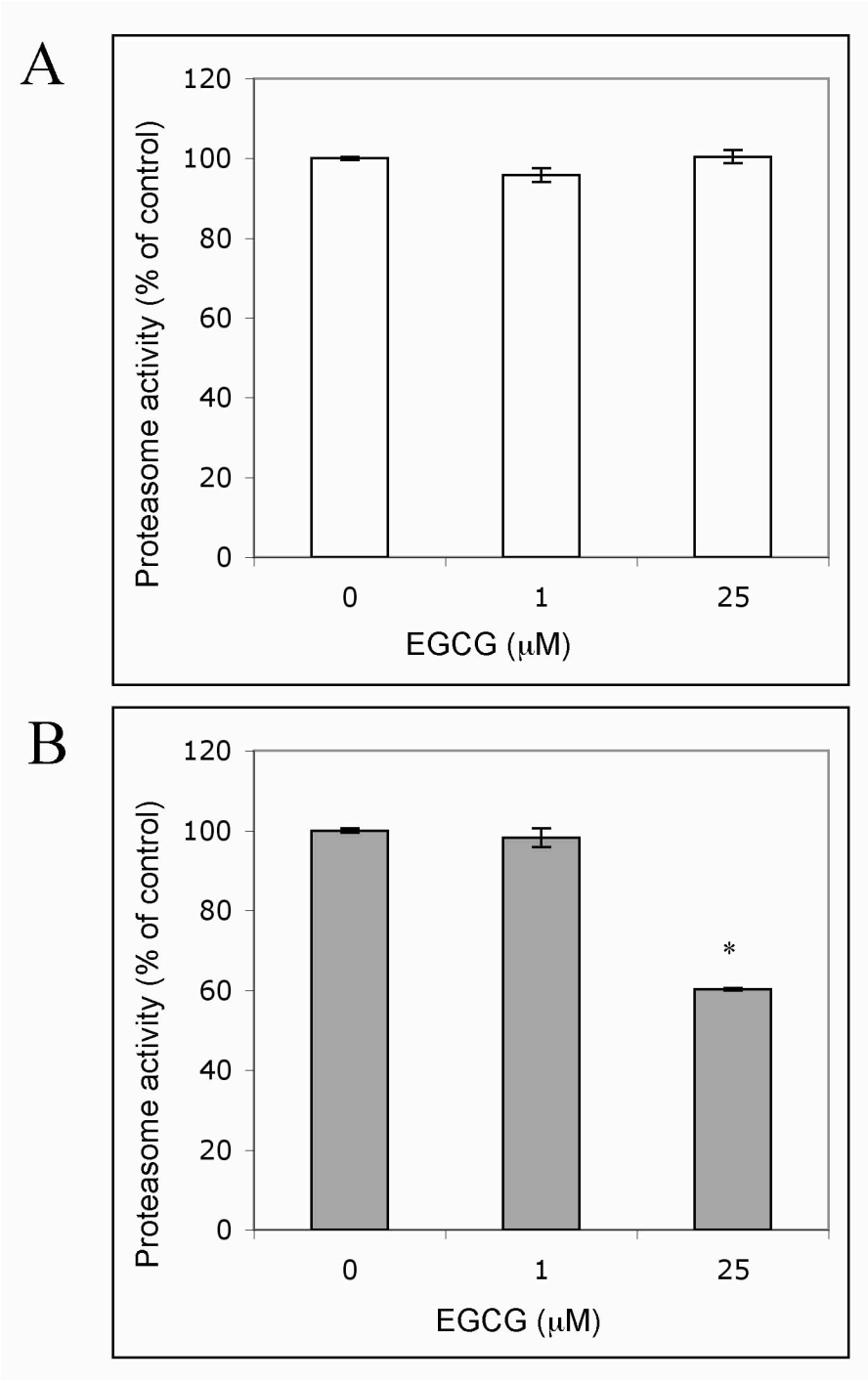

Figure 6.2. The effect of EGCG treatment on the chymotrypsin-like proteasome activity. Chymotrypsin-like activity of the proteasome was measured at (A) 7.5 h and (B) 24 h after the cultured cortical neurons were exposed to EGCG. * indicates significant difference according to ANOVA with post hoc Tukey's test.

1 μM EGCG did not show any inhibition of chymotrypsin-like activity at both 7.5 h and 24 h time points (Fig. 6.2). Taken together, the results from the chymotrypsin-like proteasomal activity assay and MTT assay show that exposure to a low dosage of EGCG (1 μM) did not induce chymotrypsin-like activity inhibition and neuronal cell death, but exposure to a high dosage of EGCG (25 μM) induced chymotrypsin-like activity inhibition and neuronal apoptosis.

6.2.2 Microarray analysis

Two EGCG treatment conditions were chosen for the microarray analysis: a low concentration (1 μM EGCG) that does not induce chymotrypsin-like proteasomal activity inhibition and neuronal apoptosis, and a high concentration (25 μM EGCG) that inhibits the chymotrypsin-like activity and induces neuronal apoptosis. Out of the 12,488 genes and ESTs from the Murine Genome U74Av2 GeneChip®, 387 were differentially expressed based on the criteria of genes showing a change of two-fold or more with a p-value of <0.01. These genes were identified and sorted according to their biological functions (Table 6.1–6.9).

6.2.3 Effect of EGCG on the protein expression of CHOP, Atf3 and the cleavage of p35

Western blot analysis shows that EGCG at high concentrations induced the expression of Atf3, but not CHOP, in the cultured cortical neurons (Fig. 6.3). This result is consistent with the microarray data (Table 6.1). There was no cleavage of p35 to p25 when the cultured cortical neurons were exposed to EGCG (25 μM), suggesting the absence of calpain activation during EGCG-induced neuronal apoptosis.

Table 6.1. Differentially expressed genes after EGCG treatment: Ubiquitin-proteasome system; heat shock proteins and molecular chaperones; response to stress; apoptosis. Gene expression is indicated as fold change ± Standard Error. Only genes differentially expressed >2-fold and significantly expressed according to one-way ANOVA, p<0.01 are included in the list.

Probe id	Symbol	Gene Title	EGCG (μM)		Genbank
			1	25	
Ubiquitin-proteasome system					
96892_at	Psma1	proteasome subunit, alpha type 1	1.81±0.41	2.08±0.35	AI836804
92544_f_at	Psma3	proteasome subunit, alpha type 3	2.15±0.41	2.14±0.35	AF055983
93988_at	Psma7	proteasome subunit, alpha type 7	1.97±0.41	2.05±0.35	AI836676
103319_at	Psmd10	proteasome 26S subunit, non-ATPase, 10	1.80±0.41	2.41±0.35	AB022022
160305_at	Psmd11	proteasome 26S subunit, non-ATPase, 11	2.14±0.41	2.53±0.35	AW121693
94302_at	Psmd4	proteasome 26S subunit, non-ATPase, 4	1.94±0.41	2.07±0.35	AF013099
98522_at	Psmd8	proteasome 26S subunit, non-ATPase, 8	1.92±0.41	2.04±0.35	AI839158
95124_I_at	Rbx1	ring-box 1	2.36±0.41	3.41±0.35	AW122337
160205_f_at	Rnf11	ring finger protein 11	2.07±0.41	2.30±0.35	AB024427
161814_f_at	Rnf19	ring finger protein (C3HC4 type) 19	3.08±0.41	2.63±0.35	AV355427
101966_s_at	Rnf13	ring finger protein 13	2.14±0.41	2.16±0.36	AF037206
101255_at	Ubb	ubiquitin B	3.00±0.41	3.26±0.35	X51703
95215_f_at	Ubc	ubiquitin C	2.71±0.41	2.95±0.35	D50527
93069_at	Ube2d2	ubiquitin-conjugating enzyme E2D 2	2.04±0.41	2.35±0.35	U62483
101581_at	Ube3a	ubiquitin protein ligase E3A	3.15±0.41	4.13±0.78	U82122
94018_at	Ubl3	ubiquitin-like 3	1.61±0.41	2.07±0.35	AW120725
93303_at	Ufd1l	ubiquitin fusion degradation 1 like	1.67±0.41	2.05±0.35	U64445
Heat shock proteins and molecular chaperones					
93743_at	Hsbp1	heat shock factor binding protein 1	2.20±0.41	2.34±0.35	AI838388
95699_f_at	2010009J04Rik	DnaJ (Hsp40) homolog, subfamily C, member 8	1.88±0.41	2.08±0.35	AI848094
97870_s_at	Ero1l	ERO1-like (S. cerevisiae)	-2.40±0.41	-1.93±0.35	AA798624
101207_at	Ppia	peptidylprolyl isomerase A	2.51±0.41	2.59±0.35	X52803
Response to stress					
95092_at	Ppp3ca	protein phosphatase 3, catalytic subunit, alpha isoform	2.05±0.41	1.98±0.35	J05479
100606_at	Prnp	prion protein	2.05±0.41	2.27±0.35	M18070
96773_at	Txndc4	thioredoxin domain containing 4 (endoplasmic reticulum)	1.97±0.41	2.62±0.35	AW125408
Apoptosis					
102727_at	Bdnf	brain derived neurotrophic factor	1.46±0.41	2.59±0.35	X55573
160696_at	Tia1	cytotoxic granule-associated RNA binding protein 1	2.20±0.42	2.07±0.35	U00689
102599_at	Tpt1	tumor protein, translationally-controlled 1	2.08±0.41	2.15±0.35	X06407

Table 6.2. Differentially expressed genes after EGCG treatment (continued): Transcription. Gene expression is indicated as fold change ± Standard Error. Only genes differentially expressed >2-fold and significantly expressed according to one-way ANOVA, p<0.01 are included in the list.

Probe id	Symbol	Gene Title	EGCG (μM)		Genbank
			1	25	
Transcription					
104155_f_at	Atf3	activating transcription factor 3	-2.58 ± 0.41	1.64 ± 0.36	U19118
95674_r_at	Basp1	brain abundant, membrane attached signal protein 1	3.16 ± 0.41	3.52 ± 0.35	AI851985
94490_at	Cnot8	CCR4-NOT transcription complex, subunit 8	1.63 ± 0.41	2.04 ± 0.35	AW122419
95460_at	Cops5	COP9 (constitutive photomorphogenic) homolog, subunit 5 (Arabidopsis thaliana)	2.46 ± 0.41	2.49 ± 0.35	U70736
160502_at	Creg	cellular repressor of E1A-stimulated genes	2.16 ± 0.42	2.80 ± 0.36	AF084524
97550_at	Hdac7a	histone deacetylase 7A	-2.20 ± 0.41	-1.99 ± 0.35	AW047228
161051_at	Hes5	hairy and enhancer of split 5 (Drosophila)	-1.12 ± 0.41	-2.34 ± 0.35	D32132
99024_at	Mad4	Max dimerization protein 4	2.15 ± 0.41	2.13 ± 0.35	U32395
104590_at	Mef2c	myocyte enhancer factor 2C	2.55 ± 0.41	2.30 ± 0.35	L13171
160138_at	Mxi1	Max interacting protein 1	1.50 ± 0.41	2.16 ± 0.35	L38822
96497_s_at	Myt1l	myelin transcription factor 1-like	1.91 ± 0.41	2.78 ± 0.35	AI848062
92893_at	Nfia	nuclear factor I/A	2.09 ± 0.41	2.28 ± 0.35	D90173
93740_at	Nsep1	nuclease sensitive element binding protein 1	3.48 ± 0.41	3.64 ± 0.35	U33196
99015_at	Pml	promyelocytic leukemia	-2.24 ± 0.41	-2.07 ± 0.35	U33626
160146_r_at	Polr2c	polymerase (RNA) II (DNA directed) polypeptide C	2.82 ± 0.41	2.65 ± 0.35	D83999
93325_at	Polr2e	polymerase (RNA) II (DNA directed) polypeptide E	1.96 ± 0.41	2.09 ± 0.35	AI845735
95003_at	Polr2k	polymerase (RNA) II (DNA directed) polypeptide K	6.43 ± 0.41	8.08 ± 0.35	AA880275
98085_f_at	Rpo1-1	RNA polymerase 1-1	2.82 ± 0.41	3.01 ± 0.35	U11248
99665_at	Satb1	special AT-rich sequence binding protein 1	2.12 ± 0.41	2.48 ± 0.35	U05252
160869_at	Sirt3	sirtuin 3 (silent mating type information regulation 2, homolog) 3 (S. cerevisiae)	2.21 ± 0.41	2.08 ± 0.35	AI849490
104158_at	Skiip	SKI interacting protein	4.23 ± 0.60	5.94 ± 0.35	AW046671
101684_r_at	Srst	simple repeat sequence-containing transcript	2.78 ± 0.41	3.86 ± 0.35	X67863
103504_at	Ssbp2	single-stranded DNA binding protein 2	2.21 ± 0.41	2.40 ± 0.35	AI837107
93918_at	Taf9	TAF9 RNA polymerase II, TATA box binding protein (TBP)-associated factor	2.69 ± 0.41	2.78 ± 0.36	AA673500
94008_at	Tceb1	transcription elongation factor B (SIII), polypeptide 1	2.04 ± 0.41	1.95 ± 0.35	AW045358
100947_at	Tcf20	transcription factor 20	3.38 ± 0.41	3.59 ± 0.35	AI847906
99603_g_at	Tieg1	TGFB inducible early growth response 1	2.08 ± 0.41	2.20 ± 0.35	AF064088
92444_f_at	Zfp1	zinc finger protein 1	1.94 ± 0.41	2.13 ± 0.35	X16493
94937_at	Zfp277	zinc finger protein 277	2.14 ± 0.41	2.89 ± 0.36	AW121594

Table 6.3. Differentially expressed genes after EGCG treatment (continued): Protein biosynthesis; protein modification. Gene expression is indicated as fold change ± Standard Error. Only genes differentially expressed >2-fold and significantly expressed according to one-way ANOVA, p<0.01 are included in the list.

Probe id	Symbol	Gene Title	EGCG (μM)		Genbank
			1	25	
Protein biosynthesis					
101213_at	Arbp	acidic ribosomal phosphoprotein P0	2.56 ± 0.41	2.60 ± 0.35	X15267
94766_at	Eef1a1	eukaryotic translation elongation factor 1 alpha 1	2.46 ± 0.41	2.60 ± 0.35	M17878
98141_at	Eif5b	eukaryotic translation initiation factor 5B	2.27 ± 0.41	3.00 ± 0.36	AA647048
98120_at	Mrpl27	mitochondrial ribosomal protein L27	1.86 ± 0.41	2.11 ± 0.35	AI844807
93859_at	Mtif2	mitochondrial translational initiation factor 2	2.39 ± 0.41	2.59 ± 0.35	AI875598
100720_at	Pabpc1	poly A binding protein, cytoplasmic 1	2.29 ± 0.41	2.04 ± 0.35	X65553
99975_at	Prkrir	protein-kinase, interferon-inducible double stranded RNA dependent inhibitor, repressor of (P58 repressor)	2.15 ± 0.41	2.25 ± 0.35	AA879937
96693_at	Rars	arginyl-tRNA synthetase	2.47 ± 0.41	2.41 ± 0.35	AI849453
94767_at	Rnu35b /// Rps11	RNA, U35b small nucleolar /// ribosomal protein S11	2.55 ± 0.41	2.69 ± 0.35	U93864
96290_f_at	Rpl21	ribosomal protein L21	2.20 ± 0.41	2.23 ± 0.35	U93863
100729_at	Rpl26	ribosomal protein L26	2.43 ± 0.41	2.69 ± 0.35	X80699
100734_at	Rpl3	ribosomal protein L3	2.34 ± 0.41	2.25 ± 0.35	Y00225
92577_f_at	Rpl37	ribosomal protein L37	2.07 ± 0.41	2.26 ± 0.35	AW047116
101129_at	Rpl5	ribosomal protein L5	1.86 ± 0.41	2.00 ± 0.35	X83590
97695_s_at	Rpl7	ribosomal protein L7	2.02 ± 0.41	2.05 ± 0.35	M29015
100694_at	Rplp1	ribosomal protein, large, P1	2.04 ± 0.41	2.05 ± 0.35	U29402
99590_at	Rps17	ribosomal protein S17	2.13 ± 0.41	2.29 ± 0.35	D25213
100686_at	Rps2	ribosomal protein S2	2.21 ± 0.41	2.10 ± 0.35	M20632
96300_f_at	Rps27	ribosomal protein S27	2.15 ± 0.41	2.49 ± 0.35	AI854238
101664_at	Rps3a	ribosomal protein S3a	2.48 ± 0.41	2.58 ± 0.35	Z83368
101212_at	Rps7	ribosomal protein S7	2.58 ± 0.41	2.57 ± 0.35	AF043285
Protein modification					
93460_at	Acvr1	activin A receptor, type 1	2.08 ± 0.42	2.20 ± 0.36	L15436
101936_at	Clk4	CDC like kinase 4	-2.29 ± 0.41	-2.33 ± 0.35	AF033566
161171_at	Dusp8	dual specificity phosphatase 8	1.52 ± 0.41	2.40 ± 0.35	AV226788
95298_at	Epha3	Eph receptor A3	2.26 ± 0.41	1.51 ± 0.36	M68513
161119_at	Epha5	Eph receptor A5	1.52 ± 0.41	2.07 ± 0.35	AI854630
92906_at	Epha7	Eph receptor A7	2.65 ± 0.41	2.56 ± 0.35	X79083
98446_s_at	Ephb4	Eph receptor B4	2.00 ± 0.41	1.99 ± 0.35	U06834
99511_at	Prkcb	protein kinase C, beta	2.07 ± 0.41	2.04 ± 0.35	X53532
97890_at	Sgk	serum/glucocorticoid regulated kinase	1.91 ± 0.41	2.16 ± 0.35	AW046181

Table 6.4. Differentially expressed genes after EGCG treatment (continued): Lipid and cholesterol biosynthesis; grwoth and development; electron transport; metal ion homeostasis. Gene expression is indicated as fold change ± Standard Error. Only genes differentially expressed >2-fold and significantly expressed according to one-way ANOVA, p<0.01 are included in the list.

Probe id	Symbol	Gene Title	EGCG (μM)		Genbank
			1	25	
Lipid and cholesterol biosynthesis					
94177_at	Hsd17b7	hydroxysteroid (17-beta) dehydrogenase 7	-1.47 ± 0.41	-2.43 ± 0.35	Y15733
95611_at	Lpl	lipoprotein lipase	1.62 ± 0.41	2.51 ± 0.35	AA726364
96909_at	Ndufab1	NADH dehydrogenase (ubiquinone) 1, alpha/beta subcomplex, 1	1.90 ± 0.41	2.21 ± 0.35	AI849803
98631_g_at	Nsdhl	NAD(P) dependent steroid dehydrogenase-like	2.31 ± 0.41	1.59 ± 0.35	AW106745
98630_at	Nsdhl	NAD(P) dependent steroid dehydrogenase-like	2.99 ± 0.41	1.85 ± 0.35	AW106745
94057_g_at	Scd1	stearoyl-Coenzyme A desaturase 1	1.01 ± 0.41	-3.66 ± 0.35	M21285
103569_at	Sh3glb1	SH3-domain GRB2-like B1 (endophilin)	2.70 ± 0.41	2.63 ± 0.35	AI842874
96534_at	Vldlr	very low density lipoprotein receptor	1.75 ± 0.42	2.58 ± 0.36	AA408956
Growth and development					
101475_at	Bmi1	B lymphoma Mo-MLV insertion region 1	3.35 ± 0.48	3.12 ± 0.35	M64068
160430_at	Catnb	catenin beta	1.86 ± 0.41	2.04 ± 0.35	M90364
100022_at	Cish	cytokine inducible SH2-containing protein	2.51 ± 0.41	3.05 ± 0.35	D89613
104386_f_at	Itgav	integrin alpha V	-1.63 ± 0.41	-2.05 ± 0.35	AI843901
93682_at	Ldb2	LIM domain binding 2	2.78 ± 0.41	2.70 ± 0.35	U89489
103549_at	Nes	nestin	-2.54 ± 0.41	-2.74 ± 0.35	AW061260
160668_at	Ogfr	opioid growth factor receptor	1.88 ± 0.41	2.10 ± 0.35	AI838195
95387_f_at	Sema4b	sema domain, immunoglobulin domain (Ig), transmembrane domain (TM) and short cytoplasmic domain, (semaphorin) 4B	7.13 ± 0.41	6.28 ± 0.40	AA266467
Electron transport					
102124_f_at	Cox4i1	cytochrome c oxidase subunit IV isoform 1	2.04 ± 0.41	2.06 ± 0.35	AI836879
100550_f_at	Cox6c	cytochrome c oxidase, subunit VIc	2.65 ± 0.41	2.73 ± 0.35	AW060422
101580_at	Cox7b	cytochrome c oxidase subunit VIIb	3.83 ± 0.41	3.93 ± 0.35	AI851220
95072_at	Cyc1	cytochrome c-1	2.58 ± 0.41	2.41 ± 0.35	AW121892
96112_at	Etfa	electron transferring flavoprotein, alpha polypeptide	2.11 ± 0.41	1.77 ± 0.35	AI851178
160194_at	Gcdh	glutaryl-Coenzyme A dehydrogenase	-2.28 ± 0.41	-2.28 ± 0.35	U18992
94208_at	Txndc7	thioredoxin domain containing 7	3.07 ± 0.41	2.45 ± 0.35	AW045202
160115_at	Txnl1	thioredoxin-like 1	2.40 ± 0.41	2.79 ± 0.35	AF052660
102000_f_at	Uqcrc2	ubiquinol cytochrome c reductase core protein 2	2.93 ± 0.41	3.31 ± 0.35	AI842835
Metal ion homeostasis					
101561_at	Mt2	metallothionein 2	-1.72 ± 0.41	-4.53 ± 0.35	K02236
95340_at	Mt3	metallothionein 3	-2.71 ± 0.41	-5.56 ± 0.35	M93310

Table 6.5. Differentially expressed genes after EGCG treatment (continued): Transmission of nerve impulse; transport. Gene expression is indicated as fold change ± Standard Error. Only genes differentially expressed >2-fold and significantly expressed according to one-way ANOVA, p<0.01 are included in the list.

Probe id	Symbol	Gene Title	EGCG (μM)		Genbank
			1	25	
Transmission of nerve impulse					
92946_f_at	Gria2	glutamate receptor, ionotropic, AMPA2 (alpha 2)	2.00 ± 0.41	2.40 ± 0.35	L32372
92392_at	Kcna3	potassium voltage-gated channel, shaker-related subfamily, member 3	2.45 ± 0.42	2.40 ± 0.36	AI850484
98339_at	Syt11	synaptotagmin 11	3.17 ± 0.41	3.29 ± 0.35	AB026808
160190_at	Syt4	synaptotagmin 4	2.87 ± 0.41	3.63 ± 0.35	U10355
Transport					
100032_at	Aaas	achalasia, adrenocortical insufficiency, alacrimia	2.03 ± 0.41	2.17 ± 0.35	X60136
101016_at	Arf1	ADP-ribosylation factor 1	2.34 ± 0.41	2.51 ± 0.35	D87898
102854_s_at	Atp7a	ATPase, Cu++ transporting, alpha polypeptide	2.09 ± 0.42	3.40 ± 0.36	U03434
94465_g_at	Clcn3	chloride channel 3	2.10 ± 0.41	2.70 ± 0.35	AF029347
103642_at	G3bp	Ras-GTPase-activating protein SH3-domain binding protein	-1.69 ± 0.41	-2.12 ± 0.35	AB001927
92749_at	Gabrb1	gamma-aminobutyric acid (GABA-A) receptor, subunit beta 1	2.42 ± 0.41	2.48 ± 0.35	U14418
161796_r_at	Kcnq1	potassium voltage-gated channel, subfamily Q, member 1	-2.72 ± 0.41	-2.94 ± 0.35	AV367240
101370_at	Kpna1	karyopherin (importin) alpha 1	1.83 ± 0.41	2.02 ± 0.35	U20619
92952_f_at	Napb	N-ethylmaleimide sensitive fusion protein attachment protein beta	3.26 ± 0.41	4.24 ± 0.35	X61455
102342_at	Nsf	N-ethylmaleimide sensitive fusion protein	2.14 ± 0.41	1.76 ± 0.35	U10120
101933_at	Rab10	RAB10, member RAS oncogene family	2.31 ± 0.41	2.49 ± 0.35	AF035646
160868_at	Rab3b	RAB3B, member RAS oncogene family	2.30 ± 0.41	2.57 ± 0.35	AI835990
98927_at	Rab6	RAB6, member RAS oncogene family	1.96 ± 0.41	2.53 ± 0.35	AI851048
104709_at	Sec23a	SEC23A (S. cerevisiae)	1.75 ± 0.41	2.00 ± 0.35	AI843665
93466_at	Sec8l1	SEC8-like 1 (S. cerevisiae)	2.93 ± 0.41	3.36 ± 0.35	AF022962
92831_at	Sfxn1	sideroflexin 1	2.22 ± 0.41	2.62 ± 0.35	AI846308
103918_at	Slc15a2	solute carrier family 15 (H+/peptide transporter), member 2	-1.01 ± 0.41	-8.64 ± 0.35	AI846682
93084_at	Slc25a4	solute carrier family 25 (mitochondrial carrier, adenine nucleotide translocator), member 4	2.32 ± 0.41	2.41 ± 0.35	U27315
104651_at	Snx14	sorting nexin 14	2.06 ± 0.41	2.38 ± 0.35	AI839611
97477_at	Timm8b	translocase of inner mitochondrial membrane 8 homolog b (yeast)	2.02 ± 0.41	2.06 ± 0.35	AW124594
93215_at	Tnfaip1	tumor necrosis factor, alpha-induced protein 1 (endothelial)	1.96 ± 0.41	2.04 ± 0.35	AF061346
101420_at	Viaat	vesicular inhibitory amino acid transporter	-4.35 ± 0.41	-3.73 ± 0.35	AJ001598
97876_at	Vps29	vacuolar protein sorting 29 (S. pombe)	2.34 ± 0.41	2.44 ± 0.35	AI842008

Table 6.6. Differentially expressed genes after EGCG treatment (continued): Cytoskeleton; cell cycle; proteolysis; calcium homeostasis and binding. Gene expression is indicated as fold change ± Standard Error. Only genes differentially expressed >2-fold and significantly expressed according to one-way ANOVA, p<0.01 are included in the list.

Probe id	Symbol	Gene Title	EGCG (μM)		Genbank
			1	25	
Cytoskeleton					
95705_s_at	Actb	actin, beta, cytoplasmic	-10.86± 0.41	-10.31± 0.35	J04181
96573_at	Actg	actin, gamma, cytoplasmic	2.65± 0.41	2.50± 0.35	M21495
93288_at	Arpc2	actin related protein 2/3 complex, subunit 2	2.30± 0.41	2.48± 0.35	AI835883
94863_r_at	Dncl2a	dynein, cytoplasmic, light chain 2A	2.47± 0.41	2.89± 0.35	AI850000
93674_at	Fgd1	FYVE, RhoGEF and PH domain containing 1	1.14± 0.41	2.29± 0.35	U22325
100398_at	Kif3a	kinesin family member 3A	2.14± 0.41	2.02± 0.35	D12645
94321_at	Krt1-10	keratin complex 1, acidic, gene 10	1.92± 0.41	2.16± 0.35	V00830
102742_g_at	Mapt	microtubule-associated protein tau	3.15± 0.41	3.49± 0.35	M18775
97909_at	Stmn1	stathmin 1	2.15± 0.41	2.26± 0.35	AI838080
96426_at	Tmsb4x	thymosin, beta 4, X chromosome	2.05± 0.41	2.13± 0.35	U38967
100342_i_at	Tuba1	tubulin, alpha 1	2.87± 0.41	2.94± 0.35	M28729
98759_f_at	Tuba2	tubulin, alpha 2	2.47± 0.41	2.39± 0.35	M28727
101543_f_at	Tuba6	tubulin, alpha 6	2.87± 0.41	2.75± 0.35	M13441
94835_f_at	Tubb2	tubulin, beta 2	2.23± 0.41	2.22± 0.35	M28739
94789_r_at	Tubb5	tubulin, beta 5	2.11± 0.41	2.02± 0.35	X04663
Cell cycle					
98478_at	Ccng2	cyclin G2	1.61± 0.41	2.18± 0.35	U95826
96236_at	Cdc16	CDC16 cell division cycle 16 homolog (S. cerevisiae)	2.27± 0.41	2.87± 0.35	AW122965
160901_at	Fos	FBJ osteosarcoma oncogene	-1.18± 0.41	3.05± 0.46	V00727
100130_at	Jun	Jun oncogene	2.28± 0.41	5.48± 0.35	X12761
92502_at	Plagl1	pleiomorphic adenoma gene-like 1	-2.20± 0.41	-2.87± 0.35	X95504
97506_at	Rnf2	ring finger protein 2	2.38± 0.41	2.36± 0.35	AI043016
98905_at	Sept7	septin 7	2.35± 0.41	2.39± 0.35	AJ223782
Proteolysis					
101040_at	Capn2	calpain 2	2.30± 0.41	2.70± 0.35	D38117
99642_i_at	Cpe	carboxypeptidase E	1.91± 0.41	2.08± 0.35	X61232
92256_at	Ctsb	cathepsin B	2.51± 0.43	2.15± 0.37	AI853714
101763_at	Gpr50	G-protein-coupled receptor 50	-1.84± 0.41	-2.53± 0.35	AF065145
102296_at	Pcsk2	proprotein convertase subtilisin/kexin type 2	1.70± 0.41	2.31± 0.35	M55669
96730_at	Tpp2	tripeptidyl peptidase II	2.34± 0.41	2.03± 0.36	X81323
Calcium homeostasis and binding					
93293_at	Calm2	calmodulin 2	2.07± 0.41	2.06± 0.35	M27844
102632_at	Calmbp1	calmodulin binding protein 1	1.64± 0.43	-2.60± 0.36	AF062378
104529_at	Caml	calcium modulating ligand	1.88± 0.41	2.06± 0.35	U21960
102197_at	Nucb2	nucleobindin 2	2.35± 0.41	2.09± 0.35	AJ222586
162428_i_at	S100a14	S100 calcium binding protein A14	-2.87± 0.41	-2.95± 0.35	AV293396

Table 6.7. Differentially expressed genes after EGCG treatment (continued): Cell signaling; cell adhesion; carbohydrate metabolism. Gene expression is indicated as fold change ± Standard Error. Only genes differentially expressed >2-fold and significantly expressed according to one-way ANOVA, p<0.01 are included in the list.

Probe id	Symbol	Gene Title	EGCG (μM)		Genbank
			1	25	
Cell signaling					
104135_at	Arl3	ADP-ribosylation factor-like 3	1.94±0.41	2.10±0.35	AW045474
103611_at	Cd47	CD47 antigen (Rh-related antigen, integrin-associated signal transducer)	1.96±0.41	2.66±0.35	AB012693
98535_at	Comt	catechol-O-methyltransferase	2.16±0.41	2.81±0.35	AF076156
97740_at	Dusp16	dual specificity phosphatase 16	1.13±0.42	2.25±0.36	AI642662
93667_at	Fbxw7	F-box and WD-40 domain protein 7, archipelago homolog (Drosophila)	2.16±0.41	2.33±0.35	AW120511
93271_s_at	Gnas	GNAS (guanine nucleotide binding protein, alpha stimulating) complex locus	2.15±0.41	2.52±0.35	AF107848
99175_at	Gng10	guanine nucleotide binding protein (G protein), gamma 10	2.12±0.41	2.45±0.35	AI843396
97004_at	Olfr71	olfactory receptor 71	-1.71±0.41	-2.24±0.35	AJ133429
102759_at	Pik3r2	phosphatidylinositol 3-kinase, regulatory subunit, polypeptide 2 (p85 beta)	1.82±0.41	2.13±0.35	Y13569
93962_at	Rap1a	RAS-related protein-1a	2.49±0.41	2.26±0.35	AI848598
160747_at	Rgs3	regulator of G-protein signaling 3	-1.71±0.41	-2.14±0.35	AI844739
162468_at	Rhoc	ras homolog gene family, member C	-1.91±0.41	-2.19±0.35	AV064502
100213_f_at	Rpl41	ribosomal protein L41	2.49±0.41	2.61±0.35	U93862
98564_f_at	Rps26	ribosomal protein S26	2.38±0.41	2.60±0.35	U67770
97243_at	Slc9a3r1	solute carrier family 9 (sodium/hydrogen exchanger), isoform 3 regulator 1	-1.85±0.41	-3.51±0.35	U74079
95669_g_at	Stmn2	stathmin-like 2	2.20±0.41	2.23±0.35	AI840972
160551_at	Vdac3	voltage-dependent anion channel 3	1.92±0.41	2.06±0.35	U30839
Cell adhesion					
104407_at	Alcam	activated leukocyte cell adhesion molecule	2.11±0.41	2.51±0.35	L25274
95661_at	Cd9	CD9 antigen	2.21±0.41	1.34±0.35	L08115
104743_at	Cdh13	cadherin 13	2.49±0.42	2.40±0.35	AB022100
92936_at	Cntn1	contactin 1	2.16±0.41	2.67±0.35	X14943
93606_s_at	Igsf4a	immunoglobulin superfamily, member 4A	2.24±0.41	1.86±0.35	AB021966
160610_at	Pcdha4	protocadherin alpha 4	1.71±0.41	2.08±0.35	D86916
92558_at	Vcam1	vascular cell adhesion molecule 1	1.32±0.41	-2.29±0.35	M84487
Carbohydrate metabolism					
161889_f_at	Aldo1	aldolase 1, A isoform	-2.76±0.41	-2.07±0.35	AV102160
160546_at	Aldo3	aldolase 3, C isoform	1.56±0.41	-2.31±0.35	AW121134
98984_f_at	Gpd2	glycerol phosphate dehydrogenase 2, mitochondrial	4.28±0.41	5.49±0.35	D50430
100573_f_at	Gpi1	glucose phosphate isomerase 1	1.71±0.41	2.02±0.35	M14220
162262_f_at	Gyg1	glycogenin 1	2.09±0.41	2.15±0.35	AV357306
104148_at	H6pd	hexose-6-phosphate dehydrogenase (glucose 1-dehydrogenase)	-2.50±0.41	-2.40±0.35	AA939571
99335_at	Hk1	hexokinase 1	2.10±0.41	1.92±0.35	J05277

Table 6.8. Differentially expressed genes after EGCG treatment (continued): Nucleobase, nucleoside, nucleotide and nucleic acid metabolism; other biological processes. Gene expression is indicated as fold change ± Standard Error. Only genes differentially expressed >2-fold and significantly expressed according to one-way ANOVA, p<0.01 are included in the list.

Probe id	Symbol	Gene Title	EGCG (μM)		Genbank
			1	25	
Nucleobase, nucleoside, nucleotide and nucleic acid metabolism					
93833_s_at	Hist1h2bc	histone 1, H2bc	2.55 ± 0.41	2.89 ± 0.35	X05862
160107_at	Hprt	hypoxanthine guanine phosphoribosyl transferase	1.86 ± 0.41	2.15 ± 0.35	K01515
102819_at	Nap1l2	nucleosome assembly protein 1-like 2	1.72 ± 0.41	2.18 ± 0.35	X92352
93831_at	Nono	non-POU-domain-containing, octamer binding protein	2.21 ± 0.41	2.21 ± 0.35	AI316087
97254_at	Rbm8	RNA binding motif protein 8	2.25 ± 0.41	2.16 ± 0.35	AA690061
160192_at	Rbmxrt	RNA binding motif protein, X chromosome retrogene	2.31 ± 0.41	2.38 ± 0.35	AF031568
103457_at	Rev3l	REV3-like, catalytic subunit of DNA polymerase zeta RAD54 like (S. cerevisiae)	2.23 ± 0.41	2.67 ± 0.35	AF083464
92196_f_at	Sf3a2	splicing factor 3a, subunit 2	-3.00 ± 0.41	-2.95 ± 0.35	X83733
97808_at	Sf3b1	splicing factor 3b, subunit 1	2.17 ± 0.41	2.59 ± 0.35	AI844532
102062_at	Smarcc1	SWI/SNF related, matrix associated, actin dependent regulator of chromatin, subfamily c, member 1	2.07 ± 0.41	2.83 ± 0.35	U85614
95049_at	Snrpd2	small nuclear ribonucleoprotein D2	3.25 ± 0.41	3.39 ± 0.35	AI837853
97486_at	U2af1	U2 small nuclear ribonucleoprotein auxiliary factor (U2AF) 1	-1.74 ± 0.41	-2.11 ± 0.35	AA693246
Other biological processes					
95745_g_at	Atp6v1a1	ATPase, H+ transporting, V1 subunit A, isoform 1	2.12 ± 0.41	2.79 ± 0.35	U13837
98066_r_at	Brd2	bromodomain containing 2	2.20 ± 0.41	2.20 ± 0.35	AL009226
92642_at	Car2	carbonic anhydrase 2	2.09 ± 0.42	-1.49 ± 0.35	M25944
103088_at	Chl1	cell adhesion molecule with homology to L1CAM	4.04 ± 0.41	5.22 ± 0.35	X94310
93582_at	Coq7	demethyl-Q 7	1.83 ± 0.41	2.11 ± 0.35	AF080580
96298_f_at	Dnclc1	dynein, cytoplasmic, light chain 1	2.29 ± 0.41	2.14 ± 0.35	AF020185
161682_f_at	Gpaa1	GPI anchor attachment protein 1	-2.82 ± 0.41	-3.04 ± 0.35	AV161234
161492_I_at	Mgat1	mannoside acetylglucosaminyltransferase 1	-3.37 ± 0.41	-2.32 ± 0.35	AV089873
96082_at	Mrpl30	mitochondrial ribosomal protein L30	2.83 ± 0.41	2.67 ± 0.35	AI850644
162168_r_at	Phgdh	3-phosphoglycerate dehydrogenase	-2.33 ± 0.43	1.79 ± 0.37	AV361953
101061_at	Ssr2	signal sequence receptor, beta	1.99 ± 0.41	2.04 ± 0.35	AI845293
162104_f_at	Tapbp	TAP binding protein	-2.88 ± 0.41	-2.10 ± 0.35	AV361189
93333_at	Tbca	tubulin cofactor a	1.83 ± 0.41	2.04 ± 0.35	U05333
160533_r_at	Tnp1	transition protein 1	2.51 ± 0.41	2.34 ± 0.35	X12521

Table 6.9. Differentially expressed genes after EGCG treatment (continued): Unknown biological processes. Gene expression is indicated as fold change ± Standard Error. Only genes differentially expressed >2-fold and significantly expressed according to one-way ANOVA, p<0.01 are included in the list.

Probe id	Symbol	Gene Title	EGCG (μM)		Genbank
			1	25	
Unknown biological processes					
102094_f_at	---	---	-1.77 ± 0.41	-2.76 ± 0.35	AI841270
101685_f_at	---	---	-1.84 ± 0.41	-2.56 ± 0.35	AI463421
92778_i_at	---	---	-1.97 ± 0.41	-2.12 ± 0.35	Z22552
162311_f_at	---	---	-2.13 ± 0.41	-2.03 ± 0.35	AV050648
161615_f_at	---	---	-2.36 ± 0.41	-1.87 ± 0.35	AV352346
103710_at	---	Transcribed sequence with weak similarity to protein ref:NP_115973.1 (H.sapiens) zinc finger protein 347; zinc finger 1111 [Homo sapiens]	1.73 ± 0.41	2.14 ± 0.35	AI037032
96526_at	---	9 days embryo whole body cDNA, RIKEN full-length enriched library, clone:D030029J20 product:unknown EST, full insert sequence	1.43 ± 0.41	2.16 ± 0.35	AW228840
95685_at	---	Adult male testis cDNA, RIKEN full-length enriched library, clone:1700092M07 product:unknown EST, full insert sequence	2.48 ± 0.41	2.28 ± 0.35	AI849678
101179_at	---	---	2.97 ± 0.41	2.35 ± 0.35	D50494
161083_at	---	Transcribed sequence with strong similarity to protein ref:NP_057365.1 (H.sapiens) STE20-like kinase; STE2-like kinase [Homo sapiens]	1.94 ± 0.41	2.43 ± 0.35	AW121616
160740_at	---	Hypothetical LOC228715 (LOC228715), mRNA	1.92 ± 0.42	2.55 ± 0.36	AA615984
98129_at	---	M.musculus mRNA for testis-specific thymosin beta-10	2.45 ± 0.41	2.62 ± 0.35	AI852553
100379_f_at	---	---	1.97 ± 0.41	3.16 ± 0.35	AI837905
96316_at	---	Transcribed sequences	2.52 ± 0.43	3.43 ± 0.37	AI839289
95714_at	0610009D07Rik	RIKEN cDNA 0610009D07 gene	2.21 ± 0.41	2.43 ± 0.35	AI226264
99143_at	0610039N19Rik	RIKEN cDNA 0610039N19 gene	1.72 ± 0.41	2.08 ± 0.35	AA614914
95458_s_at	1110001C20Rik	RIKEN cDNA 1110001C20 gene	1.66 ± 0.41	2.38 ± 0.35	AW121960
93805_at	1110003H09Rik	RIKEN cDNA 1110003H09 gene	2.08 ± 0.41	1.93 ± 0.35	AW121164
98037_at	1110003H18Rik	RIKEN cDNA 1110003H18 gene	1.94 ± 0.41	2.12 ± 0.35	AW122782
95732_at	1110005L13Rik	RIKEN cDNA 1110005L13 gene	3.12 ± 0.41	3.35 ± 0.35	AW047746
104314_r_at	1110032A03Rik	RIKEN cDNA 1110032A03 gene	3.56 ± 0.41	3.96 ± 0.70	AI851206
104077_at	1110049G11Rik	RIKEN cDNA 1110049G11 gene	1.82 ± 0.41	2.11 ± 0.35	AW121992
104076_at	1190017O12Rik	RIKEN cDNA 1190017O12 gene	2.12 ± 0.41	2.39 ± 0.35	AW122061
160184_at	1200007D18Rik	RIKEN cDNA 1200007D18 gene	-2.20 ± 0.41	-2.22 ± 0.35	AA815795
95568_at	1500011J06Rik	RIKEN cDNA 1500011J06 gene	2.18 ± 0.41	2.41 ± 0.36	AI853412
96068_at	1500034J20Rik	RIKEN cDNA 1500034J20 gene	3.69 ± 0.41	4.28 ± 0.54	AI848821
95561_at	1700013H19Rik	RIKEN cDNA 1700013H19 gene	3.12 ± 0.42	3.65 ± 0.44	AW120867
97237_at	1810003N24Rik	RIKEN cDNA 1810003N24 gene	2.10 ± 0.41	2.09 ± 0.35	AI837771
96686_i_at	2010100O12Rik	RIKEN cDNA 2010100O12 gene	2.65 ± 0.41	2.55 ± 0.35	AI853864
95105_at	2010110M21Rik	RIKEN cDNA 2010110M21 gene	1.96 ± 0.41	2.27 ± 0.35	AI847697

104620_at	2010300G19Rik	RIKEN cDNA 2010300G19 gene	2.05 ± 0.41	2.33 ± 0.35	AW123402
99187_f_at	2010315L10Rik	RIKEN cDNA 2010315L10 gene	2.33 ± 0.41	2.78 ± 0.35	AI835662
103076_at	2210412K09Rik	RIKEN cDNA 2210412K09 gene	1.81 ± 0.41	2.08 ± 0.35	AW046093
92703_at	2310032M22Rik	RIKEN cDNA 2310032M22 gene	2.23 ± 0.41	2.81 ± 0.35	AI325791
160475_at	2310034L04Rik	RIKEN cDNA 2310034L04 gene	1.87 ± 0.41	2.43 ± 0.35	AI839116
101404_at	2310061I09Rik	RIKEN cDNA 2310061I09 gene	2.12 ± 0.41	2.85 ± 0.35	AI853654
95103_at	2310065K24Rik	RIKEN cDNA 2310065K24 gene	2.10 ± 0.41	2.33 ± 0.35	AI839824
98039_at	2410015M20Rik	RIKEN cDNA 2410015M20 gene	3.37 ± 0.41	3.04 ± 0.35	AI853819
96780_at	2410022L05Rik	RIKEN cDNA 2410022L05 gene	2.23 ± 0.41	2.19 ± 0.35	AW208818
97864_at	2510049I19Rik	RIKEN cDNA 2510049I19 gene	2.32 ± 0.42	2.71 ± 0.35	AW258842
95058_f_at	2610205H19Rik	RIKEN cDNA 2610205H19 gene	2.78 ± 0.41	2.79 ± 0.35	AW121984
96688_at	2610318G18Rik	RIKEN cDNA 2610318G18 gene	2.04 ± 0.41	2.22 ± 0.35	AI845463
93768_f_at	2700059D21Rik	RIKEN cDNA 2700059D21 gene	2.33 ± 0.41	2.40 ± 0.35	AW124052
103071_at	2810429C13Rik	RIKEN cDNA 2810429C13 gene	1.77 ± 0.41	2.29 ± 0.35	AI843655
99185_at	2810443J12Rik	RIKEN cDNA 2810443J12 gene	3.35 ± 0.41	3.03 ± 0.35	AW047026
103664_r_at	2810452K22Rik	RIKEN cDNA 2810452K22 gene	1.93 ± 0.41	2.08 ± 0.35	AA959648
95135_at	3110038L01Rik	RIKEN cDNA 3110038L01 gene	-1.17 ± 0.41	-2.18 ± 0.35	AI844396
92840_at	3110079L04Rik	RIKEN cDNA 3110079L04 gene	2.26 ± 0.42	3.58 ± 0.36	AA683712
160183_f_at	3930401E15Rik	RIKEN cDNA 3930401E15 gene	2.50 ± 0.41	2.60 ± 0.35	AI846109
97437_f_at	4631416I11Rik	RIKEN cDNA 4631416I11 gene	2.83 ± 0.42	2.50 ± 0.36	AW122483
161756_at	4833420N02Rik	RIKEN cDNA 4833420N02 gene	2.04 ± 0.42	2.90 ± 0.36	AV298145
161015_at	4933402J24Rik	RIKEN cDNA 4933402J24 gene	2.00 ± 0.41	2.43 ± 0.36	AI845273
100587_f_at	5730403B10Rik	RIKEN cDNA 5730403B10 gene	2.50 ± 0.41	2.18 ± 0.35	AI843959
103978_at	5730454B08Rik	RIKEN cDNA 5730454B08 gene	1.44 ± 0.41	2.01 ± 0.35	AA666669
97916_at	5730494N06Rik	RIKEN cDNA 5730494N06 gene	1.92 ± 0.41	2.26 ± 0.35	AI116222
92992_i_at	5730497N03Rik	RIKEN cDNA 5730497N03 gene	3.60 ± 0.76	4.29 ± 0.38	AI324972
104059_at	5830451P18Rik	RIKEN cDNA 5830451P18 gene	2.05 ± 0.41	2.50 ± 0.35	AI851751
102870_at	5930418K15Rik	RIKEN cDNA 5930418K15 gene	2.38 ± 0.41	2.90 ± 0.35	AW125272
101929_at	6720463E02Rik	RIKEN cDNA 6720463E02 gene	-2.03 ± 0.41	-2.11 ± 0.35	AI836322
94895_at	9430020E02Rik	RIKEN cDNA 9430020E02 gene	2.65 ± 0.41	2.60 ± 0.35	AW122948
161104_at	9430099J10Rik	RIKEN cDNA 9430099J10 gene	3.78 ± 0.41	2.32 ± 0.35	AI846811
93427_at	9930104H07Rik	RIKEN cDNA 9930104H07 gene	2.08 ± 0.43	1.67 ± 0.38	AW122310
94663_at	AA407151	expressed sequence AA407151	-2.11 ± 0.41	-2.38 ± 0.35	AA407151
97918_at	AA536743	expressed sequence AA536743	1.55 ± 0.41	2.01 ± 0.36	AA623587
93472_at	AI413331	expressed sequence AI413331	-2.02 ± 0.41	-1.66 ± 0.35	AA796989
95503_at	AI839562	expressed sequence AI839562	2.04 ± 0.41	2.22 ± 0.35	U95498
93627_at	Ankrd28	ankyrin repeat domain 28	1.62 ± 0.41	2.21 ± 0.35	AI852287
96529_at	Ap1gbp1	AP1 gamma subunit binding protein 1	1.90 ± 0.41	2.34 ± 0.35	AW122059
93794_at	Appbp1	amyloid beta precursor protein binding protein 1	3.24 ± 0.41	3.31 ± 0.35	AI846393
97554_at	BC005624	cDNA sequence BC005624	1.95 ± 0.41	2.03 ± 0.35	AI838889
94823_at	BC029892	cDNA sequence BC029892	2.10 ± 0.41	2.24 ± 0.35	AI835315
95061_at	Bcas2	breast carcinoma amplified sequence 2	1.96 ± 0.41	2.11 ± 0.35	AI838996
100963_at	Brp17	brain protein 17	2.91 ± 0.41	2.50 ± 0.36	AI854243
103695_f_at	C330007P06Rik	RIKEN cDNA C330007P06 gene	2.11 ± 0.41	2.21 ± 0.35	AW047329
160623_at	Cdkl2	cyclin-dependent kinase-like 2 (CDC2-related kinase)	2.39 ± 0.41	2.68 ± 0.35	AI847045
92841_f_at	Chgb	chromogranin B	1.96 ± 0.41	2.88 ± 0.35	X51429
94030_at	Commd2	COMM domain containing 2	2.54 ± 0.41	2.33 ± 0.35	AI853431
96881_at	Commd6	COMM domain containing 6	2.08 ± 0.41	2.45 ± 0.35	AW049394

101976_at	Cops4	COP9 (constitutive photomorphogenic) homolog, subunit 4 (Arabidopsis thaliana)	1.97 ± 0.41	2.21 ± 0.35	AF071314
160522_at	D0H4S114	DNA segment, human D4S114	1.85 ± 0.41	2.21 ± 0.35	D45203
94526_at	D10Ertd214e	DNA segment, Chr 10, ERATO Doi 214, expressed	2.23 ± 0.41	2.49 ± 0.35	AI848453
101960_at	D10Wsu52e	DNA segment, Chr 10, Wayne State University 52, expressed	1.90 ± 0.41	2.17 ± 0.35	AI842208
103314_at	D13Ertd275e	DNA segment, Chr 13, ERATO Doi 275, expressed	1.81 ± 0.41	2.17 ± 0.35	AW046158
104714_at	D14Wsu89e	DNA segment, Chr 14, Wayne State University 89, expressed	2.08 ± 0.41	2.14 ± 0.35	AW125299
95431_at	D16Wsu109e	DNA segment, Chr 16, Wayne State University 109, expressed	2.53 ± 0.41	2.51 ± 0.35	AA623426
95432_f_at	D16Wsu109e	DNA segment, Chr 16, Wayne State University 109, expressed	3.24 ± 0.41	3.39 ± 0.35	AI844034
93841_at	D3Ertd194e	DNA segment, Chr 3, ERATO Doi 194, expressed	2.35 ± 0.41	2.59 ± 0.35	AW060249
99779_at	D6Bwg1452e	DNA segment, Chr 6, Brigham & Women's Genetics 1452 expressed	1.95 ± 0.41	2.12 ± 0.36	N28141
104418_at	D6Ertd365e	DNA segment, Chr 6, ERATO Doi 365, expressed	2.27 ± 0.41	2.08 ± 0.35	AA796868
93821_at	D8Ertd594e	DNA segment, Chr 8, ERATO Doi 594, expressed	2.61 ± 0.41	2.46 ± 0.36	AW046101
93534_at	Dcn	decorin	2.84 ± 0.41	3.15 ± 0.35	X53929
96636_at	Dctn5	dynactin 5	2.08 ± 0.41	1.90 ± 0.35	AI852649
160327_at	Dctn6	dynactin 6	2.10 ± 0.41	1.76 ± 0.35	AI848936
99096_at	Ddx24	DEAD (Asp-Glu-Ala-Asp) box polypeptide 24	1.82 ± 0.41	1.99 ± 0.35	U46690
101542_f_at	Ddx3x	DEAD/H (Asp-Glu-Ala-Asp/His) box polypeptide 3, X-linked	2.14 ± 0.41	2.27 ± 0.35	L25126
95688_at	Degs	degenerative spermatocyte homolog (Drosophila)	2.24 ± 0.41	2.25 ± 0.35	Y08460
103356_at	Dock7	dedicator of cytokinesis 7	1.70 ± 0.42	2.36 ± 0.36	AI843267
94492_at	Dstn	destrin	2.16 ± 0.41	2.31 ± 0.35	AB025406
161176_r_at	Epb7.2	erythrocyte protein band 7.2	-2.08 ± 0.41	-2.36 ± 0.35	AV230593
93309_at	Fin14	fibroblast growth factor inducible 14	2.11 ± 0.41	1.85 ± 0.35	U42386
95756_at	Ftsj3	FtsJ homolog 3 (E. coli)	2.16 ± 0.41	2.09 ± 0.36	AI839681
98048_at	Fusip1	FUS interacting protein (serine-arginine rich) 1	-2.01 ± 0.41	-2.23 ± 0.35	AF060490
96943_at	Gps1	G protein pathway suppressor 1	2.48 ± 0.41	2.32 ± 0.35	AW125234
99944_at	Hpca	hippocalcin	1.98 ± 0.41	2.27 ± 0.35	AB015200
92371_at	Hrc	histidine rich calcium binding protein	-1.48 ± 0.41	-2.68 ± 0.36	AI505355
102152_f_at	Igh-VS107	immunoglobulin heavy chain (S107 family)	-4.67 ± 0.41	-2.43 ± 0.35	M16724
93511_at	Itm2a	integral membrane protein 2A	1.51 ± 0.41	2.12 ± 0.36	L38971
101123_at	Itm2b	integral membrane protein 2B	2.00 ± 0.41	2.03 ± 0.35	U76253
160517_at	Lmnb1	lamin B1	-2.76 ± 0.41	-3.32 ± 0.35	M35153
93339_at	Mdm4	transformed mouse 3T3 cell double minute 4	-2.02 ± 0.41	-1.88 ± 0.35	AI846243
95417_at	Mgat2	mannoside acetylglucosaminyltransferase 2	2.32 ± 0.41	2.14 ± 0.35	AI117848
93787_f_at	Mrpl18	mitochondrial ribosomal protein L18	2.25 ± 0.41	2.07 ± 0.35	AI837302
92826_at	Mrps33	mitochondrial ribosomal protein S33	1.86 ± 0.41	2.02 ± 0.35	Y17852
160308_at	Msn	moesin	-2.20 ± 0.41	-2.41 ± 0.35	AI839417

104147_at	Nans	N-acetylneuraminic acid synthase (sialic acid synthase)	1.77 ± 0.41	2.09 ± 0.35	AW122052
101484_at	Nbr1	neighbor of Brca1 gene 1	1.44 ± 0.41	2.53 ± 0.35	U73039
93025_at	Ndfip1	Nedd4 family interacting protein 1	2.19 ± 0.41	2.46 ± 0.35	AI835257
101634_at	Npm1	nucleophosmin 1	2.08 ± 0.41	2.14 ± 0.35	M33212
101366_f_at	Nvl	nuclear VCP-like	3.65 ± 0.43	3.09 ± 0.42	AA250299
92848_at	Oat	ornithine aminotransferase	2.05 ± 0.41	1.71 ± 0.35	X64837
93600_at	Obrgrp	leptin receptor gene-related protein	2.40 ± 0.41	2.48 ± 0.35	AJ011565
94461_at	Pbef1	pre-B-cell colony-enhancing factor 1	1.98 ± 0.41	2.35 ± 0.35	AI852144
160899_at	Pcp4	Purkinje cell protein 4	1.76 ± 0.41	2.11 ± 0.35	X17320
101451_at	Peg3	paternally expressed 3	1.84 ± 0.43	2.77 ± 0.35	AF038939
99926_at	Pigr	polymeric immunoglobulin receptor	-2.30 ± 0.41	-2.68 ± 0.35	AB001489
96145_at	Pigt	phosphatidylinositol glycan, class T	-1.72 ± 0.41	-2.05 ± 0.35	AW211407
94445_at	Pls3	plastin 3 (T-isoform)	1.56 ± 0.41	2.25 ± 0.35	AW125273
95059_at	Pnrc2	proline-rich nuclear receptor coactivator 2	2.08 ± 0.41	1.99 ± 0.35	AW047399
102724_at	Rabep1	rabaptin, RAB GTPase binding effector protein 1	4.14 ± 0.53	4.07 ± 0.39	AI608324
98511_at	Raly	hnRNP-associated with lethal yellow	1.94 ± 0.41	2.04 ± 0.35	L17076
98602_at	Rangap1	RAN GTPase activating protein 1	2.12 ± 0.41	2.09 ± 0.35	U08110
93020_at	Rex3	reduced expression 3	2.30 ± 0.41	2.50 ± 0.35	AF051347
98119_at	Rpl30	ribosomal protein L30	1.90 ± 0.41	2.02 ± 0.35	K02928
92981_at	Scg2	secretogranin II	1.45 ± 0.41	2.20 ± 0.35	X68837
160360_at	Sep15	selenoprotein	2.10 ± 0.41	1.92 ± 0.35	AI838205
93806_at	Sh3bgrl	SH3-binding domain glutamic acid-rich protein like	2.21 ± 0.41	2.41 ± 0.35	AI848671
103813_at	Sh3yl1	Sh3 domain YSC-like 1	2.00 ± 0.41	2.79 ± 0.36	D85926
104216_at	Shoc2	soc-2 (suppressor of clear) homolog (C. elegans)	2.36 ± 0.41	1.72 ± 0.35	AF068921
93273_at	Snca	synuclein, alpha	2.24 ± 0.41	2.72 ± 0.35	AF044672
94313_at	Snrp1c	U1 small nuclear ribonucleoprotein 1C	2.21 ± 0.41	2.13 ± 0.35	X96767
160319_at	Sparcl1	SPARC-like 1 (mast9, hevin)	2.02 ± 0.41	1.60 ± 0.35	U66166
95430_f_at	Spg21	spastic paraplegia 21 homolog (human)	1.90 ± 0.41	2.00 ± 0.35	AI854154
101995_at	Sqstm1	sequestosome 1	2.21 ± 0.41	2.72 ± 0.35	U40930
96724_r_at	Ssx2ip	synovial sarcoma, X breakpoint 2 interacting protein	2.40 ± 0.41	3.13 ± 0.35	AW122911
93365_s_at	Sugt1	SGT1, suppressor of G2 allele of SKP1 (S. cerevisiae)	2.50 ± 0.41	2.91 ± 0.35	AI838149
104283_at	Tbc1d15	TBC1 domain family, member 15	1.99 ± 0.41	2.20 ± 0.35	AI037493
95101_at	Tde2	tumor differentially expressed 2	2.00 ± 0.41	2.47 ± 0.35	AI834772
95120_at	Tm4sf13	transmembrane 4 superfamily member 13	1.95 ± 0.41	2.68 ± 0.35	AI837621
98555_at	Ttc3	tetratricopeptide repeat domain 3	1.68 ± 0.41	2.00 ± 0.35	AB008516
97900_at	Txndc9	thioredoxin domain containing 9	2.19 ± 0.41	2.25 ± 0.35	AI845714
97285_f_at	Ubxd1	UBX domain containing 1	2.46 ± 0.41	2.88 ± 0.35	AW120609
160079_i_at	Wac	WW domain containing adaptor with coiled-coil	2.07 ± 0.41	2.09 ± 0.35	AI845773
100523_r_at	Wbp5	WW domain binding protein 5	2.36 ± 0.41	2.76 ± 0.35	U92454
160130_at	Wdr26	WD repeat domain 26	2.22 ± 0.41	2.43 ± 0.35	AA795284
101883_s_at	Xlr3a	X-linked lymphocyte-regulated 3a	2.17 ± 0.41	2.10 ± 0.36	L22977
94780_at	Zfp288	zinc finger protein 288	1.74 ± 0.41	2.21 ± 0.35	AI987985

104437_at	Zfp30	zinc finger protein 30	1.90 ± 0.42	2.32 ± 0.35	Z30174

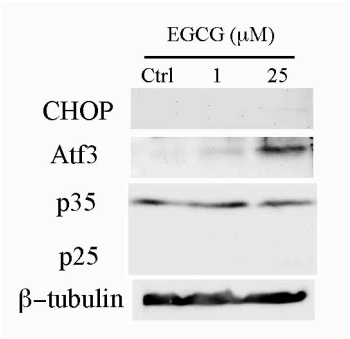

Figure 6.3. Effects of EGCG on the protein expression of CHOP, Atf3 and the cleavage of p35. Western blot analysis shows EGCG treatment induced the concentration-dependent increase of Atf3 but not CHOP expression. p35 was not cleaved to p25 during EGCG treatment. β-tubulin was the internal control for equal loading of proteins.

6.3 Discussion

6.3.1 ER stress is not involved in EGCG-induced neuronal apoptosis

The exposure of cultured cortical neurons to high concentrations of EGCG could induce neuronal apoptosis (Mandel et al, 2004). In this study, it was found that EGCG at a concentration of 25 μM could effectively inhibit chymotrypsin-like proteasomal activity and activate the apoptotic-signaling pathway through the activation of caspase-3 (Fig. 6.1). In contrast to lactacystin-induced cell death, no up-regulation of ER stress-associated genes such as the *Ddit3/CHOP* and *Atf4* was detected from the microarray data (Table 6.1). Furthermore, Western blot analysis demonstrated that the pro-apoptotic transcription factor Ddit3/CHOP protein was not expressed in cultured cortical neurons treated with a lethal dosage of EGCG, indicating the absence of ER stress in EGCG-induced neuronal cell death. Calpain activation has been associated with ER stress-mediated cell death (Rutkowski and Kaufman, 2004). The absence of p35 cleavage in the Western blot analysis of proteins extracted from cultured cortical neurons exposed to EGCG also suggests absence of calpain activation in the cell death system. Taken together, the results suggest the absence of ER stress during EGCG-induced neuronal apoptosis.

6.3.2 EGCG treatment and the up-regulation of genes encoding ubiquitin-proteasome system components

At both lethal and non-lethal concentrations, EGCG was able to induce the up-regulation of genes encoding UPS components such as proteasome subunits, ubiquitin and ubiquitin protein ligases (Table 6.1). Higher expression levels of these genes corresponded to higher concentrations of EGCG. This observation is supported by

the fact that higher concentrations of EGCG could inhibit chymotrypsin-like proteasomal activity (Fig. 6.2). Nevertheless, a non-lethal concentration of EGCG (1 μM) was also effective in up-regulating some of the genes encoding proteasome subunits such as proteasome subunit alpha type 3 (*Psma3*) and proteasome 26S subunit, non-ATPase, 11 (*Psmd11*), and also genes encoding ubiquitin b (*Ubb*), ubiquitin c (*Ubc*), ubiquitin-conjugating enzyme E2D2 (*Ube2d2*) and Ubiquitin protein ligase E3A (*Ube3a*) (Table 6.1). These results suggest that EGCG at a low concentration (1 μM) has the potential to protect neurons against the insult of accumulated unfolded proteins, since the up-regulation of UPS components has been reported to be neuroprotective by other studies (Meiners et al, 2003; Goldbaum and Richter-Landsberg, 2004)

6.3.3 The effect of EGCG on the induction of genes encoding heat shock proteins

Unlike the case in lactacystin treatment (Chapter 4), not many genes encoding HSPs were up-regulated by EGCG treatment (Table 6.1). Atf3 and c-Jun have been reported to play a major role in the transcriptional regulation of Hsp27 (Nakagomi et al, 2003). Although both *Atf3* and *c-Jun* genes were up-regulated by EGCG (25 μM) treatment, the low expression levels of the *Atf3* gene and protein (Table 6.1 and Fig. 6.3) might have contributed to the absence of *Hsp27* up-regulation in EGCG-treated cultured neurons.

6.3.4 The effect of EGCG on the regulation of lipid and cholesterol biosynthesis genes

EGCG has been reported to regulate lipid metabolism by controlling SREBP-regulated gene expression through the inhibition of proteasomes (Shay and Banz, 2005). Kuhn et al reported that the exposure of the HepG2 cell line to EGCG caused an increase in the low-density lipoprotein receptor (LDLR) protein expression (Kuhn et al, 2003). This effect of EGCG is believed to be responsible for the plasma cholesterol-lowering and heart disease-preventative effect of green tea (Kuhn et al, 2003). In this study, EGCG treatment was observed to up-regulate the expression of the very low density lipoprotein receptor gene (*Vldlr*) (Table 6.4). Vldlr is a member of the LDLR family (Goudriaan et al, 2001). The role of Vldlr in lipoprotein metabolism has been suggested by in vitro experiments showing Vldlr binding and internalizing particles that are rich in apolipoprotein E, such as very low density lipoprotein (Goudriaan et al, 2001).

Unlike with lactacystin treatment, genes involved in the synthesis of cholesterol were not down-regulated during EGCG-induced neuronal apoptosis (Table 6.4). One possible reason for this is that cultured neurons exposed to EGCG did not undergo ER stress (Fig. 6.3). A recent study demonstrated that ER stress in cells can lead to the suppression of SREBP(N)-mediated transcription of cholesterol biosynthesis genes (Zeng et al, 2004). Therefore, the absence of ER stress during EGCG-induced neuronal apoptosis might be the reason why no down-regulation of cholesterol biosynthesis genes was observed in the microarray analysis (Table 6.4).

The microarray data also shows that the gene encoding stearoyl-CoA desaturase-1 (*Scd1*) was down-regulated in neurons treated with EGCG. Scd1 is the rate-limiting enzyme in the synthesis of monosaturated fatty acids (Klaus et al, 2005). Scd1 has been reported to be down-regulated in liver cells exposed to EGCG (Klaus et al, 2005), but its role is not fully understood. A recent study proposed that Scd1 might play a major role in the process of cell regeneration (Breuer et al, 2004). Thus, the down-regulation of *Scd1* gene expression might impair neuron regeneration.

CHAPTER 7

7 General Conclusion

Proteasomal inhibition or dysfunction is likely to contribute to neuronal cell death and neurodegeneration. The study of the effects of lactacystin on cultured cortical neurons shows that proteasome inhibition can lead to neuronal apoptosis. The tumor suppressor PTEN is one possible player in neuronal apoptosis. The translocation of PTEN to the plasma membrane during neuronal cell death is of significant interest because PTEN can specifically dephosphorylate the phospholipid second messenger PtdIns(3,4,5)P_3 and act as an antagonist to the PI3-kinase/Akt survival signaling pathway. In this study, PTEN was found to be cleaved at the C-terminal end, forming a shorter or truncated 50 kDa form during lactacystin-induced neuronal apoptosis. The protease caspase-3 was found to be responsible for the cleavage of PTEN during neuronal apoptosis. Whether the cleavage of PTEN facilitates its translocation and activation is still not clear. Since the mutant PTEN without the C-terminal tail is found to have a higher phosphatase activity compared to the wild-type PTEN (personal correspondence with Heung-Chin Cheng), it is tempting to speculate that PTEN can be activated by caspase-3 cleavage during cell death.

The study of the neural membrane lipid profile initially attempted to measure the changes of PtdIns(4,5)P_2 during lactacystin-induced neuronal apoptosis, in order to complement the study of the role of PTEN in neuronal apoptosis. However, the level of PtdIns(4,5)P_2 in the cultured neurons was too minute to be detected using ESI-MS. Instead, the study of the neural lipid profile revealed the accumulation of ceramides and NAPE in the cultured cortical neurons during lactacystin-induced neuronal

apoptosis. The accumulation of ceramides in neural membranes is known to be involved in the activation of caspase-3 during apoptosis. However, the accumulation of NAPE in neural membranes during neuronal apoptosis has not been reported, since NAPE accumulation has been associated with excitotoxic or necrotic, rather than apoptotic cell death in both in vitro and in vivo systems (Hansen et al, 2001). Incidentally, NAPE is a precursor of anandamide, an endogenous cannabinoid receptor ligand. The accumulation of NAPE during neuronal injury may suggest a neuroprotective role of NAPE.

The use of microarray GeneChip® in this study has been beneficial in the understanding of the mechanisms of lactacystin-induced apoptosis. Microarray analysis of the differentially expressed genes at different time points reveals the sequence of events that leads to apoptosis. Genes that encode proteasome subunits, ubiquitin, HSPs and molecular chaperones were up-regulated at early time points, as a response to the abnormal accumulation of proteins during proteasome inhibition. Incidentally, cultured cortical neurons exposed to a lethal dose of lactacystin (1 μM) could also up-regulate the genes associated with ER stress, such as*Atf4* and *Ddit3*/*CHOP*. The early detection of the pro-apoptotic transcription factor CHOP in cultured neurons exposed to lactacystin suggests that ER stress was likely to be the main cause of lactacystin-induced neuronal apoptosis. ER stress is known to initiate other secondary pro-apoptotic responses such as the disruption of calcium homeostasis and oxidative stress in neurons. ER stress can also cause the down-regulation of genes associated with cholesterol biosynthesis, probably through a direct binding of the ER stress-activated Atf6 to SREBP, which interferes with the activation of cholesterol biosynthesis genes. The down-regulation of cholesterol

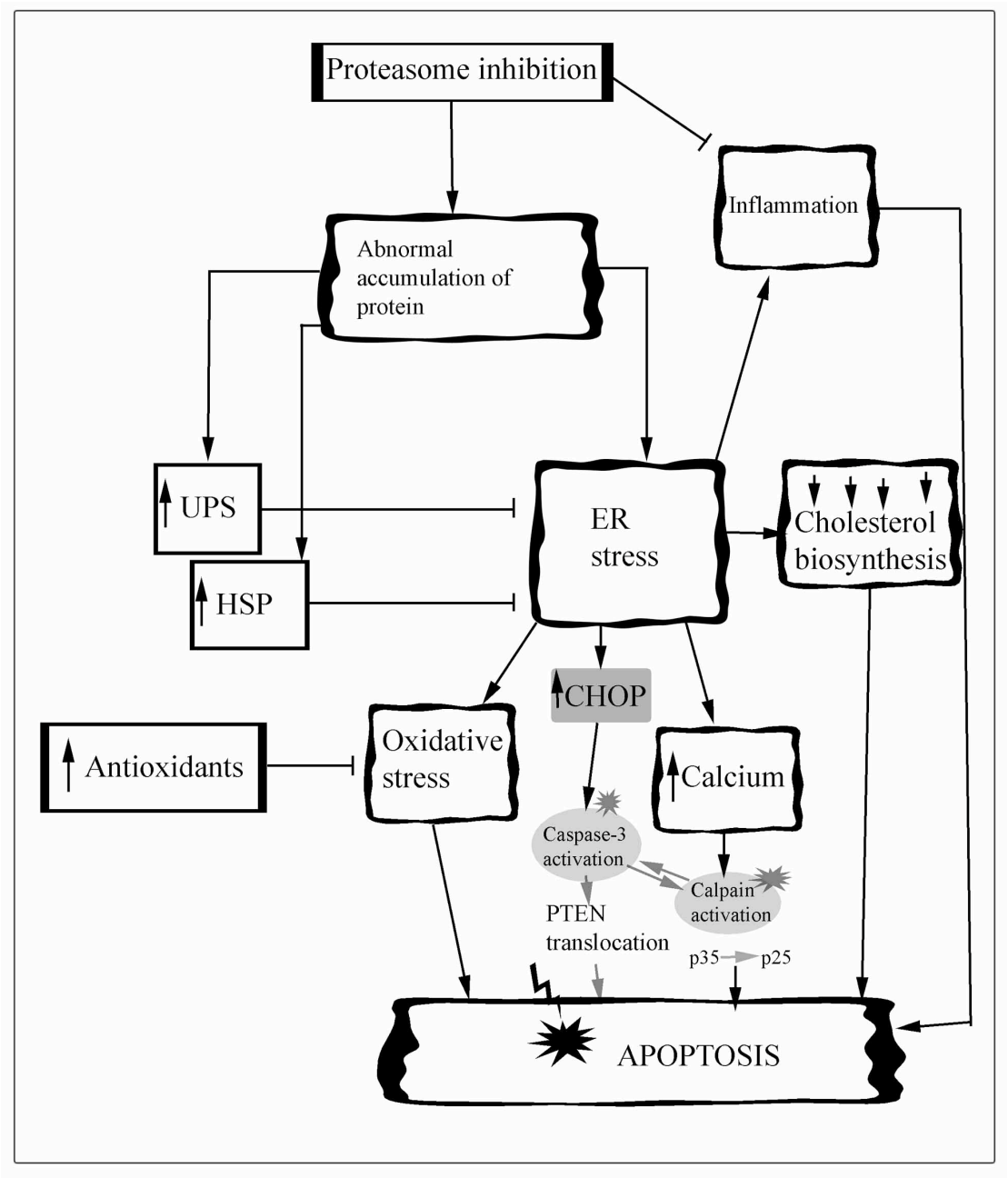

Figure 7.1. The mechanism of lactacystin-induced neuronal apoptosis. The inhibition of proteasomes by lactacystin induces the abnormal accumulation of proteins in neurons. To deal with this stress, the neurons activate the early neuroprotective responses through the up-regulation of UPS and HSPs. Exposure to lactacystin can also trigger ER stress responses, which lead to the activation of other pro-apoptotic responses such as 1) oxidative stress, 2) up-regulation of ER stress-associated pro-apoptotic transcription factor CHOP, 3) calcium disruption, 4) decrease in cholesterol biosynthesis and 5) activation of the inflammatory responses at the late phase of lactacystin treatment.

synthesis might play a role in energy conservation during apoptosis, since cholesterol biosynthesis requires a large amount of energy. Furthermore, we would expect cholesterol biosynthesis to be disrupted during ER stress, since the ER is the site of cholesterol biosynthesis. Fig. 7.1 summarizes the possible mechanism of lactacystin-induced neuronal apoptosis based on the microarray study.

Lastly, the effect of EGCG from green tea extract on cultured cortical neurons was studied as a comparison to the effect of lactacystin. EGCG is known for its neuroprotective properties, and recent studies suggest that some of the biological effect of EGCG is due to its proteasome inhibitory property. A lethal dosage of EGCG (25 μM) could activate caspase-3 and induce neuronal apoptosis. Unlike lactacystin, however, the lethal dosage of EGCG did not up-regulate the ER stress-associated pro-apoptotic transcription factor CHOP (based on the microarray and Western blot data). At a non-lethal concentration (1 μM), EGCG could induce the up-regulation of genes encoding UPS components, but was not so effective in the induction of HSP gene expression. Since EGCG can induce the up-regulation of genes encoding proteasome subunits and ubiquitin, it might be effective in protecting neurons against the accumulation of abnormal proteins under pathological conditions. Future work should study the effectiveness of EGCG in protecting neurons against the abnormal accumulation of proteins.

The microarray studies of lactacystin-induced neuronal apoptosis have revealed both potentially neuroprotective, as well as pro-apoptotic genes in the cultured cortical neurons during proteasomal inhibition. Since the dysfunction or decrease in UPS activity might play a role in the pathogenesis of neurodegenerative diseases, it is

therefore important to study the transcriptional regulation of genes associated with the UPS and HSPs as a therapeutic approach for neurodegenerative diseases.

8 REFERENCES

Adams J (2003). The development of proteasome inhibitors as anticancer drugs. Cancer Cell, 5: 417 – 421.

Alves-Rodrigues A, Gregori L and Figueiredo-Pereira ME (1998). Ubiquitin, cellular inclusions and their role in neurodegeneration. Trends Neurosci, 21: 516 – 520.

Amici M, Lupidi G, Angeletti M, Fioretti E and Eleuteri AM (2003). Peroxynitrite-induced oxidation and its effects on isolated proteasomal system. Free Radic Biol Med, 34: 987 – 996.

Antoku K, Maser RS, Scully Jr. WJ, Delach SM and Johnson DE (2001). Isolation of Bcl-2 binding proteins that exhibit homology with Bag-1 and suppressor of death domains protein. Biochem Biophys Res Commun, 286: 1003 – 1010.

Araki W and Wurtman RJ (1998). How is membrane phospholipids biosynthesis controlled in neural tissues? J Neurosci Res, 51: 667 – 674.

Ariga T, Jarvis WD and Yu RK (1998). Role of sphingolipid-mediated cell death in neurodegenerative diseases. J Lipid Res, 39: 1 – 16.

Aschner M, Cherian MG, Klaassen CD, Palmiter RD, Erickson JC and Bush AI (1997). Metallothioneins in Brain – The Role in Physiology and Pathology. Toxicol and Appl Pharmacol, 142: 229 – 242.

Backman SA, Stambolic V and Mak TW (2002). PTEN function in mammalian cell size regulation. Curr Opin neurobiol, 12: 516 – 522.

Bazan NG, Marcheselli VL and Cole-Edwards K (2005). Brain response to injury and neurodegeneration: endogenous neuroprotective signaling. Ann NY Acad Sci, 1053: 137 – 147.

Bossy-Wetzel E, Schwarzenbacher R and Lipton SA (2004). Molecular pathways to neurodegeneration. Nat Med, 10: S2 – S9.

Breuer S, Pech K, Buss A, Spitzer C, Ozols J, Hol EM, Heussen N, Noth J, Schwaiger F and Schmitt AB (2004). Regulation of stearoyl-CoA desaturase-1 after central and peripheral nerve lesions. BMC Neurosci, 5: 15 – 24.

Buccoliero R and Futerman AH (2003). The roles of ceramide and complex sphingolipids in neuronal cell function. Pharmacol Res, 47: 409 – 419.

Bush KT, Goldberg AL and Nigam SK (1997). Proteasome inhibition leads to a heat-shock response, induction of endoplasmic reticulum chaperones, and thermotolerance. J Biol Chem, 272: 9086 – 9092.

Butts BD, Hudson HR, Linseman DA, Le SS, Ryan KR, Bouchard RJ and Heidenreich KA (2005). Proteasome inhibition elicits a biphasic effect on neuronal

apoptosis via differential regulation of pro-survival and pro-apoptotic transcription factors. Mol Cell Neurosci, 30: 279 – 289.

Calignano A, La Rana G, Giuffrida A and Piomelli D (1998). Control of pain inhibition by endogenous cannabiboids. Nature, 394: 277 – 281.

Carra S, Sivilotti M, Chavez Zobel AT, Lambert H and Landry J (2005). HspB8, a small heat shock protein mutated in human neuromuscular disorders, has in vivo chaperone activity in cultured cells. Hum Mol Genet, 14: 1659 – 1669.

Carro E and Torres-Aleman I (2004). The role of insulin and insulin-like growth factor 1 in the molecular and cellular mechanisms underlying the pathology of Alzheimer's disease. Eur J Pharmacol, 490: 127 – 133.

Chapman KD (2000). Emerging physiological roles for N-acylphosphatidylethanolamine metabolism in plants: signal transduction and membrane protection. Chem Phys Lipids, 108: 221 – 230.

Chapman R, Sidrauski C and Walter P (1998). Intracellular Signaling from the endoplasmic reticulum to the nucleus. Annu Rev Cell Dev Biol, 14: 459 – 485.

Chen Y, Shertzer HG, Schneider SN, Nebert DW and Dalton TP (2005). Glutamate cysteine ligase catalysis: dependence on ATP and modifier subunit for regulation of tissue glutathione levels. J Biol Chem, in press.

Cheung NS, Pascoe CJ, Giardina SF, John CA and Beart PM (1998) Micromolar L-glutamate induces extensive apoptosis in an apoptotic-necrotic continuum of insult-dependent, excitotoxic injury in cultured cortical neurons. Neuropharmacology 37: 1419 – 1429

Cheung NS, Choy MS, Halliwell B, Teo TS, Bay BH, Lee AY, Qi RZ, Koh VH, Whiteman M, Koay ES, Chiu LL, Zhu HJ, Wong KP, Beart PM, Cheng HC (2004). Lactacystin-induced apoptosis of cultured mouse cortical neurons is associated with accumulation of PTEN in the detergent-resistant membrane fraction. Cell Mol Life Sci, 61(15): 1926-1934.

Chondrogianni N, Tzavelas C, Pemberton AJ, Nezis IP, Rivett AJ and Gonos ES (2005). Overexpression of proteasome β5 subunit increases the amount of assembled proteasome and confers ameliorated response to oxidative stress and higher survival rates. J Biol Chem, 280: 11840 – 11850.

Ciechanover A, Schwartz AL (2002). Ubiquitin-mediated degradation of cellular proteins in health and disease. Hepatology, 35: 3 – 6.

Cieslik K, Zhu Y and Wu KK (2002). Salicylate suppression macrophage nitric-oxide synthase-2 and cyclo-oxygenase-2 expression by inhabiting CCAAT/enhancer-binding protein-β binding via a common signaling pathway. J Biol Chem, 277: 49304 – 49310.

Colombaioni L and Garcia-Gil M (2004). Sphingolipid metabolites in neural signaling and functions. Brain Res Rev, 46: 328 – 355.

Cookson MR (2005). The Biochemistry of Parkinson's disease. Annu Rev Biochem, 74: 29 – 52.

Coppedè F, Armani C, Della Bidia D, Petrozzi L, Bonuccelli U and Migliore L (2005). Molecular implications of the human glutathione transferase A-4 gene (hGSTA4) polymorphisms in neurodegenerative diseases. Mutat Res, 579:107 – 114.

Consilvio C, Vinvent AM and Feldman EL (2004). Neuroinflammation, COX-2, and ALS – a dual role? Expr Neurol, 187: 1 – 10.

Cutler RG, Kelly J, Storie K, Pedersen WA, Tammara A, Hatanpaa K, Troncoso JC and Mattson MP (2004). Involvement of oxidative stress-induced abnormalities in ceramide and cholesterol metabolism in brain aging and Alzheimer's disease. Proc Natl Acad Sci USA, 101: 2070 – 2075.

Das S, Dixon JE and Cho W (2003) Membrane-binding and activation mechanism of PTEN. Proc Natl Acad Sci USA. 100: 7491 – 7496

De Vrij FMS, Sluijs JA, Gregori L, Fischer DF, Hermens WTJMC, Goldgaber D, Verhaagen J, van Leeuwen FW and Hol EM (2001). Mutant ubiquitin expressed in Alzheimer's disease causes neuronal death. FASEB J, 15: 2680 – 2688.

DeMartino GN and Slaughter CA (1999). The proteasome, a novel protease regulated by multiple mechanisms. J Biol Chem, 274: 22123 – 22126.

Di Napoli M and Papa F (2003). The proteasome system and proteasome inhibitors in stroke: controlling the inflammatory response. Curr Opin Investig Drugs, 4: 1333 – 1342.

Dick LR, Cruikshank AA, Destree AT, Grenier L, McCormack TA, Melandri FD, Nunes SL, Palombella VJ, Parent LA, Plamondon L and Stein RL (1996). Mechanistic studies on the inactivation of the proteasome by lactacystin in cultured cells. J Biol Chem, 272: 182 – 188.

Ding Q and Keller JN (2001). Proteasome and proteasome inhibition in the central nervous system. Free Radic Biol Med, 31: 574 – 584.

Eberlé D, Hegarty B, Bossard P, Ferré P, Foufelle F (2004). SREBP transcription factors: master regulators of lipid homeostasis. Biochimie, 86: 839 – 848.

Elliott PJ and Ross JS (2001). Proteasome: a new target for novel drug therapies. Am J Clin Pathol, 116: 637 – 646.

Farooqui AA, Ong W-Y, Horrocks LA (2004). Biochemical aspects of neurodegeneration in human brain: Involvement of neural membrane phospholipids and phospholipases A_2. Neurochem Res, 29: 1961 – 1977.

Franklin TB, Krueger-Naug AM, Clarke DB, Arrigo A-P, Currie RW (2005). The role of heat shock proteins Hsp70 and Hsp27 in cellular protection of the central nervous system. Int J Hyperthermia, 21: 379 – 392.

Fribley A, Zeng Q and Wang C-Y (2004). Proteasome inhibitor PS-341 induces apoptosis through induction of endoplasmic reticulum stress-reactive oxygen species in head and neck squamous cell carcinoma cells. Mol Cell Biol, 24: 9695 – 9704.

Gaczynska M, Osmulski PA and Ward WF (2001). Caretaker or undertaker? The role of the proteasome in aging. Mech Ageing Dev, 122: 235 – 254.

Gary DS and Mattson MP (2002) PTEN regulates Akt kinase activity in hippocampal neurons and increases their sensitivity to glutamate and apoptosis. Neuromol Med, 2: 261 – 269

Georgescu M, Kirsch KH, Akagi T, Shishido T and Hanafusa H (1999) The tumor-suppressor activity of PTEN is regulated by its carboxyl-terminal region. Proc Natl Acad Sci USA, 96: 10182 – 10187

Giese KC and Vierling E (2002). Changes in oligomerization are essential for the chaperone activity of a small heat shock protein in vivo and in vitro. J Biol Chem, 277: 46310 – 46318.

Gilchrist CA, Grayt DA, Stieber A, Gonatas NK and Kopito RR (2005). Effect of ubiquitin expression on neuropathogenesis in a mouse model of familial amyotrophic lateral sclerosis. Neuropathology and Applied Neurobiology, 31: 20 – 33.

Glickman MH and Raveh (2005). Proteasome plasticity. FEBS Lett, 579: 3214 – 3223.

Goldbaum O and Richter-Landsberg (2004). Proteolytic stress causes heat shock protein induction, tau ubiquitination, and the recruitment of ubiquitin to tau-positive aggregates in oligodendrocytes in culture. J Neurosci, 24: 5748 – 5757.

Goldberg AL (2003). Protein degradation and protection against misfolded or damaged proteins. Nature, 426: 895 – 899.

Goswami R and Dawson G (2000). Does Ceramide Play a Role in Neural Cell Apoptosis? J Neurosci Res, 60: 141 – 149.

Goudriaan JR, Tacken PJ, Dahlmans VEH, Gijbels MJJ, van Dijk KW, Havekes LM and Jong MC (2001). Protection from obesity in mice lacking the VLDL receptor. Arterioscler Thromb Vasc Biol, 21: 1488 – 1493.

Griffin RJ, Moloney A, Kelliher M, Johnston JA, Ravid R, Dockery P, O'Connor R and O'Neill C (2005). Activation of Akt/PKB, increased phosphorylation of Akt substrates and loss and altered distribution of Akt and PTEN features of Alzheimer's disease pathology. J Neurochemistry, 93: 105 – 117.

Groll M and Clausen T (2003). Molecular shredders: how proteasomes fulfill their role. Curr Opin Struct Biol, 13: 665 – 673.

Grune T, Jung T, Merker K, Davies KJA (2004). Decreased proteolysis caused by protein aggregates, inclusion bodies, plaques, lipofuscin, ceroid, and 'aggresomes' during oxidative stress, aging, and disease. Int J Biochem Cell Biol, 36: 2519 – 2530.

Hai T, Wolfgang CD, Marsee DK, Allen AE, Sivaprasad U (1999). ATF3 and stress responses. Gene Expr, 7: 321 – 335.

Halliwell B (2002) Hypothesis: proteasomal dysfunction: a primary event in neurogeneration that leads to nitrative and oxidative stress and subsequent cell death. Ann NY Acad Sci, 962: 182 – 194

Hampton RY (2002). ER-associated degradation in protein quality control and cellular regulation. Curr Opin Cell Biol, 14: 476 – 482.

Hansen HS, Lauritzen L, Strand AM, Vinggaard AM, Frandsen A and Schousboe A (1997). Characterization of glutamate-induced formation of N-acylphosphatidylethanolamine and N-acylethanolamine in culture neocortical neurons. J Neurochem, 69: 753 – 761.

Hansen HH, Hansen SH, Schousboe A and Hansen HS (2000). Determination of the Phospholipid Precursor of Anandamide and Other N-acylethanolamine Phospholipids Before and After Sodium Azide-Induced Toxicity in Cultured Neocortical Neurons. J Neurochem, 75: 861 – 871.

Hansen HH, Ikonomidou C, Bittigau P, Hansen SH and Hansen HS (2001). Accumulation of the anandamide precursor and other N-acylethanolamine phospholipids in infant rat models of in vivo necrotic neuronal death. J Neurochem, 76: 39 – 46.

Hegde AN (2004). Ubiquitin-proteasome-mediated local protein degradation and synaptic plasticity. Prog Neurobiol, 73: 311 – 357.

Hershko A and Ciechanover A (1998). The ubiquitin system, Annu Rev Biochem, 67: 425 – 479.

Holmback J, Karlsson AA, Arnoldsson KC (2001). Characterization of N-acylphosphatidylethanolamine and acylphosphatidylglycerol in oats. Lipids, 36: 153 – 165.

Hope AD, de Silva R, Fischer DF, Hol EM, van Leeuwen FW and Lees AJ (2003). Alzheimer's associated variant ubiquitin causes inhibition of the 26S proteasome and chaperone expression. J Neurochem, 86: 394 – 404.

Horton JD (2002). Sterol regulatory element-binding proteins: transcriptional activators of lipid synthesis. Biochem Soc Trans, 30: 1091 – 1095.

Hubatsch I, Ridderström M, Mannervik B (1998). Human glutathione transferase A4-4: an Alpha class enzyme with high catalytic efficiency in the conjugation of 4-hydroxinonenal and other genotoxic products of lipid peroxidation. J Biochem, 330: 175 – 179.

Imajoh-Ohmi S, Kawaguchi T, Sugiyama S, Tanaka K, Omura S and Kikuchi H (1995). Lactacystin, a specific inhibitor or the proteasome, induces apoptosis in human monoblast U937 cells. Biochem Biophys Res Commun, 217: 1070 – 1077.

Jiang HY, Wek SA, McGrath BC, Lu D, Hai T, Harding HP, Wang X, Ron D, Cavener DR and Wek RC (2004). Activating Transcription Factor 3 Is Integral to the Eukaryotic Initiation Factor 2 Kinase Stress Response. Mol Cell Biol, 1365 – 1377.

Joazeiro CA and Weissman (2000). RING finger proteins: mediators of ubiquitin ligase activity. Cell, 102: 549 – 552.

Jung S-H, Bang H and Young S (2005). Sample size calculation for multiple testing in microarray data analysis. Biostatistics, 6: 157 – 169.

Katayama T, Imaizumi K, Manabe T, Hitomi J, Kudo T and Tohyama M (2004). Induction of neuronal death by ER stress in Alzheimer's disease. J Chem Neuroanat, 28: 67 – 78.

Keller JN, Hanni KB, Markesbery WR (2000). Impairment proteasome function in Alzheimer's disease. J Neurochem, 75: 436 – 439.

Keller JN, Gee J, Ding Q (2002). The proteasome in brain aging. Ageing Res Rev, 1: 279 – 293.

Keller JN, Dimayuga E, Chen Q, Thorpe J, Gee J and Ding Q (2004). Autophagy, proteasomes, lipofuscin, and oxidative stress in the aging brain. Int J Biochem Cell Biol, 36: 2376 – 2391.

Klein J (2000). Membrane breakdown in acute and chronic neurodegeneration: focus on choline-containing phospholipids. J Neural Transm, 107: 1027 – 1063.

Koudinova NV, Kontush A, Berezov TT and Koudinov AR (2003). Amyloid beta, neural lipids, cholesterol & Alzheimer's disease. Neurobiol Lipids, 1: 27 – 33. available at: http://neurobiologyoflipids.org/content/1/6/

Kusakawa G, Saito T, Onuki R, Ishiguro K, Kishimoto T and Hisanaga S (2000). Calpain-dependent proteolytic cleavage of the p35 cyclin-dependent kinase 5 activator to p25. J Biol Chem, 275: 17166 – 17172.

Lachyanker MB, Sultana N, Schonhoff CM, Mitra P, Poluha W, Lambert S, Quesenberry PJ, Litofsky NS, Recht LD, Nabi R, Miller SJ, Ohta S, Neel BG and Ross AH (2000) A role for nuclear PTEN in neuronal differentiation. J. Neurosci. 20: 1404 – 1413

Lai Y, Du L, Dunsmore KE, Jenkins LW, Wong HR and Clark RSB (2005). Selectively increasing inducible heat shock protein 70 via TAT-protein transduction protects neurons from nitrosative stress and excitotoxicity. J Neurochem, 94: 360 – 366.

Lam YA, Pickart CM, Alban A, Landon M, Jamieson C, Ramage R, Mayer RJ and Layfield R (2000). Inhibition of the ubiquitin-proteasome system in Alzheimer's disease. Proc Natl Acad Sci USA, 97: 9902 – 9906.

Latchman DS (2005). HSP27 and cell survival in neurons. Int H Hyperthermia, 21: 393 – 402.

Layfield R (2000). Does an inhibition of the ubiquitin/26S proteasome pathway of protein degradation underlie the pathogenesis of non-familial Alzheimer's disease? Med Hypotheses, 56: 395 – 399.

Layfield R, Cavey JR and Lowe J (2003). Role of ubiquitin-mediated proteolysis in the pathogenesis of neurodegenerative disorders. Ageing Res Rev, 2: 343 – 356.

Lee CS, Tee LY, Warmke T, Vinjamoori A, Cai A, Fagan AM and Snider BJ (2004). A proteasomal stress response: pre-treatment with proteasome inhibitors increases proteasome activity and reduces neuronal vulnerability to oxidative injury. J Neurochem, 91: 996 – 1006.

Lee DH and Goldberg AL (1998). Proteasome inhibitors: valuable new tools for cell biologists. Trends in cell Biology, 8: 397 – 403.

Lee MS, Kwon YT, Li M, Peng J, Friedlander RM and Tsai LH (2000). Neurotoxicity induces cleavage of p35 and p25 by calpain. Nature, 405: 360 – 364.

Leslie NR, Bennett D, Gray A, Pass I, Khe H-X and Downes P (2001) Targeting mutants of PTEN reveal distinct subsets of tumour suppressor functions. Biochem J, 357: 427 – 435

Leslie NR and Downes CP (2002) The down side of PI3-kinase signalling. Cell Signal, 14: 285 – 295

Li L, Liu F and Ross AH (2003). PTEN regulation of neural development and CNS stem cells. J Cell Biochem, 88: 24 – 28.

Liang G, Wolfgang CD, Chen BP, Chen TH, Hai T (1996). ATF3 gene, genome organization, promoter, and regulation. J Biol Chem, 271: 1695 – 1701. The role of heat shock proteins Hsp70 and Hsp27 in cellular protection of the central nervous system. Int J Hyperthermia, 21: 379 – 392.

Livak KJ and Schmittgen TD (2001). Analysis of relative gene expression data using real-time quantitative PCR and the 2(-Delta Delta C(T)) Method. Methods, 25: 402 – 408.

London MK, Keck BI, Ramos PC and Dohmen RJ (2004). Regulatory mechanisms controlling biogenesis of ubiquitin and the proteasome. FEBS Lett, 567: 259 – 264.

Lopez Salon M, Morelli L, Castano EM, Soto EF and Pasquini JM (2000). Defective ubiquitination of cerebral proteins in Alzheimer's disease. J Neurosci Res, 62: 302 – 310.

Luukko K, Ylikorkala A, Tiainen M and Mäkelä TP (1999) Expression of LKB1 and PTEN tumor suppressor genes during mouse embryonic development. Mech Dev, 83: 187 – 190

Maccarrone M and Ainazzi-Agró A (2003). The endocannabinoid system, anandamide and the regulation of mammalian cell apoptosis. Cell Death Differ, 10: 946 – 955.

Maeda A, Crabb JW, Palczewski K (2005). Microsomal Glutathione S-transferase 1 in the Retinal Pigment Epithelium: Protection against Oxidative Stress and a Potential Role in Aging. Biochem, 44: 480 – 489.

Mandel S, Weinreb O, Amit T and Youdium MBH (2004). Cell signaling pathways in the neuroprotective actions of the green tea polyphenol (-)-epigallocatechin-3-gallate: implications for neurodegenerative diseases. J Neurochem, 88: 1555 – 1569.

Mandel S and Youdim MBH (2004). Catechin polyphenols: neurodegeneration and neuroprotection in neurodegenerative diseases. Free Rad Biol Med, 37: 304 – 317.

Mandel S, Grunblatt E, Riederer P, Amariglio N, Hirsch JJ, Rechavi G and Youdim MBH (2005). Gene expression profiling of sporadic Parkinson's disease substantia nigra pars compacta reveals impairment of ubiquitin-proteasome subunits, SKP1A, Aldehyde dehydrogenase, and chaperone HSC-70. Ann NY Acad Sci, 1053: 356 – 375.

Mannhaupt G, Schnall R, Karpov V, Vetter I and Feldmann (1999). Rpn4p acts as a transcription factor by binding to PACE, a nonamer box found upstream of 26S proteasomal and other genes in yeast. FEBS Lett, 450: 27 – 34.

McCullough, KD, Martindale JL, Klotz L-O, Aw T-K and Holbrook NJ (2001). Gadd153 Sensitizes Cells to Endoplasmic Reticulum Stress by Down-Regulating Bcl2 and Perturbing the Cellular Redox State. Mol Cell Biol, 21: 1249 – 1259.

McDonough H and Patterson C (2003). CHIP: a link between the chaperone and proteasome systems. Cell Stress Chaperones, 8: 303 – 308.

McNaugh KSP and CW Olanow (2005). Protein aggregation in the pathogenesis of familial and sporadic Parkinson's disease. Neurobiol Aging, in press.

Meiners S, Heyken D, Weller A, Ludwig A, Stangl K, Kloetzel, Kruger E (2003). Inhibition of proteasome activity induces concerted expression of proteasome genes and de novo formation of mammalian proteasomes. J Biol Chem, 278: 21517 – 21525.

Mendez P, Azcoitia I and Garcia-Segura LM (2005). Interdependence of estrogen and insulin-like growth factor-1 in the brain: potential for analyzing neuroprotective mechanisms. J Endocrinol, 185: 11 – 17.

Meriin AB, Gabai VL, Yaglom J, Shifrin VI and Sherman MY (1998). Proteasome inhibitors activate stress kinases and induce Hsp72. J Biol Chem, 273: 6373 – 6379.

Meriin AB and Sherman MY (2005). Role of molecular chaperones in neurodegenerative disorders. Int J Hyperhermia, 21: 403 – 419.

Mizuno Y, Hattori N, Mori H, Suzuki T, Tanaka K (2001). Parkin and Parkinson's disease. Curr Opin Neurol, 14: 477 – 482.

Moore DJ, West AB, Dawson VL and Dawson TM (2005). Molecular pathophysiology of Parkinson's disease. Annu Rev Neurosci, 28: 57 – 87.

Mosser DD, Caron AW, Bourget L, Meriin AB, Sherman MY, Morimoto RI, Massie B (2000). The chaperone function of hsp70 is required for protection against stress-induced apoptosis. Mol Cell Biol, 20: 7146 – 7159.

Nagano I, Ilieva H, Shiote M, Murakami T, Yokoyama M, Shoji M and Abe K (2005). Therapeutic benefit of intrathecal injection of insulin-like growth factor-1 in a mouse model of amyotrophic lateral sclerosis. J Neurol Sci, 235: 61 – 68.

Nakagawa A, Kainosho M and Omura S (1994). Biosynthesis of lactacystin, a novel microbial metabolite which induces differentiation of Neuro 2a cells, a mouse neuroblastoma cell line. Pure & Appl Chem, 66: 2411 – 2413.

Nakagawa T, Zhu H, Morishima N, Li E, Xu J, Yankner BA and Yuan J (2000). Caspase-12 mediates endoplasmic-reticulum-specific apoptosis and cytotoxicity by amyloid-β. Nature, 403: 98 – 103.

Nakagomi S, Suzuki Y, Namikawa K, Kiryu-Seo S and Kiyama H (2003). Expression of the activating transcription factor 3 prevents c-Jun N-terminal kinase-induced neuronal cell death by promoting heat shock protein 27 expression and Akt activation. J Neurosci, 23: 5187 – 5196.

Nam S, Smith DM and Dou QP (2001). Ester bond-containing tea polyphenols potently inhibit proteasome activity in vitro and in vivo. J Biol Chem, 276: 13322 – 13330.

Naujokat C and Hoffmann S (2002) Role and function of the 26S proteasome in proliferation and apoptosis. Lab Invest, 82: 965 – 980

Nicholson DW (1999). Caspase structure, proteolytic substrates, and function during apoptotic cell death. Cell Death Differ, 6: 1028 – 1042.

Noga M and Hayashi T (1996). Ubiquitin gene expression following transient forebrain ischemia. Brain Res Mol Brain Res, 36: 261 – 267.

Ohtsuka K and Suzuki T (2000). Roles of molecular chaperones in the nervous system. Brain Res Bull, 53: 141 – 146.

Okamoto Y, Morishita J, Wang J, Schmid PC, Krebsbach RJ, Schmid HHO and Ueda N (2005). Mammalian cells stably overexpressing N-acylphosphatidylethanolamine-hydrolysing phospholipase D exhibit significantly decreased levels of N-acylphosphatidylethanolamines. Biochem J, 389: 241 – 247.

Owen AD, Schapira AH, Jenner P and Marsden CD (1996). Oxidative stress and Parkinson's disease. Ann N Y Acad Sci, 786: 217 – 223.

Pahl H L (1999). Signal transduction from the endoplasmic reticulum to the cell nucleus. Physiol Rev, 79: 683 – 701.

Pasquini LA, Moreno MB, Adamo AM, Pasquini JM and Soto EF (2000) Lactacystin, a specific inhibitor of the proteasome, induces apoptosis and activates caspase-3 in cultured cerebellar granule cells. J Neurosci Res, 59: 601 – 611

Pasquini LA, Paez PM, Besio Moreno MAN, Pasquini JM and Soto EF (2003). Inhibition of the proteasome by lactacystin enhances oligodendeoglial cell differentiation. J Neurosci, 23: 4635 – 4644.

Patrick GN, Zukerberg L, Nikolic M, de la Monte S, Dikkes P and Tsai LH (1999). Conversion of p35 to p25 deregulates cdk5 activity and promotes neurodegeneration. Nature, 402: 615 – 622.

Pelled D, Raveh T, Riebeling C, Fridkin M, Berissi H, Futerman AH and Kimchi A (2002). Death-associated protein (DAP) kinase plays a central role in ceramide-induced apoptosis in cultured hippocampal neurons. J Biol Chem, 277: 1957 – 1961.

Perandones C, Costanzo RV, Kowaljow V, Pivetta OH, Carminatti H and Radrizzani M (2004). Correlation between synaptogenesis and the PTEN phosphatase expression in dendrites during postnatal brain development. Brain Res Mol Brain Res, 128: 8 – 19.

Pfrieger FW (2003). Cholesterol homeostasis and function in neurons of the central nervous system. Cell Mol Life Sci, 60: 1158 – 1171

Phillips JB, Williams AJ, Adams J, Elliott PJ, Tortella FC (2000). Proteasome inhibitor PS-519 reduces infarction and attenuates leukocyte infiltration in a rat model of focal cerebral ischemia. Stroke, 31: 1686 – 1693.

Pike LJ (2003). Lipid rafts: bringing order to chaos. J Lipid Res, 44: 655 – 667.

Qiu JH, Asai A, Chi S, Saito N, Hamada H, Kirino T (2000). Proteasome inhibitors induce cytochrome c-caspase-3-like protease-mediated apoptosis in cultured cortical neurons. J Neurosci, 20: 259 – 265.

Rajkumar SV, Richardson PG, Hideshima T and Anderson KC (2005). Proteasome inhibition as a novel therapeutic target in human cancer. J Clin Oncol, 23: 630 – 639.

Rao RV, Ellerby HM and Bredesen DE (2004). Coupling endoplasmic reticulum stress to the cell death program. Cell Death Differ, 11: 372 – 380.

Rao RV, Niazi K, Mollahan P, Mao X, Crippen D, Poksay KS, Chen S and Bredesen DE (2005). Coupling endoplasmic reticulum stress to the cell-death program: A novel HPS90-independent role for the small chaperone protein p23. Cell Death Differ, in press.

Reimertz C, Kögel D, Rami A, Chittenden T and Prehn JHM (2003). Gene expression during ER stress-induced apoptosis in neurons: induction of the BH3-only protein Bbc3/PUMA and activation of the mitochondrial apoptosis pathway. J Cell Biol, 162: 587 – 597.

Rockwell P, Yuan H, Magnusson R and Figueiredo-Pereira ME (2000). Proteasome inhibition in neuronal cells induces a proinflammatory response manifested by upregulation of cyclooxygenase-2, its accumulation as ubiquitin conjugates, and production of the prostaglandin PGE_2. Arch Biochem Biophys, 374: 325 – 333.

Romano MF, Festa M, Pagliuca G, Lerose R, Bisogni R, Chiurazzi F, Storti G, Volpe S, Venuta S, Turco MC, Leone A (2003). BAG3 protein controls B-chronic lymphocytic leukaemia cell apoptosis. Cell Death Differ, 10: 383 – 385.

Ross AH, Lachyankar MB and Recht LD (2001). PTEN: a newly identified regulator of neuronal differentiation. Neuroscientist, 7: 278 – 281.

Rutkowski DT and Kaufman RJ (2004). A trip to the ER: coping with stress. Trends Cell Biol, 14: 20 – 28.

Salvesen GS and Dixit VM (1997). Caspases: intracellular signaling by proteolysis. Cell, 91: 443 – 446.

Sawada H, Kohno R, Kihara T, Izumi Y, Sakka N, Ibi M, Nakanishi M, Nakamizo T, Yamakawa K, Shibasaki H, Taniguchi T and Shimohama S (2004). Proteasome mediate dopaminergic neuronal degeneration, and its inhibition causes α-synuclein inclusions. J Biol Chem, 279: 10710 – 10719.

Schroder M and Kaufman RJ (2005). ER stress and the unfolded protein response. Mutat Res, 569: 29 – 63.

Schroeder RJ, Ahmed SN, Zhu Y, London E, Brown DA (1998). Cholesterol and sphingolipid enhance the triton X-100 insolubility of glycosylphosphatidylinositol-anchored proteins by promoting the formation of detergent-insoluble ordered membrane domain. J Biol Chem, 273: 1150 – 1157.

Schulz JG, Bösel J, Stoeckel M, Megow D, Dirnagl U and Endres M (2004). HMG-CoA reductase inhibition causes neurite loss by interfering with geranylgeranylpyrophosphate synthesis. J Neurochem, 89: 24 – 32.

Shay NF and Banz WJ (2005). Regulation of gene transcription by botanicals: novel regulatory mechanisms. Annu Rev Nutr, 25: 14.1 – 14.19.

Shen and Thayer (1998). Cannabinoid receptor agonists protect cultured rat hippocampal neurons from excitotocivity, Mol Pharmacol, 54: 459 – 462.

Shen X, Zhang K and Kaufman RJ (2004). The unfolded protein response – a stress signaling pathway of the endoplasmic reticulum. J Chem Neuroanat, 28: 79 – 92.

Sherman MY and Goldberg AL (2001). Cellular Defenses against Unfolded Proteins: A Cell Biologist Thinks about Neurodegenerative Diseases. Neurons, 29: 15 – 32.

Shimura H, Hattory N, Kubo S, Mizuno Y, Askawa S, Minoshima S, Shimizu N, Iwai K, Chiba T, Tanaka K and Suzuki T (2000). Familial Parkinson disease gene product, parkin, is a ubiquitin-protein ligase. Nat Genet, 25: 302 – 305.

Sillence DJ and Allan D (1998). Evidence against an early signaling role for ceramide in Fas-mediated apoptosis. J Biochem 342: 29 – 32.

Sinor AD, Irvin SM and Greenberg DA (2000). Endocannabinoids protect cerebral cortical neurons from in vitro ischemia in rats. Neurosci Lett, 278: 157 – 160.

Sitia R and Braakman I (2003). Quality control in the endoplasmic reticulum protein factory. Nature, 426: 891 – 894.

Smart EJ, Ying YS, Mineo C and Anderson RGW (1995) A detergent-free method for purifying caveolae membrane from tissue culture cells. Proc Natl Acad Sci USA, 92: 10104 – 10108

Snyder H, Mensah K, Theisler C, Lee J, Matouschek A, Wolozin B (2003). Aggregated and monomeric alpha-synuclein bind to the S6' proteasomal protein and inhibit proteasomal function. J Biol Chem, 278: 11753 – 11759.

Song S and Jung Y (2004). Alzheimer's disease meets the ubiquitin-proteasome system. Trends Mol Med, 10: 565 – 570.

Stenzel-Poore M, Stevens SL, Xiong Z, Lessov NS, Harrington CA, Mori M, Meller R, Rosenzweig HL, Tobar E, Shaw TE, Chu X and Simon RP (2003). Effect of ischaemic preconditioning on genomic response to cerebral ischaemia: similarity to neuroprotective strategies in hibernation and hypoxia-tolerant states. The Lancet, 362: 1028 – 1037.

Suh J, Lee YA and Gwag BJ (2005). Induction and attenuation of neuronal apoptosis by proteasome inhibitors in murine cortical cell cultures. J Neurochem, 95: 684 – 694.

Sun Y, Ouwang Y-B, Xu L, Chow AM-Y, Anderson R, Hecker JG and Giffard RG (2005). The carbozyl-terminal domain of inducible Hsp70 protects from ischemic injury in vivo and in vitro. J Cereb Blood Flow Metab, 1 – 4, in press.

Takeda M, Kato H, Takamiya A, Yoshida A, Kiyama H (2000). Injury-specific expression of activating transcription factor-3 in retinal ganglion cells and its colocalized expression with phosphorylated c-Jun. Invest Ophthalmol Vis Sci, 41: 2412 – 2421.

Tanaka T, Tatsuno I, Uchida D, Moroo I, Morio H, Nakamura S, Noguchi Y, Yasuda T, Kitagawa M, Saito Y and Hirai A (2000). Geranylgeranyl-pyrophosphate, and isoprenoid of mevalonate cascade, is a critical compound for rat primary cultured cortical neurons to protect the cell death induced by 3-hydroxy-3-methylglutarul-CoA reductase inhibition. J Neuronsci, 28: 2852 – 2859.

Taylor DM, Kabashi E, Agar JN, Minotti S and Durham HD (2005). Proteasome activity or expression is not altered by activation of the heat shock transcription factor Hsf1 in cultured fibroblasts or myoblasts. Cell Stress Chaperones, 10: 230 – 241.

Torres J, Rodriguez J, Myers MP, Valiente M, Graves JD, Tonks NK and Pulido R (2003) Phosphorylation-regulated cleavage of the tumor suppressor PTEN by caspase-3: implications for the control of protein stability and PTEN-protein interactions. J Biol Chem, 278: 30652 – 30660

Travers KJ, Patil CK, Wodicka L, Lockhart DJ, Weissman JS and Walter P (2000). Functional and genomic analyses reveal an essential coordination between the unfolded protein response and ER-associated degradation. Cell, 101: 249 – 258.

Trejo JL, Carro E, Garcia-Galloway E, Torres-Aleman I (2003). Role of insulin-like growth factor 1 signaling in neurodegenerative diseases. J Mol Med, 82: 156 – 162.

Tsujino H, Kondo E, Fukuoka T, Dai Y, Tokunaga A, Miki K, Yonenobu K, Ochi T, Noguchi K (2000). Activating transcription factor 3 (ATF3) induction by axotomy in sensory and motoneurons: a novel neuronal marker of nerve injury. Mol Cell Neurosci, 15: 170 – 182.

Ueda N, Okamoto Y and Morishita J (2005). N-acylphosphatidylethanolamine-hydrolyzing phospholipase D: a novel enzyme of the β-lactamase fold family releasing anandamide and other N-acylethanolamines. Life Sci, 77: 1750 – 1758.

Veldhuis WB, van der Stelt M, Wadman MW, van Zadelhoff G, Maccarrone M, Fezza F, Veldink GA, Vliegenthart JFG, Bar PR, Nicolay K and Di Marzo V (2003). Neuroprotection by the endogenous cannabinoid anandamide and arvanil against in vivo excitotoxicity in the rat: role of vanilloid receptors and lipoxygenases. J Neurosci, 23: 4127 – 4133.

Verkhratsky A and Toescu EC (2003). Endoplasmic reticulum Ca2+ homeostasis and neuronal death. J Cell Mol Med, 7: 351 – 361.

Waite KA and Eng C (2002) Protean PTEN: form and function. Am J Hum Genet, 70: 829 – 844

Wan SB, Chen D, Dou QP and Chan TH (2004). Study of the green tea polyphenols catechin-3-gallate (CG) and epicatechin-3-gallate (EGC) as proteasome inhibitors. Bioorg Med Chem, 12: 3521 – 3527.

Wang X, Gjörloff-Wingre A, Saxena M, Pathan N, Reed JC and Mustelin T (1999) The tumor suppressor PTEN regulates T cell survival and antigen receptor signalling by acting as a phosphatidylinositol 3-phosphate. J Immunol, 164: 1934 – 1939

Wang XZ, Lawson B, Brewer JW, Zinszner H, Sanjay A, Mi LJ, Boorstein R, Kreibich, Hendershot LM and Ron D (1996). Signals from the stressed endoplasmic reticulum induce C/EBP-homologous protein (CHOP/GADD153). Mol Cell Biol, 16: 4273 – 4280.

Wang XZ, Kuroda M, Sok J, Batchvarova N, Kimmel R, Chung P, Zinszner H and Ron D (1998). Identification of novel stress-induced genes down stream of CHOP. EMBO J, 17: 3619 – 3630.

Wang ZY, Huang MT, Lou YR, Xie JG, Reuhl KR, Newmark HL, Ho CT, Yang CS, Conney AH (1994). Inhibitory effects of black tea on ultraviolet B light-induced skin carcinogenesis in 7,12-dimethylbenz[a]anthracene-initiated SKH-1 mice. Cancer Res, 54: 3428 – 3455.

Wenk MR, Lucast L, Di Paolo G, Romanelli AJ, Suchy SF, Nussbaum RL, Cline GW, Shulman GI, McMurray W and De Camilli PD (2003). Phosphoinositide profiling in complex lipid mixtures using electrospray ionization mass spectrometry. Nat Biotech, 21: 813 – 817.

Wenk MR and De Camilli PD (2004). Protein-lipid interactions and phosphoinositide metabolism in membrane traffic: insights from vesicle recycling in nerve terminals. Proc Natl Acad Sci USA, 101: 8286 – 8269.

Wilson BS, Steinberg SL, Liederman K, Pfeiffer JR, Surviladze Z, Zhang J, Samelson LE, Yang L. Kotula PG and Oliver JM (2004). Markers for detergent-resistant lipid rafts occupy distinct and dynamic domains in native membranes. Mol Biol Cell, 15: 2580 – 2592.

Wójcik C (2002). Regulation of apoptosis by the ubiquitin and proteasome pathway. J Cell Mol Med, 6: 25 – 48.

Wojcik C and DeMartino GN (2003). Intracellular localization of proteasomes. Int J Biochem Cell Biol, 35: 579 – 589.

Wojcik C and Di Napoli (2004). Ubiquitin-proteasome system and proteasome inhibition: new strategies in stroke therapy. Stroke, 35: 1506 – 1518.

Yang Y and Yu X (2003). Regulation of apoptosis: the ubiquitous way. FASEB J, 17: 790 – 799.

Yew EHJ, Cheung NS, Choy MS, Qi RZ, Lee AY, Peng ZF, Melendez AJ, Manikandan J, Koay ES, Chiu L, Ng WL, Whiteman M, Kamiah J and Halliwell B

(2005). Proteasome inhibition by lactacystin in primary neuronal cells induces both potentially neuroprotective and pro-apoptotic transcriptional responses: a microarray analysis. J Neurochem, 94: 943 – 956.

Zeng L, Lu M, Mori K, Luo S, Lee AS, Zhu Y and Shyy J Y-J (2004). ATF6 modulates SREBP2-mediated lipogenesis. The EMBO Journal, 23: 950 – 958.

Zimmermann J, Erdmann D, Lalande I, Grossenbacher R, Noorani M and Fürst P (2000). Proteasome inhibitor induced gene expression profiles reveal overexpression of transcriptional regulators ATF3, GADD153 and MAD1. Oncogene, 19: 2913 – 2920.

9 APPENDIX A: Reagents and Buffers

9.1 Western blot

5X SDS/Glycine electrophoresis running buffer: 15.1 g/L Tris base, 72 g Glycine, 5 g SDS (NUMI)
30% acrylamide, Bis solution, 37.5:1 (BioRad #161-0158)
TEMED (Fluka #87689)
Ammonium Persulfate (BioRad #161-0700)
SuperSignal® West Femto (Pierce # 34095)
SuperSignal® West Pico (Perice #34080)
SuperSignal® West Dura (Pierce #34075)
Western Blocking Reagent (Roche #1921681/1921673), or 5% Non-fat milk (Anlene™ Gold), 4% non-fat milk+1% BSA (Albumin, bovine serum Fraction V Sigma A-4503)
Complete Mini protease inhibitor tablets (Roche # 1836153)
Precision Plus Protein Standard (BioRad #161-0374)
Mild Ab stripping buffer (Chemicon #2502)
Strong Ab stripping buffer (Chemicon #2504)
Kodak BioMax film (Research Instruments)
PVDF membrane (Research Instruments)
Secondary antibodies, HRP conjugated (Pierce, BioRad, Sigma)
Beta-mercaptoethanol (Sigma #?)
Percision Plus protein™ standards (Dua Color) (#161-0374)
10_ Tris/Glycine buffer: 30.3 g/L Tris base, 144.13 g/L
Tris/Glycine transfer buffer: 1_Tris/Glycine buffer, 20% (v/v) methanol
RC DC Protein Assay (BioRad #500-0120)
Erase-It™ Background Eliminator (Pierce #21065)

9.2 Immunofluorescence

Paraformyldehyde(Sigma cat# 6148)
NH_4Cl (Merck)
PBS [80 g/L NaCl, 2 g/L KCl, 14.4 g/L Na2HPO4, 2.4 KH2PO4] NUMI
Triton X-100 (Merck)
Goat Serum (Sigma #)
Alexa Fluor® 488 goat anti-mouse IgG (H+L), cat# A-11029, Molecular Probes, storage 4C in secondary antibody box
Alexa Fluor® 488 goat anti-rabbit IgG (H+L), cat# A-11034, Molecular Probes, storage at 4C in secondary antibody box
Alexa Fluor® 594 goat anti-mouse IgG (H+L), cat# A-11032, Molecular Probes, storage at 4C in secondary antibody box
Alexa Fluor® 594 goat anti-rabbit IgG (H+L), cat# A-11037, Molecular Probes, storage at 4C in secondary antibody box
FluorSave™ Reagent, cat# 345789, Calbiochem®, Storage RT

9.3 Composition of Neurobasal Medium (Brewer et al, 1993)

Components	Mg/liter	μM
Inorganic salts		
$CaCl_2$ (Anhydrous)	200	1800
$Fe(NO_3)_3.9H_2O$	0.1	0.2
Kcl	400	5360
$MgCl_2$ (Anhydrous)	77.3	812
NaCl	3000	51300
$NaHCO_3$	2200	26000
$NaH_2PO_4.H_2O$	125	900
Other components		
D-glucose	4500	25000
Phenol red	8.1	23
HEPES	2600	10000
Sodium Pyruvate	25	230
Amino acids		
L-alanine	2	20
L-arginine-HCl	84	400
L-asparagine-H_2O	0.83	5
L-cysteine	1.21	10
L-glutamine	73.5	500
L-glutamate	-	-
Glycine	30	400
L-histidine.Hcl.H_2O	42	200
L-isoleucine	105	800
L-leucine	105	800
L-lysine.HCl	146	5
L-methionine	30	200
L-phenylalanine	66	400
L-proline	7.76	67
L-serine	42	400
L-threonine	95	800
L-tryptophan	16	80
L-tyrosine	72	400
L-valine	94	800
Vitamins		
D-Ca pantothenate	4	8
Choline chloride	2	28
Folic acid	4	8
i-linositol	7.2	40
Niacinamide	4	30
Pyridoxal.HCl	4	20
Riboflavin	0.4	1
Thiamine.HCl	4	10
Vitamin B12	0.34	0.2

9.4 Composition of B27 Medium Supplement for Neurons (Brewer et al, 1993).

Biotin	Selenium
L-carnitine	T3 (triodo-1-thyronine)
Corticosterone	DL-α-tocopherol (vitamin E)
Ethanolamine	DL-α-tocopherol acetate
D(+)-galactose	Proteins:
Glutathione (reduced)	Albumin, bovine
Linoleic acid	Catalase
Linolenic acid	Insulin
Progesterone	Superoxide dismutase
Putrescine	Transferrin
Retinyl acetate	

Brewer GJ, Torricelli JR, Evege EK and Price PJ (1993). Optimized Survival of Hippocampal Neurons in B27-Supplemented Neurobasal™, a New Serum-free Medium Combination. Journal of Neuroscience Research, 35: 567 – 576.

9.5 Microarray: Eukaryotic Target Hybridization

9.5.1 Materials needed

Bovine Serum Albumin (BSA) solution (50 mg/mL), Invitrogen Life Technologies, P/N 15561-020
Herring Sperm DNA, Promega Corporation, P/N D1811
GeneChip Eukaryotic Hybridization Control Kit, Affymetrix, P/N 900454 (30 reactions) or
P/N 900457 (150 reactions), contains Control cRNA and Control Oligo B2
Control Oligo B2, 3 nM, Affymetrix, P/N 900301 (can be ordered separately)
5M NaCl, RNase-free, DNase-free, Ambion, P/N 9760G
MES hydrate SigmaUltra, Sigma-Aldrich, P/N M5287
MES Sodium Salt, Sigma-Aldrich, P/N M5057
EDTA Disodium Salt, 0.5M solution (100 mL), Sigma-Aldrich, P/N E7889
DMSO, Sigma-Aldrich, P/N D5879
Surfact-Amps 20 (Tween-20), 10%, Pierce Chemical, P/N 28320

9.5.2 Reagent Preparation

12X MES Stock Buffer (1.22M MES, 0.89M [Na+]) for 1,000 mL:
64.61g of MES hydrate
193.3g of MES Sodium Salt
800 mL of Molecular Biology Grade water
Mix and adjust volume to 1,000 mL.
The pH should be between 6.5 and 6.7. Filter through a 0.2 _m filter.

2X Hybridization Buffer (Final 1X concentration is 100 mM MES, 1M [Na+], 20 mM EDTA, 0.01% Tween-20) for 50 mL:
8.3 mL of 12X MES Stock Buffer

17.7 mL of 5M NaCl
4.0 mL of 0.5M EDTA
0.1 mL of 10% Tween-20
19.9 mL of water
Store at 2°C to 8°C, and shield from light
Do not autoclave. Store at 2°C to 8°C, and shield from light.
Discard solution if yellow.

Eukaryotic Arrays: Washing, Staining, and Scanning
Reagents and Materials Required
R-Phycoerythrin Streptavidin, Molecular Probes, P/N S-866
20X SSPE (3M NaCl, 0.2M NaH2PO4, 0.02M EDTA), BioWhittaker Molecular Applications / Cambrex, P/N 51214
Goat IgG, Reagent Grade, Sigma-Aldrich, P/N I 5256
Anti-streptavidin antibody (goat), biotinylated, Vector Laboratories, P/N BA-0500
Reagent Preparation

Wash Buffer A: Non-Stringent Wash Buffer (6X SSPE, 0.01% Tween-20) for 1,000 mL:
300 mL of 20X SSPE
1.0 mL of 10% Tween-20
699 mL of water
Filter through a 0.2 _m filter

Wash Buffer B: Stringent Wash Buffer(100 mM MES, 0.1M [Na+], 0.01% Tween-20) for 1,000 mL:
83.3 mL of 12X MES Stock Buffer (see Section 2, Chapter 2 for reagent preparation)
5.2 mL of 5M NaCl
1.0 mL of 10% Tween-20
910.5 mL of water
Filter through a 0.2 _m filter
Store at 2°C to 8°C and shield from light

2X Stain Buffer (Final 1X concentration: 100 mM MES, 1M [Na+], 0.05% Tween-20) for 250 mL:
41.7 mL of 12X MES Stock Buffer (see Section 2, Chapter 2 for reagent preparation)
92.5 mL of 5M NaCl
2.5 mL of 10% Tween-20
113.3 mL of water
Filter through a 0.2 _m filter
Store at 2°C to 8°C and shield from light
10 mg/mL Goat IgG Stock
Resuspend 50 mg in 5 mL of 150 mM NaCl
Store at 4°C

10 APPENDIX B: The gene list of microarray analysis (lactacystin treatment): >2FC, one-way ANOVA, p<0.01

Table 10.1. Ubiquitin-proteasome System

Probe id	Symbol	Gene Title	Time points (h)				Genbank
			4.5	7.5	24	48	
100955_at	2700084L22Rik	RIKEN cDNA 2700084L22 gene	2.24 ± 0.26	1.53 ± 0.11	1.06 ± 0.11	1.38 ± 0.16	AA989957
95600_at	Arih2	ariadne homolog 2 (Drosophila)	2.61 ± 0.14	4.11 ± 0.14	1.24 ± 0.15	-1.05 ± 0.19	AJ130975
96892_at	Psma1	proteasome subunit, alpha type 1	2.79 ± 0.09	3.37 ± 0.10	2.49 ± 0.20	-1.06 ± 0.14	AI836804
92544_f_at	Psma3	proteasome subunit, alpha type 3	2.45 ± 0.09	2.83 ± 0.06	1.74 ± 0.14	-1.04 ± 0.15	AF055983
94841_at	Psma5	proteasome subunit, alpha type 5	2.16 ± 0.08	2.69 ± 0.10	2.48 ± 0.30	1.01 ± 0.21	AW048997
93988_at	Psma7	proteasome subunit, alpha type 7	2.60 ± 0.08	3.53 ± 0.07	2.35 ± 0.13	-1.09 ± 0.19	AI836676
98113_at	Psmb1	proteasome subunit, beta type 1	1.52 ± 0.07	1.80 ± 0.06	2.00 ± 0.10	1.04 ± 0.17	U60824
94219_at	Psmb2	proteasome subunit, beta type 2	-1.57 ± 0.06	2.28 ± 0.09	2.63 ± 0.39	-1.20 ± 0.22	AI853269
94025_at	Psmb3	proteasome subunit, beta type 3	2.78 ± 0.06	4.50 ± 0.20	3.22 ± 0.21	1.10 ± 0.24	AW045339
98557_f_at	Psmb4	proteasome subunit, beta type 4	2.21 ± 0.06	2.26 ± 0.07	1.95 ± 0.11	1.03 ± 0.19	U65636
101992_at	Psmb6	proteasome subunit, beta type 6	1.99 ± 0.10	2.60 ± 0.07	2.40 ± 0.16	-1.11 ± 0.18	U13393
160152_at	Psmc1	proteasome 26S subunit, ATPase 1	2.28 ± 0.12	3.79 ± 0.09	2.29 ± 0.16	-1.06 ± 0.13	U39302
95448_at	Psmc2	proteasome 26S subunit, ATPase 2	2.58 ± 0.09	2.53 ± 0.07	2.49 ± 0.26	-1.16 ± 0.13	AI839371
93734_i_at	Psmc3	proteasome 26S subunit, ATPase 3	2.71 ± 0.07	3.13 ± 0.11	2.27 ± 0.12	-1.05 ± 0.13	D49686
103319_at	Psmd10	proteasome 26S subunit, non-ATPase, 10	2.21 ± 0.10	1.19 ± 0.10	-1.21 ± 0.10	1.49 ± 0.18	AB022022
160305_at	Psmd11	proteasome 26S subunit, non-ATPase, 11	5.34 ± 0.07	5.03 ± 0.27	2.75 ± 0.17	1.02 ± 0.12	AW121693

93971_f_at	Psmd12	proteasome 26S subunit, non-ATPase, 12	3.34 ± 0.06	3.62 ± 0.20	2.56 ± 0.31	-1.09 ± 0.17	AI838669
95742_at	Psmd13	proteasome 26S subunit, non-ATPase, 13	1.59 ± 0.07	2.30 ± 0.07	1.92 ± 0.11	1.02 ± 0.15	AW045451
97274_at	Psmd14	proteasome 26S subunit, non-ATPase, 14	2.26 ± 0.06	2.72 ± 0.09	2.22 ± 0.18	-1.18 ± 0.14	Y13071
92769_at	Psmd3	proteasome 26S subunit, non-ATPase, 3	1.12 ± 0.07	2.95 ± 0.07	1.95 ± 0.12	-1.12 ± 0.11	M25149
94302_at	Psmd4	proteasome 26S subunit, non-ATPase, 4	2.85 ± 0.07	5.29 ± 0.12	3.07 ± 0.35	-1.05 ± 0.21	AF013099
96698_at	Psmd5	proteasome 26S subunit, non-ATPase, 5	1.94 ± 0.07	2.79 ± 0.13	1.46 ± 0.19	-1.06 ± 0.14	AI835520
103350_at	Psmd7	proteasome 26S subunit, non-ATPase, 7	2.38 ± 0.08	3.03 ± 0.08	1.88 ± 0.30	-1.31 ± 0.15	M64641
98522_at	Psmd8	proteasome 26S subunit, non-ATPase, 8	2.30 ± 0.13	2.38 ± 0.10	1.38 ± 0.10	-1.11 ± 0.15	AI839158
95124_i_at	Rbx1	ring-box 1	3.18 ± 0.11	2.00 ± 0.19	1.13 ± 0.15	-1.21 ± 0.17	AW122337
160205_f_at	Rnf11	ring finger protein 11	2.04 ± 0.06	1.74 ± 0.09	1.01 ± 0.11	-1.29 ± 0.11	AB024427
101966_s_at	Rnf13	ring finger protein 13	2.09 ± 0.09	3.13 ± 0.12	1.00 ± 0.10	1.13 ± 0.12	AF037206
93164_at	Rnf2	ring finger protein 2	1.79 ± 0.10	3.25 ± 0.17	-1.57 ± 0.10	-1.12 ± 0.14	Y12783
96961_at	Rnf110	ring finger protein 110	3.08 ± 0.15	1.55 ± 0.15	-1.08 ± 0.17	1.14 ± 0.17	AI503821
101069_g_at	Mkrn1	makorin, ring finger protein, 1	1.96 ± 0.09	3.10 ± 0.08	-1.25 ± 0.12	-1.32 ± 0.12	AA656621
100985_at	Siah1a	seven in absentia 1A	1.86 ± 0.07	2.33 ± 0.09	1.16 ± 0.11	-1.40 ± 0.12	Z19579
101255_at	Ubb	ubiquitin B	3.10 ± 0.07	3.62 ± 0.06	1.08 ± 0.15	-1.19 ± 0.14	X51703
95215_f_at	Ubc	ubiquitin C	4.04 ± 0.09	4.79 ± 0.07	1.39 ± 0.16	-1.25 ± 0.12	D50527
102812_i_at	Ube1dc1	ubiquitin-activating enzyme E1-domain containing 1	1.82 ± 0.11	2.30 ± 0.06	1.66 ± 0.14	1.06 ± 0.13	AW210346
93069_at	Ube2d2	ubiquitin-conjugating enzyme E2D 2	2.46 ± 0.10	2.13 ± 0.12	1.08 ± 0.14	-1.30 ± 0.13	U62483

101581_at	Ube3a	ubiquitin protein ligase E3A	3.65 ± 0.08	1.93 ± 0.09	1.24 ± 0.11	-1.20 ± 0.10	U82122
94018_at	Ubl3	ubiquitin-like 3	2.17 ± 0.06	1.57 ± 0.07	1.41 ± 0.13	1.13 ± 0.15	AW120725
95601_at	Ubqln1	ubiquilin 1	1.31 ± 0.06	2.30 ± 0.10	1.08 ± 0.10	-1.29 ± 0.17	AW125420
93303_at	Ufd1l	ubiquitin fusion degradation 1 like	2.49 ± 0.07	4.45 ± 0.07	2.05 ± 0.34	-1.43 ± 0.16	U64445
161870_at	Usp15	ubiquitin specific protease 15	-3.77 ± 0.09	-3.28 ± 0.12	-1.57 ± 0.12	1.50 ± 0.24	AV359471
99085_at	Usp3	ubiquitin specific protease 3	1.42 ± 0.14	2.55 ± 0.07	1.26 ± 0.12	1.03 ± 0.13	AI021421
99086_g_at	Usp3	ubiquitin specific protease 3	1.73 ± 0.10	2.74 ± 0.11	1.14 ± 0.12	-1.23 ± 0.15	AI021421
160724_at	Usp49	ubiquitin specific protease 49	2.06 ± 0.24	2.51 ± 0.08	-1.06 ± 0.10	-1.06 ± 0.11	AJ245617

Table 10.2. Heat shock proteins and molecular chaperone

Probe id	Symbol	Gene Title	Time points (h)				Genbank
			4.5	7.5	24	48	
104589_at	C80913	expressed sequence C80913	2.04 ± 0.10	-1.11 ± 0.06	1.38 ± 0.12	1.16 ± 0.11	AF091096
98153_at	Cct3	chaperonin subunit 3 (gamma)	2.24 ± 0.10	2.54 ± 0.08	1.79 ± 0.22	-1.17 ± 0.14	L20509
160562_at	Cct7	chaperonin subunit 7 (eta)	2.00 ± 0.10	2.09 ± 0.06	1.53 ± 0.25	-1.34 ± 0.12	Z31399
96254_at	Dnajb1	DnaJ (Hsp40) homolog, subfamily B, member 1	2.11 ± 0.20	3.52 ± 0.15	1.42 ± 0.26	-1.12 ± 0.12	AB028272
98572_at	Dnajb11	DnaJ (Hsp40) homolog, subfamily B, member 11	1.84 ± 0.10	2.21 ± 0.08	1.41 ± 0.13	-1.12 ± 0.12	AW122551
93853_at	Dnajb4	DnaJ (Hsp40) homolog, subfamily B, member 4	2.19 ± 0.16	2.69 ± 0.13	1.46 ± 0.21	-1.24 ± 0.12	AA763918
104625_at	Dnajb6	DnaJ (Hsp40) homolog, subfamily B, member 6	1.61 ± 0.21	2.16 ± 0.15	-1.30 ± 0.15	-1.03 ± 0.11	AA874130
103344_at	Dnajc1	DnaJ (Hsp40) homolog, subfamily C, member 1	2.31 ± 0.30	1.86 ± 0.09	1.42 ± 0.10	1.32 ± 0.11	L16953
94422_at	Dnajc13	DnaJ (Hsp40) homolog, subfamily C, member 13	2.12 ± 0.08	1.37 ± 0.08	1.07 ± 0.15	-1.17 ± 0.11	AI842938
102414_i_at	Dnajc3	DnaJ (Hsp40) homolog, subfamily C, member 3	2.05 ± 0.14	2.25 ± 0.15	1.31 ± 0.10	1.42 ± 0.12	U28423
93211_at	Dnajc5	DnaJ (Hsp40) homolog, subfamily C, member 5	1.41 ± 0.10	3.16 ± 0.17	-1.48 ± 0.17	-1.56 ± 0.16	AF032115
102761_at	Grpel2	GrpE-like 2, mitochondrial	2.03 ± 0.12	2.07 ± 0.17	1.15 ± 0.13	-1.20 ± 0.10	AF041060
98111_at	Hsp105	heat shock protein 105	1.57 ± 0.09	2.38 ± 0.08	2.54 ± 0.53	-1.20 ± 0.13	L40406
93875_at	Hspa1a	heat shock protein 1A	-1.27 ± 0.13	4.70 ± 0.53	13.82 ± 6.14	1.78 ± 0.53	M12571

101955_at	Hspa5	heat shock 70kD protein 5 (glucose-regulated protein)	2.20 ± 0.07	2.39 ± 0.06	1.87 ± 0.17	-1.13 ± 0.11	AJ002387
96564_at	Hspa8	heat shock protein 8	2.05 ± 0.08	1.96 ± 0.10	1.14 ± 0.14	-1.18 ± 0.10	X54401
97914_at	Hspa9a	heat shock protein, A	1.68 ± 0.07	3.68 ± 0.07	2.18 ± 0.27	1.07 ± 0.16	D17666
160139_at	Hspb8	heat shock 27kDa protein 8	-1.37 ± 0.12	1.67 ± 0.16	8.08 ± 0.47	2.22 ± 0.48	AI848798
95359_at	Hspcb	heat shock protein 1, beta	2.06 ± 0.06	2.82 ± 0.11	1.46 ± 0.20	-1.08 ± 0.17	M18186
92829_at	Hspe1	heat shock protein 1 (chaperonin 10)	1.60 ± 0.07	1.38 ± 0.06	2.34 ± 0.15	1.17 ± 0.15	U09659
101207_at	Ppia	peptidylprolyl isomerase A	2.43 ± 0.07	1.98 ± 0.06	-1.08 ± 0.10	-1.18 ± 0.13	X52803
100089_at	Ppic	peptidylprolyl isomerase C	1.20 ± 0.11	-1.27 ± 0.07	1.77 ± 0.16	2.10 ± 0.16	M74227
99350_at	Sec63	SEC63-like (S. cerevisiae)	1.70 ± 0.36	2.32 ± 0.12	1.28 ± 0.10	-1.06 ± 0.13	C76102
94817_at	Serpinh1	serine (or cysteine) proteinase inhibitor, clade H, member 1	1.14 ± 0.08	3.10 ± 0.06	6.16 ± 0.15	3.30 ± 0.43	X60676

Table 10.3. Stress

Probe id	Symbol	Gene Title	Time points (h)				Genbank
			4.5	7.5	24	48	
ER stress							
104155_f_at	Atf3	activating transcription factor 3	3.77 ± 0.13	11.13 ± 0.38	6.68 ± 1.76	2.06 ± 0.27	U19118
100599_at	Atf4	activating transcription factor 4	3.52 ± 0.06	3.73 ± 0.09	-1.03 ± 0.25	-2.13 ± 0.12	M94087
101429_at	Ddit3	DNA-damage inducible transcript 3	2.90 ± 0.10	5.01 ± 0.12	2.65 ± 0.42	1.02 ± 0.15	X67083
95057_at	Herpud1	homocysteine-inducible, endoplasmic reticulum stress-inducible, ubiquitin-like domain member 1	1.93 ± 0.08	3.18 ± 0.16	1.17 ± 0.22	-1.32 ± 0.11	AI846938
94821_at	Xbp1	X-box binding protein 1	1.99 ± 0.08	2.30 ± 0.09	-1.21 ± 0.12	-1.74 ± 0.10	AW123880
92925_at	Cebpb	CCAAT/enhancer binding protein (C/EBP), beta	-1.13 ± 0.18	4.26 ± 0.14	3.44 ± 0.34	1.32 ± 0.13	M61007
Oxidative stress							
94132_at	Gpx1	glutathione peroxidase 1	-2.11 ± 0.07	-2.43 ± 0.06	-1.10 ± 0.10	-1.02 ± 0.10	X03920
97681_f_at	Gstm3	glutathione S-transferase, mu 3	-5.19 ± 0.15	-3.77 ± 0.07	-1.11 ± 0.11	1.06 ± 0.11	J03953
93026_at	Mgst1	microsomal glutathione S-transferase 1	1.63 ± 0.14	1.07 ± 0.12	4.13 ± 0.61	2.97 ± 0.36	AW124337
93573_at	Mt1	metallothionein 1	-1.24 ± 0.07	-2.35 ± 0.06	2.98 ± 0.10	4.14 ± 1.04	V00835
101561_at	Mt2	metallothionein 2	-1.51 ± 0.06	-2.20 ± 0.06	2.22 ± 0.11	2.77 ± 0.45	K02236
95340_at	Mt3	metallothionein 3	-4.44 ± 0.06	-3.65 ± 0.06	1.15 ± 0.11	1.85 ± 0.27	M93310
100606_at	Prnp	prion protein	1.46 ± 0.08	2.09 ± 0.07	1.43 ± 0.12	-1.02 ± 0.12	M18070
100538_at	Sod1	superoxide dismutase 1, soluble	-3.26 ± 0.06	-1.50 ± 0.07	2.19 ± 0.43	1.05 ± 0.33	M35725
Other							
100081_at	Stip1	stress-induced phosphoprotein 1	1.67 ± 0.10	2.46 ± 0.10	1.25 ± 0.12	1.04 ± 0.11	U27830

Table 10.4. Inflammatory responses

Probe id	Symbol	Gene Title	Time points (h)				Genbank
			4.5	7.5	24	48	
98088_at	Cd14	CD14 antigen	-2.35 ± 0.13	-3.62 ± 0.07	-1.13 ± 0.11	1.33 ± 0.13	X13333
160511_at	Cxcl12	chemokine (C-X-C motif) ligand 12	2.37 ± 0.17	1.77 ± 0.22	-1.32 ± 0.17	-1.51 ± 0.14	L12029
103202_at	Gbp3	guanylate nucleotide binding protein 3	1.14 ± 0.18	-1.19 ± 0.15	2.87 ± 0.18	2.67 ± 0.21	AW047476
101341_at	H2-M9	histocompatibility 2, M region locus 9	-5.34 ± 0.14	-5.30 ± 0.06	-1.52 ± 0.10	-1.01 ± 0.13	AF016308
102250_at	Il27ra	interleukin 27 receptor, alpha	-2.61 ± 0.08	-2.23 ± 0.07	-1.23 ± 0.12	-1.16 ± 0.15	AF053005
93077_s_at	Ly6c	lymphocyte antigen 6 complex, locus C	-2.71 ± 0.07	-2.44 ± 0.08	-1.20 ± 0.10	-1.09 ± 0.13	D86232
96939_at	Myl9	myosin, light polypeptide 9, regulatory	1.01 ± 0.17	-1.09 ± 0.11	1.62 ± 0.16	2.18 ± 0.25	AI842649
101923_at	Pla2g7	phospholipase A2, group VII (platelet-activating factor acetylhydrolase, plasma)	-1.20 ± 0.07	-1.66 ± 0.06	-1.61 ± 0.15	2.14 ± 0.18	U34277
97944_f_at	Tcra	T-cell receptor alpha chain	-2.45 ± 0.07	-1.71 ± 0.07	-1.14 ± 0.13	1.06 ± 0.13	AF099808

Table 10.5. Cholesterol biosynthesis

Probe id	Symbol	Gene Title	Time points (h)				Genbank
			4.5	7.5	24	48	
94325_at	Hmgcs1	3-hydroxy-3-methylglutaryl-Coenzyme A synthase 1	1.39 ± 0.07	-1.22 ± 0.06	-2.85 ± 0.09	-2.07 ± 0.10	AW124932
94916_at	Cyp51	cytochrome P450, 51	-1.41 ± 0.06	-1.47 ± 0.10	-3.21 ± 0.10	-3.12 ± 0.10	AW122260
160770_at	Mvd	mevalonate (diphospho) decarboxylase	-3.06 ± 0.07	-2.61 ± 0.06	-6.96 ± 0.08	-4.98 ± 0.09	AW049778
95632_f_at	Mvk	mevalonate kinase	1.51 ± 0.15	1.17 ± 0.09	-8.26 ± 0.09	-7.52 ± 0.09	AW122653
98970_at	Ggps1	geranylgeranyl diphosphate synthase 1	2.67 ± 0.13	2.79 ± 0.18	1.06 ± 0.13	-1.30 ± 0.11	AB016044
98630_at	Nsdhl	NAD(P) dependent steroid dehydrogenase-like	1.62 ± 0.09	1.01 ± 0.06	-3.50 ± 0.09	-2.91 ± 0.10	AW106745
96269_at	Idi1	isopentenyl-diphosphate delta isomerase	-1.53 ± 0.06	-2.39 ± 0.06	-5.82 ± 0.09	-4.78 ± 0.09	AA716963
104285_at	Hmgcr	3-hydroxy-3-methylglutaryl-Coenzyme A reductase	-1.77 ± 0.06	-1.53 ± 0.06	-2.43 ± 0.10	-3.38 ± 0.09	M62766
160737_at	Lss	lanosterol synthase	-1.23 ± 0.12	-1.11 ± 0.13	-2.65 ± 0.11	-3.17 ± 0.11	AW060927
100418_at	Gng2	guanine nucleotide binding protein (G protein), gamma 2 subunit	1.39 ± 0.07	2.36 ± 0.13	-1.96 ± 0.11	-2.00 ± 0.11	AW123750

Table 10.6. Lipid

Probe id	Symbol	Gene Title	Time points (h)				Genbank
			4.5	7.5	24	48	
102381_at	Acsl4	acyl-CoA synthetase long-chain family member 4	1.05 ± 0.07	-2.08 ± 0.06	-1.92 ± 0.09	-2.37 ± 0.10	AA619207
93720_at	Agpat1	1-acylglycerol-3-phosphate O-acyltransferase 1 (lysophosphatidic acid acyltransferase, alpha)	-3.47 ± 0.08	-1.30 ± 0.06	-1.44 ± 0.11	-1.28 ± 0.11	AB005623
98372_at	Aldh1a3	aldehyde dehydrogenase family 1, subfamily A3	1.43 ± 0.29	-1.94 ± 0.29	3.25 ± 0.21	-1.31 ± 0.13	AW050387
93320_at	Cpt1a	carnitine palmitoyltransferase 1a, liver	1.03 ± 0.08	1.05 ± 0.06	2.79 ± 0.13	3.23 ± 0.49	AF017175
103581_at	Cte1	cytosolic acyl-CoA thioesterase 1	1.09 ± 0.07	-1.14 ± 0.07	1.59 ± 0.10	2.38 ± 0.37	Y14004
103924_at	D8Ertd319e	DNA segment, Chr 8, ERATO Doi 319, expressed	-2.72 ± 0.06	-1.70 ± 0.06	-1.09 ± 0.14	-1.24 ± 0.13	AW048884
94393_r_at	Elovl2	elongation of very long chain fatty acids (FEN1/Elo2, SUR4/Elo3, yeast)-like 2	-2.49 ± 0.06	-2.84 ± 0.06	-1.45 ± 0.10	-1.40 ± 0.10	AI317360
94418_at	Elovl6	ELOVL family member 6, elongation of long chain fatty acids (yeast)	1.26 ± 0.07	-1.12 ± 0.09	-2.30 ± 0.10	-2.13 ± 0.10	AI839004
98575_at	Fasn	fatty acid synthase	-1.01 ± 0.07	-1.26 ± 0.06	-2.29 ± 0.09	-2.22 ± 0.10	X13135
97518_at	Fdft1	farnesyl diphosphate farnesyl transferase 1	1.25 ± 0.08	1.71 ± 0.10	-3.17 ± 0.10	-3.22 ± 0.10	D29016
103367_at	Galgt1	UDP-N-acetyl-alpha-D-galactosamine:(N-acetylneuraminyl)-galactosylglucosylceramide-beta-1, 4-N-acetylgalactosaminyltransferase	-1.29 ± 0.09	-1.02 ± 0.08	-1.32 ± 0.10	-2.13 ± 0.11	U18975
104134_at	Gdap2	ganglioside-induced differentiation-associated-protein 2	2.17 ± 0.16	2.91 ± 0.23	1.38 ± 0.31	-1.49 ± 0.14	Y17851
94854_g_at	Gnb1	guanine nucleotide binding protein, beta 1	1.20 ± 0.07	2.26 ± 0.07	-1.59 ± 0.10	-1.81 ± 0.12	U29055
96909_at	Ndufab1	NADH dehydrogenase (ubiquinone) 1, alpha/beta subcomplex, 1	2.14 ± 0.06	1.76 ± 0.10	1.34 ± 0.10	1.06 ± 0.17	AI849803
104342_i_at	Pla2g12a	phospholipase A2, group XIIA	2.08 ± 0.12	1.10 ± 0.08	-1.02 ± 0.11	1.18 ± 0.13	AI845798
92466_at	Plcb1	phospholipase C, beta 1	-2.04 ± 0.07	-2.03 ± 0.06	-1.24 ± 0.10	-1.07 ± 0.11	U85714
92465_at	Plcb1	phospholipase C, beta 1	2.07 ± 0.13	2.02 ± 0.09	-1.67 ± 0.10	-1.57 ± 0.17	U85713
92474_at	Pld1	phospholipase D1	-1.70 ± 0.12	-2.08 ± 0.09	-1.03 ± 0.10	1.66 ± 0.19	AF083497

100927_at	Pltp	phospholipid transfer protein	-3.48 ± 0.09	-3.43 ± 0.09	1.45 ± 0.27	3.04 ± 0.12	U28960
100622_at	Prdx6	peroxiredoxin 6	1.29 ± 0.06	-1.10 ± 0.06	1.66 ± 0.23	2.26 ± 0.21	AF093857
160808_at	Prkab1	protein kinase, AMP-activated, beta 1 non-catalytic subunit	1.75 ± 0.11	2.29 ± 0.06	1.58 ± 0.15	1.06 ± 0.11	AI854287
161864_f_at	Ptdss1	phosphatidylserine synthase 1	-1.56 ± 0.13	-2.27 ± 0.08	1.19 ± 0.12	-1.18 ± 0.11	AV068306
103386_at	Pte1	peroxisomal acyl-CoA thioesterase 1	-1.08 ± 0.10	2.40 ± 0.10	-1.39 ± 0.13	-1.65 ± 0.13	AW046123
160388_at	Sc4mol	sterol-C4-methyl oxidase-like	-1.12 ± 0.07	-1.59 ± 0.06	-2.95 ± 0.10	-3.66 ± 0.09	AI848668
94056_at	Scd1	stearoyl-Coenzyme A desaturase 1	-2.08 ± 0.06	-2.02 ± 0.07	-5.64 ± 0.09	-7.42 ± 0.09	M21285
103569_at	Sh3glb1	SH3-domain GRB2-like B1 (endophilin)	2.71 ± 0.08	1.80 ± 0.11	-1.30 ± 0.11	-1.24 ± 0.16	AI842874
160865_at	Vldlr	very low density lipoprotein receptor	3.68 ± 0.16	1.83 ± 0.15	-1.68 ± 0.12	-1.46 ± 0.16	L33417

Table 10.7. Apoptosis

Probe id	Symbol	Gene Title	Time points (h)				Genbank
			4.5	7.5	24	48	
161980_f_at	Bag3	Bcl2-associated athanogene 3	1.37 ± 0.29	1.97 ± 0.24	6.36 ± 1.02	3.41 ± 0.70	AV373612
94448_at	Bcl10	B-cell leukemia/lymphoma 10	1.37 ± 0.14	2.06 ± 0.07	1.30 ± 0.10	1.11 ± 0.13	AJ006289
99018_at	Bclaf1	BCL2-associated transcription factor 1	1.21 ± 0.12	1.81 ± 0.09	-1.59 ± 0.12	1.33 ± 0.27	AA874446
102727_at	Bdnf	brain derived neurotrophic factor	2.28 ± 0.19	1.23 ± 0.10	1.56 ± 0.12	-1.17 ± 0.13	X55573
95093_at	Ccar1	cell division cycle and apoptosis regulator 1	2.63 ± 0.09	1.58 ± 0.16	-1.02 ± 0.11	-1.27 ± 0.13	AI035334
95545_at	Igf1	insulin-like growth factor 1	-4.23 ± 0.08	-2.11 ± 0.07	-1.49 ± 0.11	-1.45 ± 0.14	X04480
160309_at	Map3k7ip2	mitogen-activated protein kinase kinase kinase 7 interacting protein 2	2.00 ± 0.11	1.94 ± 0.11	1.29 ± 0.12	1.07 ± 0.15	AW259500
98110_at	Mdm2	transformed mouse 3T3 cell double minute 2	1.17 ± 0.07	1.18 ± 0.07	2.77 ± 0.41	1.26 ± 0.14	AI853375
93439_f_at	Pawr	PRKC, apoptosis, WT1, regulator	-1.10 ± 0.17	1.06 ± 0.18	1.87 ± 0.27	2.70 ± 0.34	AA260005
160696_at	Tia1	cytotoxic granule-associated RNA binding protein 1	2.41 ± 0.08	1.95 ± 0.08	1.05 ± 0.10	1.03 ± 0.11	U00689
102599_at	Tpt1	tumor protein, translationally-controlled 1	2.10 ± 0.07	2.05 ± 0.06	1.10 ± 0.11	-1.10 ± 0.13	X06407
104275_g_at	Trp53	transformation related protein 53	-1.29 ± 0.08	2.01 ± 0.14	1.36 ± 0.15	1.16 ± 0.11	AB021961
160115_at	Txnl1	thioredoxin-like 1	2.53 ± 0.09	1.79 ± 0.09	1.75 ± 0.11	1.13 ± 0.12	AF052660

Table 10.8. Proteolysis

Probe id	Symbol	Gene Title	Time points (h)				Genbank
			4.5	7.5	24	48	
94238_at	2310046G15Rik	RIKEN cDNA 2310046G15 gene	-1.24 ± 0.11	-2.06 ± 0.09	1.65 ± 0.23	3.29 ± 0.21	AW228316
101040_at	Capn2	calpain 2	2.23 ± 0.09	2.63 ± 0.12	1.57 ± 0.10	1.05 ± 0.14	D38117
93048_at	Clpp	caseinolytic protease, ATP-dependent, proteolytic subunit homolog (E. coli)	2.43 ± 0.10	3.38 ± 0.10	1.75 ± 0.18	-1.15 ± 0.19	AJ005253
160349_at	Cndp2	CNDP dipeptidase 2 (metallopeptidase M20 family)	1.56 ± 0.13	2.77 ± 0.13	1.88 ± 0.12	-1.13 ± 0.17	AI854839
92256_at	Ctsb	cathepsin B	2.85 ± 0.27	3.18 ± 0.16	2.20 ± 0.12	1.82 ± 0.20	AI853714
93810_at	Ctsd	cathepsin D	1.01 ± 0.06	1.69 ± 0.07	2.15 ± 0.13	1.91 ± 0.21	X68378
97336_at	Ctsf	cathepsin F	-2.52 ± 0.07	1.11 ± 0.08	1.09 ± 0.10	1.14 ± 0.11	AJ131851
96270_at	D11Bwg0434e	DNA segment, Chr 11, Brigham & Women's Genetics 0434 expressed	-1.66 ± 0.06	-2.15 ± 0.06	-1.18 ± 0.10	-1.09 ± 0.10	AI847092
161358_r_at	Dpep3	dipeptidase 3	-1.64 ± 0.13	-3.89 ± 0.09	-1.48 ± 0.11	-1.13 ± 0.11	AV209030
98287_at	Dpp6	dipeptidylpeptidase 6	-3.44 ± 0.07	-2.61 ± 0.06	-1.41 ± 0.11	-1.26 ± 0.14	AF092507
94380_at	Ide	insulin degrading enzyme	1.71 ± 0.07	3.48 ± 0.08	2.34 ± 0.53	-1.10 ± 0.13	AI852581
160290_at	Ide	insulin degrading enzyme	3.17 ± 0.07	3.03 ± 0.08	2.78 ± 0.43	-1.04 ± 0.10	AI574278
92607_at	Mest	mesoderm specific transcript	1.39 ± 0.07	-1.15 ± 0.08	2.56 ± 0.19	2.22 ± 0.19	AF017994
104015_at	Metap1	methionyl aminopeptidase 1	1.75 ± 0.10	2.27 ± 0.11	1.12 ± 0.19	-1.41 ± 0.12	AW047992
93981_at	Plat	plasminogen activator, tissue	1.18 ± 0.14	1.05 ± 0.10	2.66 ± 0.13	2.11 ± 0.20	J03520
161446_r_at	Prss25	protease, serine, 25	-2.11 ± 0.06	-2.26 ± 0.06	-1.32 ± 0.10	-1.06 ± 0.10	AV353694
104025_at	Thop1	thimet oligopeptidase 1	-1.49 ± 0.07	1.96 ± 0.06	-1.02 ± 0.13	-1.15 ± 0.11	AW047185
96730_at	Tpp2	tripeptidyl peptidase II	2.22 ± 0.14	2.98 ± 0.32	1.24 ± 0.10	-1.16 ± 0.13	X81323

Table 10.9. Growth and development

Probe id	Symbol	Gene Title	Time points (h)				Genbank
			4.5	7.5	24	48	
100584_at	Anxa4	annexin A4	-1.48 ± 0.18	-1.49 ± 0.22	2.69 ± 0.25	2.27 ± 0.21	U72941
93083_at	Anxa5	annexin A5	-1.32 ± 0.11	-1.01 ± 0.07	1.75 ± 0.11	2.51 ± 0.13	D63423
101475_at	Bmi1	B lymphoma Mo-MLV insertion region 1	3.02 ± 0.14	2.88 ± 0.07	1.13 ± 0.12	-1.14 ± 0.16	M64068
98066_r_at	Brd2	bromodomain containing 2	2.19 ± 0.07	2.18 ± 0.08	1.06 ± 0.20	-1.49 ± 0.11	AL009226
160430_at	Catnb	catenin beta	2.13 ± 0.07	1.84 ± 0.06	1.10 ± 0.11	-1.02 ± 0.10	M90364
103088_at	Chl1	cell adhesion molecule with homology to L1CAM	3.83 ± 0.08	1.93 ± 0.11	-1.83 ± 0.11	-1.79 ± 0.12	X94310
100022_at	Cish	cytokine inducible SH2-containing protein	2.16 ± 0.40	3.02 ± 0.14	-1.34 ± 0.10	-1.12 ± 0.10	D89613

99113_at	Cops3	COP9 (constitutive photomorphogenic) homolog, subunit 3 (Arabidopsis thaliana)	3.73 ± 0.20	3.08 ± 0.09	1.37 ± 0.17	-1.12 ± 0.18	AF071313
160098_s_at	Cryab	crystallin, alpha B	1.38 ± 0.07	2.67 ± 0.10	1.15 ± 0.12	-1.21 ± 0.11	AI842724
101450_at	Csf1	colony stimulating factor 1 (macrophage)	-1.41 ± 0.08	-1.32 ± 0.07	2.88 ± 0.24	2.02 ± 0.12	M21952
93294_at	Ctgf	connective tissue growth factor	2.94 ± 0.70	2.11 ± 0.28	14.63 ± 0.63	7.93 ± 1.62	M70642
92777_at	Cyr61	cysteine rich protein 61	1.44 ± 0.16	1.26 ± 0.17	2.69 ± 0.30	2.61 ± 0.14	M32490
97372_at	Dazap1	DAZ associated protein 1	-2.21 ± 0.10	-2.09 ± 0.08	-1.20 ± 0.10	-1.06 ± 0.11	AA880432
102896_at	Dok1	downstream of tyrosine kinase 1	3.28 ± 1.07	6.24 ± 0.31	3.79 ± 0.14	1.17 ± 0.17	U78818
97426_at	Emp1	epithelial membrane protein 1	1.18 ± 0.15	1.04 ± 0.08	4.98 ± 0.45	4.06 ± 0.14	X98471
97689_at	F3	coagulation factor III	-1.16 ± 0.11	1.42 ± 0.14	3.29 ± 0.17	2.14 ± 0.17	M26071
95637_at	Flnb	filamin, beta	-1.53 ± 0.10	1.04 ± 0.12	2.11 ± 0.15	1.63 ± 0.13	AI838592
102196_at	Gna11	guanine nucleotide binding protein, alpha 11	1.23 ± 0.14	2.15 ± 0.07	1.28 ± 0.11	-1.35 ± 0.10	U37413
95082_at	Igfbp3	insulin-like growth factor binding protein 3	1.03 ± 0.14	-1.46 ± 0.08	2.41 ± 0.17	1.47 ± 0.28	AI842277
100566_at	Igfbp5	insulin-like growth factor binding protein 5	1.65 ± 0.07	1.02 ± 0.06	-1.05 ± 0.10	2.06 ± 0.13	L12447
94335_r_at	Ina	internexin neuronal intermediate filament protein, alpha	2.19 ± 0.06	-1.37 ± 0.06	-1.61 ± 0.14	-1.52 ± 0.12	L27220
100277_at	Inhba	inhibin beta-A	-2.15 ± 0.09	-3.25 ± 0.06	-1.77 ± 0.12	-1.59 ± 0.10	X69619
160828_at	Inhbb	inhibin beta-B	-1.58 ± 0.09	-2.41 ± 0.08	-1.14 ± 0.12	1.15 ± 0.18	X69620
104386_f_at	Itgav	integrin alpha V	-1.88 ± 0.07	-2.69 ± 0.08	2.06 ± 0.13	2.23 ± 0.31	AI843901
93682_at	Ldb2	LIM domain binding 2	2.84 ± 0.18	1.69 ± 0.09	-1.89 ± 0.10	-1.80 ± 0.10	U89489
103021_r_at	Map3k1	mitogen activated protein kinase kinase kinase 1	-1.36 ± 0.19	-2.14 ± 0.11	-1.05 ± 0.18	1.39 ± 0.14	AI317205
94891_s_at	Mea1	male enhanced antigen 1	2.01 ± 0.15	2.63 ± 0.11	1.36 ± 0.10	-1.55 ± 0.15	M27938
96632_at	Morf4l2	mortality factor 4 like 2	1.84 ± 0.07	2.40 ± 0.06	1.20 ± 0.13	-1.17 ± 0.12	AB025049
92717_at	Neurod1	neurogenic differentiation 1	1.31 ± 0.08	1.27 ± 0.10	-1.78 ± 0.11	-2.58 ± 0.11	U28068
160668_at	Ogfr	opioid growth factor receptor	2.07 ± 0.13	2.92 ± 0.12	1.11 ± 0.10	-1.26 ± 0.11	AI838195
99023_at	Pafah1b2	platelet-activating factor acetylhydrolase, isoform 1b, alpha2 subunit	1.41 ± 0.13	2.41 ± 0.15	-1.03 ± 0.11	-1.84 ± 0.16	U57747

95368_at	Plxna2	plexin A2	2.24 ± 0.10	2.07 ± 0.15	-1.28 ± 0.10	-1.19 ± 0.13	D86949
93390_g_at	Prom1	prominin 1	1.00 ± 0.11	-1.54 ± 0.14	1.03 ± 0.12	2.13 ± 0.11	AF039663
97474_r_at	Ptn	pleiotrophin	-1.04 ± 0.08	-3.79 ± 0.07	1.04 ± 0.10	1.46 ± 0.13	D90225
98835_at	Sema3a	sema domain, immunoglobulin domain (Ig), short basic domain, secreted, (semaphorin) 3A	2.21 ± 0.18	1.93 ± 0.13	-1.09 ± 0.14	-1.12 ± 0.12	D85028
95387_f_at	Sema4b	sema domain, immunoglobulin domain (Ig), transmembrane domain (TM) and short cytoplasmic domain, (semaphorin) 4B	8.87 ± 0.47	3.89 ± 0.12	1.07 ± 0.20	-1.36 ± 0.17	AA266467
99911_at	Sema6b	sema domain, transmembrane domain (TM), and cytoplasmic domain, (semaphorin) 6B	-4.00 ± 0.07	-2.12 ± 0.06	-1.66 ± 0.10	-1.82 ± 0.12	AF036585
97519_at	Spp1	secreted phosphoprotein 1	2.90 ± 0.07	1.84 ± 0.07	1.00 ± 0.10	1.60 ± 0.23	X13986
103832_at	Tfip11	tuftelin interacting protein 11	2.14 ± 0.20	2.81 ± 0.15	1.15 ± 0.13	-1.21 ± 0.12	AF097181
100953_at	Timeless	timeless homolog (Drosophila)	-1.49 ± 0.07	-2.01 ± 0.07	-1.06 ± 0.10	1.23 ± 0.11	AB015598
161258_at	Wt1	Wilms tumor homolog	-3.34 ± 0.10	-3.99 ± 0.07	-1.23 ± 0.10	-1.20 ± 0.10	AV322247

Table 10.10. Regulation of transcription

Probe id	Symbol	Gene Title	Time points (h)				Genbank
			4.5	7.5	24	48	
95479_at	C1d	nuclear DNA binding protein	-1.83 ± 0.09	-2.84 ± 0.06	1.00 ± 0.12	-1.02 ± 0.13	X95591
92681_at	Magel2	melanoma antigen, family L, 2	3.33 ± 0.44	2.02 ± 0.20	1.85 ± 0.46	-1.79 ± 0.12	AJ243608
100554_at	Pdlim1	PDZ and LIM domain 1 (elfin)	-1.44 ± 0.11	-2.21 ± 0.09	1.59 ± 0.11	1.72 ± 0.15	AF053367
92280_at	Strm	striamin	-2.32 ± 0.13	-1.43 ± 0.09	1.71 ± 0.32	1.54 ± 0.22	AA867778
103762_at	2810405L04Rik	RIKEN cDNA 2810405L04 gene	1.69 ± 0.08	2.69 ± 0.08	1.55 ± 0.23	-1.31 ± 0.18	AI853340
97438_r_at	4631416I11Rik	RIKEN cDNA 4631416I11 gene	2.12 ± 0.30	1.20 ± 0.21	-1.85 ± 0.13	-1.33 ± 0.13	AW122483
97437_f_at	4631416I11Rik	RIKEN cDNA 4631416I11 gene	2.86 ± 0.30	1.56 ± 0.15	-1.09 ± 0.15	-1.52 ± 0.11	AW122483
96196_i_at	5730589K01Rik	RIKEN cDNA 5730589K01 gene	2.25 ± 0.12	2.85 ± 0.12	1.56 ± 0.13	-1.19 ± 0.11	AI851708
162010_r_at	Atf2	activating transcription factor 2	-1.02 ± 0.14	-2.51 ± 0.09	-1.24 ± 0.10	-1.14 ± 0.13	AV246802
95673_s_at	Basp1	brain abundant, membrane attached signal protein 1	2.83 ± 0.08	2.64 ± 0.07	-1.03 ± 0.12	-1.24 ± 0.13	AW124113

95674_r_at	Basp1	brain abundant, membrane attached signal protein 1	3.25 ± 0.09	2.25 ± 0.06	-1.09 ± 0.16	-1.39 ± 0.16	AI851985
100544_at	Brd7	bromodomain containing 7	1.63 ± 0.12	2.21 ± 0.14	1.12 ± 0.11	-1.30 ± 0.15	AW125534
98447_at	Cebpa	CCAAT/enhancer binding protein (C/EBP), alpha	-2.93 ± 0.07	-1.60 ± 0.07	1.11 ± 0.14	-1.09 ± 0.12	M62362
160894_at	Cebpd	CCAAT/enhancer binding protein (C/EBP), delta	-1.46 ± 0.09	-1.05 ± 0.13	2.82 ± 0.37	2.44 ± 0.11	X61800
92195_at	Cebpg	CCAAT/enhancer binding protein (C/EBP), gamma	2.08 ± 0.18	2.41 ± 0.11	1.33 ± 0.15	-1.13 ± 0.12	AB012273
103900_at	Centg3	centaurin, gamma 3	1.00 ± 0.18	2.19 ± 0.09	-1.07 ± 0.12	-1.87 ± 0.12	AW124150
94490_at	Cnot8	CCR4-NOT transcription complex, subunit 8	1.99 ± 0.17	2.03 ± 0.11	1.06 ± 0.11	-1.08 ± 0.14	AW122419
95460_at	Cops5	COP9 (constitutive photomorphogenic) homolog, subunit 5 (Arabidopsis thaliana)	2.90 ± 0.07	3.30 ± 0.08	1.55 ± 0.18	-1.07 ± 0.12	U70736
160502_at	Creg	cellular repressor of E1A-stimulated genes	3.72 ± 0.17	3.72 ± 0.33	3.45 ± 0.21	1.37 ± 0.15	AF084524
96793_at	Dmap1	DNA methyltransferase 1-associated protein 1	2.17 ± 0.16	2.74 ± 0.08	1.32 ± 0.13	1.01 ± 0.17	AI607813
96297_at	Ebna1bp2	EBNA1 binding protein 2	2.26 ± 0.13	2.51 ± 0.10	1.52 ± 0.10	1.00 ± 0.10	AI845934
160244_at	Fem1a	feminization 1 homolog a (C. elegans)	1.65 ± 0.09	2.22 ± 0.13	1.25 ± 0.10	-1.09 ± 0.13	AI836048
96046_at	Hdac1	histone deacetylase 1	1.89 ± 0.18	1.97 ± 0.07	1.19 ± 0.11	1.17 ± 0.13	X98207
97550_at	Hdac7a	histone deacetylase 7A	-2.05 ± 0.06	-1.58 ± 0.08	-1.03 ± 0.10	-1.12 ± 0.11	AW047228
103765_at	Hkr3	GLI-Kruppel family member HKR3	1.84 ± 0.41	3.35 ± 0.32	1.70 ± 0.13	1.01 ± 0.11	AA718040
100007_at	Irf2bp1	interferon regulatory factor 2 binding protein 1	-2.53 ± 0.06	-1.67 ± 0.06	-1.25 ± 0.11	-1.16 ± 0.12	AI837573
160396_at	Lass2	longevity assurance homolog 2 (S. cerevisiae)	1.47 ± 0.21	1.24 ± 0.15	2.27 ± 0.11	1.44 ± 0.12	AW121580
104590_at	Mef2c	myocyte enhancer factor 2C	1.59 ± 0.07	1.36 ± 0.10	-1.94 ± 0.10	-2.19 ± 0.13	L13171
103925_at	Mllt3	myeloid/lymphoid or mixed lineage-leukemia translocation to 3 homolog (Drosophila)	2.06 ± 0.08	1.15 ± 0.08	-1.45 ± 0.10	-1.19 ± 0.13	AW120605
96497_s_at	Myt1l	myelin transcription factor 1-like	2.24 ± 0.12	2.07 ± 0.07	-1.47 ± 0.10	-1.56 ± 0.11	AI848062
100962_at	Nab2	Ngfi-A binding protein 2	-1.42 ± 0.09	-1.28 ± 0.08	2.11 ± 0.13	1.44 ± 0.11	U47543
92562_at	Nfe2l2	nuclear factor, erythroid derived 2, like 2	1.07 ± 0.08	1.43 ± 0.08	2.99 ± 0.30	2.82 ± 0.15	U70475
99527_at	Nfe2l3	nuclear factor, erythroid derived 2, like 3	2.42 ± 0.58	2.47 ± 0.38	-4.39 ± 0.18	-1.21 ± 0.13	AB013852

102955_at	Nfil3	nuclear factor, interleukin 3, regulated	-1.02 ± 0.11	2.32 ± 0.14	1.05 ± 0.26	-1.83 ± 0.11	U83148
92747_at	Nkx2-2	NK2 transcription factor related, locus 2 (Drosophila)	-6.27 ± 0.12	-2.00 ± 0.16	1.14 ± 0.10	-1.03 ± 0.15	U31566
92956_at	Notch3	Notch gene homolog 3 (Drosophila)	-1.48 ± 0.09	-2.07 ± 0.08	1.13 ± 0.15	1.10 ± 0.12	X74760
101665_at	Nr5a1	nuclear receptor subfamily 5, group A, member 1	-2.03 ± 0.08	-2.21 ± 0.06	-1.35 ± 0.10	-1.16 ± 0.10	C85959
93740_at	Nsep1	nuclease sensitive element binding protein 1	3.42 ± 0.07	2.95 ± 0.09	1.01 ± 0.12	-1.15 ± 0.15	U33196
99158_at	Ostf1	osteoclast stimulating factor 1	-1.17 ± 0.16	-1.39 ± 0.09	2.71 ± 0.26	1.31 ± 0.13	U58888
102257_at	Pknox1	Pbx/knotted 1 homeobox	1.99 ± 0.08	2.29 ± 0.08	-1.65 ± 0.16	-1.01 ± 0.20	AF061270
99015_at	Pml	promyelocytic leukemia	-2.01 ± 0.07	-2.06 ± 0.06	-1.45 ± 0.10	1.05 ± 0.11	U33626
160146_r_at	Polr2c	polymerase (RNA) II (DNA directed) polypeptide C	2.47 ± 0.21	-1.15 ± 0.09	-1.23 ± 0.10	-1.26 ± 0.11	D83999
93325_at	Polr2e	polymerase (RNA) II (DNA directed) polypeptide E	2.03 ± 0.10	1.61 ± 0.07	1.33 ± 0.11	1.16 ± 0.13	AI845735
96306_at	Polr2i	polymerase (RNA) II (DNA directed) polypeptide I	1.76 ± 0.11	2.29 ± 0.09	1.08 ± 0.16	-1.97 ± 0.11	AI852210
95003_at	Polr2k	polymerase (RNA) II (DNA directed) polypeptide K	6.99 ± 0.18	4.09 ± 0.13	1.50 ± 0.20	1.15 ± 0.30	AA880275
102652_at	Pou3f1	POU domain, class 3, transcription factor 1	1.76 ± 0.17	-1.48 ± 0.13	-2.77 ± 0.11	1.03 ± 0.20	X56959
161347_r_at	Rpo1-1	RNA polymerase 1-1	-2.40 ± 0.08	-5.28 ± 0.10	-1.27 ± 0.10	1.04 ± 0.10	AV148041
98085_f_at	Rpo1-1 /// Rps28	RNA polymerase 1-1 /// ribosomal protein S28	3.15 ± 0.11	2.86 ± 0.07	1.12 ± 0.14	-1.03 ± 0.19	U11248
98081_at	Rpo1-3	RNA polymerase 1-3	1.96 ± 0.09	2.03 ± 0.12	1.11 ± 0.13	-1.19 ± 0.17	AI853173
102856_at	Sox10	SRY-box containing gene 10	-3.08 ± 0.08	-2.05 ± 0.08	-1.31 ± 0.11	1.08 ± 0.14	AF047389
101631_at	Sox11	SRY-box containing gene 11	2.53 ± 0.08	1.65 ± 0.17	-1.18 ± 0.10	-1.15 ± 0.13	AF009414
101684_r_at	Srst	simple repeat sequence-containing transcript	3.59 ± 0.07	3.35 ± 0.19	-1.09 ± 0.11	-1.13 ± 0.10	X67863
103504_at	Ssbp2	single-stranded DNA binding protein 2	2.11 ± 0.08	1.87 ± 0.07	-1.23 ± 0.10	-1.25 ± 0.10	AI837107
100094_at	Supt5h	suppressor of Ty 5 homolog (S. cerevisiae)	1.92 ± 0.07	2.40 ± 0.07	1.27 ± 0.14	-1.04 ± 0.14	U88539
92339_at	Taf1a	TATA box binding protein (Tbp)-associated factor, RNA polymerase I, A	1.70 ± 0.33	3.21 ± 0.08	1.38 ± 0.13	1.09 ± 0.11	Y09972
99041_at	Taf1b	TATA box binding protein (Tbp)-associated factor, RNA polymerase I, B	1.49 ± 0.08	2.08 ± 0.10	1.11 ± 0.13	-1.21 ± 0.12	Y09973

93918_at	Taf9	TAF9 RNA polymerase II, TATA box binding protein (TBP)-associated factor	2.61 ± 0.07	2.53 ± 0.08	1.18 ± 0.12	-1.11 ± 0.13	AA673500
102700_at	Tbr1	T-box brain gene 1	2.13 ± 0.10	1.44 ± 0.09	-1.09 ± 0.10	-1.19 ± 0.15	U49251
104622_at	Tcea2	transcription elongation factor A (SII), 2	1.45 ± 0.15	2.21 ± 0.28	1.16 ± 0.15	-1.12 ± 0.10	D86081
101008_at	Tcerg1	transcription elongation regulator 1 (CA150)	2.04 ± 0.16	1.89 ± 0.10	1.09 ± 0.13	-1.29 ± 0.10	AB023485
102354_at	Tcf19	transcription factor 19	1.11 ± 0.14	1.05 ± 0.14	1.35 ± 0.14	2.34 ± 0.16	AI049398
100947_at	Tcf20	transcription factor 20	3.65 ± 0.32	2.00 ± 0.28	-1.03 ± 0.11	-1.43 ± 0.19	AI847906
160363_at	Tcfl1	transcription factor-like 1	1.95 ± 0.06	2.53 ± 0.09	-1.15 ± 0.10	-1.31 ± 0.11	D43643
100935_at	Tcfl4	transcription factor-like 4	1.87 ± 0.15	2.31 ± 0.12	1.24 ± 0.10	-1.40 ± 0.13	U43548
94100_s_at	Trpc4	transient receptor potential cation channel, subfamily C, member 4	1.51 ± 0.27	-1.09 ± 0.09	-2.14 ± 0.10	-1.42 ± 0.10	AF011543
93656_g_at	Usf1	upstream transcription factor 1	-1.64 ± 0.07	2.10 ± 0.09	1.14 ± 0.15	-1.27 ± 0.12	X95316
103013_at	Usf2	upstream transcription factor 2	-1.87 ± 0.08	-2.24 ± 0.07	-1.22 ± 0.11	-1.23 ± 0.11	X77602
92444_f_at	Zfp1	zinc finger protein 1	2.46 ± 0.09	2.65 ± 0.11	-1.01 ± 0.10	-1.16 ± 0.11	X16493
102263_at	Zfp143	zinc finger protein 143	2.55 ± 0.15	2.27 ± 0.15	1.15 ± 0.23	-1.21 ± 0.10	U29513
99502_at	Zfp148	zinc finger protein 148	2.65 ± 0.14	1.49 ± 0.12	1.26 ± 0.13	1.00 ± 0.11	U80078
94937_at	Zfp277	zinc finger protein 277	2.46 ± 0.13	2.40 ± 0.15	1.17 ± 0.14	1.25 ± 0.11	AW121594
98032_at	Zfp35	zinc finger protein 35	2.01 ± 0.23	2.19 ± 0.11	1.09 ± 0.16	-1.30 ± 0.12	M36146
93350_f_at	Zfp422	zinc finger protein 422	1.87 ± 0.16	2.95 ± 0.08	-1.28 ± 0.10	-1.06 ± 0.19	AW209414
102304_f_at	Zfp61	zinc finger protein 61	2.71 ± 0.13	2.65 ± 0.17	1.02 ± 0.10	-1.27 ± 0.10	L28167
103841_at	Zfp64	zinc finger protein 64	2.03 ± 0.11	2.82 ± 0.15	1.62 ± 0.21	-1.23 ± 0.11	U49046
95521_s_at	Zfp68	zinc finger protein 68	1.85 ± 0.18	2.57 ± 0.15	-1.17 ± 0.10	-1.35 ± 0.13	AB024005
92934_at	Zfp90	zinc finger protein 90	2.38 ± 0.10	2.08 ± 0.18	-1.08 ± 0.13	-1.62 ± 0.11	X79828
96707_at	Zipro1	zinc finger proliferation 1	2.06 ± 0.07	2.50 ± 0.07	1.22 ± 0.24	-1.21 ± 0.14	D10630

Table 10.11. Regulation of cell cycle

Probe id	Symbol	Gene Title	Time points (h)				Genbank
			4.5	7.5	24	48	
96220_at	Lig3	ligase III, DNA, ATP-dependent	2.34 ± 0.13	1.43 ± 0.08	1.18 ± 0.16	-1.02 ± 0.14	AW123157
95471_at	Cdkn1c	cyclin-dependent kinase inhibitor 1C (P57)	2.36 ± 0.15	1.18 ± 0.12	1.22 ± 0.13	1.03 ± 0.11	U22399
92477_at	Spin	spindlin	1.11 ± 0.11	2.10 ± 0.13	-1.70 ± 0.10	-1.87 ± 0.19	AA681862
161931_r_at	Mki67	antigen identified by monoclonal antibody Ki 67	-4.08 ± 0.18	-1.83 ± 0.13	-1.29 ± 0.10	1.22 ± 0.13	AV309347
95610_at	Cdc5l	cell division cycle 5-like (S. pombe)	2.10 ± 0.21	2.09 ± 0.13	1.02 ± 0.16	1.03 ± 0.11	AA636547
92423_at	Pard6a	par-6 (partitioning defective 6,) homolog alpha (C. elegans)	2.02 ± 0.08	2.14 ± 0.06	-1.08 ± 0.12	-1.25 ± 0.14	AF070970

94954_at	Anapc4	anaphase promoting complex subunit 4	1.94 ± 0.07	2.08 ± 0.07	1.25 ± 0.14	-1.20 ± 0.11	AI846628
96236_at	Cdc16	CDC16 cell division cycle 16 homolog (S. cerevisiae)	3.04 ± 0.23	2.92 ± 0.11	1.81 ± 0.21	-1.34 ± 0.18	AW122965
96319_at	Cdc20	cell division cycle 20 homolog (S. cerevisiae)	1.90 ± 0.07	2.30 ± 0.07	1.50 ± 0.10	1.42 ± 0.11	AW061324
104090_at	Cdc23	CDC23 (cell division cycle 23, yeast, homolog)	1.89 ± 0.08	2.68 ± 0.15	-1.11 ± 0.18	-1.29 ± 0.14	AA657164
97527_at	Cks2	CDC28 protein kinase regulatory subunit 2	2.33 ± 0.10	2.19 ± 0.07	1.25 ± 0.11	1.64 ± 0.10	AA681998
94232_at	Ccnd1	cyclin D1	-2.21 ± 0.11	-2.31 ± 0.08	1.64 ± 0.10	1.28 ± 0.10	AI849928
102292_at	Gadd45a	growth arrest and DNA-damage-inducible 45 alpha	2.49 ± 0.12	4.20 ± 0.16	4.73 ± 0.62	1.98 ± 0.26	U00937
94482_at	Csnk2a2	casein kinase II, alpha 2, polypeptide	1.45 ± 0.21	2.04 ± 0.13	1.00 ± 0.11	-1.46 ± 0.13	AF012251
98067_at	Cdkn1a	cyclin-dependent kinase inhibitor 1A (P21)	1.27 ± 0.09	1.25 ± 0.08	3.14 ± 0.33	1.19 ± 0.17	U09507
99135_at	Cdc37	cell division cycle 37 homolog (S. cerevisiae)	1.42 ± 0.09	2.34 ± 0.06	1.08 ± 0.12	-1.06 ± 0.13	U43076
103520_at	Vegfa	vascular endothelial growth factor A	2.88 ± 0.43	4.89 ± 0.21	-1.07 ± 0.22	-1.38 ± 0.14	M95200
102821_s_at	Ran	RAN, member RAS oncogene family	2.09 ± 0.07	2.34 ± 0.08	1.40 ± 0.15	1.02 ± 0.17	L32752
101254_at	Ran	RAN, member RAS oncogene family	2.25 ± 0.07	2.14 ± 0.06	1.33 ± 0.14	1.00 ± 0.16	L32751
101959_r_at	Tfdp1	transcription factor Dp 1	2.01 ± 0.07	1.46 ± 0.06	1.14 ± 0.11	-1.06 ± 0.12	X72310
94264_at	Raf1	v-raf-1 leukemia viral oncogene 1	1.56 ± 0.07	2.22 ± 0.06	1.21 ± 0.19	-1.24 ± 0.15	AW122170
92502_at	Plagl1	pleiomorphic adenoma gene-like 1	-1.38 ± 0.12	-1.03 ± 0.07	2.04 ± 0.42	2.13 ± 0.20	X95504
93300_at	Tgfb2	transforming growth factor, beta 2	1.40 ± 0.18	-2.22 ± 0.08	1.14 ± 0.12	1.45 ± 0.16	X57413
99068_at	Anapc1	anaphase promoting complex subunit 1	1.89 ± 0.08	2.29 ± 0.08	1.39 ± 0.12	1.07 ± 0.10	X80169
160127_at	Ccng1	cyclin G1	-1.01 ± 0.07	-1.34 ± 0.06	2.59 ± 0.15	1.97 ± 0.13	L49507
98478_at	Ccng2	cyclin G2	2.24 ± 0.10	1.39 ± 0.07	-1.25 ± 0.10	-1.14 ± 0.12	U95826
100130_at	Jun	Jun oncogene	4.76 ± 0.45	8.30 ± 0.13	1.91 ± 0.42	-1.45 ± 0.14	X12761
97991_at	Kras2	Kirsten rat sarcoma oncogene 2, expressed	1.82 ± 0.13	2.06 ± 0.07	1.07 ± 0.14	-1.34 ± 0.10	X02452
96598_at	D430039C20Rik	RIKEN cDNA D430039C20 gene	2.14 ± 0.27	1.75 ± 0.10	-1.20 ± 0.10	1.03 ± 0.10	AA122714
100559_at	Dhx16	DEAH (Asp-Glu-Ala-His) box polypeptide 16	2.03 ± 0.08	2.00 ± 0.09	1.39 ± 0.13	1.03 ± 0.16	AI853344

160650_at	Polr3d	polymerase (RNA) III (DNA directed) polypeptide D	2.79 ± 0.11	2.31 ± 0.14	1.00 ± 0.10	-1.05 ± 0.11	AI844711
94820_r_at	Ccni	cyclin I	-1.33 ± 0.07	-2.73 ± 0.06	-1.38 ± 0.10	1.37 ± 0.13	AF005886

Table 10.12. Transport

Probe id	Symbol	Gene Title	Time points (h)				Genbank
			4.5	7.5	24	48	
161029_at	6330416G13Rik	RIKEN cDNA 6330416G13 gene	1.84 ± 0.25	2.37 ± 0.16	-1.07 ± 0.12	-1.44 ± 0.11	AI849583
93626_at	Abcg2	ATP-binding cassette, sub-family G (WHITE), member 2	1.40 ± 0.20	-1.20 ± 0.13	2.79 ± 0.17	1.26 ± 0.16	AF103875
92288_at	Ap1g1	adaptor protein complex AP-1, gamma 1 subunit	2.53 ± 0.10	3.99 ± 0.22	-1.48 ± 0.16	-1.50 ± 0.30	X54424
100492_at	Ap2a2	adaptor protein complex AP-2, alpha 2 subunit	-3.73 ± 0.07	1.17 ± 0.08	-1.18 ± 0.11	-1.29 ± 0.11	AW122807
103878_at	Ap3b1	adaptor-related protein complex 3, beta 1 subunit	1.78 ± 0.07	2.08 ± 0.06	1.24 ± 0.15	1.00 ± 0.15	AF103809
102704_at	Aqp4	aquaporin 4	-1.59 ± 0.08	-6.24 ± 0.09	-6.17 ± 0.10	1.22 ± 0.16	U88623
92428_at	Asna1	arsA (bacterial) arsenite transporter, ATP-binding, homolog 1	1.55 ± 0.11	2.49 ± 0.09	-1.11 ± 0.17	-1.34 ± 0.16	AF039405
93797_g_at	Atp1a1	ATPase, Na+/K+ transporting, alpha 1 polypeptide	-1.26 ± 0.10	2.16 ± 0.09	1.13 ± 0.18	1.46 ± 0.14	AW123952
96032_at	Atp5g1	ATP synthase, H+ transporting, mitochondrial F0 complex, subunit c (subunit 9), isoform 1	-3.88 ± 0.08	-2.23 ± 0.07	-1.69 ± 0.10	-1.34 ± 0.11	L19737
102854_s_at	Atp7a	ATPase, Cu++ transporting, alpha polypeptide	3.21 ± 0.13	2.24 ± 0.16	1.23 ± 0.13	1.04 ± 0.12	U03434
102786_at	Clcn3	chloride channel 3	1.51 ± 0.07	2.05 ± 0.09	1.16 ± 0.14	-1.28 ± 0.11	AI849432
94464_at	Clcn3	chloride channel 3	2.01 ± 0.06	1.25 ± 0.07	1.20 ± 0.10	-1.22 ± 0.14	AF029347
94465_g_at	Clcn3	chloride channel 3	2.23 ± 0.07	1.76 ± 0.07	1.14 ± 0.10	-1.26 ± 0.16	AF029347
95654_at	Clic1	chloride intracellular channel 1	1.45 ± 0.11	1.76 ± 0.09	3.64 ± 0.18	3.20 ± 0.45	AF109905
97248_at	Dbi	diazepam binding inhibitor	-1.52 ± 0.06	-3.44 ± 0.06	-1.91 ± 0.09	1.19 ± 0.14	X61431
104469_at	Gp38	glycoprotein 38	-1.70 ± 0.11	-2.19 ± 0.06	1.99 ± 0.13	2.67 ± 0.27	M73748
92946_f_at	Gria2	glutamate receptor, ionotropic, AMPA2 (alpha 2)	2.13 ± 0.07	1.18 ± 0.09	-1.15 ± 0.11	-1.18 ± 0.11	L32372
104684_at	Grin1	glutamate receptor, ionotropic, NMDA1 (zeta 1)	-2.44 ± 0.08	-1.47 ± 0.06	-1.32 ± 0.10	-1.11 ± 0.10	AI847120
104686_at	Grin1	glutamate receptor, ionotropic, NMDA1 (zeta 1)	-1.02 ± 0.13	2.30 ± 0.10	-1.68 ± 0.16	-1.73 ± 0.17	D10028
92392_at	Kcna3	potassium voltage-gated channel, shaker-related subfamily, member 3	2.06 ± 0.16	1.22 ± 0.12	-1.16 ± 0.10	-1.14 ± 0.12	AI850484

99450_at	Kcnq2	potassium voltage-gated channel, subfamily Q, member 2	-2.33 ± 0.08	-1.90 ± 0.07	1.03 ± 0.15	-1.24 ± 0.10	AB000503
104464_s_at	Kdelr3	KDEL (Lys-Asp-Glu-Leu) endoplasmic reticulum protein retention receptor 3	-1.45 ± 0.15	1.22 ± 0.16	2.37 ± 0.18	1.66 ± 0.17	AI642389
93993_at	Lman2	lectin, mannose-binding 2	1.97 ± 0.11	2.97 ± 0.12	1.30 ± 0.13	1.25 ± 0.10	AI851062
92952_f_at	Napb	N-ethylmaleimide sensitive fusion protein attachment protein beta	3.63 ± 0.15	2.19 ± 0.09	-1.18 ± 0.13	-1.91 ± 0.14	X61455
103953_at	Sec22l1	SEC22 vesicle trafficking protein-like 1 (S. cerevisiae)	2.36 ± 0.32	2.16 ± 0.07	1.76 ± 0.11	-1.04 ± 0.15	U91538
93711_at	Sec23a	SEC23A (S. cerevisiae)	1.55 ± 0.07	2.22 ± 0.06	-1.24 ± 0.10	-1.54 ± 0.15	D12713
161326_f_at	Serpina6	serine (or cysteine) proteinase inhibitor, clade A, member 6	-2.25 ± 0.19	-1.67 ± 0.15	1.00 ± 0.11	1.10 ± 0.12	AV104178
92831_at	Sfxn1	sideroflexin 1	2.50 ± 0.15	1.58 ± 0.08	1.04 ± 0.10	-1.08 ± 0.13	AI846308
104748_s_at	Slc1a1	solute carrier family 1 (neuronal/epithelial high affinity glutamate transporter, system Xag), member 1	1.15 ± 0.25	1.88 ± 0.17	-2.14 ± 0.15	-2.42 ± 0.15	D43797
100943_at	Slc1a4	solute carrier family 1 (glutamate/neutral amino acid transporter), member 4	1.40 ± 0.06	2.41 ± 0.10	-1.03 ± 0.26	-1.52 ± 0.10	U75215
98470_at	Slc25a14	solute carrier family 25 (mitochondrial carrier, brain), member 14	2.13 ± 0.13	2.79 ± 0.12	1.01 ± 0.16	-1.63 ± 0.15	AF076981
93084_at	Slc25a4	solute carrier family 25 (mitochondrial carrier, adenine nucleotide translocator), member 4	2.21 ± 0.07	1.96 ± 0.07	-1.05 ± 0.10	-1.19 ± 0.12	U27315
100618_f_at	Slc25a5	solute carrier family 25 (mitochondrial carrier; adenine nucleotide translocator), member 5	-1.64 ± 0.08	-2.59 ± 0.06	-1.06 ± 0.17	1.06 ± 0.13	AA062013
93804_at	Slc2a3	solute carrier family 2 (facilitated glucose transporter), member 3	1.72 ± 0.10	2.35 ± 0.13	-1.06 ± 0.12	-1.23 ± 0.10	AI854156
102683_at	Slc30a3	solute carrier family 30 (zinc transporter), member 3	-2.52 ± 0.08	-2.06 ± 0.07	-1.26 ± 0.11	-1.20 ± 0.10	U76009
101877_at	Slc31a1	solute carrier family 31, member 1	1.96 ± 0.18	2.24 ± 0.06	1.02 ± 0.11	-1.15 ± 0.11	AI854432
98457_at	Slc4a4	solute carrier family 4 (anion exchanger), member 4	-1.30 ± 0.13	-3.96 ± 0.11	-1.48 ± 0.13	1.46 ± 0.15	AF020195

161573_at	Slc4a7	solute carrier family 4, sodium bicarbonate cotransporter, member 7	-3.75 ± 0.07	-2.01 ± 0.07	-1.12 ± 0.10	1.02 ± 0.16	AV278013
93471_at	Slc4a7	solute carrier family 4, sodium bicarbonate cotransporter, member 7	-1.51 ± 0.07	-2.17 ± 0.07	1.03 ± 0.14	-1.08 ± 0.12	AI594427
161695_f_at	Slc6a4	solute carrier family 6 (neurotransmitter transporter, serotonin), member 4	-1.56 ± 0.12	-2.23 ± 0.08	-1.93 ± 0.13	1.25 ± 0.13	AV230927
96276_r_at	Smbp	SM-11044 binding protein	-1.80 ± 0.07	-2.50 ± 0.06	-1.03 ± 0.21	1.13 ± 0.16	AI843327
101906_at	Smc4l1	SMC4 structural maintenance of chromosomes 4-like 1 (yeast)	2.51 ± 0.08	1.57 ± 0.11	1.13 ± 0.10	1.66 ± 0.14	AA032310
94550_at	Snx1	sorting nexin 1	1.57 ± 0.15	2.03 ± 0.10	1.19 ± 0.10	1.05 ± 0.13	AW121324
102319_at	Snx12	sorting nexin 12	1.55 ± 0.08	3.10 ± 0.13	1.31 ± 0.12	-1.22 ± 0.13	AF062484
104651_at	Snx14	sorting nexin 14	2.03 ± 0.09	1.50 ± 0.10	1.31 ± 0.10	1.01 ± 0.11	AI839611
160635_at	Stx18	syntaxin 18	1.73 ± 0.12	2.97 ± 0.09	1.39 ± 0.13	-1.10 ± 0.10	AI849070
100933_at	Stx1a	syntaxin 1A (brain)	1.35 ± 0.08	1.34 ± 0.08	-1.98 ± 0.10	-2.29 ± 0.13	D45208
96019_at	Sypl	synaptophysin-like protein	2.22 ± 0.18	3.17 ± 0.22	1.51 ± 0.11	-1.01 ± 0.18	AI843476
98339_at	Syt11	synaptotagmin 11	2.85 ± 0.07	3.38 ± 0.11	-1.59 ± 0.17	-1.61 ± 0.19	AB026808
160190_at	Syt4	synaptotagmin 4	3.50 ± 0.20	1.10 ± 0.06	-1.45 ± 0.10	-1.40 ± 0.10	U10355
103035_at	Tap1	transporter 1, ATP-binding cassette, sub-family B (MDR/TAP)	-1.48 ± 0.15	1.05 ± 0.11	2.11 ± 0.14	1.45 ± 0.17	U60020
99481_at	Atp1a2	ATPase, Na+/K+ transporting, alpha 2 polypeptide	1.02 ± 0.08	-1.64 ± 0.07	-3.57 ± 0.09	-1.03 ± 0.26	AI839697
94739_at	Trpc1	transient receptor potential cation channel, subfamily C, member 1	1.03 ± 0.10	2.35 ± 0.10	-1.47 ± 0.10	-1.37 ± 0.13	U73625

Table 10.13. Electron transport

Probe id	Symbol	Gene Title	Time points (h)				Genbank
			4.5	7.5	24	48	
99009_at	Nnt	nicotinamide nucleotide transhydrogenase	1.89 ± 0.08	1.00 ± 0.08	1.44 ± 0.17	2.31 ± 0.30	Z49204
99985_at	Txnrd1	thioredoxin reductase 1	1.40 ± 0.06	2.37 ± 0.06	2.11 ± 0.11	1.13 ± 0.14	AB027565
160194_at	Gcdh	glutaryl-Coenzyme A dehydrogenase	-2.80 ± 0.06	-1.35 ± 0.07	-1.30 ± 0.12	-1.03 ± 0.15	U18992
102000_f_at	Uqcrc2	ubiquinol cytochrome c reductase core protein 2	3.40 ± 0.10	2.28 ± 0.11	1.19 ± 0.10	-1.03 ± 0.12	AI842835
103922_f_at	1500005G05Rik	RIKEN cDNA 1500005G05 gene	-1.38 ± 0.08	1.73 ± 0.10	4.87 ± 0.97	1.32 ± 0.34	AI839690
100550_f_at	Cox6c	cytochrome c oxidase, subunit VIc	2.68 ± 0.07	1.40 ± 0.06	1.02 ± 0.10	-1.06 ± 0.12	AW060422

96112_at	Etfa	electron transferring flavoprotein, alpha polypeptide	2.30 ± 0.08	1.42 ± 0.07	1.26 ± 0.11	1.65 ± 0.12	AI851178
98918_at	Txndc5	thioredoxin domain containing 5	-3.23 ± 0.12	-1.25 ± 0.06	1.18 ± 0.15	1.10 ± 0.17	AI841920
94209_g_at	Txndc7	thioredoxin domain containing 7	2.11 ± 0.14	3.17 ± 0.17	1.04 ± 0.10	-1.26 ± 0.10	AW045202
94208_at	Txndc7	thioredoxin domain containing 7	2.83 ± 0.07	4.28 ± 0.11	-1.33 ± 0.15	-1.48 ± 0.18	AW045202
162469_r_at	Cyc1	cytochrome c-1	-2.83 ± 0.07	-1.84 ± 0.07	-1.06 ± 0.15	-1.09 ± 0.14	AV069997
95072_at	Cyc1	cytochrome c-1	2.41 ± 0.06	1.97 ± 0.09	1.15 ± 0.11	-1.20 ± 0.13	AW121892
96773_at	Txndc4	thioredoxin domain containing 4 (endoplasmic reticulum)	2.45 ± 0.11	3.46 ± 0.11	1.38 ± 0.11	1.28 ± 0.18	AW125408

Table 10.14. Protein biosynthesis

Probe id	Symbol	Gene Title	Time points (h)				Genbank
			4.5	7.5	24	48	
100636_at	Eif4ebp1	eukaryotic translation initiation factor 4E binding protein 1	3.25 ± 0.25	3.89 ± 0.31	3.17 ± 0.33	1.55 ± 0.21	U28656
101213_at	Arbp	acidic ribosomal phosphoprotein P0	2.51 ± 0.07	2.46 ± 0.06	1.12 ± 0.11	-1.06 ± 0.15	X15267
104048_at	Cars	cysteinyl-tRNA synthetase	2.11 ± 0.07	3.77 ± 0.11	1.23 ± 0.34	-1.32 ± 0.13	AI848732
94766_at	Eef1a1	eukaryotic translation elongation factor 1 alpha 1	2.43 ± 0.06	2.62 ± 0.07	1.06 ± 0.11	-1.14 ± 0.12	M17878
160129_at	Eef1d	eukaryotic translation elongation factor 1 delta (guanine nucleotide exchange protein)	1.09 ± 0.07	2.04 ± 0.06	1.30 ± 0.10	1.16 ± 0.17	AI839632
94462_at	Eif2b1	eukaryotic translation initiation factor 2B, subunit 1 (alpha)	1.68 ± 0.23	2.25 ± 0.06	1.57 ± 0.10	-1.15 ± 0.11	AW120719
94530_at	Eif2b2	eukaryotic translation initiation factor 2B, subunit 2 beta	1.73 ± 0.07	2.77 ± 0.08	1.34 ± 0.21	-1.16 ± 0.13	AI840376
160554_at	Eif3s6	eukaryotic translation initiation factor 3, subunit 6	2.13 ± 0.19	1.19 ± 0.06	1.06 ± 0.10	1.21 ± 0.14	AI839363
100557_g_at	Eif4b	eukaryotic translation initiation factor 4B	2.01 ± 0.09	2.65 ± 0.06	-1.25 ± 0.10	1.32 ± 0.12	AW121930
98608_at	Etf1	eukaryotic translation termination factor 1	1.95 ± 0.09	2.13 ± 0.16	1.70 ± 0.14	-1.01 ± 0.14	AI845886
160451_at	Etf1	eukaryotic translation termination factor 1	2.31 ± 0.17	2.84 ± 0.09	1.40 ± 0.13	1.24 ± 0.15	D87691
160231_at	Farsla	phenylalanine-tRNA synthetase-like, alpha subunit	1.42 ± 0.07	2.91 ± 0.08	1.16 ± 0.10	-1.37 ± 0.10	AI851129
161683_r_at	Gtpbp1	GTP binding protein 1	-2.94 ± 0.07	-3.60 ± 0.06	-1.31 ± 0.09	-1.16 ± 0.10	AV239949
93752_at	Iars	isoleucine-tRNA synthetase	2.12 ± 0.07	3.22 ± 0.07	1.17 ± 0.26	-1.32 ± 0.14	AI848393

100136_at	Lamp2	lysosomal membrane glycoprotein 2	1.32 ± 0.12	1.24 ± 0.09	2.39 ± 0.12	2.48 ± 0.31	M32017
102019_at	Mrpl13	mitochondrial ribosomal protein L13	2.22 ± 0.07	2.07 ± 0.13	1.61 ± 0.10	1.15 ± 0.16	AA666635
99140_at	Mrpl16	mitochondrial ribosomal protein L16	2.31 ± 0.09	2.16 ± 0.19	1.63 ± 0.19	-1.31 ± 0.13	AW124920
98120_at	Mrpl27	mitochondrial ribosomal protein L27	1.97 ± 0.08	2.27 ± 0.07	1.56 ± 0.15	-1.05 ± 0.15	AI844807
102058_at	Mrpl9	mitochondrial ribosomal protein L9	2.03 ± 0.08	2.52 ± 0.15	1.24 ± 0.14	-1.08 ± 0.18	AI845667
97884_at	Mrps11	mitochondrial ribosomal protein S11	2.28 ± 0.08	2.10 ± 0.07	1.30 ± 0.10	1.05 ± 0.12	AI844175
95159_at	Mrps18b	mitochondrial ribosomal protein S18B	1.39 ± 0.07	2.10 ± 0.10	1.27 ± 0.10	-1.19 ± 0.12	AI846849
160423_at	Mrps2	mitochondrial ribosomal protein S2	1.85 ± 0.12	2.17 ± 0.09	1.42 ± 0.19	-1.05 ± 0.14	AI853575
93859_at	Mtif2	mitochondrial translational initiation factor 2	2.95 ± 0.19	2.34 ± 0.12	1.11 ± 0.10	1.05 ± 0.17	AI875598
95070_at	Nars	asparaginyl-tRNA synthetase	1.66 ± 0.07	2.35 ± 0.11	1.32 ± 0.19	-1.52 ± 0.12	AW125874
96693_at	Rars	arginyl-tRNA synthetase	2.10 ± 0.10	3.57 ± 0.26	2.54 ± 0.37	-1.16 ± 0.16	AI849453
94767_at	Rnu35b /// Rps11	RNA, U35b small nucleolar /// ribosomal protein S11	2.66 ± 0.07	2.27 ± 0.06	1.26 ± 0.11	-1.03 ± 0.17	U93864
100711_at	Rpl10a	ribosomal protein L10A	1.98 ± 0.10	2.15 ± 0.06	1.20 ± 0.10	1.05 ± 0.15	U12403
102109_at	Rpl13	ribosomal protein L13	2.24 ± 0.08	2.51 ± 0.07	1.30 ± 0.15	-1.01 ± 0.18	U28917
96290_f_at	Rpl21	ribosomal protein L21	2.09 ± 0.06	1.74 ± 0.08	1.10 ± 0.10	-1.07 ± 0.13	U93863
92857_at	Rpl22	ribosomal protein L22	1.74 ± 0.06	2.37 ± 0.07	1.14 ± 0.14	-1.32 ± 0.13	AI853960
100729_at	Rpl26	ribosomal protein L26	2.42 ± 0.11	2.11 ± 0.06	1.27 ± 0.12	-1.03 ± 0.15	X80699
100734_at	Rpl3	ribosomal protein L3	2.34 ± 0.08	2.32 ± 0.12	1.26 ± 0.12	-1.02 ± 0.16	Y00225
160081_at	Rpl36a	ribosomal protein L36a	2.03 ± 0.07	1.06 ± 0.12	-1.04 ± 0.10	1.14 ± 0.12	AW045418
92577_f_at	Rpl37	ribosomal protein L37	2.06 ± 0.06	1.71 ± 0.06	1.21 ± 0.10	-1.11 ± 0.13	AW047116
101129_at	Rpl5	ribosomal protein L5	2.03 ± 0.07	1.80 ± 0.06	1.27 ± 0.12	-1.03 ± 0.15	X83590
96962_at	Rpl6	ribosomal protein L6	1.84 ± 0.07	1.96 ± 0.07	1.22 ± 0.13	-1.03 ± 0.16	X81987
97695_s_at	Rpl7	ribosomal protein L7	2.12 ± 0.06	1.71 ± 0.06	1.15 ± 0.10	1.02 ± 0.12	M29015
98168_at	Rpl7a	ribosomal protein L7a	2.22 ± 0.06	2.23 ± 0.08	1.26 ± 0.13	1.00 ± 0.15	M14689
100694_at	Rplp1	ribosomal protein, large, P1	1.96 ± 0.06	2.56 ± 0.08	1.16 ± 0.13	-1.06 ± 0.15	U29402
160071_at	Rpp30	ribonuclease P/MRP 30kDa subunit (human)	1.90 ± 0.07	2.08 ± 0.10	1.04 ± 0.10	-1.41 ± 0.10	U95123
100686_at	Rps2	ribosomal protein S2	2.11 ± 0.06	2.01 ± 0.08	1.17 ± 0.10	-1.11 ± 0.12	M20632
96300_f_at	Rps27	ribosomal protein S27	2.29 ± 0.07	2.07 ± 0.10	1.27 ± 0.13	1.04 ± 0.17	AI854238
101137_at	Rps3	ribosomal protein S3	2.03 ± 0.09	2.06 ± 0.06	1.28 ± 0.13	-1.10 ± 0.16	X76772
101664_at	Rps3a	ribosomal protein S3a	2.29 ± 0.08	2.39 ± 0.07	1.16 ± 0.11	-1.04 ± 0.15	Z83368
99336_at	Rps5	ribosomal protein S5	1.98 ± 0.06	2.00 ± 0.06	1.28 ± 0.13	-1.02 ± 0.17	U78085
101577_at	Rps6	ribosomal protein S6	2.03 ± 0.13	1.76 ± 0.06	1.25 ± 0.10	1.06 ± 0.13	Z54209

101212_at	Rps7	ribosomal protein S7	2.67 ± 0.07	2.45 ± 0.06	1.15 ± 0.12	-1.09 ± 0.17	AF043285
95054_at	Tars	threonyl-tRNA synthetase	1.50 ± 0.15	2.50 ± 0.07	1.48 ± 0.22	-1.17 ± 0.13	AI849620
93564_at	Yars	tyrosyl-tRNA synthetase	1.00 ± 0.08	2.05 ± 0.09	1.14 ± 0.25	-1.70 ± 0.13	AW122542

Table 10.15. Protein transport

Probe id	Symbol	Gene Title	Time points (h)				Genbank
			4.5	7.5	24	48	
104297_at	Ipo11	importin 11	1.20 ± 0.07	2.26 ± 0.07	1.29 ± 0.17	-1.13 ± 0.15	AW124742
95034_f_at	Ipo4	importin 4	2.15 ± 0.10	1.71 ± 0.10	1.18 ± 0.10	-1.09 ± 0.13	AW212243
101104_at	Dscr3	Down syndrome critical region gene 3	1.65 ± 0.07	2.00 ± 0.13	1.13 ± 0.10	-1.09 ± 0.15	AB001990
102750_at	Apba3	amyloid beta (A4) precursor protein-binding, family A, member 3	-1.70 ± 0.09	1.85 ± 0.13	1.94 ± 0.20	1.29 ± 0.24	AF070975
94870_f_at	Sara2	SAR1a gene homolog 2 (S. cerevisiae)	2.13 ± 0.12	2.16 ± 0.07	1.37 ± 0.11	-1.22 ± 0.17	AW124226
100074_at	2400003B06Rik	RIKEN cDNA 2400003B06 gene	-6.99 ± 0.06	1.31 ± 0.20	1.59 ± 0.14	-1.34 ± 0.13	AW046723
160183_f_at	3930401E15Rik	RIKEN cDNA 3930401E15 gene	2.83 ± 0.22	1.51 ± 0.07	1.19 ± 0.14	-1.16 ± 0.10	AI846109
92968_at	Arf5	ADP-ribosylation factor 5	-2.76 ± 0.06	-1.66 ± 0.06	-1.05 ± 0.13	-1.36 ± 0.10	D87902
160868_at	Rab3b	RAB3B, member RAS oncogene family	1.71 ± 0.24	1.92 ± 0.08	-1.89 ± 0.10	-2.30 ± 0.10	AI835990
101933_at	Rab10	RAB10, member RAS oncogene family	2.55 ± 0.13	1.42 ± 0.06	-1.39 ± 0.11	-1.49 ± 0.14	AF035646
97222_at	Rab6	RAB6, member RAS oncogene family	-1.97 ± 0.06	-2.09 ± 0.07	-1.20 ± 0.10	-1.14 ± 0.11	AI845921
98927_at	Rab6	RAB6, member RAS oncogene family	2.38 ± 0.11	1.10 ± 0.08	-1.14 ± 0.14	-1.44 ± 0.10	AI851048
160795_at	Scamp1	secretory carrier membrane protein 1	1.50 ± 0.10	2.23 ± 0.12	1.11 ± 0.16	-1.58 ± 0.11	AW123662
98106_at	Timm44	translocator of inner mitochondrial membrane 44	1.87 ± 0.16	2.61 ± 0.08	1.14 ± 0.10	1.01 ± 0.12	U69898
104453_at	2310079P12Rik	RIKEN cDNA 2310079P12 gene	2.78 ± 0.12	3.44 ± 0.06	1.89 ± 0.34	-1.02 ± 0.21	AW046336
95022_at	Akap12	A kinase (PRKA) anchor protein (gravin) 12	1.19 ± 0.09	-1.03 ± 0.08	3.13 ± 0.30	1.02 ± 0.10	AB020886
99156_at	2700099C19Rik	RIKEN cDNA 2700099C19 gene	1.99 ± 0.08	1.86 ± 0.07	1.29 ± 0.12	-1.04 ± 0.17	AI853370
103642_at	G3bp	Ras-GTPase-activating protein SH3-domain binding protein	-2.09 ± 0.07	-1.94 ± 0.06	-1.02 ± 0.14	-1.04 ± 0.13	AB001927
101370_at	Kpna1	karyopherin (importin) alpha 1	2.02 ± 0.07	2.66 ± 0.14	1.14 ± 0.15	-1.37 ± 0.10	U20619
92790_at	Kpna2	karyopherin (importin) alpha 2	2.13 ± 0.16	1.39 ± 0.08	1.08 ± 0.10	1.44 ± 0.15	D55720

100710_at	Vcp	valosin containing protein	1.76 ± 0.06	2.65 ± 0.08	2.10 ± 0.28	-1.02 ± 0.14	Z14044

Table 10.16. Signal transduction

Probe id	Symbol	Gene Title	Time points (h)				Genbank
			4.5	7.5	24	48	
100439_i_at	Ank1	ankyrin 1, erythroid	-2.36 ± 0.10	-2.57 ± 0.06	-1.36 ± 0.11	-1.12 ± 0.11	U76758
100065_r_at	Gja1	gap junction membrane channel protein alpha 1	-1.68 ± 0.08	-2.55 ± 0.08	1.83 ± 0.19	1.96 ± 0.17	M63801
97195_at	Gnai1	guanine nucleotide binding protein, alpha inhibiting 1	1.53 ± 0.13	2.49 ± 0.14	-1.76 ± 0.09	-1.96 ± 0.16	U38501
100386_at	Gnaz	guanine nucleotide binding protein, alpha z subunit	1.39 ± 0.11	1.99 ± 0.10	-1.67 ± 0.12	-2.10 ± 0.11	AF056973
160747_at	Rgs3	regulator of G-protein signaling 3	-2.16 ± 0.06	-1.35 ± 0.07	-1.35 ± 0.10	-1.02 ± 0.11	AI844739
92434_at	Traip	TRAF-interacting protein	1.75 ± 0.13	2.66 ± 0.12	1.24 ± 0.10	-1.06 ± 0.12	U77844
97308_at	5730466P16Rik	RIKEN cDNA 5730466P16 gene	1.75 ± 0.08	2.51 ± 0.09	1.16 ± 0.13	-1.21 ± 0.13	AI835409
99491_at	Il10rb	interleukin 10 receptor, beta	-2.07 ± 0.16	-3.73 ± 0.07	-1.01 ± 0.11	1.25 ± 0.13	U53696
101096_s_at	Hs1bp1	HS1 binding protein	2.20 ± 0.09	2.88 ± 0.06	1.42 ± 0.14	-1.07 ± 0.13	AF023482
102255_at	Osmr	oncostatin M receptor	-1.83 ± 0.41	-1.59 ± 0.25	3.84 ± 0.17	2.70 ± 0.21	AB015978
92738_at	Gdnf	glial cell line derived neurotrophic factor	-1.89 ± 0.09	-2.64 ± 0.07	-1.05 ± 0.10	-1.01 ± 0.12	D49921
104499_at	Homer1	homer homolog 1 (Drosophila)	2.48 ± 0.22	1.89 ± 0.17	-1.08 ± 0.13	-2.12 ± 0.14	AB019479
102726_at	Tac1	tachykinin 1	2.40 ± 0.23	2.00 ± 0.17	1.97 ± 0.19	-1.14 ± 0.13	D17584
103235_at	Npy	neuropeptide Y	1.09 ± 0.08	-1.19 ± 0.06	-3.07 ± 0.09	-3.12 ± 0.10	AI848386
102379_at	Rassf1	Ras association (RalGDS/AF-6) domain family 1	1.47 ± 0.13	2.40 ± 0.11	-1.12 ± 0.10	-1.04 ± 0.13	AW049415
94290_at	Akt1s1	AKT1 substrate 1 (proline-rich)	1.59 ± 0.08	2.78 ± 0.12	1.36 ± 0.11	-1.12 ± 0.12	AW124346
98434_at	Arhgef7	Rho guanine nucleotide exchange factor (GEF7)	1.93 ± 0.09	2.45 ± 0.08	1.10 ± 0.18	-1.20 ± 0.14	U96634
96592_at	Pik3r1	phosphatidylinositol 3-kinase, regulatory subunit, polypeptide 1 (p85 alpha)	1.67 ± 0.15	2.25 ± 0.17	-2.29 ± 0.13	-1.96 ± 0.20	U50413
100057_at	2510027N19Rik	RIKEN cDNA 2510027N19 gene	2.18 ± 0.13	2.60 ± 0.09	1.78 ± 0.16	1.08 ± 0.15	AI838320
98766_at	Sh3bp5	SH3-domain binding protein 5 (BTK-associated)	1.53 ± 0.08	2.72 ± 0.19	-1.61 ± 0.10	-1.37 ± 0.11	AB016835
100024_at	Shrm	shroom	-1.26 ± 0.07	-1.66 ± 0.07	2.17 ± 0.35	2.77 ± 0.18	AI641895
96572_at	Azi2	5-azacytidine induced gene 2	2.19 ± 0.19	2.03 ± 0.10	1.24 ± 0.27	-1.41 ± 0.12	AW047232
94006_at	Azi2	5-azacytidine induced gene 2	3.29 ± 0.28	2.49 ± 0.15	-1.19 ± 0.13	-1.21 ± 0.11	AB007141

103328_at	Tank	TRAF family member-associated Nf-kappa B activator	2.65 ± 0.11	2.42 ± 0.10	1.66 ± 0.13	1.29 ± 0.14	U59864
103653_at	Mras	muscle and microspikes RAS	1.93 ± 0.14	2.24 ± 0.11	-1.01 ± 0.10	-1.24 ± 0.10	AB004879
92376_at	Rit1	Ras-like without CAAX 1	1.28 ± 0.07	1.70 ± 0.08	2.16 ± 0.34	-1.07 ± 0.11	U71205
103224_at	Rab33a	RAB33A, member of RAS oncogene family	1.04 ± 0.06	-1.27 ± 0.07	-2.04 ± 0.09	-2.33 ± 0.11	D83277
101866_at	Arfrp1	ADP-ribosylation factor related protein 1	2.02 ± 0.15	2.91 ± 0.15	1.10 ± 0.15	-1.06 ± 0.13	AW060486
102083_at	Rit2	Ras-like without CAAX 2	-2.65 ± 0.12	-1.22 ± 0.11	-1.09 ± 0.11	-1.22 ± 0.15	AF084463
93730_at	Syn1	synapsin I	2.19 ± 0.07	2.18 ± 0.06	1.35 ± 0.11	1.06 ± 0.18	AF085809

Table 10.17. Calcium binding

Probe id	Symbol	Gene Title	Time points (h)				Genbank
			4.5	7.5	24	48	
100569_at	Anxa2	annexin A2	1.45 ± 0.09	1.80 ± 0.08	4.56 ± 0.25	2.84 ± 0.43	M14044
92539_at	S100a10	S100 calcium binding protein A10 (calpactin)	-1.80 ± 0.10	-1.23 ± 0.06	4.77 ± 0.55	2.54 ± 0.22	M16465
98600_at	S100a11	S100 calcium binding protein A11 (calizzarin)	-3.12 ± 0.08	-3.10 ± 0.06	5.31 ± 0.85	8.03 ± 0.50	U41341
100959_at	S100a13	S100 calcium binding protein A13	-3.02 ± 0.08	-3.37 ± 0.13	-1.23 ± 0.12	1.52 ± 0.11	X99921
100960_g_at	S100a13	S100 calcium binding protein A13	-1.44 ± 0.11	-2.27 ± 0.07	-1.08 ± 0.10	1.42 ± 0.10	X99921
162428_i_at	S100a14	S100 calcium binding protein A14	-3.78 ± 0.06	-3.92 ± 0.06	-1.46 ± 0.10	-1.28 ± 0.12	AV293396
94886_at	Canx	calnexin	-3.08 ± 0.08	-3.06 ± 0.06	-1.14 ± 0.15	-1.16 ± 0.11	L18888
102197_at	Nucb2	nucleobindin 2	2.32 ± 0.18	1.90 ± 0.15	-1.04 ± 0.11	-1.78 ± 0.11	AJ222586

Table 10.18. DNA and RNA

Probe id	Symbol	Gene Title	Time points (h)				Genbank
			4.5	7.5	24	48	
161756_at	4833420N02Rik	RIKEN cDNA 4833420N02 gene	1.88 ± 0.14	2.28 ± 0.18	-1.37 ± 0.14	1.00 ± 0.13	AV298145
100903_at	Adprtl2	ADP-ribosyltransferase (NAD+, poly(ADP-ribose) polymerase)-like 2	2.02 ± 0.07	1.68 ± 0.07	1.25 ± 0.11	1.10 ± 0.13	AJ007780
95879_at	Asf1a	ASF1 anti-silencing function 1 homolog A (S. cerevisiae)	1.57 ± 0.09	-2.11 ± 0.08	1.03 ± 0.10	1.03 ± 0.12	C79052
96775_at	Cbx1	chromobox homolog 1 (Drosophila HP1 beta)	4.97 ± 0.10	1.47 ± 0.13	-1.36 ± 0.14	1.16 ± 0.12	X56690
94506_at	Cpsf5	cleavage and polyadenylation specific factor 5	2.43 ± 0.13	1.79 ± 0.07	1.23 ± 0.11	1.14 ± 0.16	AI853113

160751_i_at	Crnkl1	Crn, crooked neck-like 1 (Drosophila)	2.62 ± 0.08	1.87 ± 0.12	-1.03 ± 0.11	-1.10 ± 0.14	AA216808
102853_at	Cspg6	chondroitin sulfate proteoglycan 6	2.02 ± 0.07	2.09 ± 0.13	-1.02 ± 0.12	-1.19 ± 0.10	Y15128
99544_at	Dguok	deoxyguanosine kinase	2.10 ± 0.07	2.44 ± 0.12	1.29 ± 0.16	-1.08 ± 0.17	AA980916
103891_i_at	Ell2	elongation factor RNA polymerase II 2	1.69 ± 0.14	1.72 ± 0.16	3.50 ± 0.41	1.49 ± 0.15	AI197161
103036_at	G22p1	thyroid autoantigen	2.30 ± 0.15	1.78 ± 0.08	1.46 ± 0.11	1.47 ± 0.11	M38700
100371_at	Hnrpa1	heterogeneous nuclear ribonucleoprotein A1	1.51 ± 0.18	2.02 ± 0.11	-1.08 ± 0.13	-1.20 ± 0.13	U65316
97759_at	Kcnma1	potassium large conductance calcium-activated channel, subfamily M, alpha member 1	-1.13 ± 0.07	-2.82 ± 0.06	-1.44 ± 0.10	-1.45 ± 0.11	U09383
97907_at	Lsm7	LSM7 homolog, U6 small nuclear RNA associated (S. cerevisiae)	2.07 ± 0.09	1.73 ± 0.07	1.53 ± 0.11	-1.12 ± 0.17	AW049564
93356_at	Mcm7	minichromosome maintenance deficient 7 (S. cerevisiae)	1.97 ± 0.09	2.59 ± 0.08	1.14 ± 0.10	1.22 ± 0.15	D26091
94376_s_at	Mre11a	meiotic recombination 11 homolog A (S. cerevisiae)	3.09 ± 0.21	3.00 ± 0.23	1.52 ± 0.13	-1.18 ± 0.11	U60318
102819_at	Nap1l2	nucleosome assembly protein 1-like 2	2.20 ± 0.07	2.57 ± 0.11	1.24 ± 0.17	-1.33 ± 0.10	X92352
92893_at	Nfia	nuclear factor I/A	2.60 ± 0.13	1.14 ± 0.08	-1.15 ± 0.10	1.92 ± 0.17	D90173
101930_at	Nfix	nuclear factor I/X	2.32 ± 0.07	1.55 ± 0.08	-1.39 ± 0.11	1.00 ± 0.15	Y07688
93830_at	Nono	non-POU-domain-containing, octamer binding protein	2.24 ± 0.07	1.82 ± 0.09	-1.06 ± 0.10	-1.14 ± 0.13	AI851199
93831_at	Nono	non-POU-domain-containing, octamer binding protein	2.66 ± 0.10	2.71 ± 0.14	-1.10 ± 0.12	-1.05 ± 0.11	AI316087
95712_at	Orc6l	origin recognition complex, subunit 6-like (S. cerevisiae)	2.02 ± 0.11	2.51 ± 0.09	1.16 ± 0.13	-1.07 ± 0.12	AW045261
104690_at	Polm	polymerase (DNA directed), mu	-2.12 ± 0.10	-1.75 ± 0.06	-1.26 ± 0.10	-1.14 ± 0.10	AI462166
95549_at	Prim2	DNA primase, p58 subunit	2.23 ± 0.22	1.59 ± 0.10	1.23 ± 0.12	1.15 ± 0.13	D13545
96103_f_at	Rad23b	RAD23b homolog (S. cerevisiae)	1.87 ± 0.09	2.85 ± 0.18	1.77 ± 0.22	-1.24 ± 0.10	X92411
160466_at	Rae1	RAE1 RNA export 1 homolog (S. pombe)	1.56 ± 0.07	2.30 ± 0.07	1.56 ± 0.13	-1.10 ± 0.14	AI048716
97254_at	Rbm8	RNA binding motif protein 8	2.47 ± 0.10	2.57 ± 0.06	1.60 ± 0.12	-1.16 ± 0.13	AA690061
160192_at	Rbmxrt	RNA binding motif protein, X chromosome retrogene	2.43 ± 0.07	2.10 ± 0.06	1.20 ± 0.14	-1.14 ± 0.13	AF031568
160072_at	Rfc3	replication factor C (activator 1) 3	2.21 ± 0.12	2.11 ± 0.08	1.10 ± 0.10	1.08 ± 0.17	AV026570
103418_at	Rfc4	replication factor C (activator 1) 4	3.54 ± 0.17	2.36 ± 0.10	1.34 ± 0.11	1.21 ± 0.26	AW122092
92196_f_at	Sf3a2	splicing factor 3a, subunit 2	-2.77 ± 0.06	-1.44 ± 0.06	-1.08 ± 0.12	-1.11 ± 0.11	X83733

97808_at	Sf3b1	splicing factor 3b, subunit 1	2.91 ± 0.07	2.16 ± 0.11	1.23 ± 0.11	-1.13 ± 0.10	AI844532
103822_at	Sfrs16	splicing factor, arginine/serine-rich 16 (suppressor-of-white-apricot homolog, Drosophila)	1.20 ± 0.16	2.03 ± 0.11	1.28 ± 0.18	-1.01 ± 0.12	AF042799
95791_s_at	Sfrs2	splicing factor, arginine/serine-rich 2 (SC-35)	2.26 ± 0.07	2.13 ± 0.12	1.13 ± 0.12	-1.18 ± 0.10	U14648
160869_at	Sirt3	sirtuin 3 (silent mating type information regulation 2, homolog) 3 (S. cerevisiae)	1.87 ± 0.22	2.31 ± 0.10	1.10 ± 0.10	-1.38 ± 0.10	AI849490
93701_at	Smarca5	SWI/SNF related, matrix associated, actin dependent regulator of chromatin, subfamily a, member 5	2.05 ± 0.28	2.22 ± 0.13	1.31 ± 0.12	1.22 ± 0.14	AA982124
102062_at	Smarcc1	SWI/SNF related, matrix associated, actin dependent regulator of chromatin, subfamily c, member 1	2.65 ± 0.11	1.31 ± 0.12	-1.04 ± 0.12	-1.23 ± 0.13	U85614
94034_at	Smfn	small fragment nuclease	1.56 ± 0.19	1.50 ± 0.11	2.00 ± 0.16	-1.03 ± 0.11	AI839882
103302_r_at	Sox3	SRY-box containing gene 3	-3.45 ± 0.07	-2.25 ± 0.06	-1.12 ± 0.11	1.29 ± 0.11	AA866668
100957_at	Ssbp1	single-stranded DNA binding protein 1	1.83 ± 0.10	1.45 ± 0.07	2.01 ± 0.10	1.34 ± 0.13	AA881160
101356_at	Tk2	thymidine kinase 2, mitochondrial	1.63 ± 0.09	2.13 ± 0.09	-1.08 ± 0.11	-1.47 ± 0.10	AI843384
99578_at	Top2a	topoisomerase (DNA) II alpha	2.15 ± 0.07	1.56 ± 0.08	1.01 ± 0.12	1.82 ± 0.10	U01915

Table 10.19. Protein modification

Probe id	Symbol	Gene Title	Time points (h)				Genbank
			4.5	7.5	24	48	
160110_at	1300010O06Rik	RIKEN cDNA 1300010O06 gene	1.15 ± 0.08	2.28 ± 0.09	1.16 ± 0.14	-1.15 ± 0.10	AW124007
103582_r_at	6130401J04Rik	RIKEN cDNA 6130401J04 gene	2.15 ± 0.33	-1.48 ± 0.11	-1.23 ± 0.16	-1.17 ± 0.12	AI845633
103907_at	Nedd4l	neural precursor cell expressed, developmentally down-regulated gene 4-like	2.29 ± 0.07	2.73 ± 0.06	1.05 ± 0.16	-1.24 ± 0.10	AW108492
161021_at	Pak3	p21 (CDKN1A)-activated kinase 3	1.98 ± 0.13	1.14 ± 0.07	-1.20 ± 0.13	-1.80 ± 0.11	U39738
161270_i_at	Prkwnk1	protein kinase, lysine deficient 1	1.22 ± 0.13	-5.24 ± 0.07	1.55 ± 0.14	-1.07 ± 0.25	AV319920
93311_at	Clk3	CDC-like kinase 3	1.98 ± 0.07	2.25 ± 0.11	1.23 ± 0.16	-1.11 ± 0.12	AF033565
101937_s_at	Clk4	CDC like kinase 4	1.03 ± 0.08	2.58 ± 0.12	1.15 ± 0.11	-1.11 ± 0.16	AF005423
92383_at	Dyrk1a	dual-specificity tyrosine-(Y)-phosphorylation regulated kinase 1a	1.01 ± 0.17	2.91 ± 0.24	-1.03 ± 0.10	-1.23 ± 0.12	U58497

97096_at	Prkar2a	protein kinase, cAMP dependent regulatory, type II alpha	3.58 ± 0.17	3.63 ± 0.09	-2.13 ± 0.23	-1.76 ± 0.23	J02935
102063_at	Pdpk1	3-phosphoinositide dependent protein kinase-1	2.91 ± 0.28	1.55 ± 0.19	-1.02 ± 0.10	-1.23 ± 0.14	AF079535
104097_at	Bub1	budding uninhibited by benzimidazoles 1 homolog (S. cerevisiae)	2.11 ± 0.13	2.01 ± 0.19	1.00 ± 0.14	1.85 ± 0.13	AF002823
101834_at	Mapk3	mitogen activated protein kinase 3	1.97 ± 0.09	2.13 ± 0.27	-1.78 ± 0.12	1.04 ± 0.20	Z14249
98771_at	Ephb2	Eph receptor B2	2.86 ± 0.08	2.67 ± 0.13	-2.00 ± 0.17	-1.42 ± 0.17	L25890
95298_at	Epha3	Eph receptor A3	2.43 ± 0.15	2.23 ± 0.15	-1.43 ± 0.10	-1.31 ± 0.21	M68513
161119_at	Epha5	Eph receptor A5	2.28 ± 0.15	1.60 ± 0.07	-1.23 ± 0.11	-1.23 ± 0.12	AI854630
98446_s_at	Ephb4	Eph receptor B4	2.48 ± 0.09	3.16 ± 0.09	1.53 ± 0.11	-1.11 ± 0.12	U06834
161964_r_at	Prkcz	protein kinase C, zeta	-2.07 ± 0.12	-3.14 ± 0.08	-1.38 ± 0.12	-1.10 ± 0.12	AV367375
97925_at	Csnk1e	casein kinase 1, epsilon	2.88 ± 0.09	2.56 ± 0.14	1.04 ± 0.28	-1.57 ± 0.18	AB028241
98087_at	Tbk1	TANK-binding kinase 1	1.93 ± 0.27	2.61 ± 0.10	1.54 ± 0.12	1.09 ± 0.13	AW048562
97393_at	Vrk1	vaccinia related kinase 1	2.28 ± 0.12	2.00 ± 0.20	1.31 ± 0.17	1.02 ± 0.13	AF080253
92659_at	Rapgef4	Rap guanine nucleotide exchange factor (GEF) 4	1.61 ± 0.20	1.07 ± 0.19	-1.71 ± 0.11	-2.50 ± 0.13	AF115480
93285_at	Dusp6	dual specificity phosphatase 6	-2.06 ± 0.07	-1.83 ± 0.06	1.49 ± 0.10	-1.36 ± 0.11	AI845584
100908_at	Ptpra	protein tyrosine phosphatase, receptor type, A	1.44 ± 0.16	1.93 ± 0.06	-1.16 ± 0.10	-1.29 ± 0.14	M36033
160760_at	Ptprk	protein tyrosine phosphatase, receptor type, K	1.55 ± 0.07	1.23 ± 0.06	-2.20 ± 0.09	-1.44 ± 0.11	L10106
92303_at	Ptprr	protein tyrosine phosphatase, receptor type, R	2.58 ± 0.07	2.11 ± 0.07	-1.35 ± 0.10	-1.41 ± 0.10	D31898
104422_at	Ptprn	protein tyrosine phosphatase, receptor type, N	-1.22 ± 0.07	1.12 ± 0.07	2.90 ± 0.15	-1.05 ± 0.11	U11812
93219_at	Acp1	acid phosphatase 1, soluble	1.94 ± 0.12	3.74 ± 0.13	1.13 ± 0.19	-1.10 ± 0.12	Y17343
94980_at	Dusp11	dual specificity phosphatase 11 (RNA/RNP complex 1-interacting)	1.11 ± 0.15	2.08 ± 0.07	1.30 ± 0.11	1.13 ± 0.12	AI006319
92380_r_at	Ptprz1	protein tyrosine phosphatase, receptor type Z, polypeptide 1	1.45 ± 0.17	-3.42 ± 0.07	-1.81 ± 0.12	1.26 ± 0.12	AJ133130
93985_at	Tiparp	TCDD-inducible poly(ADP-ribose) polymerase	1.42 ± 0.17	2.21 ± 0.08	-1.15 ± 0.10	-2.00 ± 0.11	AW120868
104238_at	Art5	ADP-ribosyltransferase 5	-2.02 ± 0.08	-2.43 ± 0.07	-1.20 ± 0.10	1.09 ± 0.11	U60881

161492_i_at	Mgat1	mannoside acetylglucosaminyltransferase 1	-2.72 ± 0.07	-3.21 ± 0.06	-1.02 ± 0.13	-1.03 ± 0.11	AV089873
100684_at	Prkcsh	protein kinase C substrate 80K-H	1.09 ± 0.08	2.04 ± 0.07	1.30 ± 0.15	1.10 ± 0.14	U92794
102047_at	Nmt1	N-myristoyltransferase 1	2.84 ± 0.12	3.45 ± 0.11	2.46 ± 0.20	1.23 ± 0.15	AF043326
161682_f_at	Gpaa1	GPI anchor attachment protein 1	-3.57 ± 0.07	-2.88 ± 0.07	-1.90 ± 0.13	-1.08 ± 0.15	AV161234

Table 10.20. Cytoskeleton

Probe id	Symbol	Gene Title	Time points (h)				Genbank
			4.5	7.5	24	48	
162379_r_at	Vim	vimentin	-8.34 ± 0.07	-7.48 ± 0.08	-1.49 ± 0.10	-1.01 ± 0.12	AV245272
93100_at	Acta2	actin, alpha 2, smooth muscle, aorta	-2.11 ± 0.07	-4.06 ± 0.08	1.68 ± 0.37	3.89 ± 0.49	X13297
95705_s_at	Actb	actin, beta, cytoplasmic	-10.94 ± 0.06	-6.82 ± 0.05	1.45 ± 0.22	-1.67 ± 0.26	J04181
96573_at	Actg	actin, gamma, cytoplasmic	2.40 ± 0.06	2.17 ± 0.06	-1.10 ± 0.10	-1.13 ± 0.11	M21495
102108_f_at	Myh9	myosin heavy chain IX	1.69 ± 0.31	1.30 ± 0.07	3.20 ± 0.24	1.82 ± 0.16	AI505453
100923_at	Myo10	myosin X	1.31 ± 0.07	1.03 ± 0.08	1.48 ± 0.14	2.09 ± 0.13	AJ249706
96426_at	Tmsb4x	thymosin, beta 4, X chromosome	2.12 ± 0.07	1.75 ± 0.06	-1.04 ± 0.11	-1.19 ± 0.12	U38967
93541_at	Tagln	transgelin	-1.63 ± 0.09	-2.06 ± 0.07	2.53 ± 0.49	4.16 ± 0.53	Z68618
100398_at	Kif3a	kinesin family member 3A	2.05 ± 0.08	1.69 ± 0.11	1.13 ± 0.14	1.06 ± 0.13	D12645
161003_at	Kif3b	kinesin family member 3B	1.58 ± 0.09	2.19 ± 0.09	-3.12 ± 0.11	-1.51 ± 0.22	D26077
94835_f_at	Tubb2	tubulin, beta 2	2.03 ± 0.06	2.31 ± 0.08	1.03 ± 0.10	-1.37 ± 0.11	M28739
94789_r_at	Tubb5	tubulin, beta 5	2.20 ± 0.06	2.71 ± 0.07	1.03 ± 0.13	-1.28 ± 0.13	X04663
98759_f_at	Tuba2	tubulin, alpha 2	2.16 ± 0.09	2.48 ± 0.06	1.08 ± 0.12	-1.19 ± 0.13	M28727
160462_f_at	Tubb3	tubulin, beta 3	1.64 ± 0.07	2.04 ± 0.07	-1.03 ± 0.10	-1.29 ± 0.11	AW050256
101419_at	Tubb4	tubulin, beta 4	-2.16 ± 0.06	-1.56 ± 0.06	-1.17 ± 0.12	-1.70 ± 0.10	M28730
99924_at	Tubg1	tubulin, gamma 1	2.00 ± 0.12	2.48 ± 0.17	1.09 ± 0.11	-1.04 ± 0.14	AW121845
100342_i_at	Tuba1	tubulin, alpha 1	2.54 ± 0.09	2.84 ± 0.08	1.03 ± 0.11	-1.21 ± 0.12	M28729
101543_f_at	Tuba6	tubulin, alpha 6	2.41 ± 0.06	3.07 ± 0.06	1.06 ± 0.12	-1.19 ± 0.14	M13441
102742_g_at	Mapt	microtubule-associated protein tau	3.07 ± 0.07	2.10 ± 0.06	-1.16 ± 0.12	-1.51 ± 0.11	M18775
99541_at	Kif11	kinesin family member 11	2.01 ± 0.13	1.08 ± 0.07	-1.10 ± 0.11	1.41 ± 0.14	AJ223293
101929_at	6720463E02Rik	RIKEN cDNA 6720463E02 gene	-2.25 ± 0.06	2.00 ± 0.06	1.28 ± 0.10	-1.50 ± 0.11	AI836322
97276_at	Ckap1	cytoskeleton-associated protein 1	1.98 ± 0.10	1.81 ± 0.13	1.27 ± 0.18	-1.36 ± 0.14	AI853425
160461_f_at	2310057H16Rik	RIKEN cDNA 2310057H16 gene	-1.07 ± 0.12	1.43 ± 0.06	2.94 ± 0.26	2.18 ± 0.13	AW215736
97909_at	Stmn1	stathmin 1	2.11 ± 0.08	2.21 ± 0.06	-1.15 ± 0.10	-1.29 ± 0.12	AI838080

Table 10.21. Cell adhesion

Probe id	Symbol	Gene Title	Time points (h)				Genbank
			4.5	7.5	24	48	
104407_at	Alcam	activated leukocyte cell adhesion molecule	2.94 ± 0.09	-1.22 ± 0.07	-1.25 ± 0.15	-1.18 ± 0.14	L25274
98140_at	Cdh1	cadherin 1	-2.68 ± 0.07	-2.72 ± 0.09	-1.25 ± 0.10	-1.16 ± 0.13	X60961
104743_at	Cdh13	cadherin 13	1.93 ± 0.18	1.29 ± 0.10	-1.74 ± 0.10	-2.45 ± 0.10	AB022100
95898_at	Cdh4	cadherin 4	2.30 ± 0.08	1.55 ± 0.07	-1.12 ± 0.10	-1.03 ± 0.11	X69966
101701_at	Cdh8	cadherin 8	1.98 ± 0.16	1.13 ± 0.09	-2.37 ± 0.10	-1.42 ± 0.14	X95600

94305_at	Col1a1	procollagen, type I, alpha 1	-1.71 ± 0.38	-8.55 ± 0.07	-1.14 ± 0.22	1.38 ± 0.22	U03419
161156_r_at	Col1a2	procollagen, type I, alpha 2	-2.53 ± 0.11	-2.69 ± 0.06	-1.37 ± 0.11	-1.23 ± 0.11	AV230631
101093_at	Col4a1	procollagen, type IV, alpha 1	-1.66 ± 0.07	-2.24 ± 0.07	1.18 ± 0.10	1.21 ± 0.16	M15832
92567_at	Col5a2	procollagen, type V, alpha 2	1.02 ± 0.16	-1.40 ± 0.08	2.05 ± 0.33	2.12 ± 0.38	L02918
102070_at	Col9a3	procollagen, type IX, alpha 3	-2.19 ± 0.08	-1.67 ± 0.07	1.04 ± 0.11	1.26 ± 0.13	AW212495
93529_at	D8Wsu49e	DNA segment, Chr 8, Wayne State University 49, expressed	-1.57 ± 0.07	-2.08 ± 0.07	-1.44 ± 0.10	-1.19 ± 0.10	AW125219
160649_at	Gp1bb	glycoprotein Ib, beta polypeptide	-1.09 ± 0.09	-1.04 ± 0.09	-2.14 ± 0.10	-1.84 ± 0.11	AB001419
95511_at	Itga6	integrin alpha 6	1.63 ± 0.12	1.43 ± 0.11	2.19 ± 0.13	1.77 ± 0.15	X69902
92366_at	Lama2	laminin, alpha 2	2.42 ± 0.13	1.62 ± 0.20	1.40 ± 0.12	-1.22 ± 0.15	U12147
99669_at	Lgals1	lectin, galactose binding, soluble 1	-1.06 ± 0.07	-1.03 ± 0.06	4.01 ± 0.36	5.89 ± 0.72	X15986
161708_f_at	Mpdz	multiple PDZ domain protein	-1.01 ± 0.39	-3.97 ± 0.16	1.48 ± 0.14	1.29 ± 0.17	AV244715
96582_at	Ncam2	neural cell adhesion molecule 2	2.05 ± 0.21	1.79 ± 0.11	-1.79 ± 0.10	-1.07 ± 0.18	AF001287
160469_at	Thbs1	thrombospondin 1	-2.17 ± 0.07	-3.20 ± 0.06	2.16 ± 0.39	2.91 ± 0.31	M62470
92558_at	Vcam1	vascular cell adhesion molecule 1	1.04 ± 0.08	-1.25 ± 0.08	1.37 ± 0.11	1.97 ± 0.13	M84487
94963_at	Vcl	vinculin	-1.10 ± 0.09	1.25 ± 0.11	2.07 ± 0.14	1.92 ± 0.26	AI462105

Table 10.22. Energy

Probe id	Symbol	Gene Title	Time points (h)				Genbank
			4.5	7.5	24	48	
97525_at	Gyk	glycerol kinase	1.78 ± 0.19	2.49 ± 0.11	1.89 ± 0.22	1.01 ± 0.13	U48403
94367_at	AA407809	expressed sequence AA407809	1.59 ± 0.08	2.13 ± 0.07	1.09 ± 0.11	-1.21 ± 0.10	AI850362
102783_at	2310009E04Rik	RIKEN cDNA 2310009E04 gene	-2.81 ± 0.10	-2.72 ± 0.10	-1.25 ± 0.12	1.05 ± 0.10	AI131744
93268_at	Glo1	glyoxalase 1	-1.80 ± 0.06	-2.28 ± 0.06	1.09 ± 0.11	1.15 ± 0.11	AI852001
93007_at	Npy1r	neuropeptide Y receptor Y1	1.92 ± 0.10	1.15 ± 0.15	-4.01 ± 0.15	-2.59 ± 0.14	Z18280
104148_at	H6pd	hexose-6-phosphate dehydrogenase (glucose 1-dehydrogenase)	-2.07 ± 0.08	-2.00 ± 0.06	1.05 ± 0.11	-1.13 ± 0.11	AA939571
98984_f_at	Gpd2	glycerol phosphate dehydrogenase 2, mitochondrial	3.92 ± 0.22	2.12 ± 0.14	1.19 ± 0.12	-1.54 ± 0.10	D50430
160921_at	Acas2l	acetyl-Coenzyme A synthetase 2 (AMP forming)-like	-2.16 ± 0.07	-2.19 ± 0.06	-1.23 ± 0.10	1.61 ± 0.21	AW125884
92800_i_at	Atp5c1	ATP synthase, H+ transporting, mitochondrial F1 complex, gamma polypeptide 1	2.50 ± 0.12	1.66 ± 0.10	1.01 ± 0.10	-1.07 ± 0.15	AI836694
100573_f_at	Gpi1	glucose phosphate isomerase 1	1.93 ± 0.07	2.49 ± 0.13	3.13 ± 0.16	1.28 ± 0.21	M14220
161889_f_at	Aldo1	aldolase 1, A isoform	-2.51 ± 0.06	-1.28 ± 0.06	1.71 ± 0.10	1.06 ± 0.17	AV102160

160546_at	Aldo3	aldolase 3, C isoform	1.22 ± 0.06	-1.40 ± 0.07	-2.71 ± 0.10	1.25 ± 0.21	AW121134
162032_f_at	Pkm2	pyruvate kinase, muscle	-2.69 ± 0.07	-2.86 ± 0.07	1.15 ± 0.14	-1.02 ± 0.16	AV368209
93271_s_at	Gnas	GNAS (guanine nucleotide binding protein, alpha stimulating) complex locus /// GNAS (guanine nucleotide binding protein, alpha stimulating) complex locus	2.25 ± 0.09	2.57 ± 0.06	-1.03 ± 0.14	-1.22 ± 0.13	AF107848

Table 10.23. Other biological processes

Probe id	Symbol	Gene Title	Time points (h)				Genbank
			4.5	7.5	24	48	
98037_at	1110003H18Rik	RIKEN cDNA 1110003H18 gene	2.13 ± 0.07	1.51 ± 0.06	1.34 ± 0.10	1.03 ± 0.15	AW122782
99658_f_at	1110025H10Rik	RIKEN cDNA 1110025H10 gene	-1.46 ± 0.14	-2.99 ± 0.07	-1.08 ± 0.12	-1.14 ± 0.10	AW047907
160590_r_at	1810030M08Rik	RIKEN cDNA 1810030M08 gene	1.64 ± 0.07	2.05 ± 0.08	1.02 ± 0.13	-1.11 ± 0.10	AI853323
160595_at	2310042P20Rik	RIKEN cDNA 2310042P20 gene	2.08 ± 0.08	1.73 ± 0.21	1.10 ± 0.10	-1.34 ± 0.12	AI842450
96096_f_at	2610207I16Rik	RIKEN cDNA 2610207I16 gene	1.11 ± 0.08	1.03 ± 0.08	1.27 ± 0.13	2.03 ± 0.23	AI648018
100032_at	Aaas	achalasia, adrenocortical insufficiency, alacrimia	2.98 ± 0.14	1.42 ± 0.13	1.22 ± 0.10	1.17 ± 0.11	X60136
99559_at	Aldh3a2	aldehyde dehydrogenase family 3, subfamily A2	1.76 ± 0.07	2.30 ± 0.14	1.39 ± 0.19	-1.14 ± 0.16	U14390
161401_f_at	Aldh3a2	aldehyde dehydrogenase family 3, subfamily A2	2.17 ± 0.17	1.39 ± 0.14	1.24 ± 0.12	-1.10 ± 0.12	AV276715
101447_at	Apc	adenomatosis polyposis coli	1.77 ± 0.07	2.72 ± 0.08	-1.49 ± 0.10	-1.29 ± 0.11	M88127
95144_at	Arpc1a	actin related protein 2/3 complex, subunit 1A	1.73 ± 0.06	2.17 ± 0.06	1.06 ± 0.15	-1.16 ± 0.14	AB024984
95133_at	Asns	asparagine synthetase	1.74 ± 0.07	3.13 ± 0.13	1.11 ± 0.24	-1.50 ± 0.17	U38940
96951_at	Atp6v1d	ATPase, H+ transporting, V1 subunit D	2.14 ± 0.14	1.65 ± 0.08	1.17 ± 0.10	-1.09 ± 0.13	AI839795
100996_at	AU041707	expressed sequence AU041707	2.53 ± 0.32	2.70 ± 0.23	-1.53 ± 0.17	-1.42 ± 0.16	AF015811
95469_at	Btd	biotinidase	-2.16 ± 0.09	-1.68 ± 0.09	-1.17 ± 0.10	-1.05 ± 0.10	AA734444
92642_at	Car2	carbonic anhydrase 2	-1.12 ± 0.11	1.27 ± 0.10	2.42 ± 0.11	1.31 ± 0.16	M25944
94241_at	Coasy	Coenzyme A synthase	1.42 ± 0.09	2.02 ± 0.07	1.58 ± 0.19	-1.07 ± 0.13	AI837229
98535_at	Comt	catechol-O-methyltransferase	2.23 ± 0.11	1.39 ± 0.07	1.13 ± 0.11	-1.06 ± 0.12	AF076156
98505_i_at	Cpox	coproporphyrinogen oxidase	2.03 ± 0.12	2.51 ± 0.16	1.32 ± 0.17	-1.13 ± 0.12	D16333
103492_at	Cpxm1	carboxypeptidase X 1 (M14 family)	1.16 ± 0.35	3.05 ± 0.22	3.44 ± 0.21	1.38 ± 0.18	AF077738
97724_at	Cry2	cryptochrome 2 (photolyase-like)	1.85 ± 0.26	3.47 ± 0.09	-1.75 ± 0.17	-1.29 ± 0.22	AB003433

95620_at	Dhrs7	dehydrogenase/reductase (SDR family) member 7	1.60 ± 0.09	2.16 ± 0.09	1.70 ± 0.10	1.52 ± 0.13	AW120882
103550_at	Ednrb	endothelin receptor type B	1.63 ± 0.09	-3.50 ± 0.07	-1.62 ± 0.10	1.98 ± 0.17	U32329
103342_at	Eed	embryonic ectoderm development	2.05 ± 0.13	1.76 ± 0.08	1.41 ± 0.12	1.19 ± 0.14	U78103
98121_at	Fnta	farnesyltransferase, CAAX box, alpha	1.60 ± 0.07	2.00 ± 0.06	1.20 ± 0.14	-1.03 ± 0.13	D49744
93750_at	Gsn	gelsolin	-1.66 ± 0.12	1.05 ± 0.10	1.83 ± 0.27	2.21 ± 0.26	J04953
160101_at	Hmox1	heme oxygenase (decycling) 1	1.11 ± 0.14	2.34 ± 0.11	5.39 ± 0.82	2.23 ± 0.49	X56824
162460_f_at	Igbp1	immunoglobulin (CD79A) binding protein 1	-1.08 ± 0.10	-2.40 ± 0.13	1.08 ± 0.13	1.42 ± 0.16	AV048486
101102_at	Igbp1	immunoglobulin (CD79A) binding protein 1	2.10 ± 0.08	2.55 ± 0.07	1.06 ± 0.12	1.57 ± 0.21	AJ223156
93795_at	Itpa	inosine triphosphatase (nucleoside triphosphate pyrophosphatase)	2.11 ± 0.10	1.63 ± 0.08	1.25 ± 0.13	-1.04 ± 0.12	AW124626
93374_at	Jph3	junctophilin 3	-2.50 ± 0.08	-2.63 ± 0.06	-1.46 ± 0.12	-1.41 ± 0.11	AI836349
161796_r_at	Kcnq1	potassium voltage-gated channel, subfamily Q, member 1	-2.37 ± 0.07	-4.41 ± 0.07	-1.56 ± 0.10	-1.19 ± 0.12	AV367240
103630_at	Lars	leucyl-tRNA synthetase	1.85 ± 0.06	2.97 ± 0.08	1.42 ± 0.29	-1.30 ± 0.14	AI844089
103377_at	Lrp2	low density lipoprotein receptor-related protein 2	-1.72 ± 0.14	-2.24 ± 0.11	2.00 ± 0.13	1.60 ± 0.43	AW259788
99632_at	Mad2l1	MAD2 (mitotic arrest deficient, homolog)-like 1 (yeast)	2.11 ± 0.09	1.35 ± 0.10	1.17 ± 0.10	1.31 ± 0.11	U83902
160637_at	Mocs2	molybdenum cofactor synthesis 2	2.18 ± 0.09	1.51 ± 0.07	1.33 ± 0.12	-1.04 ± 0.11	AW060325
96082_at	Mrpl30	mitochondrial ribosomal protein L30	2.23 ± 0.27	2.33 ± 0.12	1.27 ± 0.12	-1.04 ± 0.10	AI850644
100046_at	Mthfd2	methylenetetrahydrofolate dehydrogenase (NAD+ dependent), methenyltetrahydrofolate cyclohydrolase	1.95 ± 0.06	2.55 ± 0.07	-1.05 ± 0.24	-1.88 ± 0.15	J04627
160463_at	Myd116	myeloid differentiation primary response gene 116	1.93 ± 0.09	4.30 ± 0.09	2.71 ± 0.47	1.12 ± 0.15	X51829
161000_i_at	Nusap1	nucleolar and spindle associated protein 1	1.52 ± 0.16	-1.35 ± 0.08	-1.36 ± 0.12	1.82 ± 0.13	AA275196
104139_at	P4ha1	procollagen-proline, 2-oxoglutarate 4-dioxygenase (proline 4-hydroxylase), alpha 1 polypeptide	1.42 ± 0.12	1.95 ± 0.09	2.04 ± 0.20	1.19 ± 0.11	U16162
98021_at	Paf53	RNA polymerase I associated factor	1.90 ± 0.12	2.36 ± 0.11	1.57 ± 0.14	-1.11 ± 0.11	D14336

160788_at	Pes1	pescadillo homolog 1, containing BRCT domain (zebrafish)	1.87 ± 0.07	2.73 ± 0.11	1.41 ± 0.12	-1.07 ± 0.14	AI846045
94491_at	Pex13	peroxisomal biogenesis factor 13	1.61 ± 0.11	2.54 ± 0.10	-1.09 ± 0.10	-1.23 ± 0.11	AW123194
95074_at	Pex19	peroxisome biogenesis factor 19	-1.57 ± 0.10	-2.16 ± 0.07	-1.31 ± 0.10	-1.03 ± 0.14	AW125309
96295_at	Psat1	phosphoserine aminotransferase 1	1.63 ± 0.08	2.47 ± 0.08	1.30 ± 0.16	1.33 ± 0.15	AW122030
93542_at	Pter	phosphotriesterase related	1.33 ± 0.15	1.02 ± 0.12	1.56 ± 0.11	3.54 ± 0.51	U28016
160314_at	Pyp	pyrophosphatase	2.11 ± 0.07	2.33 ± 0.06	1.38 ± 0.15	-1.33 ± 0.14	AI839803
162317_r_at	Rps12	ribosomal protein S12	-5.09 ± 0.18	1.30 ± 0.19	1.13 ± 0.22	-1.23 ± 0.16	AV064697
93899_at	Rps6kb1	ribosomal protein S6 kinase, polypeptide 1	1.93 ± 0.16	2.05 ± 0.11	-1.25 ± 0.13	-1.21 ± 0.11	AJ000654
100732_at	Rps8	ribosomal protein S8	1.46 ± 0.06	1.97 ± 0.07	1.33 ± 0.12	-1.07 ± 0.14	X73829
102769_f_at	Sc5d	sterol-C5-desaturase (fungal ERG3, delta-5-desaturase) homolog (S. cerevisae)	1.87 ± 0.10	-1.14 ± 0.10	-2.09 ± 0.11	-2.05 ± 0.13	AB016248
95049_at	Snrpd2	small nuclear ribonucleoprotein D2	3.17 ± 0.12	2.52 ± 0.18	1.21 ± 0.12	-1.10 ± 0.19	AI837853
101061_at	Ssr2	signal sequence receptor, beta	1.92 ± 0.07	2.01 ± 0.10	1.45 ± 0.10	1.00 ± 0.14	AI845293
95436_at	Sst	somatostatin	1.35 ± 0.11	1.64 ± 0.08	-1.19 ± 0.19	-4.06 ± 0.10	X51468
94564_at	Sult4a1	sulfotransferase family 4A, member 1	1.40 ± 0.13	3.05 ± 0.07	-2.26 ± 0.16	-2.37 ± 0.19	AF059257
93413_at	Terf2	telomeric repeat binding factor 2	2.95 ± 0.17	1.97 ± 0.10	1.05 ± 0.16	-1.09 ± 0.18	AF003000
160533_r_at	Tnp1	transition protein 1	2.19 ± 0.17	1.51 ± 0.14	-1.22 ± 0.12	-1.14 ± 0.12	X12521
94381_at	Umpk	uridine monophosphate kinase	1.43 ± 0.08	2.15 ± 0.16	1.37 ± 0.13	-1.31 ± 0.10	L31783
99126_at	Xist	inactive X specific transcripts	2.68 ± 0.07	-1.31 ± 0.11	1.39 ± 0.11	1.17 ± 0.22	L04961
101890_f_at	Zrf2	zuotin related factor 2	2.23 ± 0.08	2.81 ± 0.13	1.57 ± 0.25	-1.16 ± 0.16	U53208

Table 10.24. Unknown biological processes

Probe id	Symbol	Gene Title	Time points (h)				Genbank
			4.5	7.5	24	48	
96264_at	0610008 N23Rik	RIKEN cDNA 0610008N23 gene	1.62 ± 0.07	2.91 ± 0.09	1.09 ± 0.14	-1.16 ± 0.14	AW061235
95677_at	0610009 C03Rik	RIKEN cDNA 0610009C03 gene	1.87 ± 0.08	2.80 ± 0.09	1.51 ± 0.22	-1.22 ± 0.17	AA881621
160267_at	0610009 E20Rik	RIKEN cDNA 0610009E20 gene	-2.12 ± 0.07	-2.48 ± 0.07	1.05 ± 0.13	1.06 ± 0.12	AI845987
96079_at	0610010 K06Rik	RIKEN cDNA 0610010K06 gene	1.52 ± 0.08	2.67 ± 0.10	1.01 ± 0.18	-1.43 ± 0.14	AI853881
95634_at	0610010 K14Rik	RIKEN cDNA 0610010K14 gene	2.21 ± 0.11	2.12 ± 0.11	1.10 ± 0.11	-1.01 ± 0.16	AI848107

95636_at	0610010 K14Rik	RIKEN cDNA 0610010K14 gene	2.37± 0.09	2.15± 0.09	-1.04± 0.10	1.03±0.24	AW123628
97242_at	0610010 O12Rik	RIKEN cDNA 0610010O12 gene	1.32± 0.07	2.06± 0.16	1.36± 0.14	-1.01±0.13	AI849011
95045_at	0610012 D09Rik	RIKEN cDNA 0610012D09 gene	2.05± 0.10	1.72± 0.09	-1.05± 0.12	-1.19±0.14	AI844469
97012_f_at	0610033 H09Rik	RIKEN cDNA 0610033H09 gene	3.00± 0.23	2.44± 0.27	1.73± 0.14	1.08±0.18	AI838702
99143_at	0610039 N19Rik	RIKEN cDNA 0610039N19 gene	2.19± 0.08	2.01± 0.07	1.52± 0.12	1.16±0.11	AA614914
98615_at	0610041 E09Rik	RIKEN cDNA 0610041E09 gene	2.28± 0.13	1.35± 0.07	1.41± 0.10	1.05±0.11	AW049570
104400_at	0610042 I15Rik	RIKEN cDNA 0610042I15 gene	2.11± 0.10	2.97± 0.10	-1.80± 0.21	-1.98±0.17	AF076956
95458_s_at	1110001 C20Rik	RIKEN cDNA 1110001C20 gene	2.45± 0.07	1.27± 0.08	-1.10± 0.15	-1.06±0.10	AW121960
93805_at	1110003 H09Rik	RIKEN cDNA 1110003H09 gene	2.22± 0.12	1.54± 0.10	1.23± 0.10	-1.03±0.12	AW121164
94340_at	1110004 L07Rik	RIKEN cDNA 1110004L07 gene	1.57± 0.06	2.14± 0.11	1.58± 0.35	-1.52±0.12	AW124224
95732_at	1110005 L13Rik	RIKEN cDNA 1110005L13 gene	3.23± 0.12	2.17± 0.09	1.20± 0.10	-1.11±0.16	AW047746
103439_at	1110007 H17Rik	RIKEN cDNA 1110007H17 gene	-2.64± 0.07	-1.23± 0.10	-1.64± 0.11	-1.39±0.10	AW045417
97305_at	1110017 C15Rik	RIKEN cDNA 1110017C15 gene	2.34± 0.16	2.46± 0.07	1.47± 0.12	-1.08±0.14	AW123267
95592_at	1110019 N10Rik	RIKEN cDNA 1110019N10 gene	2.75± 0.07	2.64± 0.07	1.34± 0.22	-1.29±0.17	AW046785
103773_at	1110020 K19Rik	RIKEN cDNA 1110020K19 gene	1.66± 0.09	3.01± 0.46	1.06± 0.15	-1.30±0.13	AW047874
104314_r_at	1110032 A03Rik	RIKEN cDNA 1110032A03 gene	3.12± 0.95	4.51± 0.25	-1.08± 0.16	-1.03±0.19	AI851206
96604_at	1110032 N12Rik	RIKEN cDNA 1110032N12 gene	1.89± 0.19	2.23± 0.11	1.57± 0.17	-1.23±0.12	AW125827
94233_at	1110038 F14Rik	RIKEN cDNA 1110038F14 gene	1.95± 0.08	2.02± 0.09	1.69± 0.20	1.15±0.11	AW048642
160619_at	1110063 F24Rik	RIKEN cDNA 1110063F24 gene	1.40± 0.08	2.17± 0.07	1.25± 0.20	-1.22±0.12	AI843727
160184_at	1200007 D18Rik	RIKEN cDNA 1200007D18 gene	-2.35± 0.06	-1.09± 0.06	-1.12± 0.11	-1.28±0.14	AA815795
97401_at	1300006 C06Rik	RIKEN cDNA 1300006C06 gene	2.05± 0.07	2.57± 0.11	1.10± 0.11	-1.22±0.12	AW124244
93301_at	1300007 B12Rik	RIKEN cDNA 1300007B12 gene	2.08± 0.11	2.24± 0.11	1.04± 0.14	-1.47±0.12	AW124624

98049_at	1300018I05Rik	RIKEN cDNA 1300018I05 gene	1.44± 0.13	2.00± 0.06	1.22± 0.14	-1.04±0.12	AI853458
96732_at	1500001L20Rik	RIKEN cDNA 1500001L20 gene	-2.18± 0.07	-2.28± 0.07	1.01± 0.14	-1.04±0.17	AI851081
160723_at	1500001M20Rik	RIKEN cDNA 1500001M20 gene	1.84± 0.11	2.08± 0.12	1.06± 0.11	-1.20±0.15	AW124848
95568_at	1500011J06Rik	RIKEN cDNA 1500011J06 gene	2.90± 0.11	1.97± 0.12	1.18± 0.13	-1.07±0.12	AI853412
103885_at	1500019O16Rik	RIKEN cDNA 1500019O16 gene	1.93± 0.07	2.53± 0.12	1.07± 0.10	1.07±0.13	AW049156
98891_at	1600012H06Rik	RIKEN cDNA 1600012H06 gene	1.75± 0.13	2.19± 0.27	1.04± 0.10	-1.16±0.11	AW011716
160975_at	1700024K14Rik	RIKEN cDNA 1700024K14 gene	-1.56± 0.11	-2.19± 0.11	1.32± 0.18	1.34±0.22	AI504338
101568_at	1700024N20Rik	RIKEN cDNA 1700024N20 gene	1.76± 0.08	2.78± 0.12	1.38± 0.15	1.01±0.15	AW227620
161004_at	1700097N02Rik	RIKEN cDNA 1700097N02 gene	-2.14± 0.12	-3.37± 0.06	-1.03± 0.11	-1.01±0.10	AA250414
161109_at	1810013L24Rik	RIKEN cDNA 1810013L24 gene	2.06± 0.18	1.27± 0.09	1.10± 0.11	-1.10±0.13	AV335391
96743_at	1810035L17Rik	RIKEN cDNA 1810035L17 gene	2.02± 0.07	1.41± 0.06	1.76± 0.10	1.09±0.16	AA958560
98958_at	1810057B09Rik	RIKEN cDNA 1810057B09 gene	2.15± 0.12	-1.62± 0.07	-1.34± 0.10	-1.21±0.11	AA759910
95699_f_at	2010009J04Rik	RIKEN cDNA 2010009J04 gene	1.92± 0.07	2.08± 0.06	1.31± 0.14	-1.03±0.15	AI848094
96686_i_at	2010100O12Rik	RIKEN cDNA 2010100O12 gene	2.08± 0.12	1.68± 0.07	1.26± 0.10	-1.01±0.16	AI853864
104620_at	2010300G19Rik	RIKEN cDNA 2010300G19 gene	2.07± 0.07	1.92± 0.08	-1.03± 0.15	-1.73±0.10	AW123402
99187_f_at	2010315L10Rik	RIKEN cDNA 2010315L10 gene	2.45± 0.15	2.73± 0.08	1.98± 0.22	-1.03±0.21	AI835662
96761_at	2210409B01Rik	RIKEN cDNA 2210409B01 gene	-2.18± 0.10	-2.30± 0.07	-1.09± 0.11	-1.13±0.10	AF109906
103076_at	2210412K09Rik	RIKEN cDNA 2210412K09 gene	2.08± 0.11	-1.02± 0.08	1.09± 0.12	1.24±0.10	AW046093
95075_at	2310006I24Rik	RIKEN cDNA 2310006I24 gene	2.17± 0.10	2.02± 0.08	-1.01± 0.11	-1.30±0.10	AW229141
103874_r_at	2310015N07Rik	RIKEN cDNA 2310015N07 gene	2.78± 0.31	1.21± 0.22	1.41± 0.18	-1.02±0.15	AA684456
98942_r_at	2310032D16Rik	RIKEN cDNA 2310032D16 gene	-2.99± 0.10	-4.97± 0.06	1.03± 0.19	1.14±0.30	AW125284
104218_s_at	2310032M22Rik	RIKEN cDNA 2310032M22 gene	2.77± 0.13	1.28± 0.11	-1.31± 0.10	1.14±0.12	AI507524

92703_at	2310032 M22Rik	RIKEN cDNA 2310032M22 gene	3.33± 0.15	1.95± 0.08	-1.05± 0.14	-1.37±0.13	AI325791
160475_at	2310034 L04Rik	RIKEN cDNA 2310034L04 gene	2.42± 0.07	2.94± 0.15	1.25± 0.24	-1.28±0.10	AI839116
94978_at	2310037 I24Rik	RIKEN cDNA 2310037I24 gene	1.85± 0.13	2.34± 0.06	1.41± 0.18	-1.14±0.11	AI839775
104117_at	2310040 A13Rik	RIKEN cDNA 2310040A13 gene	1.93± 0.16	1.74± 0.09	-1.11± 0.12	1.23±0.13	AI836641
101404_at	2310061 I09Rik	RIKEN cDNA 2310061I09 gene	2.73± 0.15	2.13± 0.12	1.50± 0.15	-1.21±0.14	AI853654
95103_at	2310065 K24Rik	RIKEN cDNA 2310065K24 gene	2.38± 0.12	2.36± 0.11	1.22± 0.17	-1.24±0.15	AI839824
104100_at	2310075 E07Rik	RIKEN cDNA 2310075E07 gene	-3.46± 0.10	-2.52± 0.07	1.31± 0.14	1.65±0.11	AI845915
95449_at	2310075 G12Rik	RIKEN cDNA 2310075G12 gene	-3.12± 0.11	-1.83± 0.06	-1.10± 0.11	1.16±0.12	AW049793
95501_at	2410001 C21Rik	RIKEN cDNA 2410001C21 gene	1.61± 0.08	2.21± 0.07	1.02± 0.11	-1.21±0.12	AW122970
93138_at	2410012 H22Rik	RIKEN cDNA 2410012H22 gene	1.09± 0.08	1.49± 0.10	2.20± 0.13	1.26±0.16	AI853219
98039_at	2410015 M20Rik	RIKEN cDNA 2410015M20 gene	2.37± 0.15	1.90± 0.13	1.08± 0.10	1.08±0.12	AI853819
104641_f_at	2410018 L13Rik	RIKEN cDNA 2410018L13 gene	1.31± 0.06	2.45± 0.09	-1.30± 0.19	-1.98±0.14	AI643393
98344_f_at	2410018 L13Rik	RIKEN cDNA 2410018L13 gene	2.06± 0.11	2.09± 0.13	-1.01± 0.11	-2.14±0.11	AI850438
161906_f_at	2410022 L05Rik	RIKEN cDNA 2410022L05 gene	-3.11± 0.09	-3.26± 0.06	-1.28± 0.10	-1.61±0.12	AV113045
101047_at	2410026 K10Rik	RIKEN cDNA 2410026K10 gene	-2.47± 0.07	-1.09± 0.06	1.22± 0.17	-1.26±0.12	AW123697
95138_at	2510001 I10Rik	RIKEN cDNA 2510001I10 gene	1.16± 0.07	2.21± 0.11	1.68± 0.12	1.24±0.11	AI836568
98528_at	2510006 D16Rik	RIKEN cDNA 2510006D16 gene	1.79± 0.08	2.33± 0.07	1.24± 0.21	-1.27±0.15	AI854901
97864_at	2510049 I19Rik	RIKEN cDNA 2510049I19 gene	3.66± 0.36	2.42± 0.13	1.15± 0.17	1.26±0.17	AW258842
98134_at	2610101 N10Rik	RIKEN cDNA 2610101N10 gene	1.35± 0.07	2.00± 0.10	1.17± 0.17	-1.07±0.10	AW048639
162057_f_at	2610103 J23Rik	RIKEN cDNA 2610103J23 gene	2.19± 0.19	1.65± 0.06	1.05± 0.12	1.07±0.13	AV269118
93802_at	2610103 J23Rik	RIKEN cDNA 2610103J23 gene	5.92± 0.55	3.46± 0.62	1.56± 0.19	1.12±0.21	AA815890
160177_at	2610203 K23Rik	RIKEN cDNA 2610203K23 gene	2.10± 0.07	2.29± 0.09	1.59± 0.19	-1.01±0.14	AW123805

95058_f_at	2610205 H19Rik	RIKEN cDNA 2610205H19 gene	2.54± 0.08	1.41± 0.10	1.20± 0.10	-1.02±0.13	AW121984
98973_at	2610318 G08Rik	RIKEN cDNA 2610318G08 gene	3.15± 0.22	4.09± 0.35	1.39± 0.18	1.10±0.11	AA982595
96688_at	2610318 G18Rik	RIKEN cDNA 2610318G18 gene	2.01± 0.14	1.31± 0.07	-1.15± 0.12	-1.10±0.10	AI845463
101524_at	2610510 D13Rik	RIKEN cDNA 2610510D13 gene	2.35± 0.21	1.55± 0.07	-1.20± 0.10	-1.16±0.11	AI851595
160223_at	2610511 O17Rik	RIKEN cDNA 2610511O17 gene	2.24± 0.19	2.10± 0.13	1.45± 0.11	-1.06±0.14	AW047172
92268_at	2700007 P21Rik	RIKEN cDNA 2700007P21 gene	2.60± 0.10	4.08± 0.22	1.49± 0.21	1.06±0.14	AI854851
100306_at	2700007 P21Rik	RIKEN cDNA 2700007P21 gene	2.70± 0.22	6.66± 0.34	1.29± 0.18	-1.13±0.15	AI510297
93768_f_at	2700059 D21Rik	RIKEN cDNA 2700059D21 gene	2.42± 0.08	2.33± 0.13	1.01± 0.12	-1.28±0.11	AW124052
104470_at	2700066 J21Rik	RIKEN cDNA 2700066J21 gene	2.61± 0.67	4.61± 0.13	1.77± 0.22	1.20±0.18	AI957346
160752_at	2810002 D13Rik	RIKEN cDNA 2810002D13 gene	-4.05± 0.17	-1.20± 0.14	-1.13± 0.10	1.00±0.13	AA667021
104089_at	2810026 P18Rik	RIKEN cDNA 2810026P18 gene	3.53± 0.23	5.50± 0.23	1.35± 0.11	1.05±0.10	AW045664
99466_at	2810031 J10Rik	RIKEN cDNA 2810031J10 gene	1.29± 0.15	2.27± 0.10	-1.49± 0.15	-1.38±0.16	AI845653
95150_at	2810052 M02Rik	RIKEN cDNA 2810052M02 gene	1.58± 0.14	2.45± 0.15	1.16± 0.10	-1.11±0.13	AI852196
95451_at	2810405 J04Rik	RIKEN cDNA 2810405J04 gene	1.45± 0.07	2.21± 0.09	1.12± 0.16	-1.27±0.13	AA855382
160278_at	2810428 I15Rik	RIKEN cDNA 2810428I15 gene	1.24± 0.11	2.88± 0.09	2.15± 0.33	-1.29±0.14	AI854550
103071_at	2810429 C13Rik	RIKEN cDNA 2810429C13 gene	3.33± 0.10	2.52± 0.09	1.22± 0.11	1.35±0.13	AI843655
99185_at	2810443 J12Rik	RIKEN cDNA 2810443J12 gene	2.49± 0.08	2.08± 0.09	1.26± 0.11	-1.25±0.11	AW047026
103664_r_at	2810452 K22Rik	RIKEN cDNA 2810452K22 gene	2.12± 0.09	1.39± 0.09	1.13± 0.11	-1.29±0.11	AA959648
92840_at	3110079 L04Rik	RIKEN cDNA 3110079L04 gene	4.91± 0.58	6.87± 0.17	1.54± 0.32	1.04±0.12	AA683712
101998_at	4833420 G17Rik	RIKEN cDNA 4833420G17 gene	2.28± 0.07	2.10± 0.14	1.02± 0.11	1.19±0.11	AW125086
104356_at	4921516 M08Rik	RIKEN cDNA 4921516M08 gene	3.39± 0.22	1.75± 0.25	1.10± 0.13	1.13±0.11	AI465543
97798_at	4930504 E06Rik	RIKEN cDNA 4930504E06 gene	1.31± 0.08	2.55± 0.22	1.45± 0.23	-1.01±0.12	AW121496

104485_at	4930527 D15Rik	RIKEN cDNA 4930527D15 gene	1.57± 0.50	2.82± 0.14	1.21± 0.11	1.07±0.14	AI552398
104640_f_at	4930553 M18Rik	RIKEN cDNA 4930553M18 gene	2.20± 0.09	2.91± 0.20	1.34± 0.12	-1.13±0.11	AI464596
104639_i_at	4930553 M18Rik	RIKEN cDNA 4930553M18 gene	3.05± 0.35	5.24± 0.18	1.13± 0.24	1.12±0.28	AI464596
95123_at	4930566 A11Rik	RIKEN cDNA 4930566A11 gene	2.16± 0.08	1.85± 0.08	-1.24± 0.17	-1.37±0.12	AI844003
104243_r_at	4930578 F06Rik	RIKEN cDNA 4930578F06 gene	2.80± 0.20	1.28± 0.15	1.40± 0.12	-1.05±0.14	AI835622
160279_at	4930588 M11Rik	RIKEN cDNA 4930588M11 gene	1.92± 0.07	2.67± 0.12	1.66± 0.19	-1.10±0.17	AW123632
99988_at	4933427 L07Rik	RIKEN cDNA 4933427L07 gene	1.07± 0.07	2.00± 0.13	1.31± 0.14	-1.02±0.11	AW122115
101001_at	5031439 A09Rik	RIKEN cDNA 5031439A09 gene	-1.16± 0.08	-1.19± 0.07	1.83± 0.11	2.03±0.26	AI647612
95140_at	5230400 G24Rik	RIKEN cDNA 5230400G24 gene	1.86± 0.12	2.15± 0.07	-1.08± 0.13	-1.17±0.12	AI842068
97357_at	5430401 D19Rik	RIKEN cDNA 5430401D19 gene	1.43± 0.07	-1.07± 0.06	-2.23± 0.11	-1.59±0.13	AI426400
100587_f_at	5730403 B10Rik	RIKEN cDNA 5730403B10 gene	2.99± 0.43	1.91± 0.08	1.08± 0.10	1.01±0.12	AI843959
92992_i_at	5730497 N03Rik	RIKEN cDNA 5730497N03 gene	4.26± 0.39	3.11± 0.32	-1.20± 0.12	1.12±0.15	AI324972
160119_at	5730592 L21Rik	RIKEN cDNA 5730592L21 gene	1.00± 0.07	2.04± 0.11	1.18± 0.15	-1.18±0.11	AI845538
93579_at	5830427 H10Rik	RIKEN cDNA 5830427H10 gene	1.84± 0.07	1.98± 0.15	1.26± 0.16	-1.10±0.14	AW121613
104059_at	5830451 P18Rik	RIKEN cDNA 5830451P18 gene	2.26± 0.15	2.33± 0.09	1.05± 0.12	-1.27±0.11	AI851751
102964_at	6230400 O18Rik	RIKEN cDNA 6230400O18 gene	1.83± 0.17	2.88± 0.10	1.43± 0.18	-1.40±0.12	AW122326
94415_at	6230421 P05Rik	RIKEN cDNA 6230421P05 gene	2.82± 0.13	2.26± 0.15	1.58± 0.20	-1.03±0.14	AA710439
161114_i_at	6330509 M23Rik	RIKEN cDNA 6330509M23 gene	2.15± 0.23	1.78± 0.17	-1.15± 0.11	-1.74±0.10	AV330064
94426_at	6330575 P11Rik	RIKEN cDNA 6330575P11 gene	2.72± 0.11	2.86± 0.08	-1.04± 0.26	-2.08±0.18	AI851052
96833_at	8430423 A01Rik	RIKEN cDNA 8430423A01 gene	1.30± 0.08	2.39± 0.12	1.07± 0.11	-1.27±0.16	AW048468
96539_at	9330147 J08Rik	RIKEN cDNA 9330147J08 gene	-1.66± 0.07	-2.40± 0.07	-1.56± 0.11	-1.12±0.10	AW212071
94895_at	9430020 E02Rik	RIKEN cDNA 9430020E02 gene	2.66± 0.10	1.58± 0.07	1.06± 0.12	-1.05±0.17	AW122948

104444_at	9430098 E02Rik	RIKEN cDNA 9430098E02 gene	2.01 ± 0.11	1.72 ± 0.10	1.05 ± 0.10	-1.50 ± 0.15	AA689927
161104_at	9430099 J10Rik	RIKEN cDNA 9430099J10 gene	3.82 ± 0.25	1.91 ± 0.22	1.10 ± 0.17	1.79 ± 0.13	AI846811
104486_at	A2m	alpha-2-macroglobulin	-1.04 ± 0.15	-1.72 ± 0.09	-1.14 ± 0.14	2.69 ± 0.44	AI850558
97118_at	A630007 B06Rik	RIKEN cDNA A630007B06 gene	1.53 ± 0.08	2.29 ± 0.16	1.23 ± 0.20	-1.14 ± 0.12	AI159700
103303_at	A730019 I05Rik	RIKEN cDNA A730019I05 gene	-1.32 ± 0.09	-2.62 ± 0.08	1.27 ± 0.20	1.50 ± 0.29	AA798246
103688_at	A830006 N08Rik	RIKEN cDNA A830006N08 gene	-1.27 ± 0.17	1.10 ± 0.12	-1.51 ± 0.10	-2.27 ± 0.10	AW122834
94663_at	AA4071 51	expressed sequence AA407151	-2.46 ± 0.08	-2.56 ± 0.07	-1.37 ± 0.12	1.00 ± 0.12	AA407151
160713_at	AA4079 30	expressed sequence AA407930	2.08 ± 0.07	3.61 ± 0.21	2.74 ± 0.52	1.01 ± 0.15	AI841579
161376_f_at	AA4079 30	expressed sequence AA407930	2.12 ± 0.25	1.79 ± 0.20	1.07 ± 0.16	-1.40 ± 0.15	AV243059
97918_at	AA5367 43	expressed sequence AA536743	2.48 ± 0.13	1.59 ± 0.09	1.26 ± 0.14	1.40 ± 0.13	AA623587
94486_at	AA9597 42	expressed sequence AA959742	1.47 ± 0.06	2.27 ± 0.09	1.56 ± 0.18	-1.09 ± 0.16	AW125178
94359_at	AA9605 58	expressed sequence AA960558	-2.01 ± 0.06	-1.74 ± 0.06	-1.24 ± 0.12	-1.39 ± 0.10	AI849556
101006_at	Acat2	acetyl-Coenzyme A acetyltransferase 2	1.10 ± 0.07	-2.20 ± 0.06	-3.50 ± 0.09	-2.90 ± 0.10	M35797
104578_f_at	Actn1	actinin, alpha 1	-1.01 ± 0.08	1.26 ± 0.06	2.13 ± 0.11	1.70 ± 0.17	AI195392
99949_at	AI22578 2	expressed sequence AI225782	1.19 ± 0.07	2.03 ± 0.06	1.14 ± 0.15	-1.29 ± 0.10	AW060324
93472_at	AI41333 1	expressed sequence AI413331	-2.05 ± 0.07	-1.97 ± 0.07	1.03 ± 0.11	1.02 ± 0.10	AA796989
160297_at	AI41363 1	expressed sequence AI413631	2.17 ± 0.11	1.52 ± 0.12	1.83 ± 0.11	1.12 ± 0.15	AW121431
95503_at	AI83956 2	expressed sequence AI839562	2.13 ± 0.07	1.65 ± 0.06	-1.01 ± 0.11	-1.41 ± 0.12	U95498
93168_at	AI85262 9	expressed sequence AI852629	2.65 ± 0.58	-1.94 ± 0.20	-1.63 ± 0.11	-1.25 ± 0.14	AI852629
97369_g_at	Akap1	A kinase (PRKA) anchor protein 1	1.30 ± 0.16	2.20 ± 0.15	-1.31 ± 0.11	-1.26 ± 0.10	U95145
95001_at	Akap8	A kinase (PRKA) anchor protein 8	-1.02 ± 0.09	2.10 ± 0.29	1.26 ± 0.14	-1.12 ± 0.11	AB028920
101947_at	Akap8l	A kinase (PRKA) anchor protein 8-like	1.09 ± 0.11	2.69 ± 0.10	1.56 ± 0.21	1.13 ± 0.13	AB028921

93464_at	Akap9	A kinase (PRKA) anchor protein (yotiao) 9	1.54 ± 0.08	-3.17 ± 0.07	-1.27 ± 0.10	-1.35 ± 0.14	AI561567
103790_at	Alg3	asparagine-linked glycosylation 3 homolog (yeast, alpha-1,3-mannosyltransferase)	-2.13 ± 0.07	-1.88 ± 0.06	1.03 ± 0.14	-1.13 ± 0.11	AI846632
95590_at	Alg5	asparagine-linked glycosylation 5 homolog (yeast, dolichyl-phosphate beta-glucosyltransferase)	1.32 ± 0.08	2.59 ± 0.19	1.48 ± 0.11	-1.06 ± 0.18	AA615951
98477_s_at	Ank3	ankyrin 3, epithelial	2.03 ± 0.13	1.85 ± 0.13	-1.26 ± 0.10	-1.61 ± 0.11	L40632
93627_at	Ankrd28	ankyrin repeat domain 28	2.05 ± 0.13	1.95 ± 0.14	1.50 ± 0.15	-1.16 ± 0.13	AI852287
102815_at	Anxa11	annexin A11	-6.37 ± 0.18	-6.68 ± 0.13	1.41 ± 0.16	1.85 ± 0.11	U65986
101393_at	Anxa3	annexin A3	-1.81 ± 0.18	-2.57 ± 0.24	12.33 ± 3.14	9.26 ± 0.80	AJ001633
96529_at	Ap1gbp1	AP1 gamma subunit binding protein 1	2.77 ± 0.22	1.93 ± 0.13	-1.29 ± 0.12	-1.10 ± 0.13	AW122059
93794_at	Appbp1	amyloid beta precursor protein binding protein 1	3.45 ± 0.16	1.85 ± 0.13	1.13 ± 0.13	-1.21 ± 0.14	AI846393
102677_at	Arhgdig	Rho GDP dissociation inhibitor (GDI) gamma	-1.21 ± 0.07	-1.02 ± 0.07	-1.75 ± 0.10	-2.56 ± 0.10	U73198
98490_at	Arl10c	ADP-ribosylation factor-like 10C	-1.53 ± 0.07	2.23 ± 0.09	-1.19 ± 0.11	-1.07 ± 0.16	AA822412
95136_at	Arl6ip4	ADP-ribosylation factor-like 6 interacting protein 4	2.46 ± 0.21	1.96 ± 0.14	1.53 ± 0.17	-1.07 ± 0.13	AW049185
93288_at	Arpc2	actin related protein 2/3 complex, subunit 2	2.26 ± 0.10	1.86 ± 0.09	1.04 ± 0.10	-1.22 ± 0.12	AI835883
97259_at	Arpp19	cAMP-regulated phosphoprotein 19	2.17 ± 0.18	2.12 ± 0.10	1.05 ± 0.10	-1.12 ± 0.11	AJ005983
102980_at	AW536594	expressed sequence AW536594	2.03 ± 0.09	2.62 ± 0.08	1.78 ± 0.35	-1.30 ± 0.10	AI849119
104005_at	B4galt2	UDP-Gal:betaGlcNAc beta 1,4-galactosyltransferase, polypeptide 2	-1.02 ± 0.07	2.35 ± 0.10	-1.75 ± 0.17	-1.88 ± 0.14	AB019541
95156_g_at	B830022L21Rik	RIKEN cDNA B830022L21 gene	1.92 ± 0.08	2.49 ± 0.20	-1.04 ± 0.19	-1.87 ± 0.17	AI853875
93900_at	Bat2	HLA-B associated transcript 2	1.42 ± 0.21	3.01 ± 0.12	-1.67 ± 0.13	-1.69 ± 0.18	AW050268
101582_at	BC003262	cDNA sequence BC003262	1.54 ± 0.10	2.18 ± 0.07	1.34 ± 0.15	-1.34 ± 0.13	AI853259
103930_at	BC004022	cDNA sequence BC004022	2.20 ± 0.08	1.71 ± 0.07	1.41 ± 0.10	-1.08 ± 0.11	AI413179
97554_at	BC005624	cDNA sequence BC005624	2.04 ± 0.14	2.16 ± 0.07	1.37 ± 0.13	-1.01 ± 0.15	AI838889
104037_at	BC016108	cDNA sequence BC016108	1.77 ± 0.17	2.46 ± 0.48	1.24 ± 0.12	-1.24 ± 0.13	AI834891

	98	BC016198					
93004_r_at	BC018242	cDNA sequence BC018242	-2.04± 0.07	-1.65± 0.06	-1.57± 0.10	-1.21±0.10	AI842887
96560_at	BC029719	cDNA sequence BC029719	-1.46± 0.16	-2.48± 0.07	-1.17± 0.10	1.26±0.11	AA648027
94823_at	BC029892	cDNA sequence BC029892	2.12± 0.07	2.01± 0.09	1.16± 0.11	-1.04±0.16	AI835315
104366_at	BC039093	cDNA sequence BC039093	-1.33± 0.11	-2.12± 0.07	-1.31± 0.10	1.02±0.10	AW047831
97490_at	Bcl7b	B-cell CLL/lymphoma 7B	1.68± 0.17	2.08± 0.11	1.25± 0.10	-1.24±0.13	AJ011145
98052_at	Bet1l	blocked early in transport 1 homolog (S. cerevisiae)-like	2.09± 0.08	2.30± 0.07	1.15± 0.10	-1.03±0.12	AF003999
101961_at	Bub3	budding uninhibited by benzimidazoles 3 homolog (S. cerevisiae)	2.13± 0.08	2.16± 0.10	1.05± 0.14	1.00±0.13	U67327
103695_f_at	C330007P06Rik	RIKEN cDNA C330007P06 gene	2.17± 0.20	1.58± 0.07	1.24± 0.10	1.16±0.12	AW047329
103908_at	C330016H24Rik	RIKEN cDNA C330016H24 gene	1.12± 0.08	2.43± 0.08	1.10± 0.13	-1.45±0.11	AW121857
100410_at	C330027G06Rik	RIKEN cDNA C330027G06 gene	3.24± 0.31	1.82± 0.15	1.14± 0.15	-1.04±0.16	AW122781
98948_at	C77032	EST C77032	2.18± 0.11	2.43± 0.11	2.04± 0.17	-1.01±0.11	AI785289
104157_at	C78212	expressed sequence C78212	2.21± 0.17	1.46± 0.17	1.19± 0.11	-1.33±0.14	AW125643
101596_at	C78859	expressed sequence C78859	1.27± 0.17	1.08± 0.16	1.88± 0.16	-1.37±0.14	C78859
94990_at	C78915	expressed sequence C78915	1.26± 0.08	2.11± 0.07	1.20± 0.10	-1.22±0.14	AI854725
93741_at	C87860	expressed sequence C87860	1.63± 0.09	2.15± 0.07	1.36± 0.14	-1.11±0.11	AA693066
104529_at	Caml	calcium modulating ligand	2.41± 0.08	2.65± 0.10	1.27± 0.16	-1.40±0.11	U21960
97930_f_at	Cd151	CD151 antigen	1.01± 0.07	1.43± 0.10	2.80± 0.14	1.84±0.31	AF033620
160493_at	Cd63	Cd63 antigen	-1.66± 0.07	-1.50± 0.06	2.33± 0.10	1.99±0.29	D16432
103016_s_at	Cd68	CD68 antigen	-1.39± 0.11	1.01± 0.09	3.10± 0.23	2.79±0.51	X68273
94084_at	Cdc26	cell division cycle 26	2.14± 0.07	2.24± 0.09	1.33± 0.10	-1.04±0.13	AI842888
160623_at	Cdkl2	cyclin-dependent kinase-like 2 (CDC2-related kinase)	1.22± 0.09	1.34± 0.09	-1.44± 0.12	-2.15±0.11	AI847045
102804_at	Ceacam2	CEA-related cell adhesion molecule 2	-2.82± 0.07	-2.94± 0.06	-1.36± 0.10	-1.29±0.11	X67279
99486_at	Cenpb	centromere autoantigen B	1.42± 0.09	2.13± 0.07	1.10± 0.15	-1.06±0.13	X55038
162251_f_at	Centg2	centaurin, gamma 2	-1.51± 0.08	-3.15± 0.09	-1.38± 0.10	-1.22±0.12	AV335015
92841_f_at	Chgb	chromogranin B	2.24± 0.07	1.55± 0.08	-1.27± 0.10	-1.38±0.12	X51429
160330_at	Chordc1	cysteine and histidine-rich domain (CHORD)-containing, zinc-	1.66± 0.07	3.00± 0.07	1.56± 0.20	-1.24±0.10	AW122453

		binding protein 1					
94030_at	Commd2	COMM domain containing 2	2.42 ± 0.09	2.19 ± 0.09	1.27 ± 0.12	-1.23 ± 0.14	AI853431
96881_at	Commd6	COMM domain containing 6	2.36 ± 0.12	1.89 ± 0.10	1.51 ± 0.13	-1.08 ± 0.14	AW049394
104302_f_at	Commd9	COMM domain containing 9	2.99 ± 0.12	2.17 ± 0.21	1.30 ± 0.12	1.02 ± 0.11	AI851085
101976_at	Cops4	COP9 (constitutive photomorphogenic) homolog, subunit 4 (Arabidopsis thaliana)	2.30 ± 0.07	2.46 ± 0.07	1.34 ± 0.13	-1.05 ± 0.13	AF071314
101580_at	Cox7b	cytochrome c oxidase subunit VIIb	2.38 ± 0.08	1.16 ± 0.06	1.05 ± 0.10	1.00 ± 0.12	AI851220
97352_f_at	Coxvib2	cytochrome c oxidase subunit VIb, testes-specific	-1.93 ± 0.08	-3.61 ± 0.08	1.00 ± 0.27	2.66 ± 0.11	AW123567
103334_at	Crcp	calcitonin gene-related peptide-receptor component protein	1.99 ± 0.11	1.98 ± 0.10	1.09 ± 0.17	-1.63 ± 0.11	AF028242
161942_f_at	Cwf19l1	CWF19-like 1, cell cycle control (S. pombe)	1.99 ± 0.74	2.12 ± 0.18	-1.38 ± 0.11	1.23 ± 0.15	AV337197
96526_at	D030029J20Rik	9 days embryo whole body cDNA, RIKEN full-length enriched library, clone:D030029J20 product:unknown EST, full insert sequence	1.60 ± 0.07	2.12 ± 0.17	1.03 ± 0.16	-1.14 ± 0.11	AW228840
160803_at	D0H8S2298E	DNA segment, Human S2298E	1.84 ± 0.27	1.73 ± 0.09	2.28 ± 0.11	-1.32 ± 0.12	D88447
92649_at	D0HXS9928E	DNA segment, human DXS9928E	1.71 ± 0.07	2.01 ± 0.08	1.54 ± 0.13	-1.12 ± 0.15	Y18505
94526_at	D10Ertd214e	DNA segment, Chr 10, ERATO Doi 214, expressed	2.13 ± 0.11	2.05 ± 0.07	1.07 ± 0.11	-1.39 ± 0.15	AI848453
104087_at	D10Ertd641e	DNA segment, Chr 10, ERATO Doi 641, expressed	1.38 ± 0.11	2.00 ± 0.14	1.00 ± 0.12	-1.33 ± 0.14	AI840598
99087_at	D10Ertd749e	DNA segment, Chr 10, ERATO Doi 749, expressed	1.98 ± 0.07	2.35 ± 0.07	1.50 ± 0.14	-1.33 ± 0.12	AW060179
160455_s_at	D10Ertd749e	DNA segment, Chr 10, ERATO Doi 749, expressed	2.03 ± 0.08	2.57 ± 0.07	1.57 ± 0.16	-1.32 ± 0.12	AW123786
101960_at	D10Wsu52e	DNA segment, Chr 10, Wayne State University 52, expressed	2.16 ± 0.07	2.14 ± 0.08	1.28 ± 0.12	-1.06 ± 0.12	AI842208
96189_at	D11Ertd416e	DNA segment, Chr 11, ERATO Doi 416, expressed	2.10 ± 0.15	1.06 ± 0.15	1.36 ± 0.10	1.21 ± 0.12	AW046184
160772_i_at	D11Ertd730e	DNA segment, Chr 11, ERATO Doi 730, expressed	1.92 ± 0.11	2.69 ± 0.09	1.41 ± 0.21	1.00 ± 0.16	AW214428

98635_at	D11Moh 35	DNA segment, Chr 11, KL Mohlke 35	1.59 ± 0.09	2.23 ± 0.13	1.05 ± 0.18	-1.44 ± 0.10	AI854629
95480_at	D11Wsu 68e	DNA segment, Chr 11, Wayne State University 68, expressed	1.78 ± 0.17	2.01 ± 0.15	-1.05 ± 0.10	1.07 ± 0.14	AI847163
160587_at	D12Ertd 604e	DNA segment, Chr 12, ERATO Doi 604, expressed	2.11 ± 0.28	1.74 ± 0.08	1.18 ± 0.18	-1.48 ± 0.15	AW050018
160957_at	D12Ertd 7e	DNA segment, Chr 12, ERATO Doi 7, expressed	2.13 ± 0.24	2.02 ± 0.14	1.16 ± 0.18	-1.24 ± 0.14	AI156978
94451_at	D13Wsu 123e	DNA segment, Chr 13, Wayne State University 123, expressed	1.75 ± 0.08	2.33 ± 0.10	1.16 ± 0.10	-1.13 ± 0.10	AI787627
160964_at	D16Bwg 1494e	DNA segment, Chr 16, Brigham & Women's Genetics 1494 expressed	-2.19 ± 0.07	-1.92 ± 0.07	-1.09 ± 0.10	-1.15 ± 0.11	AI838494
95431_at	D16Wsu 109e	DNA segment, Chr 16, Wayne State University 109, expressed	2.88 ± 0.08	2.08 ± 0.06	1.03 ± 0.10	-1.25 ± 0.11	AA623426
95432_f_at	D16Wsu 109e	DNA segment, Chr 16, Wayne State University 109, expressed	3.00 ± 0.07	2.78 ± 0.10	-1.04 ± 0.11	-1.57 ± 0.10	AI844034
160310_at	D19Bwg 1357e	DNA segment, Chr 19, Brigham & Women's Genetics 1357 expressed	1.99 ± 0.07	2.31 ± 0.13	1.34 ± 0.11	-1.34 ± 0.11	AW046771
95679_at	D19Ertd 144e	DNA segment, Chr 19, ERATO Doi 144, expressed	1.48 ± 0.07	2.14 ± 0.10	1.23 ± 0.20	-1.33 ± 0.15	AI835912
160685_at	D5Ertd3 63e	DNA segment, Chr 5, ERATO Doi 363, expressed	1.49 ± 0.08	2.00 ± 0.07	-1.21 ± 0.15	-1.10 ± 0.15	AI153037
104116_at	D5Ertd5 93e	DNA segment, Chr 5, ERATO Doi 593, expressed	2.26 ± 0.21	2.47 ± 0.27	2.83 ± 0.46	-1.48 ± 0.13	AW124049
104717_at	D5Ertd6 89e	DNA segment, Chr 5, ERATO Doi 689, expressed	1.79 ± 0.09	2.01 ± 0.10	-1.04 ± 0.15	-1.22 ± 0.13	AI848330
104418_at	D6Ertd3 65e	DNA segment, Chr 6, ERATO Doi 365, expressed	2.47 ± 0.09	1.54 ± 0.11	-1.20 ± 0.10	-1.24 ± 0.12	AA796868
103861_s_at	D7Wsu128e	DNA segment, Chr 7, Wayne State University 128, expressed	1.62 ± 0.07	3.86 ± 0.10	1.88 ± 0.13	-1.14 ± 0.11	AA388099
103862_r_at	D7Wsu128e	DNA segment, Chr 7, Wayne State University 128, expressed	1.96 ± 0.08	3.01 ± 0.11	1.51 ± 0.11	-1.05 ± 0.10	AA388099
97863_at	D8Ertd3 54e	DNA segment, Chr 8, ERATO Doi 354, expressed	-1.15 ± 0.07	-1.23 ± 0.06	2.16 ± 0.19	1.20 ± 0.24	AW125274
96125_at	Daxx	Fas death domain-associated protein	2.09 ± 0.07	2.60 ± 0.08	-1.21 ± 0.20	-1.24 ± 0.12	AF110520
96636_at	Dctn5	dynactin 5	1.80 ± 0.06	2.11 ± 0.07	1.04 ± 0.13	-1.12 ± 0.12	AI852649

103460_at	Ddit4	DNA-damage-inducible transcript 4	2.36 ± 0.11	3.79 ± 0.19	1.11 ± 0.17	-1.03 ± 0.19	AI849939
100037_at	Ddx18	DEAD (Asp-Glu-Ala-Asp) box polypeptide 18	1.82 ± 0.23	2.98 ± 0.16	1.01 ± 0.12	-1.12 ± 0.21	AW213225
160492_at	Ddx18	DEAD (Asp-Glu-Ala-Asp) box polypeptide 18	2.11 ± 0.08	2.51 ± 0.12	1.56 ± 0.20	-1.01 ± 0.11	AI648005
99096_at	Ddx24	DEAD (Asp-Glu-Ala-Asp) box polypeptide 24	1.82 ± 0.10	3.05 ± 0.07	1.35 ± 0.16	-1.30 ± 0.13	U46690
101542_f_at	Ddx3x	DEAD/H (Asp-Glu-Ala-Asp/His) box polypeptide 3, X-linked	2.87 ± 0.20	1.18 ± 0.06	1.16 ± 0.15	-1.05 ± 0.14	L25126
92226_at	Ddx50	DEAD (Asp-Glu-Ala-Asp) box polypeptide 50	1.80 ± 0.07	2.12 ± 0.10	1.38 ± 0.21	-1.09 ± 0.13	AA866971
95688_at	Degs	degenerative spermatocyte homolog (Drosophila)	2.08 ± 0.09	2.05 ± 0.07	1.44 ± 0.11	-1.07 ± 0.12	Y08460
160892_at	Dlgh3	discs, large homolog 3 (Drosophila)	1.14 ± 0.15	2.14 ± 0.16	-1.32 ± 0.11	-1.53 ± 0.10	D87117
101975_at	Dlk1	delta-like 1 homolog (Drosophila)	-1.87 ± 0.10	-2.55 ± 0.06	-1.35 ± 0.12	1.27 ± 0.11	Z12171
97220_at	Dscr2	Down syndrome critical region homolog 2 (human)	2.18 ± 0.10	1.98 ± 0.08	1.43 ± 0.15	-1.19 ± 0.15	AW122732
94492_at	Dstn	destrin	2.16 ± 0.06	1.57 ± 0.07	1.04 ± 0.12	-1.27 ± 0.14	AB025406
96814_r_at	DXImx46e	DNA segment, Chr X, Immunex 46, expressed	1.22 ± 0.20	2.17 ± 0.29	-1.23 ± 0.11	1.20 ± 0.11	AI852973
99366_at	E030024M05Rik	RIKEN cDNA E030024M05 gene	-1.32 ± 0.13	1.01 ± 0.10	3.48 ± 0.21	3.24 ± 0.34	AI553536
103708_at	Eif1a	eukaryotic translation initiation factor 1A	1.66 ± 0.07	1.99 ± 0.09	1.11 ± 0.13	-1.36 ± 0.11	AI132207
98141_at	Eif5b	eukaryotic translation initiation factor 5B	3.76 ± 0.11	1.78 ± 0.13	1.52 ± 0.14	-1.30 ± 0.11	AA647048
92317_at	Elavl2	ELAV (embryonic lethal, abnormal vision, Drosophila)-like 2 (Hu antigen B)	2.11 ± 0.13	-1.03 ± 0.07	-1.30 ± 0.11	-1.27 ± 0.12	U29088
92361_at	Elavl4	ELAV (embryonic lethal, abnormal vision, Drosophila)-like 4 (Hu antigen D)	2.16 ± 0.11	1.09 ± 0.09	-1.35 ± 0.11	-1.45 ± 0.13	D31953
100051_at	Epb7.2	erythrocyte protein band 7.2	-1.98 ± 0.06	-2.35 ± 0.08	-1.24 ± 0.13	1.25 ± 0.14	U17297
103263_at	Epc1	enhancer of polycomb homolog 1 (Drosophila)	1.89 ± 0.07	2.50 ± 0.07	-1.05 ± 0.14	-1.22 ± 0.13	AF079765
104006_at	Eps15	epidermal growth factor receptor pathway substrate 15	1.78 ± 0.09	3.26 ± 0.38	1.02 ± 0.10	1.16 ± 0.11	L21768

103859_at	Eral1	Era (G-protein)-like 1 (E. coli)	1.09 ± 0.15	2.76 ± 0.10	-1.01 ± 0.15	1.13 ± 0.14	AA863768
98525_f_at	Erdr1	erythroid differentiation regulator 1	1.64 ± 0.12	3.02 ± 0.07	1.51 ± 0.24	-1.12 ± 0.18	AJ007909
96031_r_at	Fbxl5	F-box and leucine-rich repeat protein 5	1.89 ± 0.14	1.25 ± 0.11	1.07 ± 0.12	1.21 ± 0.11	AW259411
160424_f_at	Fdps	farnesyl diphosphate synthetase	-1.19 ± 0.06	-1.34 ± 0.06	-3.84 ± 0.10	-4.54 ± 0.10	AI846851
99098_at	Fdps	farnesyl diphosphate synthetase	1.22 ± 0.06	1.21 ± 0.06	-4.21 ± 0.10	-4.63 ± 0.09	AW045533
96569_at	Fignl1	fidgetin-like 1	-2.61 ± 0.07	-3.11 ± 0.06	-1.17 ± 0.10	1.13 ± 0.11	AA266298
160648_at	Fignl1	fidgetin-like 1	-2.00 ± 0.07	-2.25 ± 0.07	-1.04 ± 0.10	1.61 ± 0.10	AI047076
93309_at	Fin14	fibroblast growth factor inducible 14	2.53 ± 0.07	2.01 ± 0.06	1.42 ± 0.17	-1.13 ± 0.16	U42386
104600_at	Fip1l1	FIP1 like 1 (S. cerevisiae)	2.51 ± 0.12	2.68 ± 0.13	1.45 ± 0.11	1.28 ± 0.11	AI841692
93443_at	Fndc1	fibronectin type III domain containing 1	-3.37 ± 0.11	-1.90 ± 0.09	-1.38 ± 0.10	1.08 ± 0.16	AW212271
98817_at	Fst	follistatin	1.30 ± 0.10	-1.19 ± 0.06	-2.06 ± 0.11	-2.20 ± 0.11	Z29532
95756_at	Ftsj3	FtsJ homolog 3 (E. coli)	2.38 ± 0.12	1.92 ± 0.14	1.75 ± 0.10	-1.03 ± 0.11	AI839681
98075_at	G431001I09Rik	RIKEN cDNA G431001I09 gene	2.34 ± 0.07	2.08 ± 0.06	1.23 ± 0.11	1.05 ± 0.12	AW121683
93011_at	Gabarapl1	gamma-aminobutyric acid (GABA(A)) receptor-associated protein-like 1	1.66 ± 0.08	2.62 ± 0.06	1.71 ± 0.27	-1.18 ± 0.12	AW123904
98531_g_at	Gas5	growth arrest specific 5	2.25 ± 0.07	3.20 ± 0.08	2.08 ± 0.20	1.30 ± 0.14	AI849615
92783_at	Gh	growth hormone	-1.67 ± 0.08	-2.37 ± 0.09	-1.07 ± 0.12	-1.17 ± 0.10	X02891
100592_at	Ghitm	growth hormone inducible transmembrane protein	1.18 ± 0.06	2.52 ± 0.09	1.73 ± 0.12	1.09 ± 0.12	AI929971
96943_at	Gps1	G protein pathway suppressor 1	2.47 ± 0.06	2.40 ± 0.09	1.27 ± 0.11	-1.21 ± 0.13	AW125234
99160_s_at	Grina	glutamate receptor, ionotropic, N-methyl D-asparate-associated protein 1 (glutamate binding)	-1.03 ± 0.09	2.13 ± 0.07	-1.28 ± 0.12	-1.35 ± 0.17	AW227647
96085_at	Gsta4	glutathione S-transferase, alpha 4	1.17 ± 0.10	1.03 ± 0.08	5.07 ± 0.12	4.56 ± 1.18	L06047
160225_at	Gtf2b	general transcription factor IIB	2.75 ± 0.11	3.31 ± 0.13	1.50 ± 0.31	1.04 ± 0.16	AI840450
104402_at	Gtf3c4	general transcription factor IIIC, polypeptide 4	1.89 ± 0.23	2.66 ± 0.10	1.39 ± 0.17	-1.22 ± 0.15	AA030469
160172_at	Gtl2	GTL2, imprinted maternally expressed untranslated	1.24 ± 0.07	2.80 ± 0.23	1.96 ± 0.25	-1.13 ± 0.10	Y13832

		mRNA					
160176_at	Hirip5	histone cell cycle regulation defective interacting protein 5	2.30 ± 0.07	2.29 ± 0.09	1.63 ± 0.11	-1.20 ± 0.21	AJ132616
94805_f_at	Hist1h2ac	histone 1, H2ac	4.05 ± 0.10	3.04 ± 0.10	1.03 ± 0.14	1.03 ± 0.21	M33988
94832_at	Hnrph2	heterogeneous nuclear ribonucleoprotein H2	1.05 ± 0.11	-2.07 ± 0.07	1.01 ± 0.13	1.01 ± 0.11	U58105
160316_at	Hnrpu	heterogeneous nuclear ribonucleoprotein U	-2.45 ± 0.07	-1.72 ± 0.07	1.50 ± 0.20	-1.32 ± 0.12	AA981581
98090_at	Hrb2	HIV-1 Rev binding protein 2	4.04 ± 0.21	3.24 ± 0.24	1.75 ± 0.11	-1.10 ± 0.13	AW210014
99109_at	Ier2	immediate early response 2	1.77 ± 0.08	3.53 ± 0.07	1.72 ± 0.14	1.24 ± 0.18	M59821
94384_at	Ier3	immediate early response 3	4.75 ± 0.30	7.40 ± 0.48	7.33 ± 0.22	1.29 ± 0.28	X67644
102152_f_at	Igh-VS107	immunoglobulin heavy chain (S107 family)	-3.88 ± 0.07	-3.28 ± 0.08	-1.36 ± 0.10	-1.12 ± 0.10	M16724
160397_at	Ik	IK cytokine	2.04 ± 0.08	1.35 ± 0.09	1.24 ± 0.10	1.05 ± 0.10	AI790328
162006_r_at	Immt	inner membrane protein, mitochondrial	-1.34 ± 0.07	-3.01 ± 0.07	-1.32 ± 0.10	-1.07 ± 0.10	AV334115
161407_i_at	Inpp1	inositol polyphosphate-1-phosphatase	-1.88 ± 0.06	-2.01 ± 0.08	1.17 ± 0.11	-1.09 ± 0.12	AV312395
104735_at	Kctd12	potassium channel tetramerisation domain containing 12	2.01 ± 0.14	-1.14 ± 0.06	-1.38 ± 0.09	-1.30 ± 0.10	AI842065
102644_at	Kdt1	kidney cell line derived transcript 1	1.34 ± 0.11	2.07 ± 0.13	2.65 ± 0.24	2.43 ± 0.10	U13371
100571_at	Laptm4b	lysosomal-associated protein transmembrane 4B	-1.32 ± 0.07	-1.08 ± 0.07	2.34 ± 0.22	1.80 ± 0.38	AW123934
103523_at	Leng8	leukocyte receptor cluster (LRC) member 8	-5.32 ± 0.11	-1.12 ± 0.13	1.43 ± 0.24	1.10 ± 0.10	AI851703
98059_s_at	Lmna	lamin A	1.26 ± 0.07	2.82 ± 0.19	3.54 ± 0.18	1.34 ± 0.18	D49733
101214_f_at	LOC14433	similar to glyceraldehyde-3-phosphate dehydrogenase	2.78 ± 0.07	3.07 ± 0.11	1.51 ± 0.17	-1.07 ± 0.16	M32599
161392_f_at	Lrpb7	leucine rich protein, B7 gene	-1.69 ± 0.12	-2.23 ± 0.06	-1.40 ± 0.10	1.00 ± 0.11	AV257486
92564_at	Lrrfip1	leucine rich repeat (in FLII) interacting protein 1	2.84 ± 0.35	1.22 ± 0.26	3.92 ± 0.30	2.37 ± 0.22	AI891475
98440_at	Ltb4dh	leukotriene B4 12-hydroxydehydrogenase	1.13 ± 0.22	1.33 ± 0.16	10.74 ± 1.04	6.95 ± 1.90	AA596710
104368_at	Mapre3	microtubule-associated protein, RP/EB family, member 3	-3.10 ± 0.07	-1.84 ± 0.08	-1.17 ± 0.12	1.05 ± 0.15	U51204

103553_at	Mcm10	minichromosome maintenance deficient 10 (S. cerevisiae)	2.11 ± 0.29	1.85 ± 0.23	1.29 ± 0.12	-1.17 ± 0.13	AA867646
95417_at	Mgat2	mannoside acetylglucosaminyl transferase 2	2.17 ± 0.07	1.58 ± 0.12	1.25 ± 0.10	-1.14 ± 0.11	AI117848
96258_at	Mgst3	microsomal glutathione S-transferase 3	-2.19 ± 0.07	1.51 ± 0.07	-1.27 ± 0.10	-1.83 ± 0.11	AI843448
104752_at	Mmrp19	monocyte macrophage 19	1.76 ± 0.08	2.29 ± 0.08	1.13 ± 0.13	1.12 ± 0.17	AB028863
103468_at	Mns1	meiosis-specific nuclear structural protein 1	1.85 ± 0.23	1.12 ± 0.15	1.04 ± 0.17	2.06 ± 0.13	D14849
96151_at	Mocos	molybdenum cofactor sulfurase	2.25 ± 0.28	2.16 ± 0.29	3.26 ± 0.13	1.08 ± 0.13	AA839813
97803_at	Mpp1	membrane protein, palmitoylated	-1.56 ± 0.07	-2.07 ± 0.08	-1.03 ± 0.10	1.04 ± 0.11	U38196
100886_f_at	Mrpl45	mitochondrial ribosomal protein L45	2.27 ± 0.10	2.62 ± 0.10	1.04 ± 0.11	1.04 ± 0.12	AI841415
96861_at	Mrpl50	mitochondrial ribosomal protein L50	1.59 ± 0.19	2.31 ± 0.10	-1.30 ± 0.13	1.00 ± 0.15	AI852376
160621_at	Mrps22	mitochondrial ribosomal protein S22	1.88 ± 0.13	2.08 ± 0.08	1.69 ± 0.15	-1.28 ± 0.11	AI852322
92826_at	Mrps33	mitochondrial ribosomal protein S33	2.08 ± 0.13	-1.02 ± 0.06	-1.16 ± 0.10	-1.28 ± 0.11	Y17852
95730_at	Mrps34	mitochondrial ribosomal protein S34	1.04 ± 0.17	2.57 ± 0.20	1.96 ± 0.17	-1.13 ± 0.18	AI840884
104186_at	Msl2	male-specific lethal-2 homolog (Drosophila)	2.07 ± 0.09	1.67 ± 0.12	1.18 ± 0.10	-1.05 ± 0.12	AA739263
160308_at	Msn	moesin	-2.05 ± 0.07	-1.19 ± 0.08	5.12 ± 0.35	2.80 ± 0.61	AI839417
103044_g_at	Mtcp1	mature T-cell proliferation 1	-2.25 ± 0.10	-1.64 ± 0.06	-1.17 ± 0.10	-1.11 ± 0.11	Z35294
103264_at	Mtmr1	myotubularin related protein 1	1.23 ± 0.08	1.21 ± 0.08	-2.22 ± 0.10	-1.03 ± 0.21	AF073997
96285_at	Myadm	myeloid-associated differentiation marker	-2.24 ± 0.10	-3.54 ± 0.07	-1.10 ± 0.12	1.03 ± 0.10	AJ001616
104147_at	Nans	N-acetylneuraminic acid synthase (sialic acid synthase)	1.94 ± 0.09	2.73 ± 0.13	-1.20 ± 0.10	-1.20 ± 0.12	AW122052
103791_at	Narg1	NMDA receptor-regulated gene 1	1.77 ± 0.19	1.99 ± 0.08	1.12 ± 0.12	1.02 ± 0.11	AW048763
93246_at	Narg1	NMDA receptor-regulated gene 1	2.02 ± 0.12	1.10 ± 0.06	1.21 ± 0.18	-1.08 ± 0.11	AW260482
160398_at	Nol7	nucleolar protein 7	2.48 ± 0.10	1.34 ± 0.07	1.66 ± 0.12	1.22 ± 0.12	AW124661
101634_at	Npm1	nucleophosmin 1	2.49 ± 0.07	1.92 ± 0.07	1.17 ± 0.10	1.01 ± 0.14	M33212
93673_at	Nrtn	neurturin	-1.84 ± 0.08	-2.51 ± 0.09	-1.02 ± 0.11	-1.05 ± 0.16	U78109

103868_at	Nufip1	nuclear fragile X mental retardation protein interacting protein	1.51 ± 0.19	2.85 ± 0.32	1.61 ± 0.17	-1.42 ± 0.17	AA681274
101366_f_at	Nvl	nuclear VCP-like	3.47 ± 0.26	2.60 ± 0.20	1.26 ± 0.11	-1.26 ± 0.11	AA250299
93600_at	Obrgrp	leptin receptor gene-related protein	2.16 ± 0.12	1.47 ± 0.06	-1.25 ± 0.11	1.01 ± 0.13	AJ011565
100626_at	Odf2	outer dense fiber of sperm tails 2	1.64 ± 0.19	3.04 ± 0.31	1.08 ± 0.10	-1.16 ± 0.16	AF034105
92500_at	Odz3	odd Oz/ten-m homolog 3 (Drosophila)	2.01 ± 0.12	-1.26 ± 0.07	-1.47 ± 0.10	-1.13 ± 0.12	AB025412
97581_at	Odz4	odd Oz/ten-m homolog 4 (Drosophila)	-1.85 ± 0.08	-2.41 ± 0.07	-1.32 ± 0.11	1.08 ± 0.11	AF059485
99549_at	Ogn	osteoglycin	1.03 ± 0.31	-6.87 ± 0.19	1.62 ± 0.49	4.77 ± 0.64	D31951
103388_at	P42pop	Myb protein P42POP	-3.59 ± 0.06	-3.12 ± 0.07	-1.25 ± 0.13	-1.10 ± 0.12	AW047050
100720_at	Pabpc1	poly A binding protein, cytoplasmic 1	2.02 ± 0.12	2.02 ± 0.06	1.01 ± 0.11	1.01 ± 0.16	X65553
94461_at	Pbef1	pre-B-cell colony-enhancing factor 1	2.32 ± 0.14	2.06 ± 0.12	-1.11 ± 0.12	-1.10 ± 0.11	AI852144
160899_at	Pcp4	Purkinje cell protein 4	2.04 ± 0.07	1.34 ± 0.06	-1.39 ± 0.11	-1.23 ± 0.12	X17320
98056_at	Phlda3	pleckstrin homology-like domain, family A, member 3	-2.49 ± 0.07	1.20 ± 0.11	2.67 ± 0.13	1.38 ± 0.15	AI846214
99926_at	Pigr	polymeric immunoglobulin receptor	-4.91 ± 0.11	-3.78 ± 0.06	-1.42 ± 0.09	-1.11 ± 0.10	AB001489
94445_at	Pls3	plastin 3 (T-isoform)	2.46 ± 0.09	1.59 ± 0.08	1.91 ± 0.15	1.17 ± 0.10	AW125273
96136_at	Pmscl2	polymyositis/scleroderma autoantigen 2	1.89 ± 0.23	3.27 ± 0.24	1.73 ± 0.29	-1.08 ± 0.12	AI553452
104378_at	Pon2	paraoxonase 2	-1.01 ± 0.19	-1.02 ± 0.09	1.68 ± 0.20	2.12 ± 0.15	L48514
97979_at	Ppp1r7	protein phosphatase 1, regulatory (inhibitor) subunit 7	2.15 ± 0.09	2.41 ± 0.10	1.30 ± 0.12	-1.13 ± 0.11	AI849126
95631_at	Ppp4c	protein phosphatase 4, catalytic subunit	1.52 ± 0.10	3.06 ± 0.09	1.11 ± 0.11	1.02 ± 0.11	AF088911
93010_at	Pqbp1	polyglutamine binding protein 1	2.16 ± 0.18	2.37 ± 0.09	1.02 ± 0.10	-1.49 ± 0.10	AJ250406
97496_f_at	Prkcdbp	protein kinase C, delta binding protein	1.17 ± 0.23	1.23 ± 0.18	5.96 ± 0.65	3.36 ± 0.17	AW048944
160197_at	Pycrl	pyrroline-5-carboxylate reductase-like	1.37 ± 0.12	2.50 ± 0.10	1.59 ± 0.17	-1.09 ± 0.10	AW060487
161006_at	R75096	expressed sequence R75096	-2.93 ± 0.10	-3.07 ± 0.07	-1.36 ± 0.10	-1.38 ± 0.11	AI853978
101381_at	Rabep1	rabaptin, RAB GTPase binding effector protein 1	1.97 ± 0.25	2.73 ± 0.08	1.06 ± 0.15	-1.47 ± 0.10	D86066

102724_at	Rabep1	rabaptin, RAB GTPase binding effector protein 1	5.36 ± 0.50	3.28 ± 0.26	-1.14 ± 0.10	-1.43 ± 0.10	AI608324
95077_at	Rabggtb	RAB geranylgeranyl transferase, b subunit	2.60 ± 0.09	3.77 ± 0.07	1.51 ± 0.26	-1.04 ± 0.10	U12922
103840_at	Rad17	RAD17 homolog (S. pombe)	2.37 ± 0.15	1.68 ± 0.09	1.49 ± 0.10	-1.08 ± 0.12	AJ011923
96154_at	Renbp	renin binding protein	-2.12 ± 0.14	-1.31 ± 0.09	1.32 ± 0.14	1.28 ± 0.12	AA600645
93020_at	Rex3	reduced expression 3	2.21 ± 0.15	1.77 ± 0.06	1.12 ± 0.12	-1.56 ± 0.10	AF051347
96653_at	Rnaset2	ribonuclease T2	1.22 ± 0.07	-1.03 ± 0.07	2.15 ± 0.13	1.54 ± 0.24	AI851762
98915_at	Rnf149	ring finger protein 149	1.00 ± 0.11	1.48 ± 0.11	2.22 ± 0.23	1.05 ± 0.11	AI849082
161814_f_at	Rnf19	ring finger protein (C3HC4 type) 19	4.51 ± 0.12	2.67 ± 0.18	-1.03 ± 0.10	-1.48 ± 0.10	AV355427
102131_f_at	Rnf20	ring finger protein 20	-3.05 ± 0.08	-2.93 ± 0.06	1.01 ± 0.13	1.08 ± 0.13	AU014874
93518_at	Rnps1	ribonucleic acid binding protein S1	1.49 ± 0.07	2.04 ± 0.09	-1.01 ± 0.19	-1.35 ± 0.10	X70067
97838_at	Rnu22	RNA, U22 small nucleolar	3.38 ± 0.13	4.31 ± 0.22	2.16 ± 0.19	1.14 ± 0.12	AA684508
160514_at	Rp9h	retinitis pigmentosa 9 homolog (human)	1.92 ± 0.07	2.12 ± 0.10	-1.02 ± 0.10	-1.26 ± 0.12	D78255
100213_f_at	Rpl41	ribosomal protein L41	2.34 ± 0.06	2.85 ± 0.08	1.03 ± 0.12	-1.13 ± 0.14	U93862
98564_f_at	Rps26	ribosomal protein S26	2.28 ± 0.07	2.09 ± 0.10	1.07 ± 0.10	-1.10 ± 0.15	U67770
92981_at	Scg2	secretogranin II	2.41 ± 0.09	1.29 ± 0.07	1.47 ± 0.19	-1.77 ± 0.11	X68837
95986_at	Scospondin	subcommissural organ spondin	-1.97 ± 0.11	-2.17 ± 0.08	-1.59 ± 0.10	-1.04 ± 0.10	C79529
95104_at	Sdc2	syndecan 2	-2.08 ± 0.07	-2.34 ± 0.07	1.22 ± 0.11	1.33 ± 0.12	U00674
95664_at	Sec14l1	SEC14-like 1 (S. cerevisiae)	2.21 ± 0.08	3.43 ± 0.09	-1.43 ± 0.11	-1.44 ± 0.13	AW048159
103871_at	Sec23ip	Sec23 interacting protein	2.02 ± 0.12	2.37 ± 0.16	1.36 ± 0.17	-1.04 ± 0.13	AW123729
162420_r_at	Selk	selenoprotein K	-1.36 ± 0.07	-2.05 ± 0.07	1.29 ± 0.10	-1.34 ± 0.12	AV290470
98905_at	Septin7	septin 7	2.51 ± 0.06	2.60 ± 0.11	1.02 ± 0.13	-1.06 ± 0.13	AJ223782
96060_at	Serpinb6a	serine (or cysteine) proteinase inhibitor, clade B, member 6a	-1.34 ± 0.08	1.02 ± 0.06	2.29 ± 0.18	1.42 ± 0.15	U25844
99494_at	Serpini1	serine (or cysteine) proteinase inhibitor, clade I, member 1	2.08 ± 0.07	1.84 ± 0.07	-1.55 ± 0.15	-1.22 ± 0.15	AJ001700
101861_at	Sgce	sarcoglycan, epsilon	1.87 ± 0.08	2.10 ± 0.13	1.20 ± 0.10	1.13 ± 0.10	AF031919
93806_at	Sh3bgrl	SH3-binding domain glutamic acid-rich protein like	2.43 ± 0.09	1.72 ± 0.11	-1.19 ± 0.11	1.01 ± 0.12	AI848671
104216_at	Shoc2	soc-2 (suppressor of clear) homolog (C. elegans)	1.63 ± 0.25	2.50 ± 0.18	-1.51 ± 0.10	-1.17 ± 0.16	AF068921

98800_at	Slc23a3	solute carrier family 23 (nucleobase transporters), member 3	-2.48 ± 0.12	-2.94 ± 0.08	-1.25 ± 0.10	-1.36 ± 0.10	U25739
104200_at	Slc5a6	solute carrier family 5 (sodium-dependent vitamin transporter), member 6	-2.48 ± 0.07	-2.76 ± 0.08	-1.30 ± 0.13	-1.24 ± 0.12	AW048729
98553_at	Slmap	sarcolemma associated protein	1.79 ± 0.08	2.02 ± 0.18	1.82 ± 0.19	-1.22 ± 0.13	AW124175
98991_at	Smarcad 1	SWI/SNF-related, matrix-associated actin-dependent regulator of chromatin, subfamily a, containing DEAD/H box 1`	1.85 ± 0.14	2.23 ± 0.09	1.03 ± 0.13	-1.17 ± 0.13	X69942
100887_at	Smc6l1	SMC6 structural maintenance of chromosomes 6-like 1 (yeast)	2.16 ± 0.09	1.71 ± 0.11	-1.24 ± 0.10	1.14 ± 0.12	AI838562
96712_at	Smoc1	SPARC related modular calcium binding 1	-2.49 ± 0.07	-2.45 ± 0.07	1.01 ± 0.16	2.07 ± 0.41	AI848508
93273_at	Snca	synuclein, alpha	1.50 ± 0.06	1.01 ± 0.06	-2.81 ± 0.10	-2.98 ± 0.09	AF044672
100510_at	Sncb	synuclein, beta	-2.38 ± 0.07	-2.75 ± 0.06	-1.46 ± 0.13	-1.37 ± 0.10	AI839708
94313_at	Snrp1c	U1 small nuclear ribonucleoprotein 1C	2.45 ± 0.07	2.04 ± 0.10	1.54 ± 0.12	1.01 ± 0.12	X96767
100101_at	Snrpa	small nuclear ribonucleoprotein polypeptide A	1.73 ± 0.08	2.11 ± 0.07	1.28 ± 0.16	-1.15 ± 0.11	L15447
93832_at	Spag7	sperm associated antigen 7	1.23 ± 0.07	2.04 ± 0.07	1.14 ± 0.11	-1.04 ± 0.11	AI854541
97160_at	Sparc	secreted acidic cysteine rich glycoprotein	1.28 ± 0.07	-1.84 ± 0.10	3.00 ± 0.17	3.64 ± 0.59	X04017
160319_at	Sparcl1	SPARC-like 1 (mast9, hevin)	1.05 ± 0.07	-1.21 ± 0.06	-2.20 ± 0.10	-1.37 ± 0.10	U66166
94387_at	Spata5	spermatogenesis associated 5	1.94 ± 0.11	2.87 ± 0.19	1.36 ± 0.26	-1.47 ± 0.19	AF016544
98428_at	Spg4	spastic paraplegia 4 homolog (human)	1.49 ± 0.08	2.20 ± 0.08	-1.34 ± 0.10	-1.37 ± 0.10	AJ246002
161054_at	Spock1	sparc/osteonectin, cwcv and kazal-like domains proteoglycan 1	-2.65 ± 0.07	-1.49 ± 0.06	-1.70 ± 0.10	-2.85 ± 0.10	X92864
101995_at	Sqstm1	sequestosome 1	3.11 ± 0.06	5.59 ± 0.09	3.58 ± 0.34	1.17 ± 0.27	U40930
92579_at	Ssb	Sjogren syndrome antigen B	2.21 ± 0.15	1.07 ± 0.07	1.05 ± 0.12	-1.06 ± 0.10	L00993
96724_r_at	Ssx2ip	synovial sarcoma, X breakpoint 2 interacting protein	2.55 ± 0.24	2.07 ± 0.07	-1.03 ± 0.10	1.07 ± 0.11	AW122911
97310_at	St13	suppression of tumorigenicity 13	1.59 ± 0.09	2.54 ± 0.06	1.39 ± 0.14	1.14 ± 0.10	AW124318

103286_at	Stam2	signal transducing adaptor molecule (SH3 domain and ITAM motif) 2	1.65 ± 0.41	2.41 ± 0.23	-1.05 ± 0.12	1.00 ± 0.12	AB012611
93366_r_at	Sugt1	SGT1, suppressor of G2 allele of SKP1 (S. cerevisiae)	2.17 ± 0.11	1.64 ± 0.15	1.15 ± 0.12	1.05 ± 0.11	AI838149
93365_s_at	Sugt1	SGT1, suppressor of G2 allele of SKP1 (S. cerevisiae)	2.96 ± 0.19	2.44 ± 0.19	1.20 ± 0.12	1.04 ± 0.13	AI838149
94368_at	Supv3l1	suppressor of var1, 3-like 1 (S. cerevisiae)	2.43 ± 0.11	2.56 ± 0.19	1.58 ± 0.17	-1.02 ± 0.12	AW049139
101031_at	Surf1	surfeit gene 1	1.76 ± 0.10	2.28 ± 0.10	1.85 ± 0.25	-1.10 ± 0.14	M14689
104283_at	Tbc1d15	TBC1 domain family, member 15	3.18 ± 0.11	3.82 ± 0.22	1.98 ± 0.14	1.39 ± 0.12	AI037493
95101_at	Tde2	tumor differentially expressed 2	2.29 ± 0.09	1.14 ± 0.08	1.15 ± 0.10	-1.07 ± 0.10	AI834772
101551_s_at	Tes	testis derived transcript	1.35 ± 0.08	1.51 ± 0.08	-1.40 ± 0.22	-2.31 ± 0.10	X78989
99144_s_at	Tgoln1	trans-golgi network protein	1.74 ± 0.18	3.11 ± 0.10	1.25 ± 0.16	1.14 ± 0.20	D50031
99057_at	Thy1	thymus cell antigen 1, theta	-2.55 ± 0.07	-1.59 ± 0.06	1.50 ± 0.22	-1.29 ± 0.11	M12379
160678_at	Tm4sf12	transmembrane 4 superfamily member 12	1.13 ± 0.11	-2.02 ± 0.08	1.05 ± 0.14	2.26 ± 0.21	AA871166
95120_at	Tm4sf13	transmembrane 4 superfamily member 13	2.33 ± 0.08	1.19 ± 0.09	-1.28 ± 0.10	-1.33 ± 0.11	AI837621
92437_at	Tm7sf2	transmembrane 7 superfamily member 2	-1.29 ± 0.11	-1.09 ± 0.07	-4.50 ± 0.10	-2.69 ± 0.10	AW047445
95383_at	Tm7sf2	transmembrane 7 superfamily member 2	-1.11 ± 0.07	-1.28 ± 0.06	-1.71 ± 0.10	-2.18 ± 0.10	AI415418
160472_r_at	Tmeff1	transmembrane protein with EGF-like and two follistatin-like domains 1	1.24 ± 0.08	-2.59 ± 0.07	-1.67 ± 0.11	-1.15 ± 0.10	AI837838
100039_at	Tmem4	transmembrane protein 4	2.86 ± 0.24	2.93 ± 0.13	1.34 ± 0.10	1.25 ± 0.17	AW125880
92942_at	Trim21	tripartite motif protein 21	-1.99 ± 0.09	-2.24 ± 0.07	-1.32 ± 0.12	1.18 ± 0.17	AA138192
101372_at	Trip13	thyroid hormone receptor interactor 13	2.42 ± 0.29	1.99 ± 0.25	2.20 ± 0.35	-1.30 ± 0.13	AI852645
96921_at	Ttc1	tetratricopeptide repeat domain 1	1.62 ± 0.12	2.88 ± 0.20	1.76 ± 0.16	1.04 ± 0.10	AW060765
97900_at	Txndc9	thioredoxin domain containing 9	2.28 ± 0.07	1.92 ± 0.09	1.15 ± 0.15	-1.17 ± 0.13	AI845714
102817_at	U2af1-rs1	U2 small nuclear ribonucleoprotein auxiliary factor (U2AF) 1, related sequence 1	2.07 ± 0.08	1.97 ± 0.08	1.36 ± 0.24	-1.13 ± 0.11	S69507
100717_at	U90926	cDNA sequence U90926	-2.99 ± 0.07	-3.01 ± 0.06	-1.38 ± 0.10	1.02 ± 0.10	U90926

		U90926					
97285_f_at	Ubxd1	UBX domain containing 1	2.25 ± 0.22	2.23 ± 0.07	1.07 ± 0.11	-1.01 ± 0.14	AW120609
100091_at	Ugalt2	UDP-galactose translocator 2	2.10 ± 0.11	1.86 ± 0.06	1.26 ± 0.15	-1.28 ± 0.14	D87990
102317_at	Vamp4	vesicle-associated membrane protein 4	-1.34 ± 0.07	-2.07 ± 0.07	-1.18 ± 0.10	-1.29 ± 0.10	AF061516
160079_i_at	Wac	WW domain containing adaptor with coiled-coil	2.37 ± 0.07	1.92 ± 0.09	-1.02 ± 0.10	-1.24 ± 0.10	AI845773
100523_r_at	Wbp5	WW domain binding protein 5	2.20 ± 0.14	1.14 ± 0.08	1.24 ± 0.14	1.03 ± 0.13	U92454
100522_s_at	Wbp5	WW domain binding protein 5	2.31 ± 0.11	1.58 ± 0.07	1.07 ± 0.15	1.03 ± 0.11	U92454
160130_at	Wdr26	WD repeat domain 26	2.40 ± 0.09	1.86 ± 0.09	1.43 ± 0.12	-1.15 ± 0.12	AA795284
100348_at	X83313	EST X83313	-80.41 ± 0.03	-25.86 ± 0.04	1.37 ± 0.18	-1.98 ± 0.77	AW214136
96018_r_at	Zdhhc5	zinc finger, DHHC domain containing 5	1.02 ± 0.09	-2.21 ± 0.06	-1.02 ± 0.10	-1.15 ± 0.10	AI853561
104582_g_at	Zdhhc6	zinc finger, DHHC domain containing 6	2.23 ± 0.09	2.32 ± 0.18	1.32 ± 0.10	1.01 ± 0.12	AI845438
95533_at	Zfp106	zinc finger protein 106	-1.11 ± 0.07	-2.61 ± 0.07	-1.82 ± 0.12	1.18 ± 0.14	AW048037
99001_at	Zfp292	zinc finger protein 292	2.40 ± 0.11	1.11 ± 0.11	-1.11 ± 0.13	-1.15 ± 0.10	AF017806
100897_f_at	Zfp297	zinc finger protein 297	-2.37 ± 0.11	-1.31 ± 0.11	1.20 ± 0.16	1.11 ± 0.17	AF100956
104437_at	Zfp30	zinc finger protein 30	2.42 ± 0.16	1.51 ± 0.08	1.21 ± 0.14	-1.21 ± 0.15	Z30174
93324_at	Zfp36l1	zinc finger protein 36, C3H type-like 1	1.27 ± 0.11	-1.39 ± 0.07	1.28 ± 0.10	2.24 ± 0.14	M58566
98277_at	Zfpn1a4	zinc finger protein, subfamily 1A, 4 (Eos)	-2.06 ± 0.09	-1.47 ± 0.08	-1.18 ± 0.10	-1.16 ± 0.10	AB017615
103753_at	Zzz3	zinc finger, ZZ domain containing 3	3.06 ± 0.10	2.43 ± 0.18	1.29 ± 0.15	1.05 ± 0.11	AI159572
101217_at		---	-11.95 ± 0.15	-3.15 ± 0.11	-1.30 ± 0.10	1.06 ± 0.12	D18865
161737_at		---	-5.94 ± 0.08	-2.93 ± 0.17	1.13 ± 0.12	-1.05 ± 0.13	AV312560
101863_at		---	-5.45 ± 0.18	-1.42 ± 0.22	-1.18 ± 0.13	1.00 ± 0.16	C78246
103709_at		---	-5.41 ± 0.12	-3.78 ± 0.07	-1.27 ± 0.10	1.24 ± 0.18	AA763466
95891_at		Hypothetical LOC328660 (LOC328660), mRNA	-3.83 ± 0.10	-2.60 ± 0.09	-1.48 ± 0.10	1.10 ± 0.13	AI591977
102094_f_at		---	-2.78 ± 0.06	-2.83 ± 0.06	-1.10 ± 0.11	1.25 ± 0.15	AI841270
161535_at		---	-2.76 ± 0.07	-3.37 ± 0.06	-1.31 ± 0.11	-1.23 ± 0.11	AV234882
161124_at		---	-2.49 ± 0.07	-2.88 ± 0.07	-1.33 ± 0.10	-1.06 ± 0.10	AV237354
161196_r_at		---	-2.42 ± 0.08	-2.50 ± 0.06	-1.35 ± 0.12	1.19 ± 0.15	AV254135
102348_at		---	-2.41 ± 0.07	-4.37 ± 0.06	1.66 ± 0.25	1.17 ± 0.19	AI551087
101685_f_at		---	-2.32 ± 0.07	-2.60 ± 0.06	-1.34 ± 0.10	-1.36 ± 0.12	AI463421
162311_f_at		---	-2.22 ± 0.07	-3.54 ± 0.08	-1.11 ± 0.10	-1.20 ± 0.10	AV050648

92778_i_at	---	-2.09± 0.10	-1.91± 0.07	-1.16± 0.11	-1.04±0.10	Z22552
161615_f_at	---	-1.99± 0.07	-2.36± 0.08	-1.22± 0.10	-1.07±0.10	AV352346
162496_r_at	---	-1.87± 0.07	-2.31± 0.08	-1.74± 0.10	-1.07±0.12	AV153195
162292_r_at	---	-1.54± 0.11	-2.52± 0.07	1.01± 0.11	-1.12±0.10	AV377060
104363_at	Similar to corneodesmosin precursor; S protein; differentiated keratinocyte S protein precursor (LOC195357), mRNA	-1.54± 0.09	-2.29± 0.13	1.42± 0.10	1.24±0.13	AA763213
102091_f_at	---	-1.25± 0.14	-2.35± 0.10	1.03± 0.10	-1.14±0.13	AA407599
161528_r_at	---	-1.14± 0.11	-3.51± 0.11	-1.99± 0.10	-1.06±0.14	AV227261
101216_at	---	1.15± 0.11	-2.21± 0.08	-1.09± 0.11	-1.63±0.13	R75193
92269_r_at	Peg10 mRNA for paternally expressed 10, complete cds	1.33± 0.19	-1.80± 0.14	2.19± 0.22	1.84±0.12	AI836610
96215_f_at	CDNA clone MGC:67258 IMAGE:6413648, complete cds	1.37± 0.12	2.27± 0.08	1.58± 0.16	-1.05±0.13	AI153421
103467_g_at	4 days neonate male adipose cDNA, RIKEN full-length enriched library, clone:B430101C18 product:HYPOTHETICAL 19.9 KDA PROTEIN homolog [Homo sapiens], full insert sequence	1.69± 0.10	2.11± 0.07	1.08± 0.16	-1.40±0.14	AA790056
101179_at	---	2.00± 0.07	1.83± 0.08	-1.20± 0.14	-1.16±0.13	D50494
103710_at	Transcribed sequence with weak similarity to protein ref:NP_115973.1 (H.sapiens) zinc finger protein 347; zinc finger 1111 [Homo sapiens]	2.19± 0.11	1.27± 0.08	-1.05± 0.10	-1.02±0.10	AI037032
96579_at	Transcribed sequences	2.20± 0.21	1.86± 0.19	1.13± 0.13	1.13±0.13	AA267568
98129_at	M.musculus mRNA for testis-specific thymosin beta-10	2.35± 0.10	2.65± 0.12	-1.06± 0.11	-1.24±0.14	AI852553
101732_at	---	2.36± 0.20	2.10± 0.14	-1.13± 0.11	-1.12±0.11	M12039

95685_at	Adult male testis cDNA, RIKEN full-length enriched library, clone:1700092M07 product:unknown EST, full insert sequence	2.55 ± 0.08	3.74 ± 0.11	1.22 ± 0.18	-1.30 ± 0.13	AI849678
161083_at	Transcribed sequence with strong similarity to protein ref:NP_057365.1 (H.sapiens) STE20-like kinase; STE2-like kinase [Homo sapiens]	2.58 ± 0.09	1.97 ± 0.09	-1.03 ± 0.10	-1.40 ± 0.10	AW121616
100379_f_at	---	2.80 ± 0.11	1.75 ± 0.11	1.91 ± 0.14	-1.12 ± 0.10	AI837905
96316_at	Transcribed sequences	3.01 ± 0.23	1.82 ± 0.15	-1.08 ± 0.12	1.21 ± 0.15	AI839289